

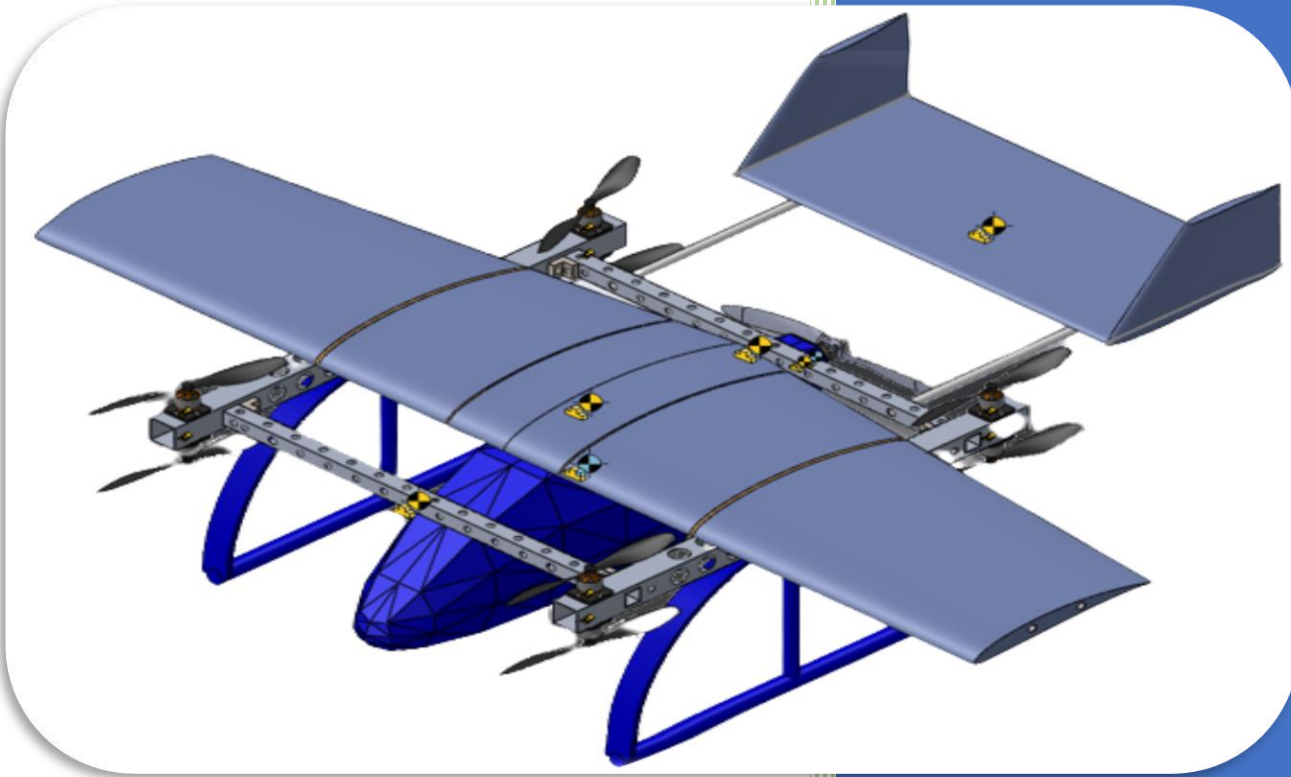


Cairo University  
Faculty of Engineering  
Aerospace Department



2022

# Urban Air Mobility (eVTOL)



**Submitted By:**

**Ahamed Khalil Yehia**

**Eyad Osama Mohamed**

**Romany Farouk Mozarie**

**Omar Khaled El-Said**

**Mahmoud Ahmed Mohamed**

**Under the supervision of :**

**Dr. Ayman Hamdy Kassem**

## Acknowledgement

---

### Acknowledgement

First and always, the prayerful thanks to our **Superb Bestows (Al-Wahhab) ALLAH** who gives us everything we have. His guidance and care made this study came to light.

We would like to thank **Professor Dr. Ayman Hamdy Kassem** for his assistance, advice and support throughout this research.

Special thanks to **Professor Dr. Osama Mohamady**, their great help.

Special thanks to **Eng. Wessam Ahmad** and **Eng. Mohamed Hetta** for their patience & great help.

Thanks to **SSTL** and **UDC members** for their hospitality and providing the needed components.

## **Abstract**

---

### **Abstract:**

**Urban Air Mobility (UAM)** is the use of small, highly automated aircraft to transport passengers or cargo at low altitudes in urban and suburban areas developed in response to traffic congestion. It usually refers to current and emerging technologies such as conventional helicopters and unmanned aerial vehicles (UAVs). Vertical take-off and landing aircraft (VTOL), electric propulsion aircraft and vertical take-off and landing aircraft (eVTOL) are characterized by the use of several electric-powered rotors or lift and propulsion fans, and in our project we have used eight motors installed on a frame made of aluminum as we used blue foam in the manufacture of some parts of the vehicle such as fuselage, wing and tail and introduced the concept of coaxial for a number of reasons including reducing the weight of the vehicle and reducing the space it occupies for ease of movement and also for the sake of Safety, when one or more motor vehicles are disabled, the vehicle is able to control and fly, which is called fault tolerance control. Finally, this project is a gateway to promoting the world of mobility in the future, reducing traffic congestion and reducing pollution.

# Table Of Contents

---

## Table Of Contents

Acknowledgement .....	i
Abstract: .....	ii
Table Of Contents .....	iii
Table Of Figures .....	vi
Abbreviations and Acronyms: .....	xii
Nomenclature: .....	xiii
Chapter One:Introduction: .....	1
1.1. Urban Air Mobility (UAM) .....	2
1.2. Unmanned Aerial Vehicle (UAV) .....	2
1.3. Electric vertical take-off and landing (eVTOL) .....	2
1.4. literature Review .....	4
1.4.1. Full-Scale Review .....	5
1.4.2. Wing Review .....	7
1.4.3. Tail Review .....	7
1.4.4. ECAA .....	8
1.4.5. Conclusion: .....	8
1.5. Coaxial Performance: .....	9
Chapter Two:Preliminary Design .....	10
2.1. Introduction .....	11
2.2. Weight Estimation .....	11
2.2.1 Roskam Method .....	11
2.2.2 Breakdown Method .....	14
2.2.3 Dynamic Scaling .....	16
2.2.4 Matching plot .....	17
2.3. Motor Selection: .....	19
2.3.1. Multi rotor .....	19
2.3.2. Single motor .....	20
2.4. Blade selection .....	23
2.4.1 Two Blade Propeller .....	23
2.4.2 Three Blade Propeller .....	24
2.5. Battery selection .....	26

# Table Of Contents

---

2.5.1 Lithium-ion Battery .....	26
2.5.2 Lithium-Polymer battery .....	26
2.6 Sizing frame .....	28
2.7 Material selection .....	28
Chapter Three: Aerodynamics.....	29
3.1. Introduction: .....	30
3.2. Fuselage design.....	30
3.2.1 Results:.....	32
3.3. Wing design .....	32
3.3.1 Span and chord .....	33
3.3.2 Airfoil Selection .....	33
3.3.3 Tail Design .....	36
3.3.4 Modified wing.....	38
3.3.5 Modified Model .....	42
3.3.6 Conclusion: .....	43
3.4. Wing loading.....	43
3.4.1. Sizing of the Wing .....	45
3.4.2 Sizing of the control surfaces .....	46
3.5. XFLR5 Aircraft Analysis .....	47
3.5.1 XFLR5 Results .....	48
Chapter Four: Structure .....	53
4.1 Introduction: .....	54
4.2 Main Frame:.....	54
4.2.1 Cross Section Selection:.....	54
4.2.2 Configuration Selection:.....	57
4.2.3 Weight Reduction: .....	63
4.3 landing Skid:.....	66
4.3.1 Static Structure Analysis .....	67
4.3.2 Impact Analysis:.....	71
4.4 Fuselage: .....	73
4.4.1 Static Structure Analysis .....	74
4.4.2 Fuselage installation: .....	76
4.5 Wing:.....	76
4.5.1 Static Structure Analysis .....	77

# Table Of Contents

---

<b>4.5.2 Wing installation:</b> .....	79
<b>4.5.3 Wing Spar Static Structure Analysis</b> .....	79
<b>4.6 Tail</b> .....	81
<b>4.6.1 Tail installation:</b> .....	81
<b>4.6. Tail Spar Static Structure Analysis:</b> .....	82
<b>4.7 Assembled Structure:</b> .....	84
<b>Chapter Five: Experimental Study</b> .....	87
<b>5.1. Introduction</b> .....	88
<b>5.2. Coaxial Rotors</b> .....	88
<b>5.3. Battery Comparison</b> .....	89
<b>5.3.1. One motor with a propeller 1045</b> .....	89
<b>5.3.2. One motor with a propeller 1245</b> .....	91
<b>5.3.3. Two motors with two propellers 1045</b> .....	93
<b>5.3.4 Two motors with two propellers 1245</b> .....	95
<b>5.4. Propeller Comparison</b> .....	97
<b>5.4.1. One motor with a 2Cell battery</b> .....	97
<b>5.4.2. One motor with a 3Cell battery</b> .....	99
<b>5.4.3. Two motors with two propellers of the same size using a 2Cell Battery</b> .....	101
<b>5.4.4. Two motors with two propellers of the same size using a 3Cell Battery</b> .....	103
<b>5.4.5. Two motors with two different propellers using a 3Cell Battery</b> .....	105
<b>5.5. And vice versa Vertical Spacing Comparison</b> .....	107
<b>5.5.1. Two motors with two propellers 1045 using a 2Cell Battery:</b> .....	107
<b>5.6. Efficiency</b> .....	109
<b>Chapter Six: Hardware and Electronics</b> .....	110
<b>6.1. Introduction</b> .....	111
<b>6.2. Brushless DC Electric Motor (BLDC Motor)</b> .....	111
<b>6.3. Electronic Speed Controller (ESC)</b> .....	111
<b>6.4. Power Distribution Board</b> .....	114
<b>6.5. Arduino Board</b> .....	115
<b>6.6. Sensors</b> .....	119
<b>6.6.1 Inertial Measurement Unit (IMU)</b> .....	119
<b>6.6.2. Altitude Sensor</b> .....	130
<b>6.6.3 Global Positioning System (GPS)</b> .....	133
<b>6.6.4 Transmitter and Receiver</b> .....	135

# Table Of Contents

---

<b>6.6.5 Airspeed Sensor .....</b>	<b>137</b>
<b>6.7. Arducopter.....</b>	<b>137</b>
<b>    Chapter Seven:Octa-Quad Modeling .....</b>	<b>141</b>
<b>7.1. Introduction.....</b>	<b>142</b>
<b>7.2. Transition from earth axes to body axes.....</b>	<b>143</b>
<b>7.3. Kinetics.....</b>	<b>144</b>
<b>    7.3.1 Forces .....</b>	<b>144</b>
<b>    7.3.2 moments .....</b>	<b>145</b>
<b>7.4. Kinematics .....</b>	<b>145</b>
<b>7.5. Modeling .....</b>	<b>147</b>
<b>7.6. Forces in body .....</b>	<b>149</b>
<b>    7.6.1 Forces in body x-axis.....</b>	<b>149</b>
<b>    7.6.2 Forces in body z-axis.....</b>	<b>149</b>
<b>7.7. Moments about body axes .....</b>	<b>150</b>
<b>7.8. Modeling Parameters.....</b>	<b>151</b>
<b>7.9 Mission Modeling:.....</b>	<b>151</b>
<b>    7.9.1. Takeoff and landing.....</b>	<b>152</b>
<b>    7.9.2. Cruise .....</b>	<b>154</b>
<b>    Chapter Eight: Octa-quad Control and Simulation .....</b>	<b>156</b>
<b>8.1. Takeoff and Landing: .....</b>	<b>157</b>
<b>    8.1.1. Altitude Controller.....</b>	<b>157</b>
<b>    8.1.2. Roll Controller .....</b>	<b>158</b>
<b>    8.1.3. Pitch Controller .....</b>	<b>159</b>
<b>    8.1.4. Yaw Controller .....</b>	<b>160</b>
<b>8.2. Cruise:.....</b>	<b>161</b>
<b>8.3. Simulation.....</b>	<b>162</b>
<b>    8.3.1. Results .....</b>	<b>163</b>
<b>    References.....</b>	<b>167</b>
<b>References:.....</b>	<b>168</b>
<b>    Appendix A .....</b>	<b>170</b>
<b>    Appendix B.....</b>	<b>174</b>

# Abbreviations and Acronyms

---

## Table Of Figures

Figure 1: VTOL Oprating Range .....	4
Figure 2:embeds 36 electric motors in tilting wings and canards .....	6
Figure 3:six ducts for extended operational range.....	6
Figure 4:conventional configuration .....	7
Figure 5: Wing position configurations .....	7
Figure 6: Tail configurations .....	8
Figure 7: Single Motor VS Coaxial Motors .....	9
Figure 8:Roscom Matching .....	13
Figure 9:Simple Matching.....	13
Figure 10:Roscom Matching eVTOL.....	14
Figure 11:Ehang 216.....	16
Figure 12:Ehang VT-30 .....	16
Figure 13: Matching Plot.....	16
Figure 14: optimum design points .....	18
Figure 15: Stall Speed.....	18
Figure 16: Motors .....	19
Figure 17:Data sheet of motor and specifications .....	19
Figure 18: motor characteristic at full throttle data from ecalc .....	20
Figure 19: motor characteristic at full throttle .....	22
Figure 20:Better components.....	22
Figure 21: Blade selection .....	23
Figure 22:Lithium-ion Battery .....	26
Figure 23:Lithium-Polymer battery .....	26
Figure 24: 2 Cell VS 3 Cell Battery .....	27
Figure 25: 3 Cell Battery .....	27
Figure 26:Standard Man standing approach .....	30
Figure 27: Standard Man sitting approach .....	30
Figure 28: Cabin and Baggage Hold dimension.....	30
Figure 29: fuselage cross section.....	31
Figure 30: Fuselage Side section: Front Cone .....	31
Figure 31: fuselage top section.....	32
Figure 32: Fuselage Parameters .....	32
Figure 33: NACA 0009 Airfoil .....	32
Figure 34: Wing geometric homebuilt .....	33
Figure 35: Airfoil Selection Flow chart.....	34
Figure 36: Airfoil SG6043 .....	34
Figure 37: wing model in 3d.....	35
Figure 38: Aerodynamic theoretical analysis of wing.....	35
Figure 39: Tail and wing airfoil geometric homebuilt A .....	36
Figure 40: Wing and tail 3D model .....	37
Figure 41: Wing and tail aerodynamic theoretical analysis.....	38
Figure 42: modified wing top view .....	38
Figure 43: Modified wing in 3D .....	39
Figure 44: Modified wing theoretical analysis.....	40

## Abbreviations and Acronyms

---

Figure 45: Modified wing drag analysis.....	41
Figure 46: Modified Wing Induced Drag analysis .....	41
Figure 47: Modified Model Theoretical Analysis.....	42
Figure 48: Stall Speed Determination .....	44
Figure 49: XFLR5 Analysis.....	48
Figure 50: cm VS alpha Curve .....	48
Figure 51: Aerodynamic stability .....	48
Figure 52 : cl VS cm Curve .....	49
Figure 53: cl VS alpha Curve.....	50
Figure 54: Velocity Vs Cm Curve.....	50
Figure 55: Longitudinal Eigenvalue .....	52
Figure 56: Lateral Eigenvalue .....	52
Figure 57:Structure Analysis (Square cross section (1.5×1.5 ×0.1 cm) .....	55
Figure 58: Structure Analysis (Square cross section (2.5×2.5 ×0.1 cm) .....	55
Figure 59: Structure Analysis (Square cross section 4×4×0.1 cm) .....	56
Figure 60: The first design and its dimensions.....	56
Figure 61:The first design and its dimensions .....	57
Figure 62: The first design Total deformation .....	57
Figure 63: The first design Stress .....	58
Figure 64: The first design Strain.....	58
Figure 65: The Second design and its dimensions.....	59
Figure 66: The second design Total deformation.....	59
Figure 67: The second design Stress.....	60
Figure 68: The second design Strain .....	60
Figure 69: The Coaxial design and its dimensions .....	61
Figure 70: The Coaxial design Total deformation .....	61
Figure 71: The Coaxial design Stress .....	62
Figure 72: The Coaxial design Strain.....	62
Figure 73: The Coaxial drilled design and its dimensions.....	63
Figure 74: The Coaxial drilled design Total deformation .....	64
Figure 75: The Coaxial drilled design Stress .....	64
Figure 76: The Coaxial drilled design Strain .....	65
Figure 77: The Coaxial frame Implemented design.....	66
Figure 78: The Landing skid Implemented design .....	67
Figure 79: Frist Design of The Landing skid and its dimensions .....	67
Figure 80: Frist Design of The Landing skid Total deformation.....	68
Figure 81: Frist Design of The Landing skid Stress.....	68
Figure 82: Frist Design of The Landing skid Strain .....	69
Figure 83: Second Design of The Landing skid and its dimensions .....	69
Figure 84: Second Design of The Landing skid Total deformation.....	70
Figure 85: Second Design of The Landing skid Stress.....	70
Figure 86: Frist Design of The Landing skid Strain .....	71
Figure 87: The Impact test of the Landing skid.....	72
Figure 88: Implemented design .....	73
Figure 89: Fuselage CAD design and Implemented design.....	74
Figure 90: Fuselage CAD design Total deformation .....	74

## Abbreviations and Acronyms

---

Figure 91: Fuselage CAD design Stress .....	75
Figure 92: Fuselage CAD design Strain.....	75
Figure 93:Fuselage installation .....	76
Figure 94: Wing dimension .....	77
Figure 95: Wing CAD design Total deformation.....	77
Figure 96: Wing CAD design Stress.....	78
Figure 97: Wing CAD design Strain .....	78
Figure 98: Wing Frame installation .....	79
Figure 99: Wing Spar CAD design Total deformation.....	79
Figure 100: Wing Spar CAD design Stress.....	80
Figure 101: Wing Spar CAD design Strain .....	80
Figure 102: Tail CAD design .....	81
Figure 103: Tail Frame installation.....	81
Figure 104: Two Way Elbow (3D printed) .....	82
Figure 105: Tail Spar CAD design Total deformation .....	82
Figure 106: Tail Spar CAD design Stress .....	83
Figure 107: Tail Spar CAD design Strain.....	83
Figure 108: Assembly Exploded view.....	84
Figure 109: Final Assembly.....	85
Figure 110: Final Assembly dimensions (mm) .....	85
Figure 111: Implemented design .....	86
Figure 112: Coaxial test rig .....	88
Figure 113:One motor using 2Cell battery with propeller 1045 .....	89
Figure 114 :One motor using 3Cell battery with propeller 1045 .....	89
Figure 115 :One motor using 3Cell battery with propeller 1245 .....	91
Figure 116 : One motor using 2Cell battery with propeller 1245.....	91
Figure 117 :Two motors using 2Cell battery with propellers 1045 .....	93
Figure 118 :Two motors using 3Cell battery with propellers 1045 .....	93
Figure 119 :Two motors using 2Cell battery with propellers 1245 .....	95
Figure 120 :Two motors using 3Cell battery with propellers 1245 .....	95
Figure 121 :One motor using 2Cell battery with propeller 1045 .....	97
Figure 122 :One motor using 2Cell battery with propeller 1245 .....	97
Figure 123 :One motor using 3Cell battery with propeller 1245 .....	99
Figure 124 :One motor using 3Cell battery with propeller 1045 .....	99
Figure 125 :Two motors using 2Cell battery with propellers 1245 .....	101
Figure 126 :Two motors using 2Cell battery with propellers 1045 .....	101
Figure 127 :Two motors using 3Cell battery with propellers 1245 .....	103
Figure 128 :Two motors using 3Cell battery with propellers 1045 .....	103
Figure 129 :Upper 1045 & Lower 1245.....	105
Figure 130 :Upper 1245 & Lower 1045.....	105
Figure 131 :Vertical spacing 16cm .....	107
Figure 132 :Vertical spacing 14cm .....	107
Figure 133 :Efficiency .....	109
Figure 134: Pulse Width Modulation .....	112
Figure 135: Servo PWM.....	112
Figure 136: Servo motor connections Arduino board .....	114

## Abbreviations and Acronyms

---

Figure 137: Power Distribution Board.....	115
Figure 138: Arduino Uno Pinout .....	117
Figure 139:Arduino Uno .....	117
Figure 140: Arduino Mega Pinout.....	118
Figure 141: Arduino Mega .....	119
Figure 142: Magnetometer device .....	120
Figure 143: BMX055.....	121
Figure 144: Digital interface of the device .....	121
Figure 145: BMX055 Basic Description.....	122
Figure 146: <i>I2C</i> connection.....	123
Figure 147: connections and the corresponding addresses .....	123
Figure 148: <i>I2C</i> scan .....	124
Figure 149: Accelerometer Register Map .....	125
Figure 150: Gyroscope Range.....	126
Figure 151: Gyroscope Register Map.....	127
Figure 152:Magnetometer Register Map.....	128
Figure 153: BMP180 .....	130
Figure 154: pressure and temperature sensor algorithm .....	130
Figure 155: pressure and temperature sensor algorithm with example .....	131
Figure 156: Altitude in Standard atmosphere.....	132
Figure 157: BMP180 measurement .....	132
Figure 158: Triangulation .....	133
Figure 159: GPS module with Anttena .....	134
Figure 160 : Coordinates of Aerospace Engineering department building .....	135
Figure 161: Blynk IoT .....	135
Figure 162: ESP8266.....	136
Figure 163: Serial Peripheral Interface (SPI) .....	136
Figure 164: nRF24L01.....	137
Figure 165: Arducopter .....	137
Figure 166: mission planner.....	139
Figure 167: The configuration we have to use to our Arducopter.....	139
Figure 168: Coordinate Frames.....	142
Figure 169: Transition from Body Axes to Earth Axes .....	143
Figure 170 :The arrangement of the motors and the direction of their rotation .....	147
Figure 171:Comparison between two different motors .....	148
Figure 172 :Comparison between two different motors .....	149
Figure 173: Altitude Controller Step Response.....	157
Figure 174: Roll Controller Step Response .....	158
Figure 175: Pitch Controller Step Response.....	159
Figure 176: Yaw Controller Step Response.....	160
Figure 177: Controlling the cruise speed on Simulink .....	162

## **Abbreviations and Acronyms**

---

### **Abbreviations and Acronyms:**

<b>UAM</b> .....	<b>Urban Air Mobility</b>
<b>VTOL</b> .....	<b>Vertical Take-Off and Landing</b>
<b>eVTOL</b> .....	<b>electric propulsion aircraft and vertical take-off and landing aircraft</b>
<b>UAV</b> .....	<b>Unmanned Aerial Vehicle</b>
<b>STOL</b> .....	<b>Short Take-Off and Landing</b>
<b>ABC</b> .....	<b>Aircraft-Body-Centered (frame, assumed as body fixed frame)</b>
<b>MOS</b> .....	<b>Margin Of Safety</b>
<b>FOS</b> .....	<b>Factor OF Safety</b>
<b>DC</b> .....	<b>Direct Current</b>
<b>BLDC</b> .....	<b>Brushless Direct Current</b>
<b>ESC</b> .....	<b>Electronic Speed Control</b>
<b>PWM</b> .....	<b>Pulse Width Modulation</b>
<b>IMU</b> .....	<b>Inertial Measurement Unit</b>
<b>c.g.</b> .....	<b>Center of gravity</b>
<b>DOF</b> .....	<b>Degree of freedom</b>
<b>SISO</b> .....	<b>Single input single output</b>
<b>PD</b> .....	<b>Proportional derivative</b>
<b>PI</b> .....	<b>Proportional integral</b>
<b>GPS</b> .....	<b>Global positioning system</b>
<b>PWM</b> .....	<b>Pulse Width Modulation</b>
<b>SPI</b> .....	<b>Serial peripheral interface</b>
<b>PS</b> .....	<b>Protocol select</b>
<b>MSB</b> .....	<b>Most significant bit</b>
<b>LSB</b> .....	<b>Least significant bit</b>
<b>AHRS</b> .....	<b>Attitude and heading reference system</b>
<b>MEMS</b> .....	<b>Micro-electro-mechanical system</b>

## **Abbreviations and Acronyms**

---

<b>MARG</b> .....	<b>Magnetic, angular rates, and gravity</b>
<b>RF</b> .....	<b>Radio frequency</b>
<b>BLDC motor</b> .....	<b>Brushless direct current motor</b>
<b>PDB</b> .....	<b>Power distribution board</b>

## Nomenclature

---

### Nomenclature:

$\rho$	Air density
$P$	Pressure
$P_0$	Static pressure
$V$	Air speed
$\phi$	Roll angle in earth reference axes, rotation angle about x-axis of earth reference frame
$\theta$	Pitch angle in earth reference axes, rotation angle about y-axis of earth reference frame
$\psi$	Yaw angle in earth reference axes, rotation angle about z-axis of earth reference frame
$x_E, y_E, z_E$	Earth reference axes
$x_B, y_B, z_B$	Body fixed axes
$R_{BE}$	Coordinate transformation matrix from body-fixed axes to earth axes
$R_{EB}$	Coordinate transformation matrix from earth axes to body-fixed axes
$m$	Vehicle's mass
$g$	Gravity of earth
$\vec{F}$	Force vector in body-fixed axes
$F_x$	Force component in x-axis of body-fixed frame
$F_y$	Force component in y-axis of body-fixed frame
$F_z$	Force component in z-axis of body-fixed frame
$\vec{V}_B$	Velocity vector in body-fixed axes
$u$	Velocity component in x-axis of body-fixed frame
$v$	Velocity component in y-axis of body-fixed frame
$w$	Velocity component in z-axis of body-fixed frame
$\vec{\omega}$	Angular velocity vector about body-fixed axes
$p$	Roll rate in body fixed axes, angular velocity about x-axis of body fixed frame
$q$	Pitch rate in body fixed axes, angular velocity about y-axis of body fixed frame

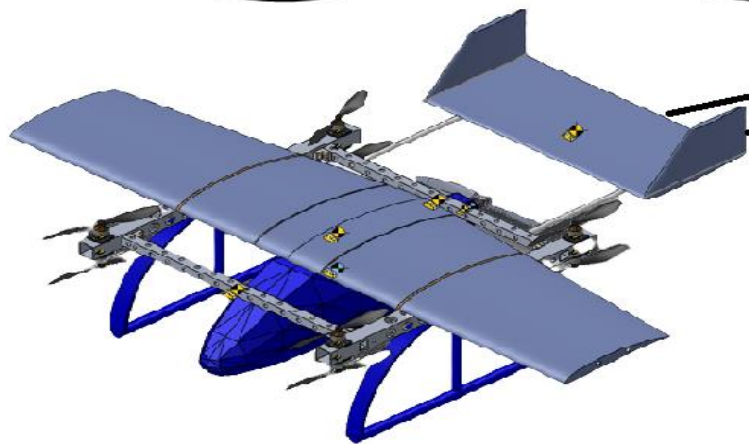
## Nomenclature

---

$r$	..... Yaw rate in body fixed axes, angular velocity about z-axis of body fixed frame
$\vec{M}$	..... Moment vector in body-fixed axes
$L$	..... Moment about x-axis of body-fixed frame
$M$	..... Moment about in y-axis of body-fixed frame
$N$	..... Moment about in z-axis of body-fixed frame
$I$	..... Inertia matrix of the vehicle
$I_{xx}$	..... Moment of inertia around body-fixed x-axis when the body rotates around its x-axis
$I_{yy}$	..... Moment of inertia around body-fixed y-axis when the body rotates around its y-axis
$I_{zz}$	..... Moment of inertia around body-fixed z-axis when the body rotates around its z-axis
$I_{xy}$	..... Moment of inertia around body-fixed y-axis when the body rotates around its x-axis
$I_{yx}$	..... Moment of inertia around body-fixed x-axis when the body rotates around its y-axis
$I_{xz}$	..... Moment of inertia around body-fixed z-axis when the body rotates around its x-axis
$I_{zx}$	..... Moment of inertia around body-fixed x-axis when the body rotates around its z-axis
$I_{yz}$	..... Moment of inertia around body-fixed z-axis when the body rotates around its y-axis
$I_{zy}$	..... Moment of inertia around body-fixed y-axis when the body rotates around its z-axis
$K_t$	..... Thrust coefficient of motor
$K_r$	..... Torque coefficient of motor
$Th_i$	..... Throttle input to the motor
$Th_{late}$	..... Throttle input to control roll angle $\phi$
$Th_{long}$	..... Throttle input to control pitch angle $\theta$
$Th_{norm}$	..... Throttle input to control yaw angle $\psi$
$Th_z$	..... Throttle input to control Thrust in z-axis
$Th_x$	..... Throttle input to control Thrust in x-axis

# **Chapter One:**

# **Introduction**



## 1.1. Urban Air Mobility (UAM)

Urban air mobility (UAM) offers a new way for us to commute to work and transport goods using electric vertical take-off and landing aircraft (eVTOLs). Similar to the helicopter, this new breed of aircraft is somewhere between commercial airplanes and remotely controlled drones, configured to carry large payloads and people. UAM will open traffic lanes in the sky. It represents nothing short of a giant leap forward in transportation,

Urban air mobility (UAM), also called flying taxi, is defined in a 2018 National Aeronautics and Space Administration (NASA) paper “as safe and efficient air traffic operations in a metropolitan area for manned aircraft and unmanned aircraft systems (UAS)”. It will use highly automated aircraft that will operate and transport passengers or cargo at lower altitudes within urban and suburban areas and is considered a subset of advanced aerial mobility.

A growing number of players, led by aerospace, automobile, and technology companies, are working on urban air mobility solutions. The first generation of full-scale demonstrators are flying today, and limited commercial flights are possible within the next five years. Of course, progress is never a straight line, especially in technology, regulatory and industry transformations as significant as introducing a new transportation system. As a consequence, forecasts of the size of the global market for eVTOLs by 2030 vary widely

## 1.2. Unmanned Aerial Vehicle (UAV)

Unmanned Aerial Vehicle (UAV) is a type of aircraft which has no pilot or passenger on board. UAVs include both autonomously controlled (drones) and remotely piloted vehicles (RPVs) controlled via Radio transmitter. UAVs are commonly used in situations where there is high risk in sending a human piloted aircraft or where using a manned aircraft is impractical

## 1.3. Electric vertical take-off and landing (eVTOL)

Electric vertical take-off and landing (eVTOL) vehicles are light commercial aircraft that can take off and land vertically like helicopters and fly forward like airplanes. Unlike helicopters, they use batteries instead of fuel for propulsion and are more maneuverable, less complex, and more efficient than helicopters. They are designed to fly at a lower altitude than commercial aircraft and will be either piloted or autonomous.

Much of the eVTOL investment to date has been focused on design what the aircraft looks like, how it is powered, and how it performs as well as how to make it as safe or safer than commercial aircraft aviation and how to create an amazing customer experience. The design criteria include:

- **Payload.** The range for air taxis is from a single-person (100 kgs) to a nine-person-plus-baggage (960 kg) payload. Companies like Lilium and Joby Aviation are focused on a five-passenger eVTOL, while Volocopter and Ehang are opting for a more compact solution. EASA and FAA are recommending setting the maximum take-off weight for eVTOLs at 3,175 kg.

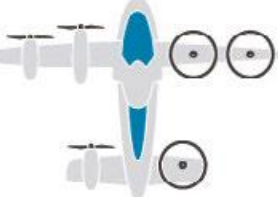
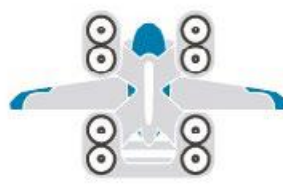
- **Safety.** To fly above populated areas, eVTOLs will be required to be at least as safe as general aviation aircraft. However, with rapid growth expected in the number of eVTOLs operating in city skies, regulators may impose more stringent safety standards than those that apply to general aviation.

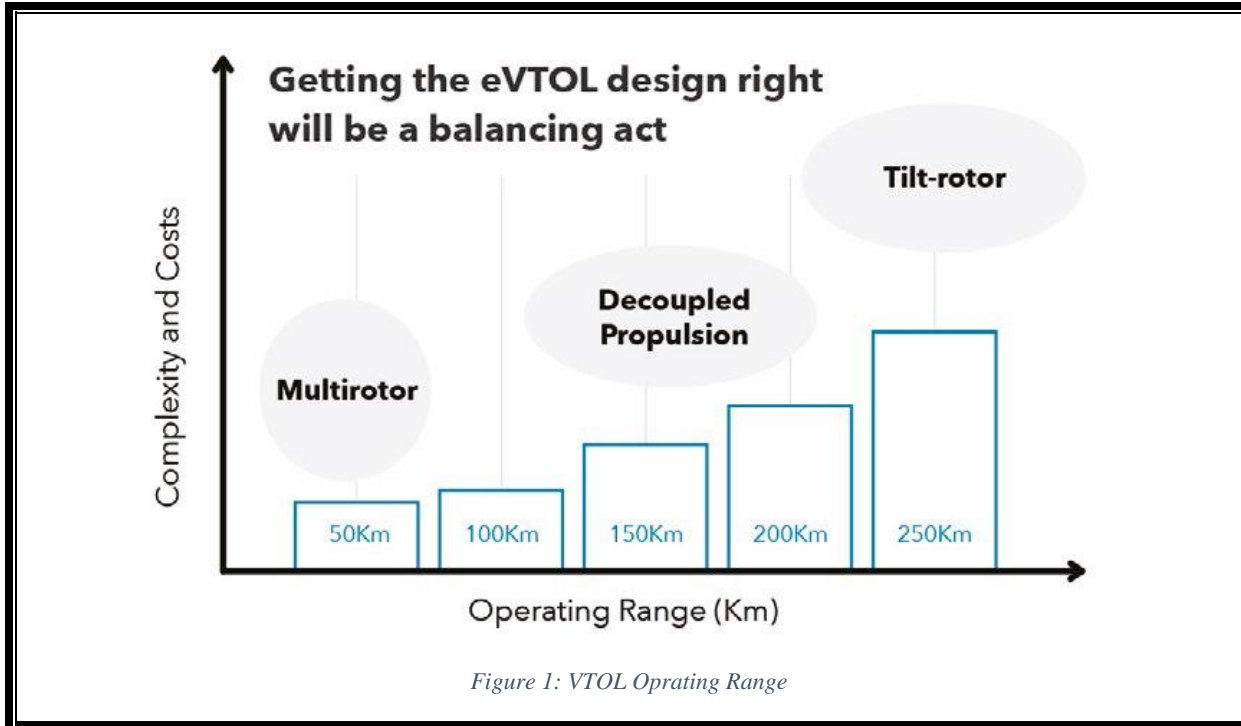
- **Noise.** Sound pollution, both frequency and decibel level, is a serious issue for operating eVTOLs in urban environments. Uber has a set of requirements that specify eVTOLs must be 15 decibels (dB) less noisy than existing light helicopters, which is about 70 dB at 500 feet versus 85 dB for a typical helicopter. In comparison, the noise from a commercial jet at 25 meters is 150 dB, while a quiet rural area is 30 dB.
- **Cost.** As part of the mobility-as-a-service revolution, eVTOLs will be managed by service provider and will likely not be sold to private customers. The service providers will purchase fleets of eVTOLs that will be part of an on-demand business service. This model will allow them to minimize per-vehicle

product costs, and drive down the passenger cost-per-mile, which will help drive the success of the commercial eVTOL ventures.

### Three key eVTOL configurations

Much of the focus today is on three propulsion system alternatives, which differ dramatically from traditional helicopters.

Multirotor	Tilt-rotor	Decoupled-propulsive
		
<p>Multirotor eVTOLs are wingless aircraft. They are very efficient while hovering and suited for low-noise applications. However, they are less efficient while cruising, with a top speed of about 90 km/h and a maximum range of 40-50 km. Still, they are a viable alternative to today's helicopters because they are quieter, cheaper to operate, and have no harmful emissions.</p>	<p>Tilt-rotor or vectored-thrust eVTOLs have multiple propellers or fans that can be tilted to transition from vertical to horizontal flight and can reach speeds of up to 300 km/h and a range of 300 km. Tilting the propellers, and controlling the direction of thrust stabilizes the vehicle's attitude and angular velocity. Tilt-rotors are more complex than multirotor as all the actuators that tilt the engines need to be fully redundant and certified for multiple failures. This redundancy adds weight and cost and requires more time for certification.</p>	<p>Decoupled-propulsive, lift-and-cruise configurations have multiple fixed vertical propellers and a pusher to transition from vertical to horizontal flight. They can reach speeds of up to 250 km/h and have a range of up to 150-200 km. Decoupled propulsive systems can deliver higher performance than multirotor, but lower than tilt rotors.</p>



## ❖ Applications

Its ability to VTOL and hover in the position with proper stability and maneuverability brings many mission options into possibilities. This makes the Unmanned Aerial Vehicle (UAV) versatile and may be used for various purposes. Few application areas are described here

**Aerial surveillance:** UAV these days are widely used for aerial surveillance. Aerial surveillance drones include conservation drones mostly used for wildlife conservation. It is also used by different organizations like military forums for aerial surveillance for their specific purpose.

**Photogrammetry:** Different organizations use this vehicle for photogrammetric purposes where the high-resolution aerial images taken by the UAV is used for generating 3D images of the landscapes and generating maps.

**Delivery robot:** These days different companies are using UAV as their delivery Kit or robot. Domino's Pizza uses its Dom copter (Oct-copter) for delivering Pizza to its customers.

**Precision farming:** Developed countries are using this vehicle for precision farming where the crops are continuously inspected and the corresponding actions are taken for greater productivity.

**Rescue missions:** This vehicle could also be used for rescue purposes and delivering medicine kits for casualties where manned vehicles are riskier to take.

## 1.4. literature Review

Its purpose is to build a proper background of what countries are aspiring to achieve, for more realistic thoughts to enter the field of competition.

### 1.4.1. Full-Scale Review

This section reviews the UAM airplanes of publicly available information or just announced by the industry company.

❖ There are basically four configurations in this field:

- 1) Multicopters:** The aircraft is built like a helicopter and the lift is produced exclusively by rotors.
- 2) Vectored Thrust:** The lift is produced by wings during the flight while thrust is produced by the same engines by a tilting mechanism.
- 3) Lift + Cruise:** The lift is produced by wings during the flight but the thrust is produced by a set of fixed motors different from the motors producing lift during hover or by the same engines by tilting the whole aircraft in the direction of the slipstream like a helicopter.
- 4) Augmented Lift:** Not VTOL; however, the wing is supplied with high lift devices that provide short distances take-off.

Multicopters	Vectored Thrust
 VoloCity	 JOBY S4
Lift + Cruise	Augmented Lift
 Eve UAM Solutions	 Airflow Ravn
 Beta Technologies ALIA	 Electra

❖ The decentralized propulsion and multiple small rotors are to ensure quiet transport for urban environments.

	Archer Maker eVTOL	Velocity	Eve Urban Air Mobility Solutions
Number of Rotors	6 + 6 tiltrotors	18	8 + 2 pushers
Number of Passengers	2	2	5

Some of them are designed to fly without a pilot and deploys a whole-vehicle parachute in case of a failure like the German-built Lilium. One of the more futuristic designs. Lilium Jet has space for

seven passengers including a seat for pilot, and it embeds 36 electric motors in tilting wings and canards.



Figure 2: embeds 36 electric motors in tilting wings and canards

## ❖ Almost all of them are electric.

**1) Gas Vehicles:** In the first decade of the 20th century, investors were drawn to another aircraft that was to spawn a new air taxi industry, the Very Light Jet (VLJ). The VLJ was expected to revolutionize on-demand short trips with low purchase and operating costs, all thanks to new technologies, and not as high-risk ones as eVTOL, yet it seems there's no progress that lives up to the expectations.

**2) Electric Vehicles:** They are likely to be much quieter and environmental friendly. The disadvantage of electric propulsion is its energy density. Gram for gram, fossil fuels carry as much as 100 times the energy of batteries. Advertised eVTOL ranges are short because they have to be. BETA recently announced the longest known flight by an eVTOL: 205 miles, a short distance which a single tank of gas can get in almost any car or airplane. What's more, batteries cannot be refueled quickly. Recharge times vary depending on factors like temperature, but can take up to a couple of hours. The commercial aviation industry relies on turning its airplanes around rapidly, a pace eVTOLs simply cannot match unless drained batteries can be swapped with fresh ones, a task that would add cost and risk to every flight. And like a cellphone battery, eVTOL batteries degrade over time and will need to be replaced. Although batteries have much lower energy density than liquid fuel, the Nexus offsets this by cruising on an airplane wing as well as lift generated by the six ducts for extended operational range.

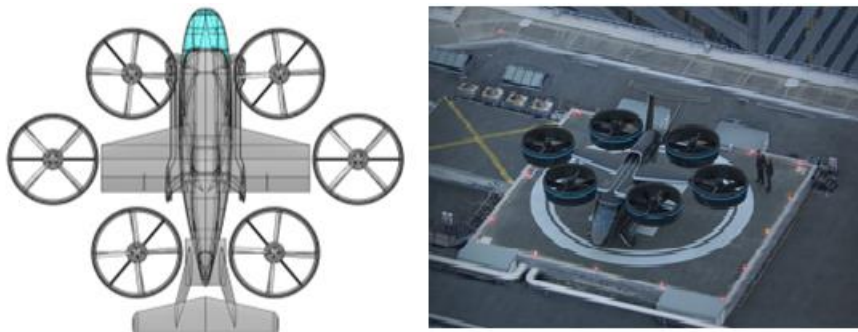


Figure 3:six ducts for extended operational range

### 1.4.2. Wing Review

The wing configuration is centered around four configurations:

- 1) **Conventional:** A wing and aft tail (e.g. Nexus).
- 2) **Canard:** A wing and front tail (e.g. Lilium).
- 3) **Tandem:** Front and rear wings (e.g. Eve).
- 4) **Three Surfaces:** A wing, aft and front tails (e.g ATEA).

Most airplanes are of a conventional configuration. With certain exceptions. One reason is that the database and the experience dealing with conventional configurations is very large. This database is narrow and even non-existent in some of the other configurations.



Figure 4:conventional configuration

-  The high wing is mostly used since the low altitude is full of weather hazards like wind and turbulence over buildings that need higher stability in roll, moreover, there is actually no need for rolling since the mounted rotors can provide pure rotation in yaw. A high visual resolution for a pilot is also needed.

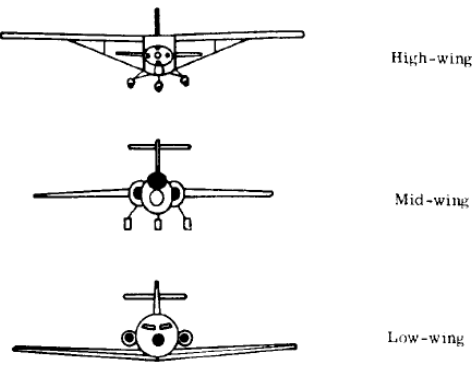


Figure 5: Wing position configurations

-  The ‘wing fold’ mechanism is found in some cargo airplanes (e.g Pipistrel Nuuva V300).

### 1.4.3. Tail Review

A standard tail is rather to make the controllability a function of engine power but could cause significant tail fatigue at high engine power, could be solved using dihedral or some other configurations:

Three configurations are found frequently used in UAMs:

- 1) **T-tail:** The Horizontal Tail (HT) is away from the slipstream.
- 2) **Twin tail:** The HT is either mounted low for less vortices at its tip or mounted high for the same function in T-tail.
- 3) **V-tail:** HT & Vertical Tail (VT) are integrated together. Is lighter with aerodynamic benefits but complex in control.

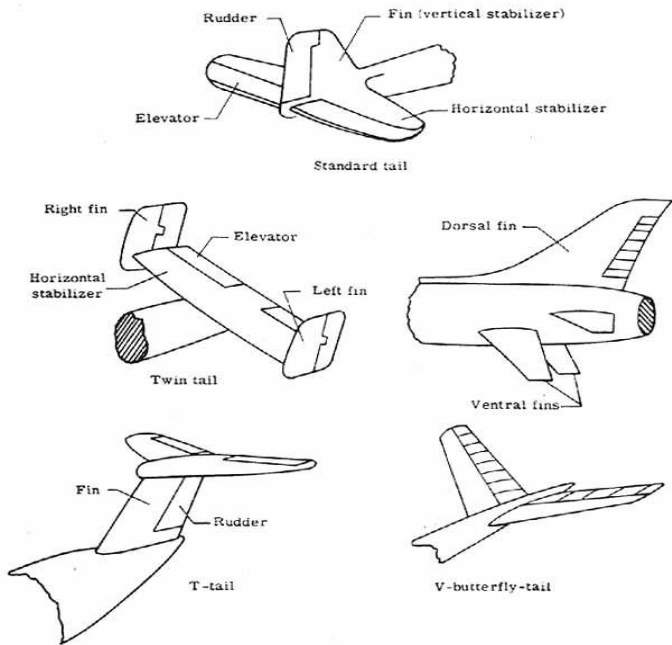


Figure 6: Tail configurations

#### 1.4.4. ECAA

Must be put in consideration the legislation of security and safety for the approval of Egyptian Civil Aviation Authorities, the regulator of the civil aviation activities, including management of air traffic in Egypt, in order to be approved as a certified vehicle and start operations

The authorities that shall be determined by decree from the minister of civil aviation for the practice of fixed competencies indicated in this law, A civil aviation authority is supposed to regulate civil aviation to promote safety, developing and operating a system of air traffic control and navigation for aircrafts, developing and carrying out programs to control aircraft noise and other environmental effects of civil aviation

A flight permit is a limited approval issued by the CAA to undertake a certain aerial operation in the territory of the republic, including civil airports , civil airplanes and the airplanes of the state including personnel.

#### 1.4.5. Conclusion:

The race is about low acoustic, cheaper, safer and non-polluting. If we can have something that possesses optimum values through all of them, it would be revolutionary enough to compete as a main power.

### 1.5. Coaxial Performance:

In designing a micro multi-rotor vehicle is an adequate choice of propulsion system. The original quadrotor concept, introduced in 2000s, evolved into many various solutions. Nowadays, the tri-, quad-, hexa- and octocopters are available on the market

In our Project, we focus on few multirotor designs, with so called x8 quadrotor or octa quad among them. This configuration of multirotor extends original quadcopter concept by increasing the total thrust output of platform thanks to additional set of motors. On each side, there are two identical rotors installed, one above another. The propellers rotate in opposite directions, which equalizes the momentum of platform. The upper propeller works as a tractor, while the lower unit is a pusher. As a result, the total thrust of propulsion unit is increased with similar physical volume in comparison to single propeller

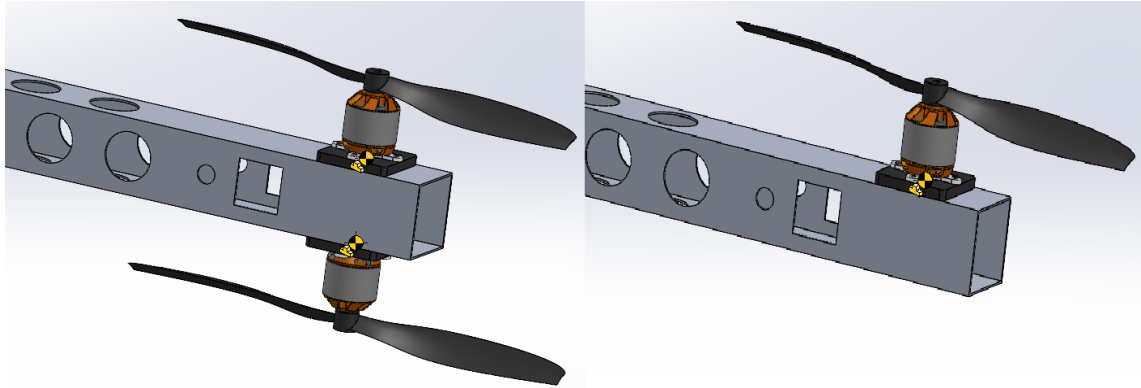


Figure 7: Single Motor VS Coaxial Motors

However, considering that a lower propeller operates in a prop wash of upper unit, the total thrust performance of coaxial propulsion is lower comparing to two separated propellers.

- ❖ performance of coaxial propulsion in UAVs, and efficiency of such propulsion design according to Glauert's theory with varying motors' speed or spacing and propellers' diameter and pitch.

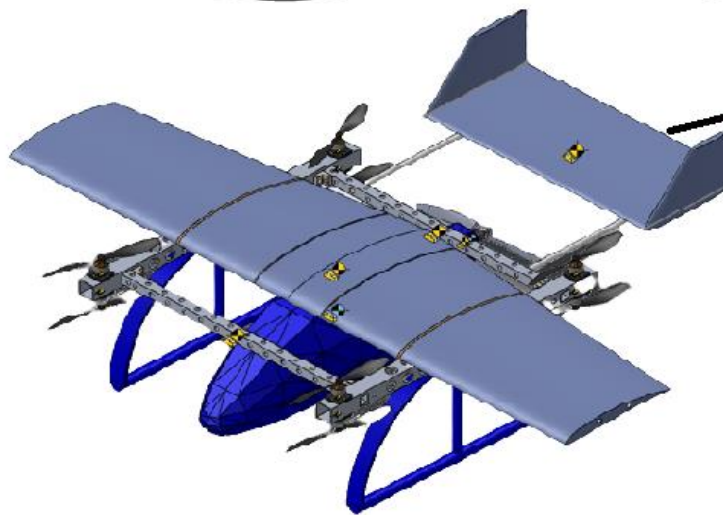
#### Advantages of Coaxial:

- ❖ When there are more than 5 motors present, it provides redundancy: if one motor fails the aircraft can still maintain balance in the air and allow it to land safely
- ❖ Reducing the dimensions of the frame and then reducing its weight
- ❖ Possibility to make the frame foldable for better mobility

#### Disadvantages of Coaxial:

- ❖ Some 10-30% loss in power efficiency. Basically, the bottom motor is just turning in already sped-up air, it's losing efficiency
- ❖ Propellers can get caught by obstacles more easily as pilots could oversee them
- ❖ Because the propellers are located above and below the arms, they are hard to hide from the camera's view
- ❖ Difficult to find appropriate landing gear

# **Chapter Two: preliminary Design**



## 2.1. Introduction

The preliminary design stage makes use of extensive mathematical optimization. The objective of the optimization process is to design a geometry and propulsion system to maximize the range which implies minimizing power and maximizing cruise efficiency. In our case, we have divided the optimization and design process into seven stages.

**requirements of Our project:**

- ✈ Vertical take-off and landing, and hovering at least 3 min – Subscale
- ✈ Relatively high cruise speed of 160 km/h – Full scale
- ✈ Endurance is at least 5 min, – Subscale
- ✈ Payload is 500 g – Subscale
- ✈ Payload is 200 kg – Full scale

## 2.2. Weight Estimation

For this section, it is important to estimate time to stay in air, and to achieve a better performance with minimum weight and allowable material.

### 2.2.1 Roskam Method

The maximum take-off weight  $W_{TO}$  can be obtained from historical data for general aircraft conceptual design, Roskam assumed the relation the take-off weight to empty weight of fuel airplanes, it's used and explained precisely in his reference [2].

A convenient way to break down  $W_{TO}$  as follows:

$W_{TO} = W_{OE} + W_{PL}$	$W_{TO}$	the take-off gross weight (kg)
	$W_{OE}$	the airplane operating weight empty (OWE)
	$W_{PL}$	the payload weight (kg)
$W_{OE} = W_E + W_{crew}$	$W_E$	the empty weight (kg)
	$W_{crew}$	the weight of the crew required to operate the airplane (in this case it equals zero)
$W_E = W_{ME} + W_{BC} + W_{FEQ}$	$W_{ME}$	the manufacturer's empty weight (green weight (kg))
	$W_{BC}$	the weight of all battery cells
	$W_{FEQ}$	the fixed equipment weight if it is found (kg). Fixed equipment weight can include

Substituting yields the take-off gross weight as:

$$W_{TO} = W_E + W_{PL}$$

And the empty weight is

$$W_E = W_{TO} - W_{PL}$$

Since there exists a linear relationship between  $\log W_{TO}$  and  $\log W_E$  as follows

$$\log W_{TO} = A + B \cdot \log W_E$$

Where  $A$  and  $B$  are the regression line constants, are determined from fitting collected data to of similar UAM and eVTOL types to straight lines. The samples below are for UAM aircrafts that are announced by its organization.

UAM name	Payload ( <b>kg</b> )	Empty Weight ( <b>kg</b> )	Take-off Weight ( <b>kg</b> )
JOBY S4	500	1315	1815
Pipistrel Nuuva V300	300	1240	1700
Beta Technologies ALIA	635	2539.7	3174.7
Elroy Air Chaparral	226.8	550	800
V400	100	300	400
French ASCENDANCE ATEA HYBRID-ELECTRIC VTOL AIRCRAFT	445	1550	2000
JAUNT JOURNEY	453.6	1633	2721.6
Kitty Hawk	100	274.7	374.7
Ehang VT-30	200	700	900
Dufour Aerospace aEro 3	749.8	2050	2800

#### Criteria

1. lift+cruise and vectored thrust types are only included
2. cargo and passenger only were also considered at payload  $\geq 100$  kg
3. aircraft with multiple mission goals are excluded

While the data collected for eVTOL drones, attached in the Appendix B.1 Data are manipulated using MATLAB codes Appendix C.1 & 2, to obtain the regression line constants.

## UAM

### Roskam Matching

$$A = 0.13193, B = 1.0018$$

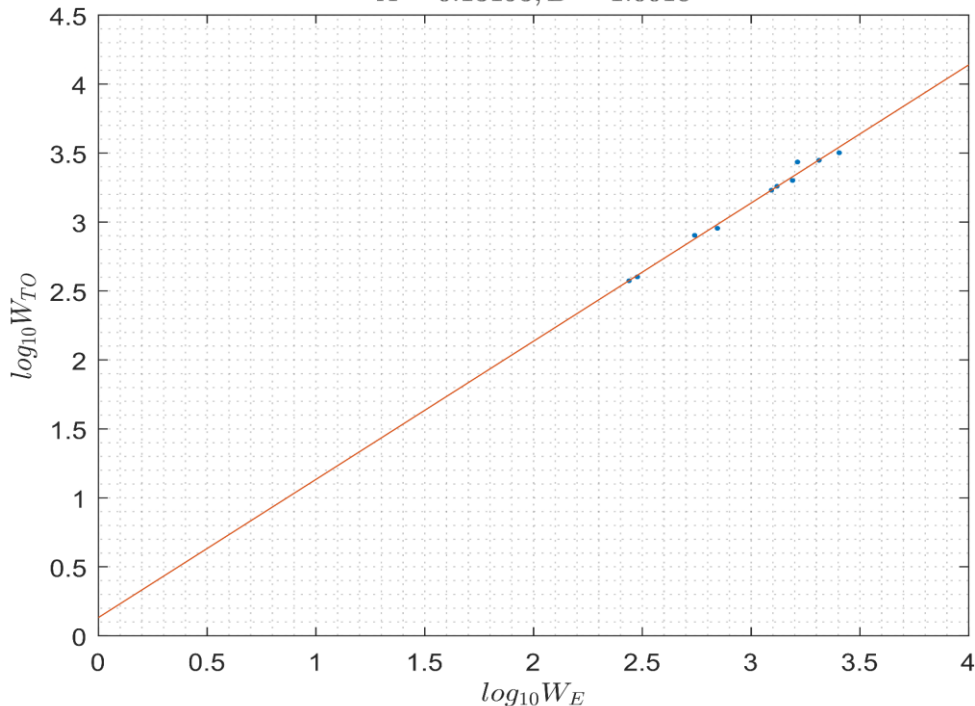
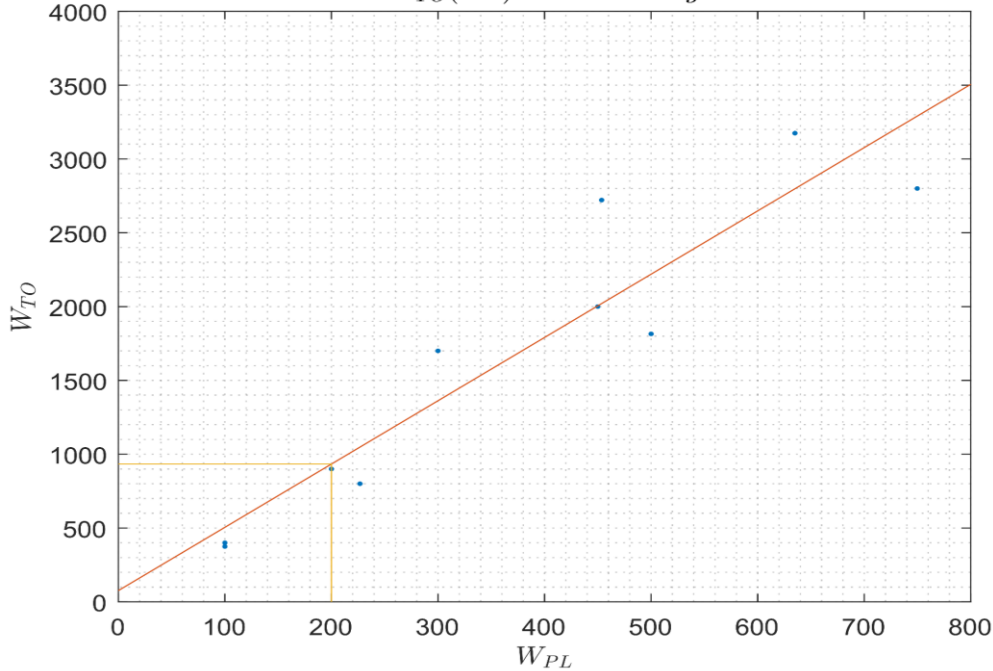


Figure 8: Roskam Matching

$W_{PL} = 200 \text{ kg}$
$W_{TO} = 540 \text{ kg}$
$W_E = 340 \text{ kg}$

### Simple Matching

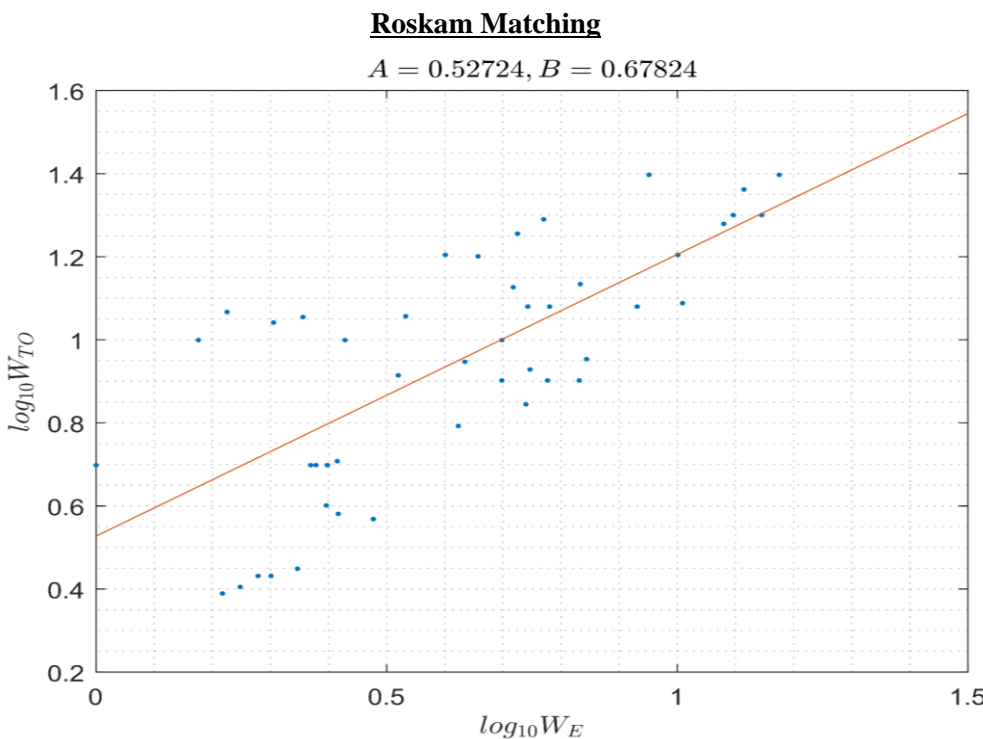
$$W_{TO}(200) = 933.2695 \text{ kg}$$



$W_{PL} = 200 \text{ kg}$
$W_{TO} = 933 \text{ kg}$
$W_E = 733 \text{ kg}$

Figure 9: Simple Matching

## eVTOL “octocopters”



### 2.2.2 Breakdown Method

Another method is by easily stating the required components and summatting what its weight  $W_{TO}$  is expected to be

For an octocopter, taking the average maximum takeoff weight about 3500 grams, and payload about 500 grams, so here we make first iteration about main components

DRONE COAXIAL ALONE		
Components	Number	weight gm
Brushless motor	8	480
Battery	4	1600
Propeller	8	160
ESC	8	320
Frame	1	850
Controller	1	50
Payload	1	500
<b>TOTAL WEIGHT</b>		<b>3960</b>

Based on previous projects from literature review We need to make a second iteration but after selection the motor type, and battery type and quantity.

For an eVTOL, taking the average maximum takeoff weight to be about 6000 grams, and payload 500 grams, so here we make the first iteration about main components. Here are the total components of all the model.

eVTOL		
Components	Number	weight gm
Brushless motor	8	480
Battery	4	1600
Propeller	8	160
ESC	8	360
Frame	1	850
Scorpion SII-4020-420(420)	1	288
Lipo 3000mAh-35/50C	1	480
APC Propeller Thin Electric 14 x 8,5 E	1	50
<b>WING AND TAIL</b>	<b>1</b>	<b>500</b>
<b>FUSELAGE</b>	<b>1</b>	<b>500</b>
<b>PAYOUT</b>	<b>1</b>	<b>500</b>
controller	1	20
<b>TOTAL WEIGHT</b>		<b>5788</b>

By considering the extra components and structures of VTOL systems, the initial take-off weight is determined as 6 kg.

One of the design requirements of the eVTOL is to carry a payload of 0.5 kg weight. As  $W_{TO}$  is about 6 kg., then  $W_E$  can be found as 5.5kg.

$$W_{TO} = W_E + W_{PL}$$

### Conclusion

Estimating the total weight allows the design lift coefficient to be found at the time of cruising, which is the design condition. The design lift coefficient is calculated which will lead the selection of the wing profile.

For eVTOL, it wasn't very necessary to depend on roscams method since we already have a primary design and can easily state the missing components and estimate their weights. The breakdown method is assured to be a lot more accurate to pass with its results

for UAM, Roscams matching results were not very satisfying since the take-off weight was way low compared to other airplanes of the same type, to have clear vision, the results are comparable to a multirotor model Ehang 216 than Ehang VT-30, reference 7 for more collected data

$$\begin{aligned}W_E &= 380 \text{ kg} \\W_{TO} &= 600 \text{ kg} \\W_{PL} &= 220 \text{ kg}\end{aligned}$$



Figure 11:Ehang 216



Figure 12:Ehang VT-30

$$\begin{aligned}W_E &= 700 \text{ kg} \\W_{TO} &= 900 \text{ kg} \\W_{PL} &= 200 \text{ kg}\end{aligned}$$

Figure 13: Matching Plot

### 2.2.3 Dynamic Scaling

The simplest type of dynamic free-flight model is known as the rigid-body model. As implied by the name, a rigid-body model does not attempt to simulate flexible structural properties such as aero elastic bending modes or flutter properties of the full-scale article. However, even these simple models must be scaled according to mandatory relationships in each of the primary units of mass, length, and time to provide flight motions and test results directly applicable to the corresponding full-scale aircraft. Units of model length such as wingspan are, of course, scaled from geometric ratios between the model and full-scale vehicle, units of model mass (weight) are scaled from those of the full-scale vehicle on the basis of a parameter known as the relative density factor (measure of model mass density relative to an atmospheric sample), and model time is scaled on the basis of a parameter known as the Froude number (ratio of inertial to gravitational effects). From these relationships, other physical quantities such as linear velocity and angular velocity can be derived. For most applications, the model and full-scale aircraft are tested in the same gravitational field, and therefore linear accelerations are equal between model and full scale. To conduct meaningful tests using free-flight models, the scaling procedures must be followed during the construction, testing, and data analysis of a dynamic model. Simply scaling geometric dimensional characteristics without regard for other parameters can produce completely misleading results.

Many of the free-flight dynamic model tests conducted by the NACA and NASA in research efforts have involved investigations of rigid models for conditions in which Mach number and compressibility were not major concerns. For these incompressible flow conditions, the required scale factors for dynamic models are given in the following table: Appendix A.5

Linear dimension	Scale Factor ( $n$ )
Relative density ( $m/\rho L^3$ )	1
Froude number ( $V^2/gL$ )	1
Angle of attack	1
Linear acceleration	1
Weight, mass	$n^3/\sigma$
Moment of inertia	$n^5/\sigma$
Linear velocity	$n^{1/2}$
Angular velocity	$n^{-1/2}$
Time	$n^{1/2}$
Reynolds number ( $VL/v$ )	$n^{1.5}vv_0$
Where $\sigma$ is the ratio of air density to that at sea level ( $\rho/\rho_0$ ), and $v$ is the value of kinematic viscosity.	

Applying these relations at given MGTOW for both full “933 kg” and subscale “6 kg”, we get scale factor  $n = 0.18$

Note:  $\sigma = 0.907755$  at  $h = 1000$  m.

#### 2.2.4 Matching plot

Estimation of wing area "a" and Take-off power

One of the first tasks in any new aircraft design is to perform a constraint analysis Using a special graph called a constraint analysis graph. The primary advantage of this

Graph is that it can be used to assess the required wing area and power plant for the design, such that it will meet all performance requirements. Constraint analysis is used to assess the relative significance of performance constraints on the design. This is done by plotting the constraints on a special two-dimensional graph called the design space (see Figure 13). Commonly the two axes represent characteristics such as (y-axis) thrust-to-weight ratio ( $T/W$ ) and (x-axis) wing loading ( $W/S$ ). The graph is then read by noting that any combinations of  $W/S$  and  $T/W$  that are above the constraint curves will result in a design that meets those requirements. The white-colored region in the figure is the domain of acceptable solutions. The shaded region represents unacceptable solutions. For instance, Design A would meet the T-O run and climb requirements, design C would meet none, and design E all but the climb. Design F meets all requirements. The graph allows the designer to see at a glance the combination of  $W/S$  and  $T/W$  that allows the requirements to be met.

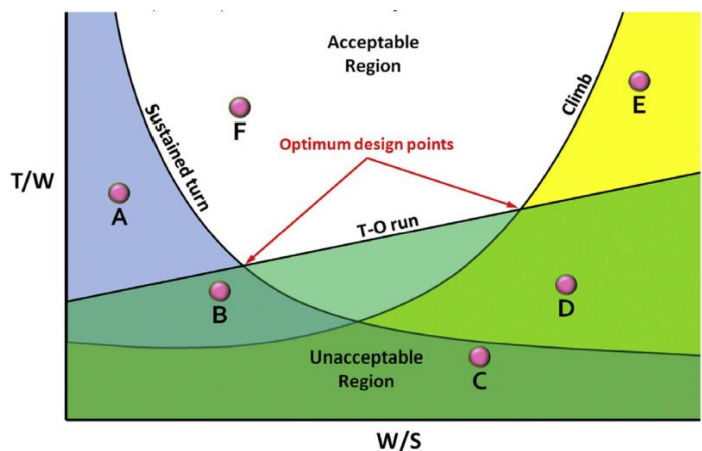


Figure 14: optimum design points

### For – Subscale

Considering the simple but most effective flight regime cruise conditions, the design maximum lift coefficient for the eVTOL is assumed to be 1.5, and Stall velocity 40 kmph  
The wing area of the VTOL could now estimated to be  $0.52 \text{ m}^2$  according to lift equation, this is called sizing to stall

$$W = L = 0.5 \rho_{\infty} V_{\infty}^2 S_{WING} C_L$$

Taking into account Cruise flight velocity, is a mission requirement and it is given as 68 km/h after scalation, explained briefly in reference 3

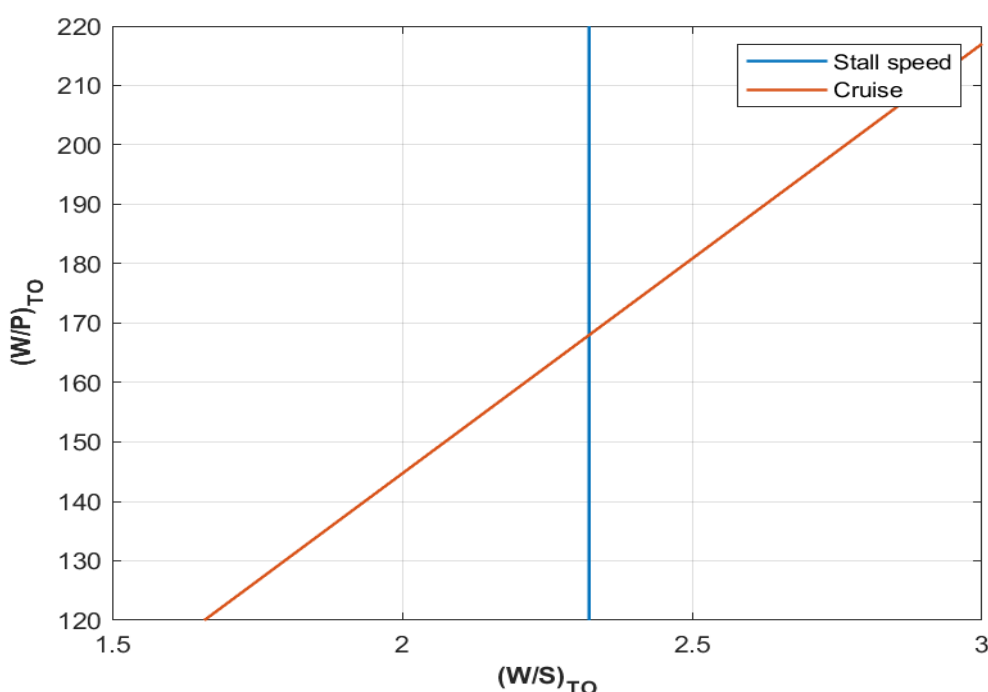


Figure 15: Stall Speed

## 2.3. Motor Selection:

### 2.3.1. Multi rotor

Our goals here to choose the best motor for our mission, and available motors in our zone so we make some searching for selection motor.

These data are from the datasheet of these motors.



Figure 16: Motors

	<b>Motor</b>	<b>Weight gm</b>	<b>Max Thrust gm</b>	<b>Thrust/weight</b>	<b>Max current A</b>	<b>Max power W</b>	<b>Availability</b>
1	Emax CF2822	40	700	17.5	14	145	available
2	Emax A2212 6T 2200 KV	52	1000	19.23	21.5	239	available
3	Turnigy D2836/8	70	1100	15.7	18	336	Not available
4	Bumble Bee MBR-BB-01	80	1150	14.375	19	210	Not available

Here we found the brushless motor Emax A2212 6T is available, and it has max thrust to weight ratio, and it preferred due to low cost.

From data sheet of motor and specifications. We compare the motor rpm and the lift expected for gross weight.

MODEL	KV (rpm/V)	Voltage (V)	Prop	Load Current(A)	Power (W)	Pull (g)	Efficiency (g/W)	Lipo Cell	Weight (g)
A2212	930	11.1	1060	9.8	109	660	6.1	2-4S	52
	1000		1047	15.6	173	885	5.1		
	1400		9050	19.0	210	910	4.3		
	1800		8060	20.8	231	805	3.5		
	2200		6030	21.5	239	732	3.1		
	2450		6030	25.2	280	815	2.9	2-3S	

Figure 17: Data sheet of motor and specifications

Generally speaking the more Kv a motor has, the more RPM and more power. For example, a 2200Kv motor would be faster than a 900Kv motor. If Kv is like horsepower, then turns is the physical attribute of a motor.

Here we can choice 2200kv and 2450 kv due to high power, and high thrust with small propeller than other with fixed voltage 11.1 V. The first choice is 2450 kV, but from another view 2450 kv is not available in our zone so we decided to choose second choice 2200kv.

### 2.3.2. Single motor

Here we using motor database, and program setup called (ecalc) to make iteration, and compare between scorpions' motor kv about what we choice for best motor can give us the response we need.

Manufacturer	Model	GR	Kv	Kt	Rm ( $\Omega$ )	Io (A)	Max P in (W)	Max V	weight (g)
Scorpion	SII-4020-630 (630)	1	630	1.52E-02	0.034	1.54	1500	22.2	288
	SII-4020-540 (540)		540	1.77E-02	0.034	1.22	1850	22.2	288
	SII-4020-420 (420)		420	2.28E-02	0.034	0.91	1500	22.2	288
	SII-4025-520 (520)		520	1.84E-02	0.016	1.4	2000	22.2	353
	SII-4025-440 (440)		440	2.17E-02	0.025	1.1	2000	25.9	353
	SII-4025-330 (330)		330	2.90E-02	0.037	0.74	2000	29.6	353
	SII-4035-450 (450)		450	2.13E-02	0.026	1.71	2960	37	435
	SII-4035-380 (380)		380	2.52E-02	0.025	1.52	2600	44.4	435
	SII-4035-330 (330)		330	2.90E-02	0.031	1.41	2400	40.7	435
	SII-4035-250 (250)		250	3.83E-02	0.037	0.69	2700	44.4	450

We choice SII-4020-420 (420) due to small weight and current initial.

Before starting the experimental study we can showing motor characteristic at full throttle data from ecalc.

By using ecalc we test this motor with our mission, and give us efficacy,

We used lipo 3000 mAh 35/50 C 6 cell (22.2 V) battery, and ESC max 50A and 1485 propeller to achieve our mission.

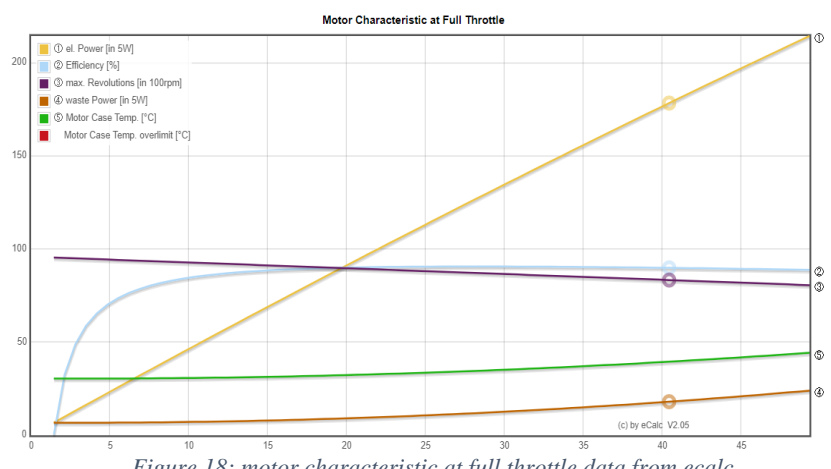
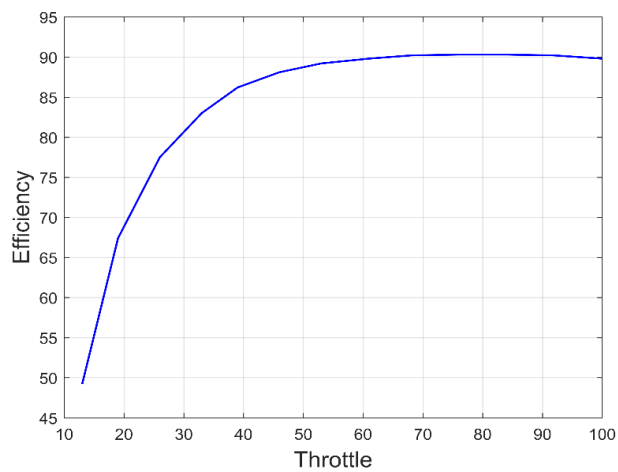
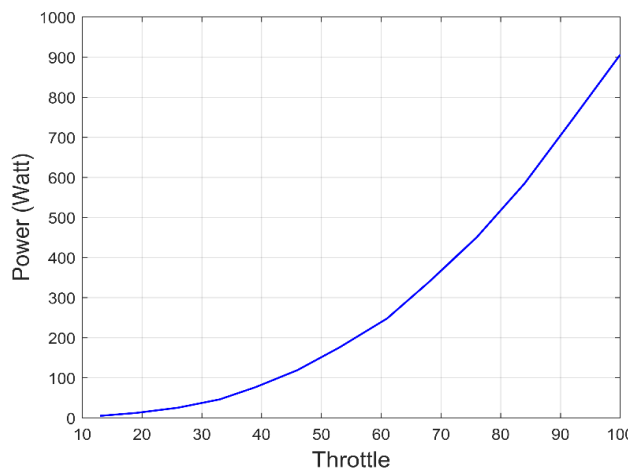
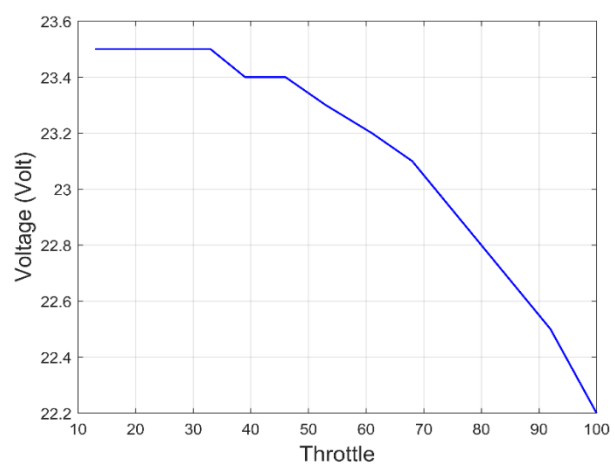
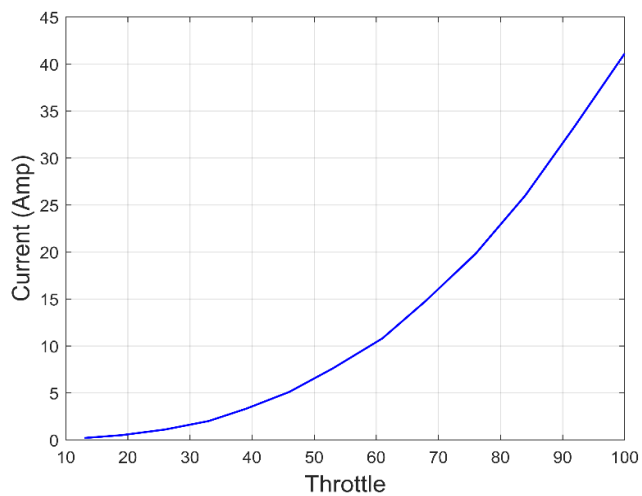


Figure 18: motor characteristic at full throttle data from ecalc



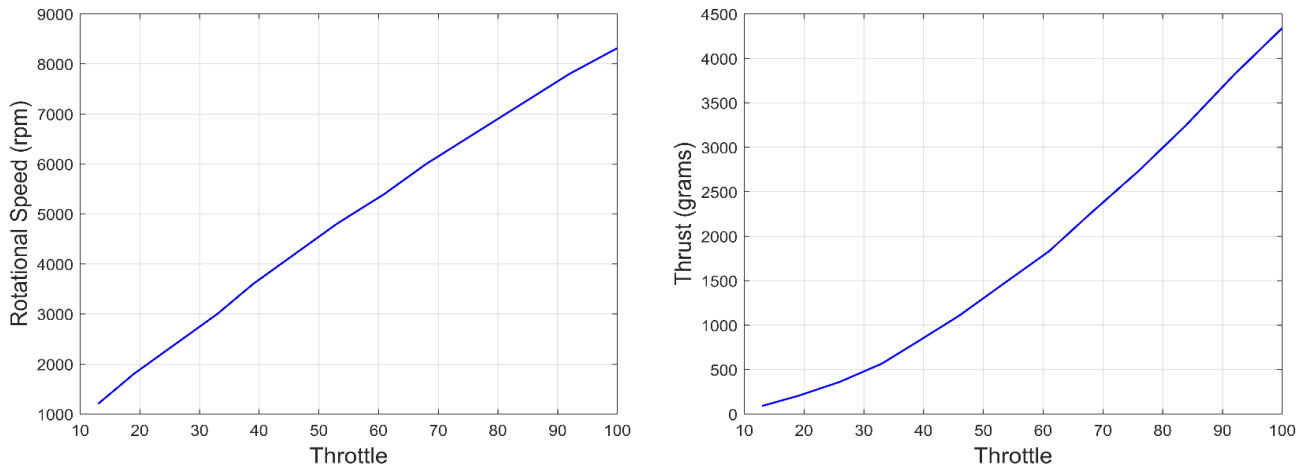


Figure 19: motor characteristic at full throttle

We Can see our result for motor with battery and our constrains like maximum takeoff weight and cruise speed, so we achieve it and by numerical test and it much better. But most of these components doesn't available.

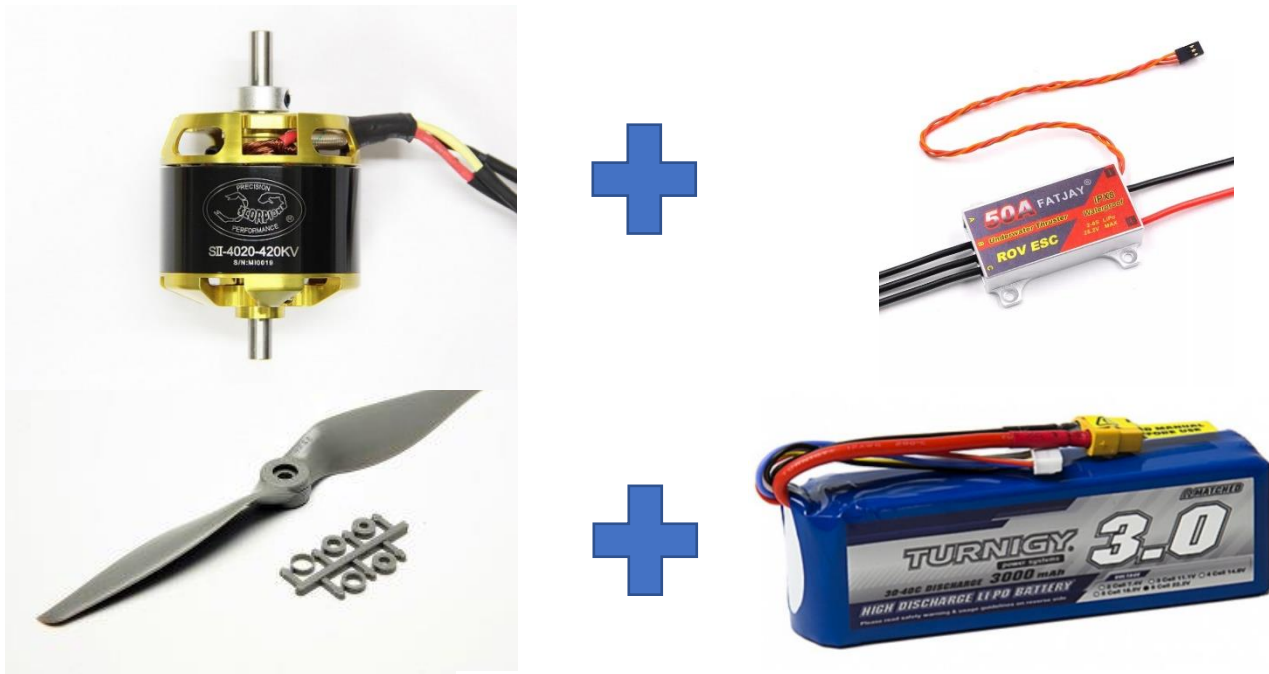


Figure 20:Better components

## 2.4. Blade selection

Let's start to identify propeller: Each brushless motor has a Propeller installed on top of it. Similar to the wheels of a car, it is the most important component of drones. A propeller is necessary for drones to fly. Propellers can have two or three blades and come in a variety of sizes and designs. Every propeller has two important elements. The first is pitch, while the second is diameter. The blades of a propeller are described by  $A * B$

Where A is the diameter (in inch) of the blade. B is the pitch (in inch) of the blade.

Diameter is the length of the propeller measured vertically, or the distance the blade tips make across the circle as the propeller turns.

Pitch represents the twisted present on the propeller's blade. It is the distance that a propeller would move in one revolution if it were moving through a soft solid, like a screw in wood or we can say it is the distance, the propeller will be pulled forward after one full rotation. If the propeller's pitch is 4.5 inch its means after one rotation propeller will move forward 4.5 inches.

Pitch provides an effective area whereas diameter provides an area. The propeller will produce more thrust and be able to lift more weight if we use it with a greater pitch for the same diameter, but it will also need more electricity. More speed and maneuverability are offered by a high RPM, but less weight can be lifted. With a high pitch propeller and a motor that manages fewer revolutions but greater torque, the drone can be flown steadily while carrying large loads. We require a 1:2 ratio between weight and thrust in order to fly a quadcopter.

$\text{power (watts)} = k_p * D^4 * P * \text{RPM}^3$	$K_p$	for midsized propellers $K_p$ value is 1.2
	$D$	Diameter of propellers
	$P$	Pitch

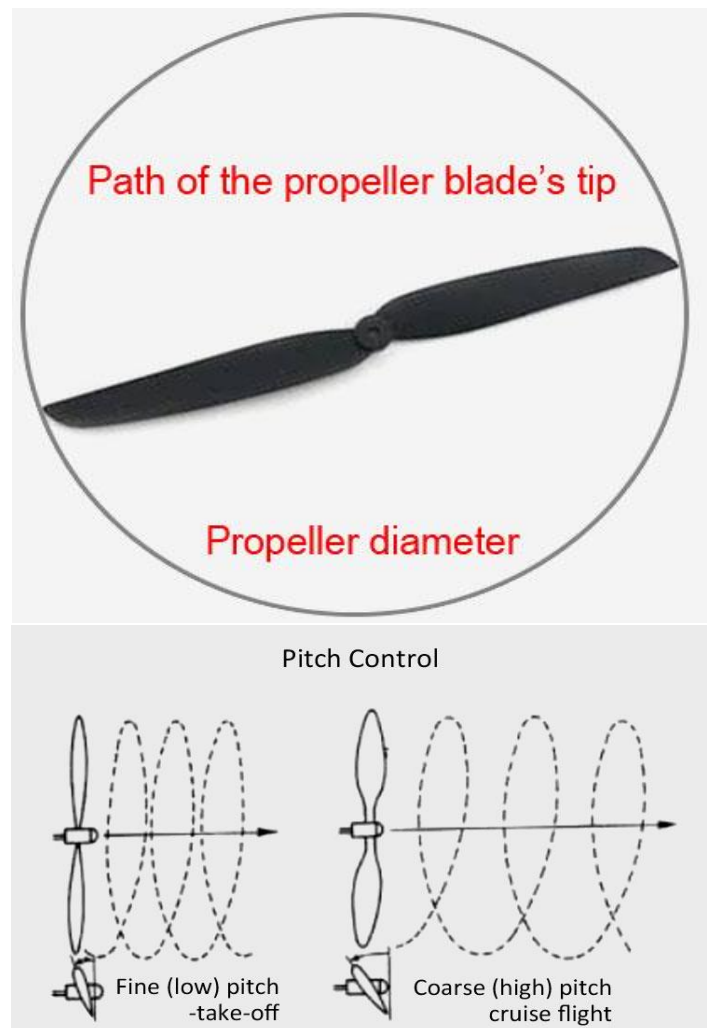


Figure 21: Blade selection

Drone flight is significantly influenced by the position of the propellers. Propellers may appear to be mirror pictures of each other, much as our hands are mirror images of one another, but they are not the same. For this reason, we need to be aware of their shape.

### 2.4.1 Two Blade Propeller

2 blade drone propellers have two blades, as the name says. When all other factors are equal, the mechanical efficiency of a drone's propellers increases as the number of blades reduces, which is why two-blade propellers are more efficient than three-blade propellers. Thrust

propels a drone into the air. Thrust allows the drone to overcome drag and its own weight and eventually climb into the sky. While a two-blade prop is more economical, it produces less thrust, making it unsuitable for large drones with powerful engines.

2 blade propellers will perform particularly well on drones where a quick motor reaction is necessary but the complete thrust is not as important. Because ultralight racing drones are so light, the amount of push required is small, and having two-blade propellers will result in higher reaction and speed.

#### Advantages and Disadvantages of Two Blade Propeller

Advantages	Disadvantages
It has higher efficiency as compared to three blades.	Two blades propeller makes more noise.
It provides faster speed as compared to three blades.	There are more affected by wind.
It is more durable than a three-blade prop if your copter is going to be crash.	Two blades propeller provides less stability as compared to three blades propeller.
Making a foldable design for drones with two blades props is much easier.	

#### 2.4.2 Three Blade Propeller

Three blades propeller contains three blades that work together to provide increased thrust. Thrust is important for raising up your drone, and three blades propeller can handle greater weight because of more thrust. Manufacturers frequently employ three-blade props on bigger drones since they have more powerful motors and require a lot of force to achieve lift. Due to the tremendous thrust generated by 3 blade props, they are also more stable, which is why 3 blade prop drones feel more gripping when doing fast maneuvers. Another feature of three blades propeller is that they can fly smoothly even if they aren't completely balanced. This is in contrast to two-blade props, which must be completely balanced and in excellent condition in order to fly smoothly; otherwise, they will begin to produce unpleasant vibrations when spinning

### Advantages and Disadvantages of Three Blades Propeller

Advantages	Disadvantages
Three blades propeller provides the best balance of efficiency, thrust, and grip.	It is not efficient as compared to two blades propeller.
Three blades propeller provides a very stable flight and can do quick maneuvers smoothly.	It is not fast.
It creates very little noise as compared to two blades propeller.	Three blades propeller is not portable.
It is less affected by wind and blade tips have better tracking with 3 blades.	These are more susceptible to damage in the crush.

A propeller's number of blades is not always a good thing. A propeller with more blades vibrates less and is hence quieter. Also, it generates higher thrust at a given RPM. As opposed to a propeller with fewer blades, it will also be heavier and, more crucially, less effective. Due to its effectiveness and portability, 2-blade propellers are typically found on drones. They are lightweight, portable, and surprisingly impact-resistant thanks to their elasticity. They are regarded as the preferred choice for drone pilots because of their inexpensive cost as well.

So we decided to choice two blade propeller.

We discovered that each motor requires a specific set of propellers in order to operate at its best.

Motor	Battery	Propeller	Maximum Thrust
Emax A2212 6T 2200 KV	Lipo battery (11.1v -5200 mAH-35C)	5 x 4	395
Emax A2212 6T 2200 KV	Lipo battery (11.1v -5200 mAH-35C)	6035	475
Emax A2212 6T 2200 KV	Lipo battery (11.1v -5200 mAH-35C)	8045	650
Emax A2212 6T 2200 KV	Lipo battery (11.1v -5200 mAH-35C)	9045	750
Emax A2212 6T 2200 KV	Lipo battery (11.1v -5200 mAH-35C)	1045	1200

Tests shows that (1045) propeller gives us higher thrust than other propellers and it is availability, so it our choice.

## 2.5. Battery selection

There is a lot of type of batters we can use for brushless motor, but we can consider talk about two type that most common on our field of eVTOL.

### 2.5.1 Lithium-ion Battery

The chemical electrolyte between the positive and negative electrodes of lithium-ion and lithium-polymer batteries is the main difference between the two types of batteries.

Lithium-ion and lithium-polymer batteries each have advantages and disadvantages. Lithium-ion batteries often have higher power densities and lower prices than lithium-polymer batteries. The efficiency of lithium-ion batteries is astounding. Li-ion in a flexible battery case.

Lithium-ion batteries are highly unstable, ageing, and intrinsically unstable. Since Li-ion batteries have gained popularity in.



Figure 22:Lithium-ion Battery

### 2.5.2 Lithium-Polymer battery:

Li-Po batteries, on the other hand, are typically robust and flexible. Particularly in terms of their body size and shape.

Additionally, they have a very low profile, are lightweight, and are less likely to leak electrolyte. But Li-Po batteries aren't perfect because they cost a lot more to make and have a lower energy density and longevity than lithium-ion batteries.



Figure 23:Lithium-Polymer battery

So we choice the lithium –polymer due to safety and lightweight to save sum weight.

The brushless motor Emax A2212 6T 2200 KV can use battery 2-3 cell so we compared with thrust and efficiency. And the capacity to response our mission's requirements such endurance. And maximum current for all eight motors.

To calculate endurance we do some calculations as a function of capacity of battery in (mAh), the higher (mAh) then the longer battery will stay.

- ↗ Maximum current of motor is 21.5, so for eight motors →  $21.5 \times 8 = 172 \text{ Amp}$
- ↗ In order to electronics take (2 Amp) as calculated by adding this to previous number

$$\rightarrow 172 + 2 = 174 \text{ Amp}$$

- ↗ For endurance 3 minute the capacity will be →  $174000 * \frac{3}{60} = 8700 \text{ mAh}$
- ↗ For availability we have battery 2 cell and 3 cell 5200 mAh 35c that produce →  $\text{max current} = 5200 * 35 = 182000 \text{ m amp}$ , that bigger than 174000 m amp, that required from eight motor, but we need two or more to achieve 3 minutes at least.

#### For the voltage

we tested the brushless motor Emax A2212 6T 2200KV with propeller 1045 to compare between there, and choice the best choice

Throttle %	2cell (7.4) lipo battery 5200 mAh 35 c weight (260)	3cell (11.1) lipo battery 5200 mAh 35 c Weight (411)
0	0	0
15	10	30
20	50	90
25	70	140
30	120	230
35	170	320
40	230	440
45	290	530
50	360	630
55	430	710
60	500	790

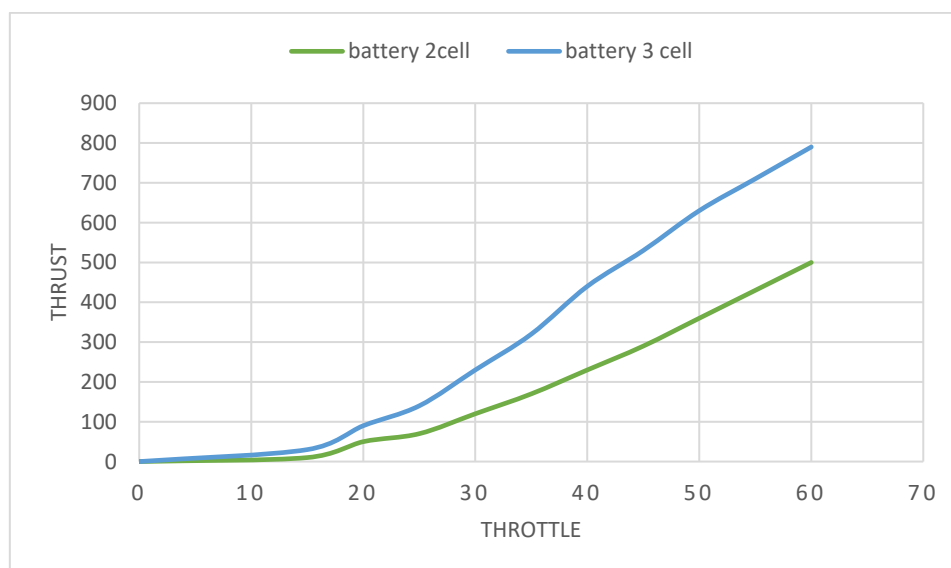


Figure 24: 2 Cell VS 3 Cell Battery



Figure 25: 3 Cell Battery

We can see from tests the battery 3cell give us more thrust, so we choice 3cell (11.1) lipo battery 5200 mAh 35 c.

## 2.6 Sizing frame

The frame size of a drone is the distance from opposite corner motors. The frame is used for mounting and holding all other items and plane. There are many different types and sizes of multi-rotor frames. Due to our aerodynamic we have to estimate the range of structure frame with plane, and the propeller diameter and with the distance between motors and the distance between propeller and the wing to will not affect to aerodynamics and safety. Also, literature review on previous project about eVTOL helped us to estimate the range of distance. The frame is quadcopter X8 and the distance between motors is 650 mm.

## 2.7 Material selection

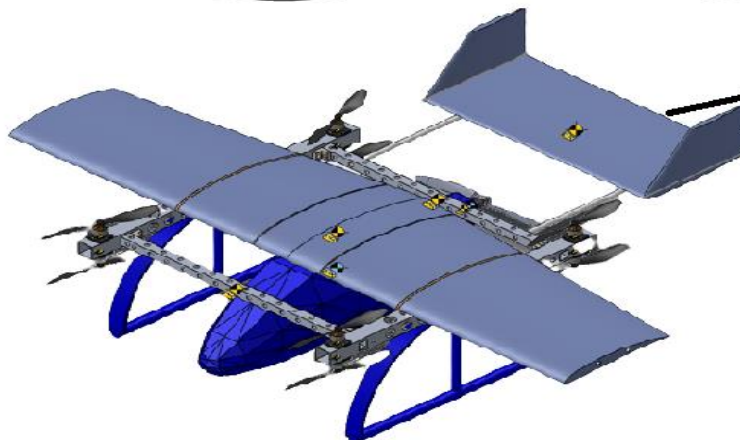
By searching generally in eVTOL and different multi-rotor we have reached to several types of materials used in this field, and these are our results that we reached:

Material	Density ( $kg/m^3$ )	$F_{yield}$ (MPa)	$F_{ult}$ (MPa)	$\tau_u$ (MPa)	G (MPa)	E (MPa)
Blue foam	35					
White foam	28					
Carbon fiber	1800		4000			227500
Aluminum bars	2700	145	241	165		68300
Acrylic	1180		72	110	3170	2960
Plywood	780		31			60
MDF	600		24			28
PVC	1450		41		2070	2410

For multi-rotor we have tried some of these materials and we found that the simplest, available and minimum cost material is aluminum, which is high in density than the others but with some machinery we can reduce the total weight of the airframe. And for fixed wing we used blue foam and white foam due to minimum mass density and available and less cost than carbon fiber

# **Chapter Three:**

# **Aerodynamics**



### 3.1. Introduction:

The transition aerodynamics will compromise the cruise wing sizing; therefore, it is important to be able to optimize this. To ensure the feasibility of the concept, cruise flight must be high-performing with minimum drag, so as to increase the range of the vehicle and provide sufficient electrical autonomy. This poses a significant design challenge, for which optimization algorithms can be employed to define wing and fuselage shapes capable of maximizing performance.

### 3.2. Fuselage design

Using Standard Man approach

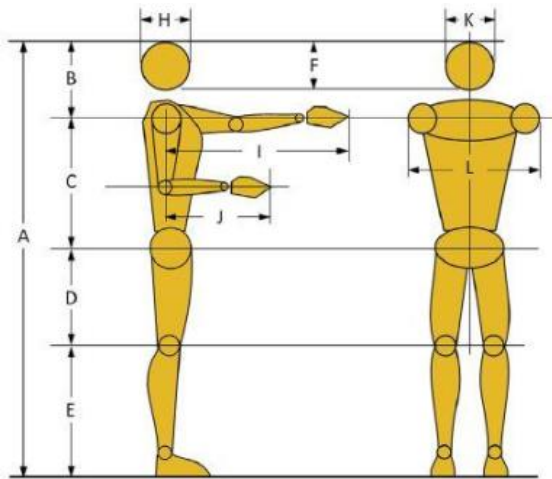


Figure 26: Standard Man standing approach

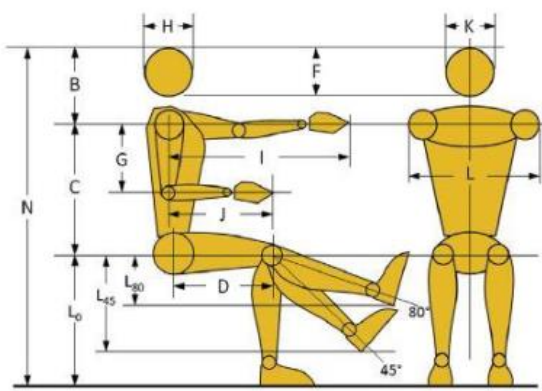


Figure 27: Standard Man sitting approach

For two series seats, we find the following data:

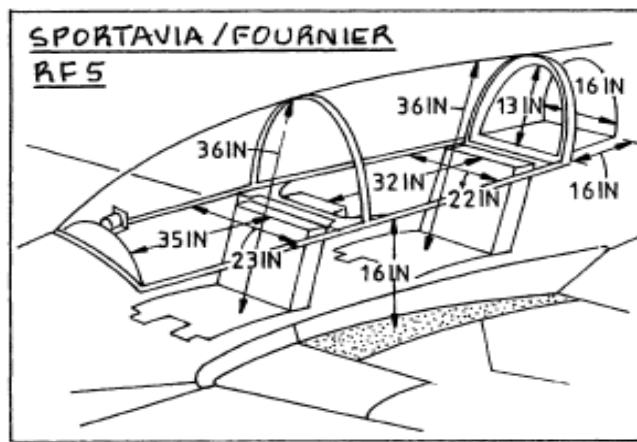


Figure 28: Cabin and Baggage Hold dimension

From “Part III Airplane Design”, and EV review we designed the next fuselage cross sections to meet a mission requirement

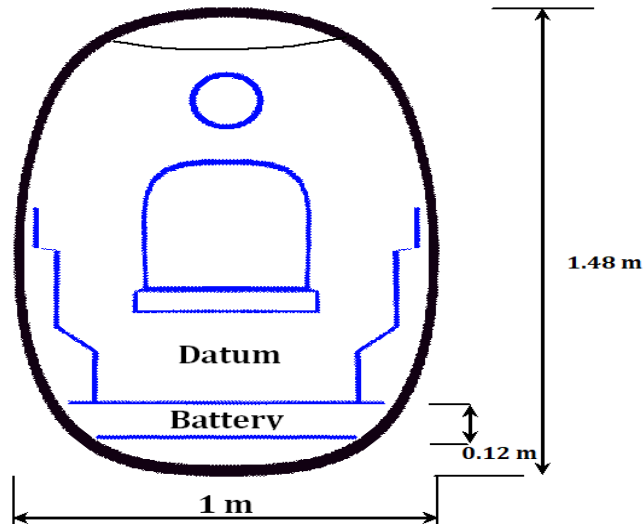


Figure 29: fuselage cross section

The front and rear cones were supposed to match that in the NZ Wisk (Kitty Hawk) Cora illustrated in its FAA design application. appendix{xx}



Figure 30: Fuselage Side section: Front Cone

The deflections happened during the design process then detected later

Designed by ramp scaling to the thrust engine diameter

The top cross section is designed to be in streamlined shape like an airfoil, while the interior boundaries are kept as mentioned in figure 27 or higher.

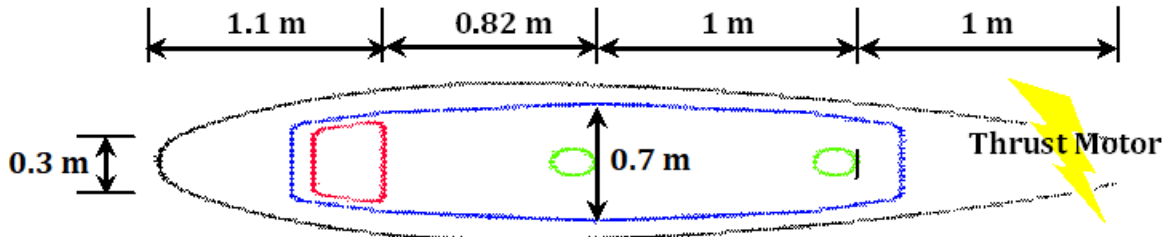


Figure 31: fuselage top section

Note: The interior details/regions were heavily based on EV references

XFLR5 is a software initially designed to parametrically model and create body conformal. However, it has been continuously updated and it was successfully employed in this work to parametrize both the wing and fuselage geometry and to create a near field wing mesh, suitable for adjoint studies

### 3.2.1 Results:

1.  $l_f = 3.92 \text{ m}$
2.  $d_{eff} = 1.22 \text{ m}$
3.  $\theta_{fc} = 26^\circ$
4. width after scaling  $D = 18 \text{ cm}$

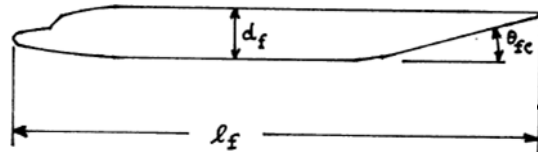


Figure 32: Fuselage Parameters

### 3.3. Wing design

The overall structural configuration is to be a cantilever high wing made of foam and spars



Figure 33: NACA 0009 Airfoil

### 3.3.1 Span and chord

The total lift area to be is determined to be  $0.52 \text{ m}^2$

For a mission commitment of having a short wingspan, Aspect Ratio is assumed low  $\text{AR} = 4.5$   
considering the aircraft fall under the homebuilt category

Table 6.1 Homebuilt Airplanes: Wing Geometric Data

Type	Dihedral Angle, $\Gamma_w$	Incidence Angle, $i_w$	Aspect Ratio, $A$	Sweep Angle, $\Lambda_{c/4}$	Taper Ratio, $\lambda_w$	Max. Speed, $V_{max}$	Wing Type
		root/tip deg.		deg.		kts	
PIK-21	0	0	3.8	0	1.0	NA	ctl/low
Durable							
RD-03C	6.5	3/0	7.0	0	0.51	182	ctl/mid
PIEL							
CP-750	5.7	4.2	5.9	0	0.55	183	ctl/low
CP-90	5.7	3	5.4	0	0.44	171	ctl/low
POTTIER							
P-50R	4.4	NA	5.1	2	0.54	167	ctl/low
P-70S	0	2	4.8	0	1.0	129	ctl/mid
O-O							
Aerosport	2.5	NA	5.7	0	1.0	76	ctl/low
Aerocar							
Micro-Imp	0	4	4.7	0	1.0	260	ctl/high
Coats							
SA-III	4	1.5	5.6	0	1.0	165	ctl/low
Sequoia							
300	3	3.5/1.5	6.9	0	0.55	243	ctl/low
Ord-Hume							
OH-4B	3	3	5	5.0	1.0	95	brcd/parasol
Procter							
Petrel	5	0	6.6	0	1.0	113	ctl/low
Bede BD-8	0	3	3.9	0	1.0	238	ctl/low

ctl = cantilever    brcd = braced (strutted)

Figure 34: Wing geometric homebuilt

$$\text{Span } b = \sqrt{S_{tot} \times AR} = \sqrt{0.52 \times 4.5} = 1.52 \text{ m}$$

$$c = \frac{b}{AR} = \frac{1.52}{4.5} = 0.338 \text{ m}$$

### 3.3.2 Airfoil Selection

From equation of lift, taking  $V_{cruise} = 18 \text{ m/s}$  &  $S_{wing} = 0.52 \text{ m}^2$  we can calculate  $C_{L CRUISE}$

$$W = L = 0.5 \rho_\infty V_\infty^2 S_{WING} C_L$$

$$C_{L CRUISE} = 0.57$$

$$C_{2D} = \frac{C_{L 3D}}{1 - \frac{C_L}{\pi AR}} = 0.59$$

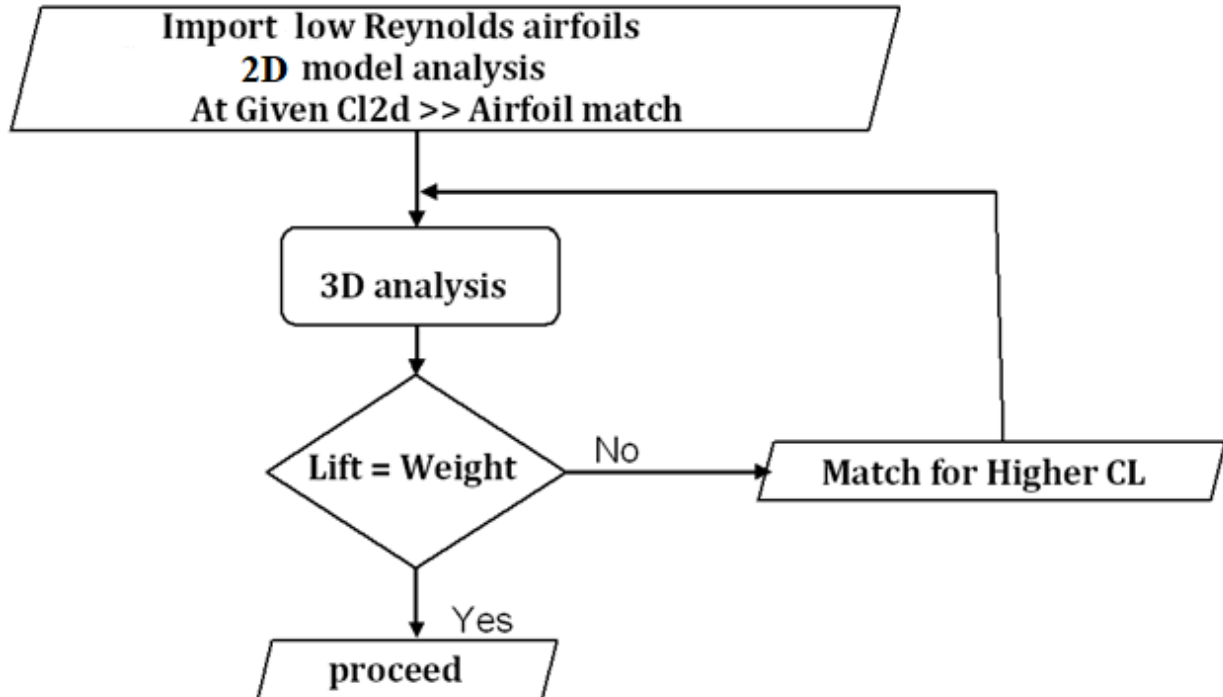


Figure 35: Airfoil Selection Flow chart

Aerodynamic analysis is done in XFLR5. It is a software initially designed to parametrically model and create body conformal. However, it has been continuously updated and it was successfully employed in this work to parametrize both the wing and fuselage geometry and to create a near field wing mesh, suitable for adjoint studies

SG6043 is to be selected. Incidence and twist angles of  $0^\circ$  are sufficient for achieving both, the longitudinal stability and the required cruise lift-coefficient  $CL_{cr}$ , for more details proceed to section "Longitudinal stability".

A dihedral angle is supposed to not be necessary when it's a high wing

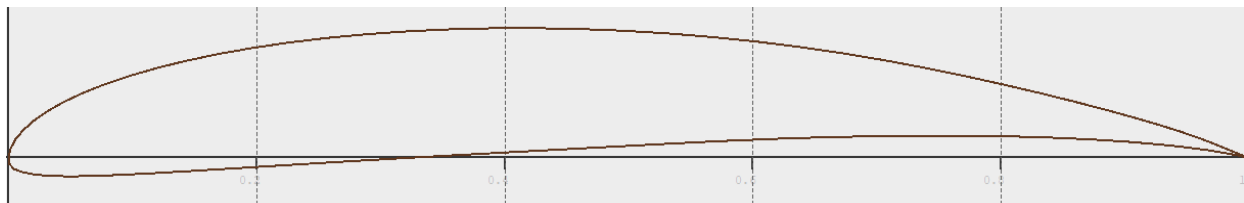


Figure 36: Airfoil SG6043

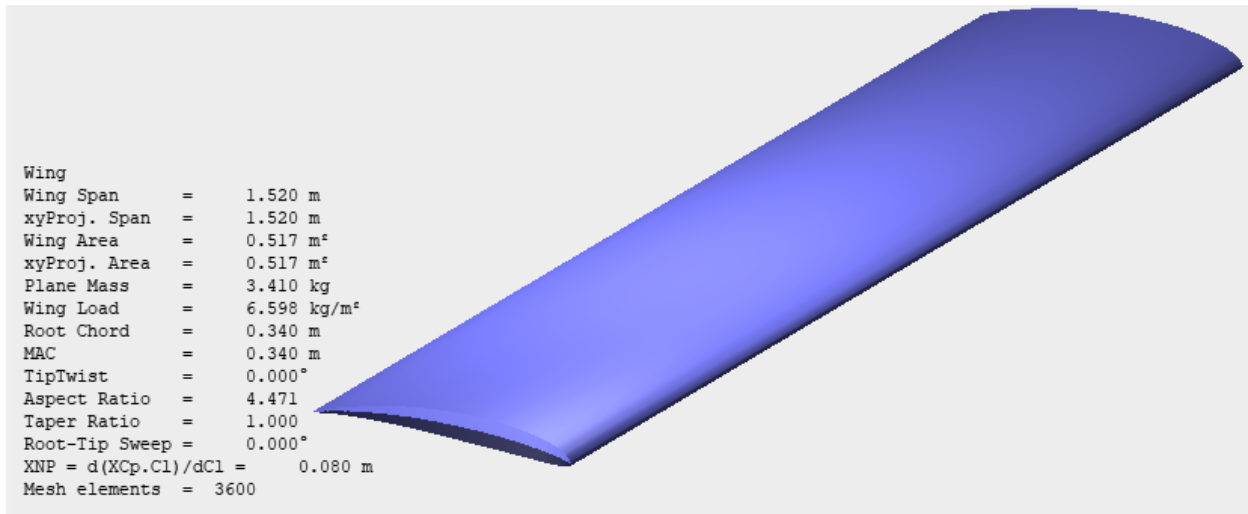


Figure 37: wing model in 3d

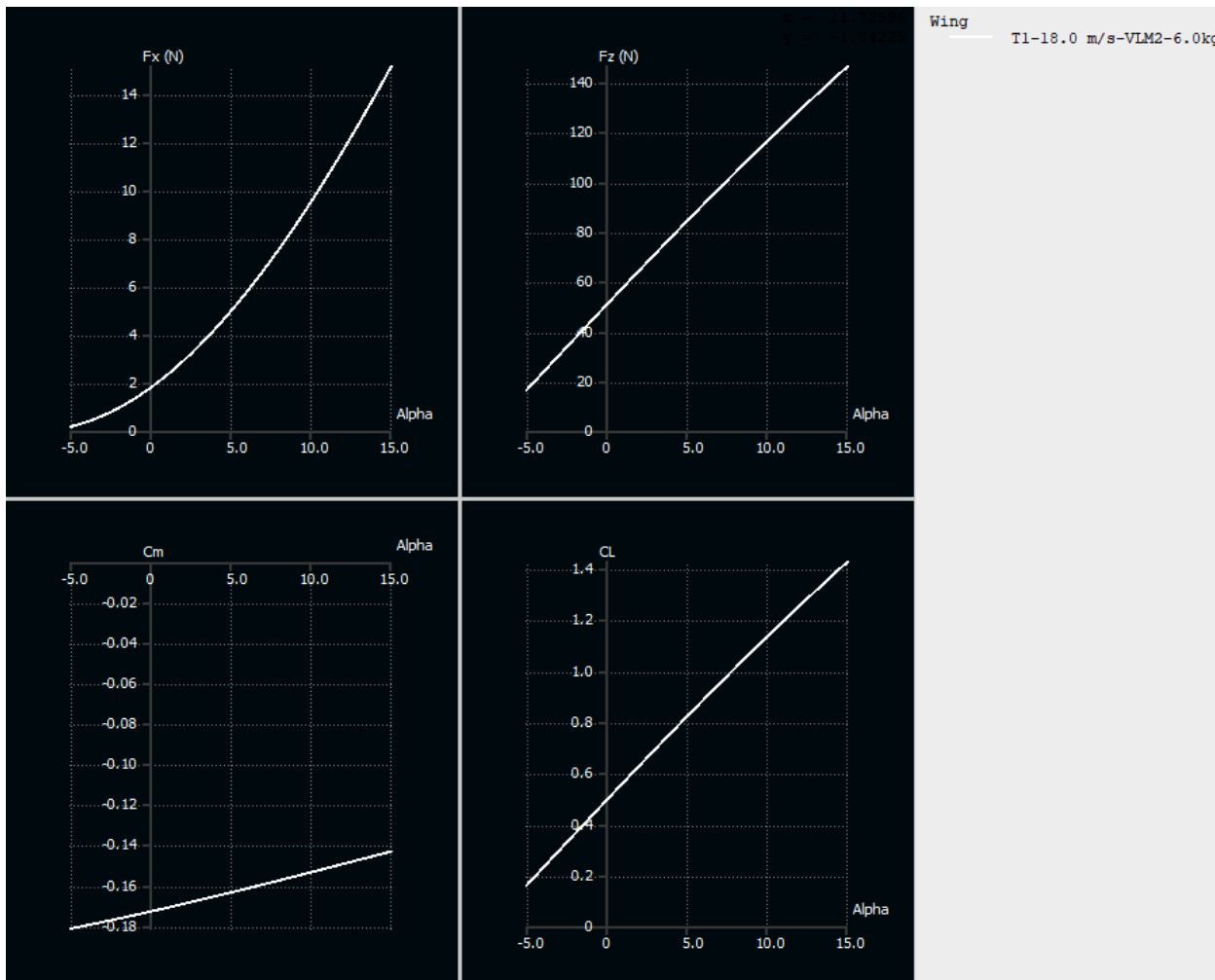


Figure 38: Aerodynamic theoretical analysis of wing

### 3.3.3 Tail Design

Horizontal tail (HT) is needed to stabilize the airplane in longitudinal, for a conventional airplane an aft horizontal tail is used. Longitudinal stability is the tendency of the aircraft to counter induced moments about the longitudinal axis, whether caused by wind, the wing, or the fuselage. For simplicity, the fuselage contribution is assumed to be replaced with a mounted area section. The tail span was assumed to equal 0.6, the assumption is made beside the process of frame sizing to fit between the two directional bars. From the table below, it's assumed that  $V_H = 0.62$

Table 3.1a) Homebuilt Airplanes: Horizontal Tail Volume and Elevator Data

Type	Wing Area S ft <sup>2</sup>	Wing mac c	Wing Airfoil root/tip	Hor. Tail Area S <sub>h</sub> ft <sup>2</sup>	S <sub>e</sub> /S <sub>h</sub>	x <sub>h</sub>	$\bar{V}_h$	Elevator Chord root/tip fr.c <sub>h</sub>
PIK-21	76.4	4.50	64212	10.4	0.45	10.1	0.30	0.45
Durable								
RD-03C	119	4.30	23018/23012	22.2	0.33	11.3	0.49	.47/.32
PIEL								
CP-750	118	3.82	23012	23.5	0.51	12.6	0.66	.55/.47
CP-90	104	3.81	NA	22.3	0.50	11.8	0.66	.56/.38
POTTIER								
P-50R	80.7	3.74	23015/23012	13.4	0.52	10.6	0.47	.50/.55
P-70S	77.5	4.10	4415	14.5	0.60	9.68	0.44	0.60
O-O								
Aerosport	80.7	3.77	23012	15.4	0.48	10.6	0.54	0.48
Aerocar								
Micro-Imp	81.0	3.00	GA(Pc)-1	11.7	0.25	6.27	0.30	.28/.33
Coats								
SA-III	112	4.50	63415	16.5	0.46	10.9	0.36	0.46
Sequoia								
300	130	4.37	64,A215/64A210	25.5	0.43	13.2	0.59	0.43
Ord-Hume								
OH-4B	125	5.25	RAF48	25.4	0.49	11.1	0.43	0.49
Procter								
Petrel	135	4.54	3415	26.0	0.52	12.2	0.52	0.52
Bede BD-8	96.7	5.0	63,015	19.4	0.14	7.64	0.31	0.17

\* Unless otherwise indicated.

Figure 39: Tail and wing airfoil geometric homebuilt A

Tail moment arm is assumed to equal 65 cm during the conceptual designing

$$\frac{S_{tail}}{S_{wing}} = \frac{c_{wing} V_H}{L_{HT\ arm}} = \frac{0.338 * 0.62}{0.65} = 0.322$$

$$c_{tail} = \frac{0.322 * 0.52}{0.6} = 28\ cm$$

**Airfoil: NACA 0009**

The incidence angle to obtain stability is found to be  $i_h = -4^\circ$

The next analysis are obtained

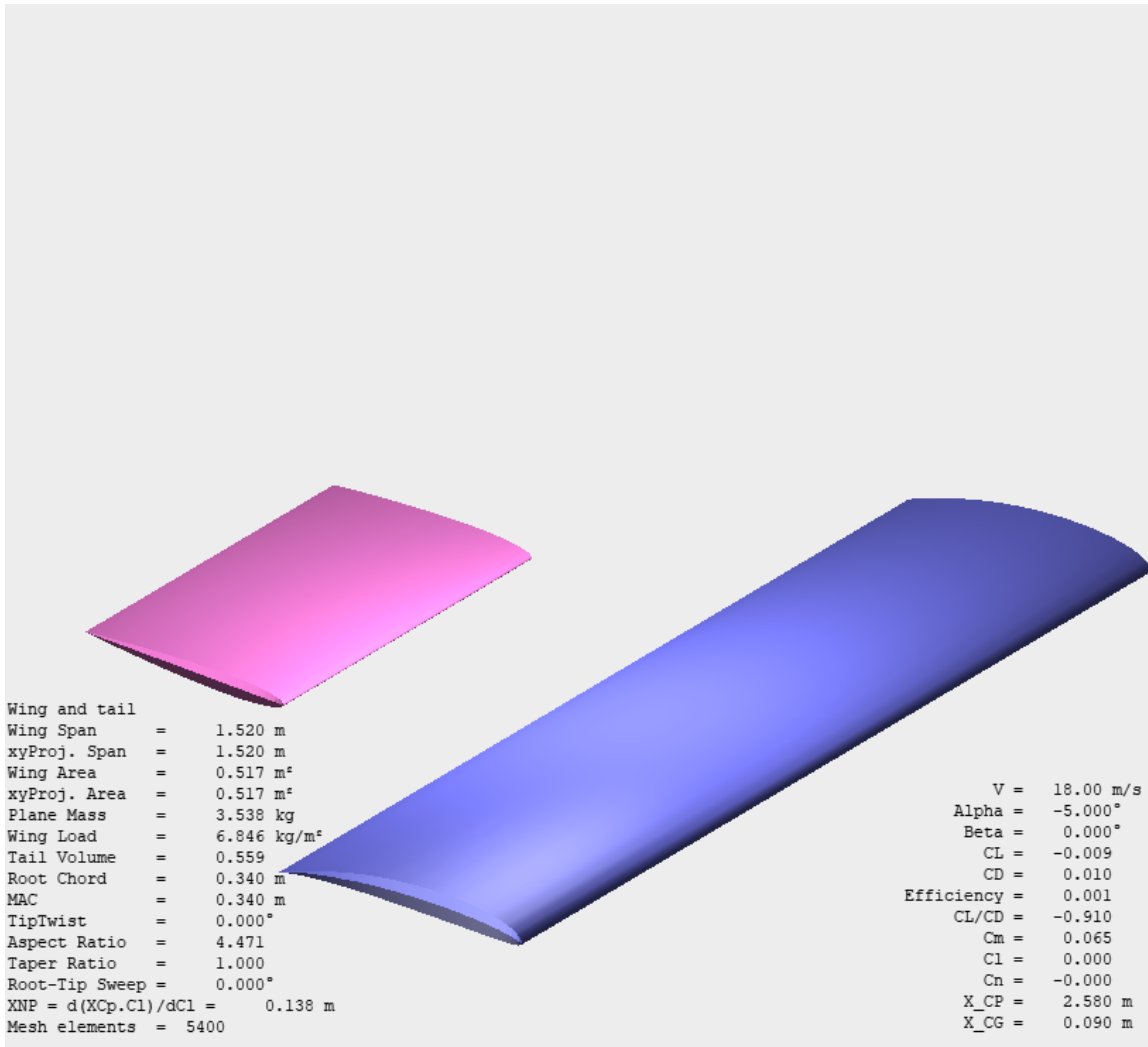


Figure 40: Wing and tail 3D model

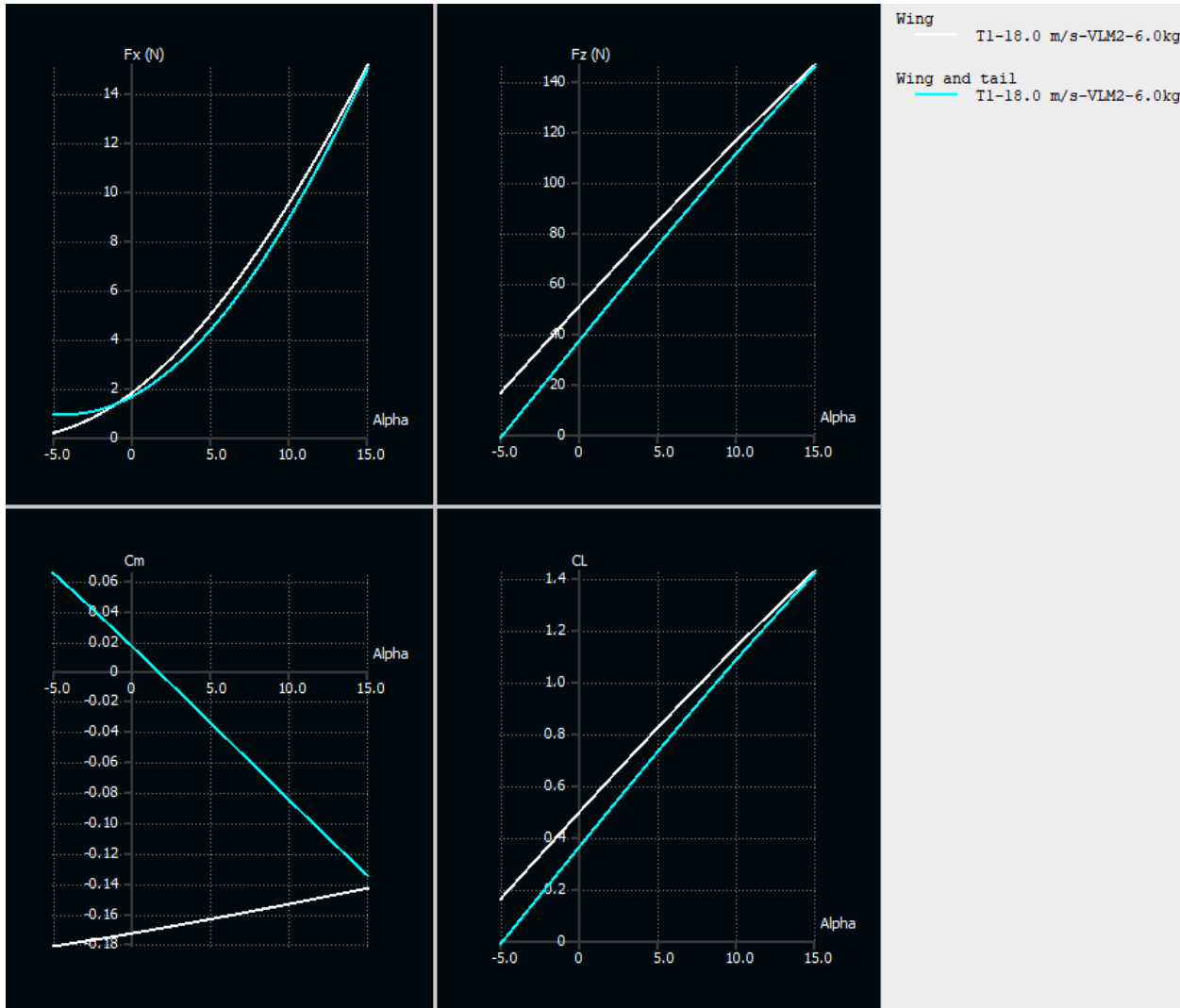


Figure 41: Wing and tail aerodynamic theoretical analysis

### 3.3.4 Modified wing

The wing is divided into two sections, the mid-section of the wing would be a constant chord mounted on top of the fuselage have a width  $D = 18 \text{ cm}$  and the outboard sections are tapered. This added an additional constraint to maximizing aerodynamic efficiency.

$$AR = 4.5$$

$$b = 1.52 \text{ m}$$

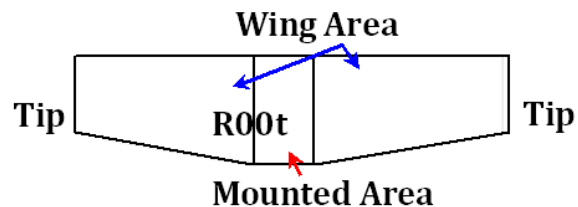


Figure 42: modified wing top view

Assume  $c_r = 38 \text{ cm}$

$$S_{tot} = 18 c_r + (b - 18)(c_t + 0.5 \times (c_r - c_t))$$

$$5200 = 684 + 134(c_t + 0.5 \times (38 - c_t))$$

$$c_t = 29 \text{ cm}$$

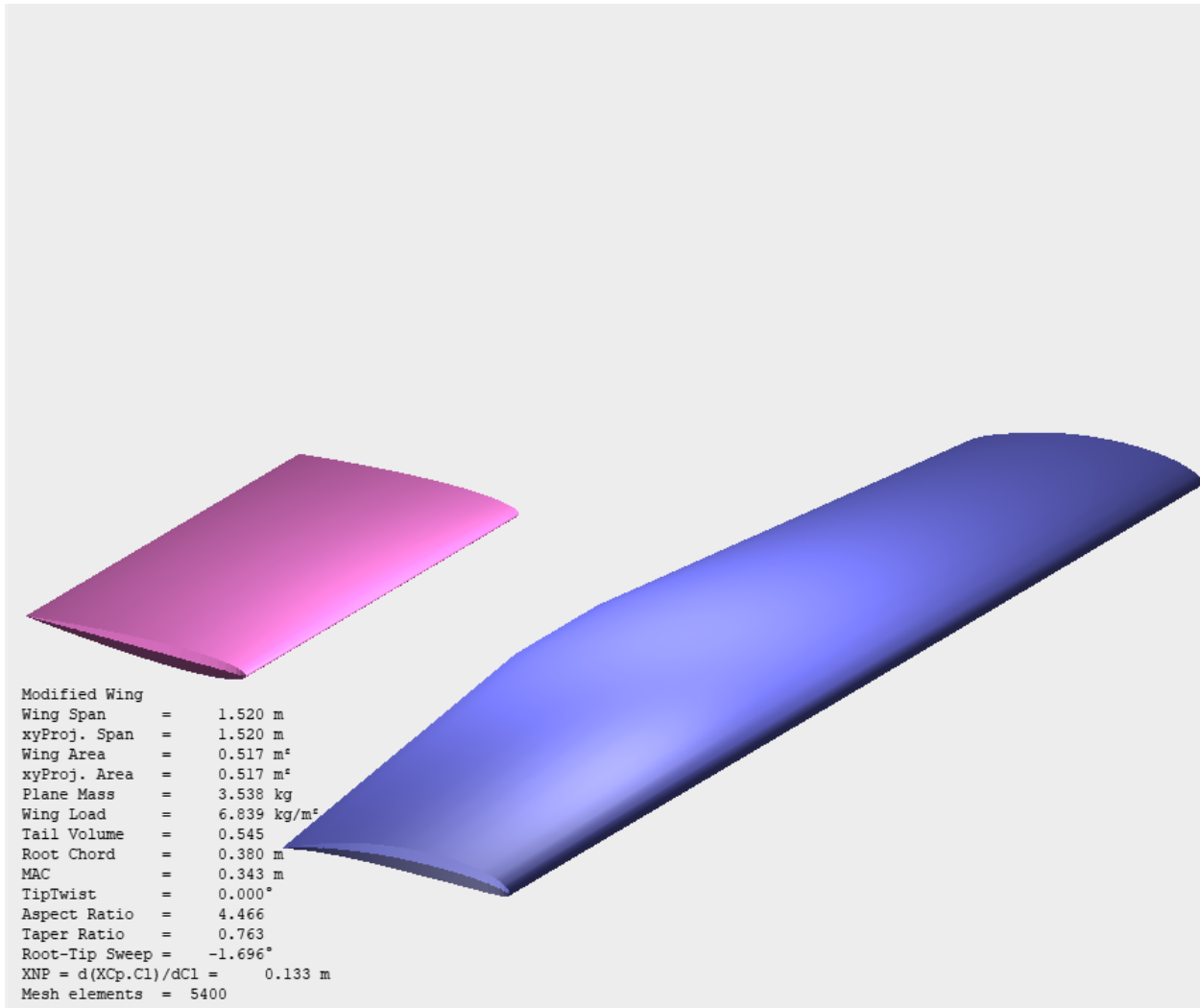


Figure 43: Modified wing in 3D

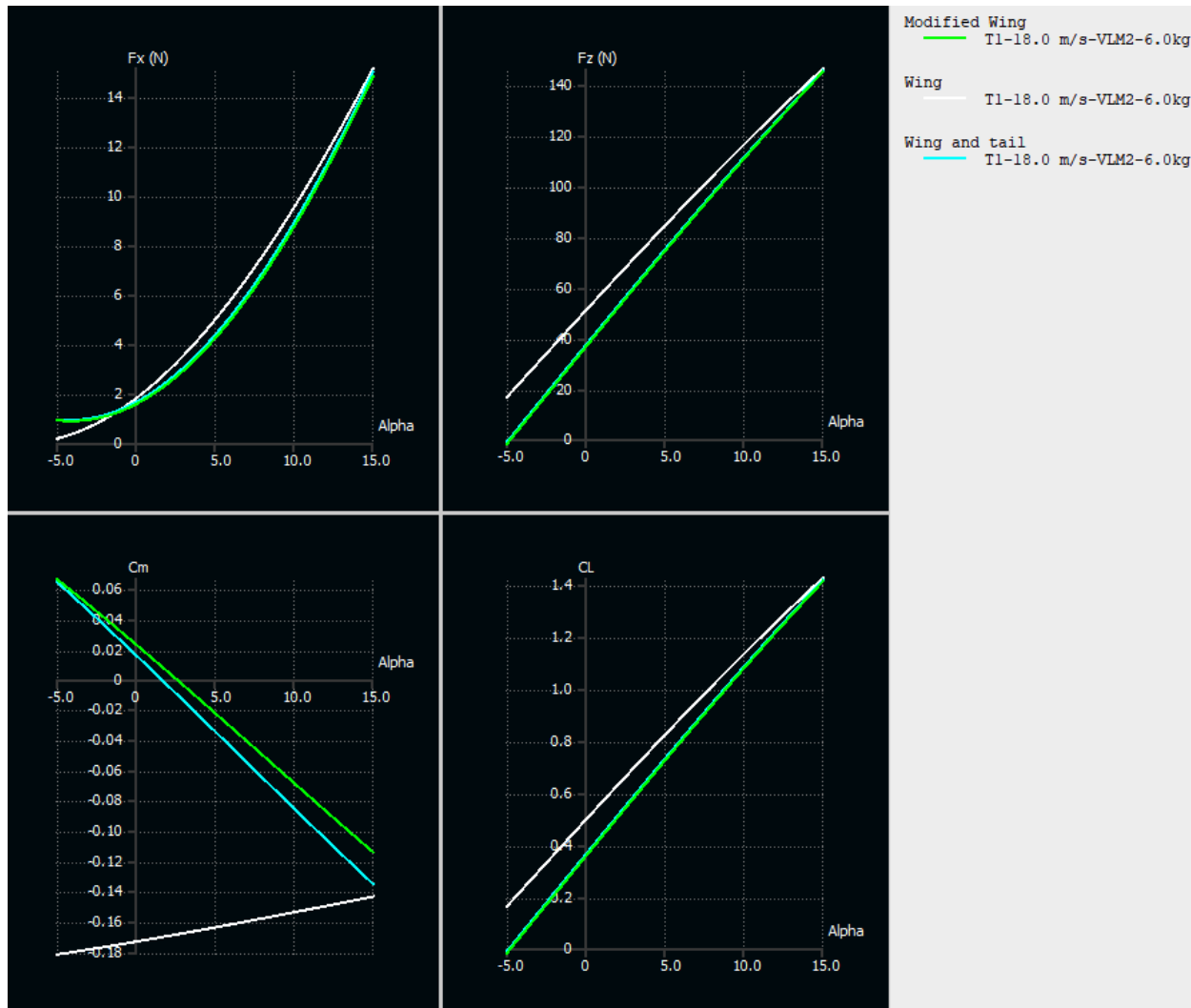


Figure 44: Modified wing theoretical analysis

The modification in taper reduced the total drag force by reducing the induced vortices at tips

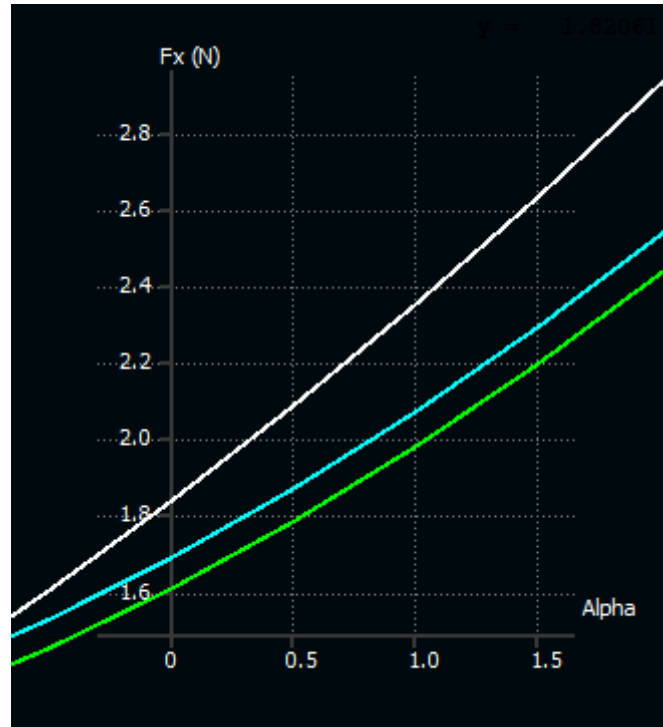


Figure 45: Modified wing drag analysis

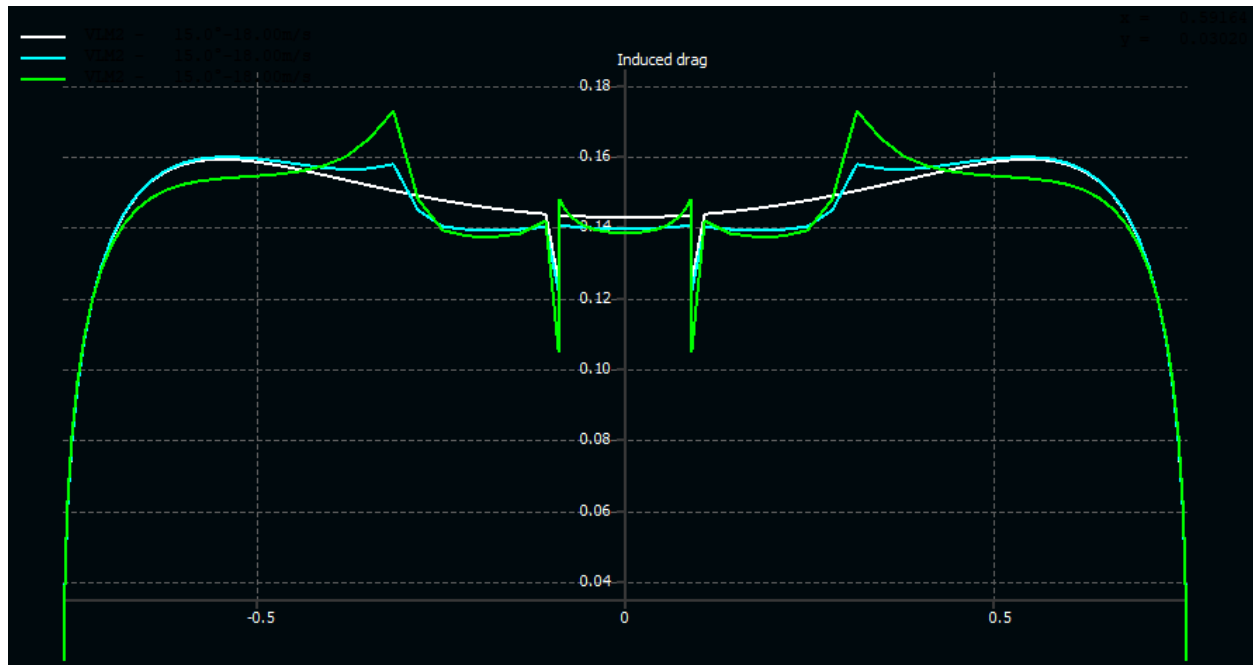


Figure 46: Modified Wing Induced Drag analysis

### 3.3.5 Modified Model

Iterating with tail parameters, we achieved a better stability in longitudinal at

1. Tail moment arm = 65 cm
2.  $i_h = -3^\circ$
3. tail span = 70 cm

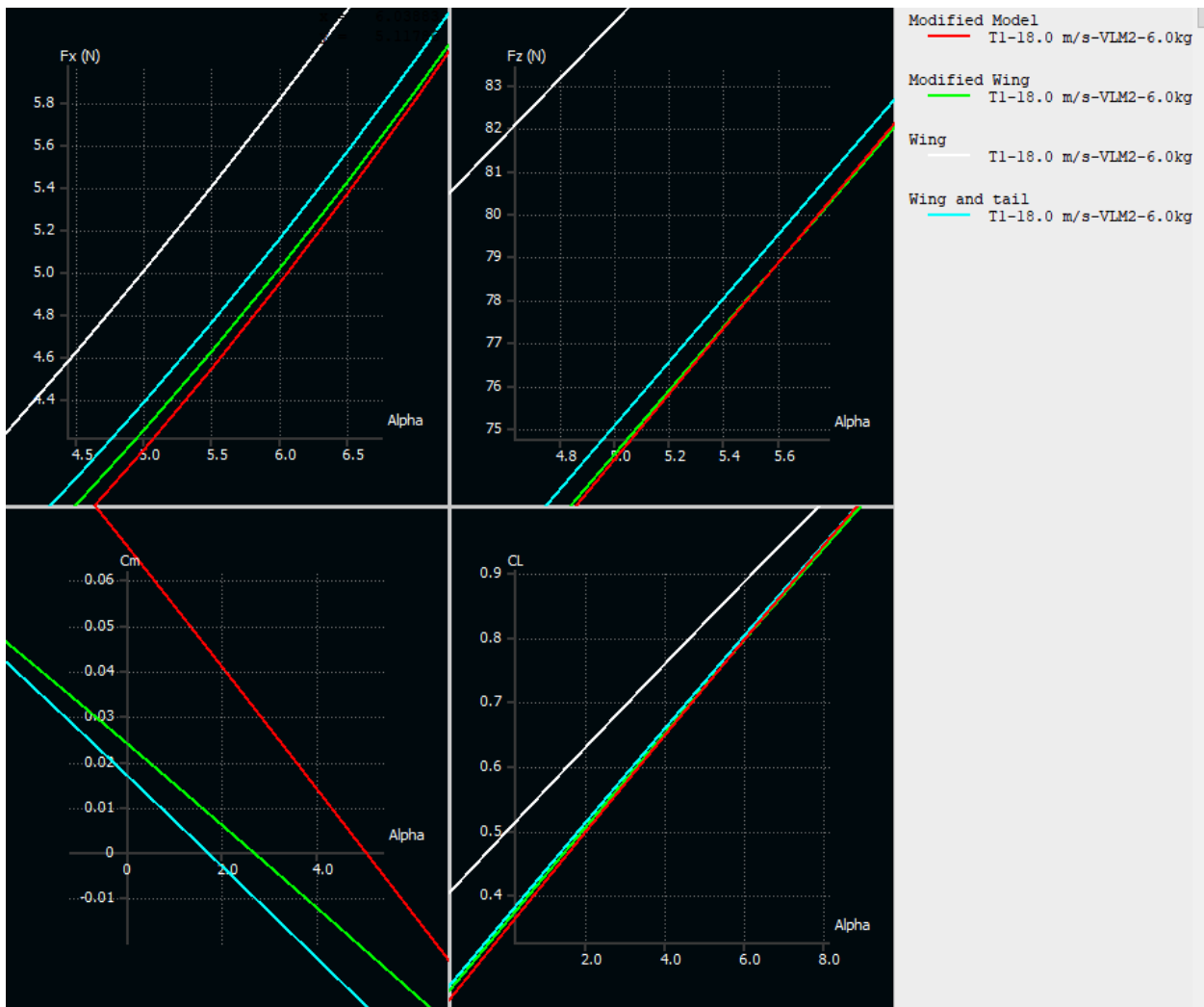


Figure 47: Modified Model Theoretical Analysis

### 3.3.6 Conclusion:

Estimate	Value
Wing Area	0.52m <sup>2</sup>
Mean Aero. Chord	0.343m
Span	1.52 m

## 3.4. Wing loading

The wing loading is the weight of the aircraft divided by the area of the reference (not exposed) wing. Wing loading directly affects stall speed, climb rate, take-off and landing distances as well as turning performance. Also, it determines the design lift coefficient, and impacts drag through its effect upon wetted area and wing span. There are many methods of calculating wing loading in aircraft designs according to the design requirements. In this study, stall speed and cruise speed are chosen as constraints in wing loading calculations.

According to the two methods, the calculations are made separately and the selection of the smaller value between the two values are made. The smallest value is chosen such that, if the wing is large enough to minimize the wing loading; it is highly possible that the wing will satisfy all other requirements

### Stall speed constraint

The stall speed of an aircraft is directly determined by the wing loading and the maximum lift coefficient. Stall speed is a major contributor to flying safety, with a substantial number of fatal accidents. Wing loading from stall speed is calculated as shown:

$$\frac{w}{s} = 0.5 \rho_{\infty} V_{stall} C_L$$

$$C_{L,max} = 0.9 C_{L,max} \cos(\lambda_{C/4})$$

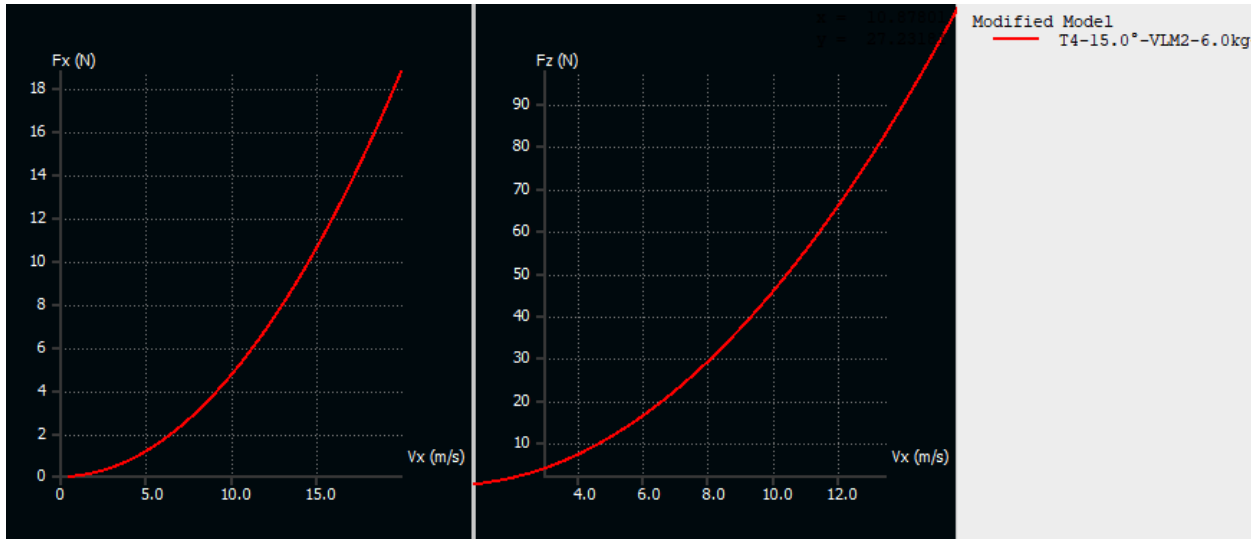


Figure 48: Stall Speed Determination

### Cruise speed constraint

During cruise flight, the lift equals the weight so that the lift coefficient equals the wing loading divided by the dynamic pressure. In the case of propeller aircraft, the transport coefficient changes in direct proportion to the square root of the drag factor. At the same time, drag due to lift factor ( $K$ ) value deals with the performance of the wing characteristics of the aircraft, and the growth of this value reduces aerodynamic performance. In addition, it is necessary to determine the drag coefficient that affects the entire VTOL-FW UAV to calculate the cruise speed requirement and wing loading. For this, the method given in Eq. is found for all components of VTOL-FW separately and zero lift drag coefficient is calculated. Expressions for cruise-speed constraint method are given:

$$\frac{w}{s} = q_{\infty} \sqrt{\pi A Re C_{D_0}}$$

$$K = \frac{1}{\pi A R e}$$

$$\text{Where } e = 1.78(1 - 0.045AR^{0.68}) - 0.64$$

$$C_L = \sqrt{\pi A Re C_{D_0}}$$

$$C_L = \sqrt{C_{D_0}/3K}$$

### 3.4.1. Sizing of the Wing

Finding the wing loading value allows to determine the true value of the wing area. Actual wing area value is calculated as  $0.51 \text{ m}^2$  for the wing loading value of  $9.874 \text{ kg/ms}^2$  calculated for 6 kg take-off weight. Calculation of the wing area provides the determination of wing geometric characteristics such as wing root and tip chord length as well as average aerodynamic chord length with the selected taper ratio value in

Parameter	Symbol	Value	Unit
Aspect Ratio	AR	4.466	—
Wing Span	b	1.52	m
Empty Weight	$W_e$	5.5	kg
Take-off Weight	$W_{TO}$	6	kg
Design Lift Coefficient	$C_{L,design}$	0.4	—
Cruise Speed	$V_{cruise}$	?	km/h
Taper Ratio	$\lambda$	0.763	—
Wing Twist	—	-1.696	Degree
Airfoil	—	SG6043	—

$$c_r = \frac{2S_{Wing}}{b(1 + \lambda)}$$

$$c_t = \lambda c_r$$

Parameter	Symbol	Value	Unit
Stall speed	$V_{Stall}$	39.6	Km/h
Maximum lift coefficient	$C_{L,max}$	1.8	—
Wing loading-stall speed	$(\frac{W}{S})_{stallspeed}$	183.8	$\text{Kg/m}^2$

Oswald span efficiency	e	0.918	-
Skin friction coefficient	C <sub>f</sub>	0.00615	-
Multirotor drag coefficient	CD <sub>MR</sub>	0.021	-

$$\underline{c} = \frac{2}{3} c_r \frac{1 + \lambda + \lambda^2}{1 + \lambda}$$

### 3.4.2 Sizing of the control surfaces

Historical trend shows that the tail moment arm of this type of the aircraft is generally between 0.6 and 0.7. Taking the horizontal tail volume ratio ( $V_{HT}$ ) as 0.5 for a homebuilt aircraft horizontal tail wing area and other specifications can be found out. For an arbitrary aircraft, a vertical tail has to be a little bit closer to the wing than the horizontal tail. This is to prevent the vertical tail to be masked by the wakes created by the horizontal tail. Therefore, with arbitrarily

Parameter	Symbol	value	Unit
Wing area	Swing	0.52	m
Wing root chord	c <sub>r</sub>	0.38	m
Wing tip chord	c <sub>t</sub>	0.29	m
Mean aerodynamic chord	c	0.3	m
Horizontal tail area	S <sub>HT</sub>	0.2	m
Horizontal tail moment arm	I <sub>HT</sub>	0.625	m
Vertical tail area	S <sub>VT</sub>	0.07	m
Vertical tail moment arm	I <sub>VT</sub>	0.625	m

$$V_{HT} = \frac{l_{HT} S_{HT}}{\underline{c} S}$$

$$V_{VT} = \frac{l_{VT} S_{VT}}{b S}$$

### 3.5. XFLR5 Aircraft Analysis

The estimated root stall and tip stall values of the wing were determined in XFLR5<sup>11</sup> as 2D airfoils. As the root stalls before the tip, the maximum angle of attack is taken to be  $9 - 2.6 = 6.4$ . Allowing for a 10% de-rating due to inaccuracies in a linear solver predicting flow separation, the maximum  $C_L$  of the aircraft was determined as 0.83. This corresponds to a stall speed of 17.54m/s. The transition velocity is taken as 1.2 times higher than the stall speed which gives 21.05m/s. This is clearly a large transition speed and flaps may be required to reduce this speed. Detailed information on the wing is shown

Property	Wing	Horizontal Tail	Vertical Tail (one)
Area	0.52m <sup>2</sup>	0.2m <sup>2</sup>	0.07m <sup>2</sup>
Span/Semi Span	1.520m	0.7m	0.3m
Aspect Ratio	4.466	2.50	1.25
Taper Ratio	0.763	1.00	0.71
Mean Aero. Chord	0.3427m	0.280m	0.2422m
Root Airfoil	SG6043	NSCA-0009	NSCA-0009
Root Chord	0.38m	0.28m	0.28m
Tip Airfoil	SG6043	NSCA-0009	NSCA-0009
Tip Chord	0.29m	0.28m	0.20m
Tilt Angle	0	-3	0
Root to tip sweep	-1.7	0	21.8

### 3.5.1 XFLR5 Results

#### The Pressure Coefficient:

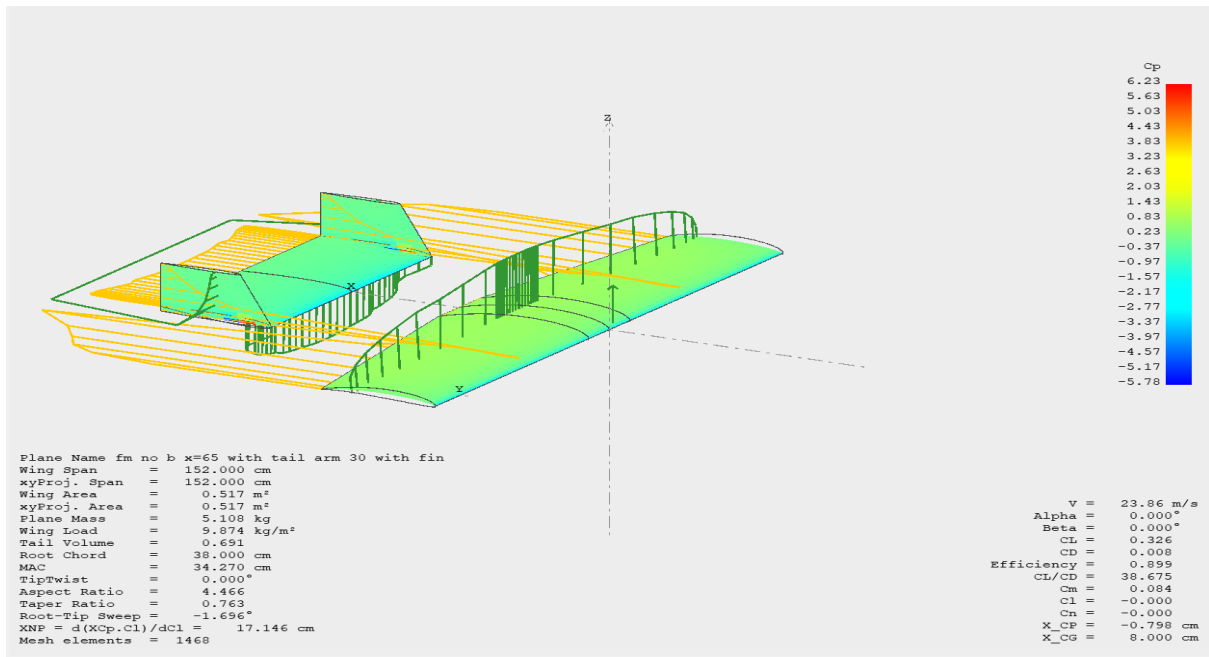


Figure 49: XFLR5 Analysis

#### Aerodynamic stability:

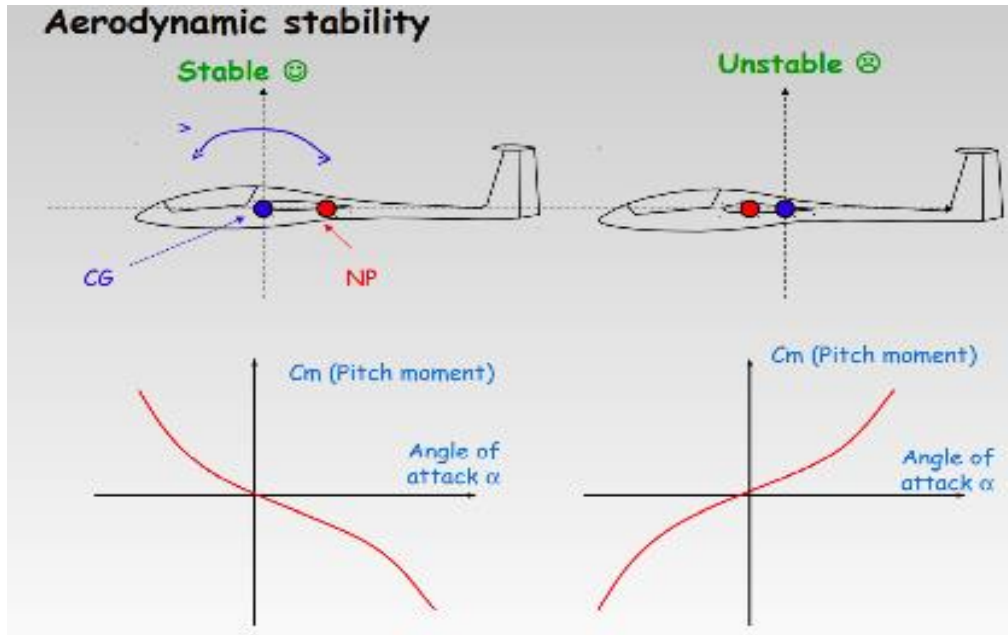
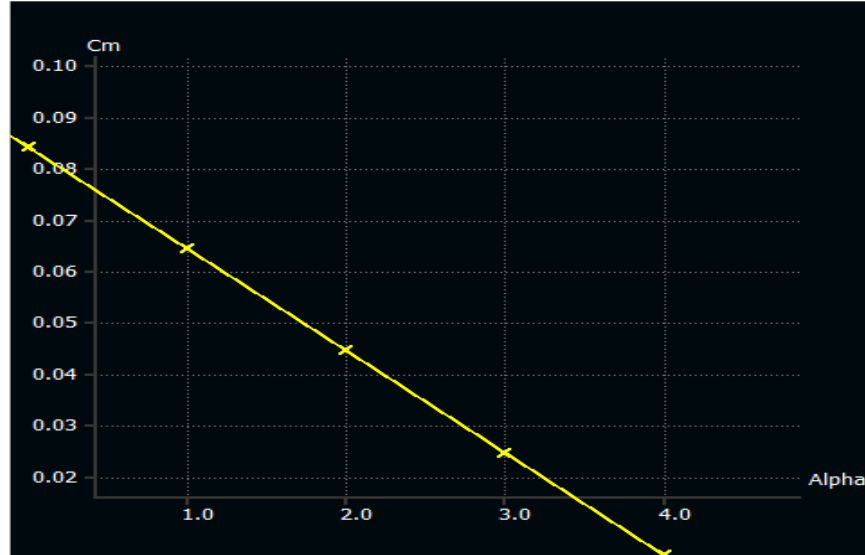


Figure 51: Aerodynamic stability



Negative slope = Stability, the curve's slope is also the strength of the stabilizing force, depending on the CG position, get the balance angle  $\alpha_e$  such that  $C_m = 0$

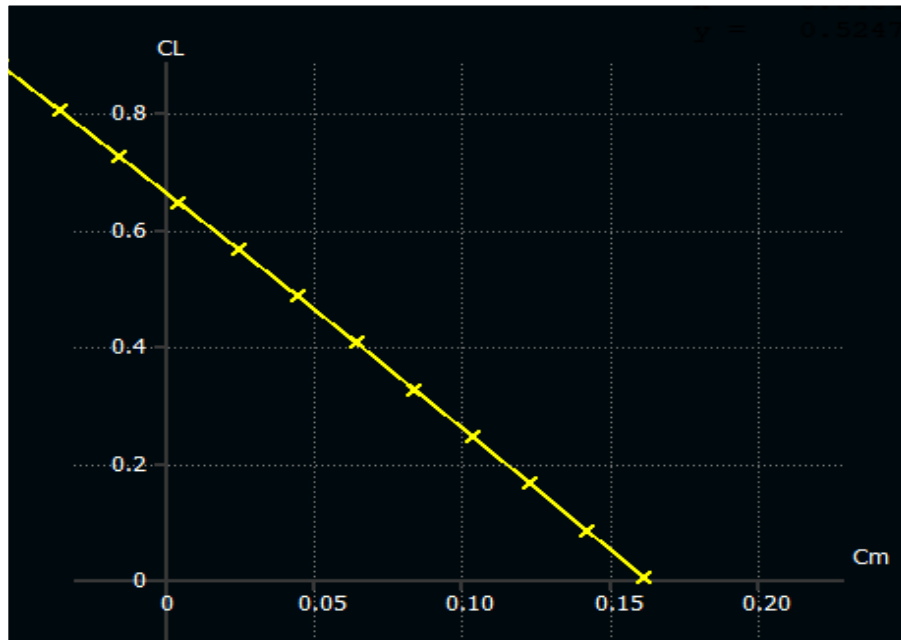


Figure 52 :  $c_l$  VS  $c_m$  Curve

We can get  $c_{mo} = 0.17$

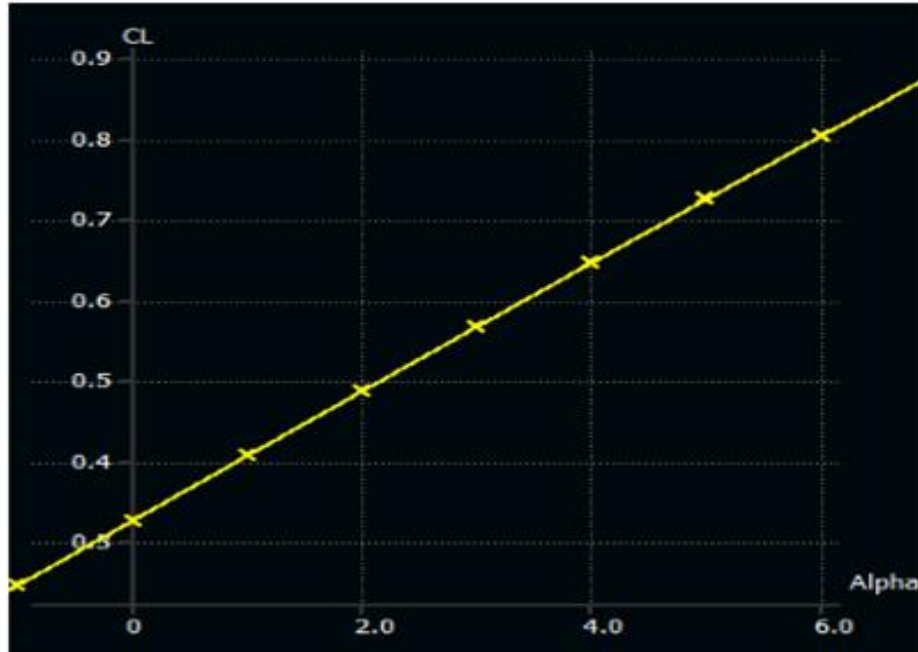


Figure 53:  $cl$  VS  $\alpha$  Curve

Check that  $Cl > 0$  for  $\alpha = \alpha_0$

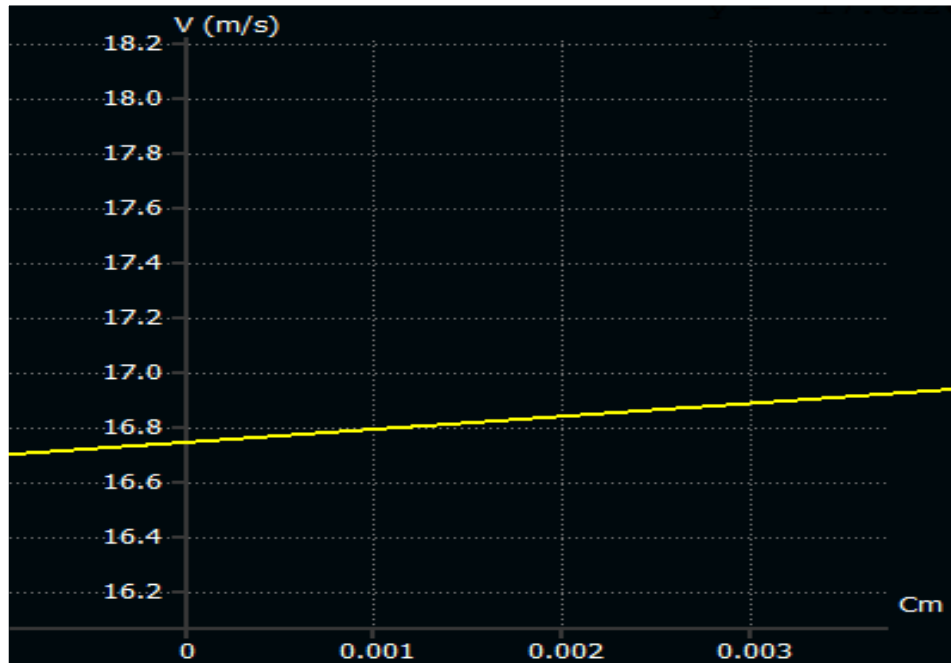


Figure 54: Velocity Vs  $Cm$  Curve

Check that  $V = V_{cruise}$  @  $Cm = 0$

---

### The Static Margin:

Knowing the NP position and the targeted SM, the CG position can be deduced...

$$X_{CG} = X_{NP} - MAC \times SM,$$

OR we can check the static margin range after the iterations the range (+0.05 .....+0.15).

$$SM = \frac{X_{NP} - X_{CG}}{MAC_{wing}}$$

### Dynamic stability:

The aerodynamic derivatives were calculated in XFLR5 and used to solve the linearized longitudinal and lateral stability equations presented in Nelson. The results are shown in

Longitudinal	Eigenvalue
Short Period	$-3.9514 \pm 5.3436i$
Phugoid	$-0.00006 \pm 0.8338i$

Lateral	Eigenvalue
Roll Subsidence	-8.6328
Dutch Roll	$-0.7456 \pm 3.3388i$
Spiral	0.385

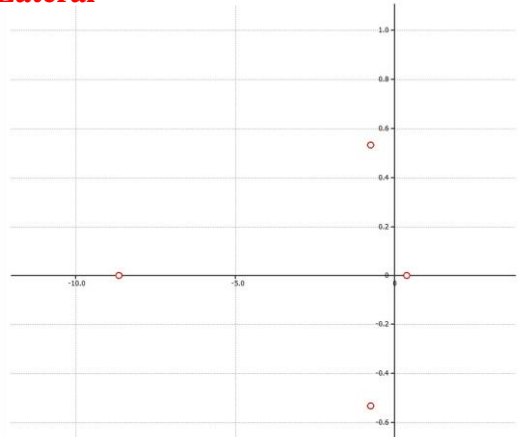
**Lateral**

Figure 56: Lateral Eigenvalue

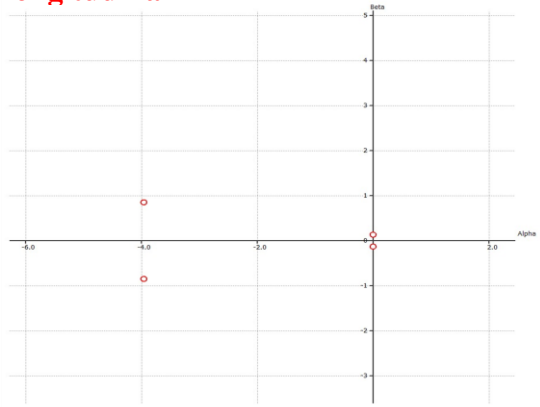
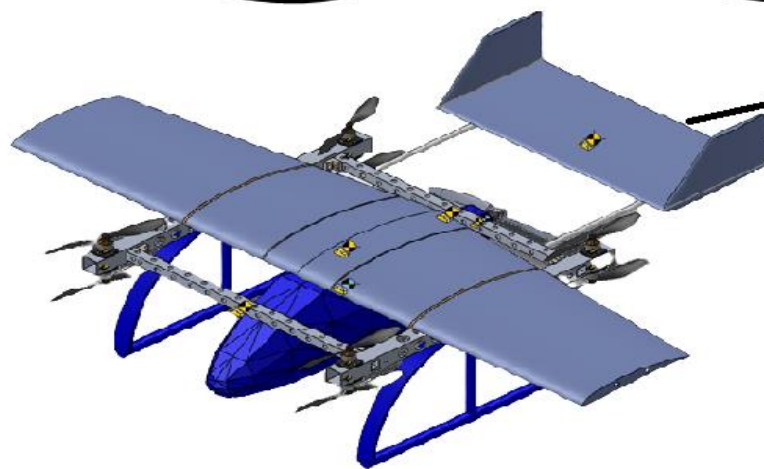
**Longitudinal**

Figure 55: Longitudinal Eigenvalue

# **Chapter Four:**

# **Structure**



## 4.1 Introduction:

To design a small-scale VTOL UAV, it is important to limit certain parameters of sizes to a practically reasonable figure so that other parameters concerning dimensions would be feasible for fabrication. The design parameters chosen should also obey known theoretical concepts and equations to confirm that the VTOL UAV will be able to accomplish stable and safety flights across all its flight modes. The general procedures to determine basic structural design parameters are:

- ❖ Estimate the All-Up-Weight of the aircraft
- ❖ Wing Design: Determine the size of the wing loading, wingspan, aspect ratio and chord
- ❖ Fuselage Design: Determine the size of the fuselage
- ❖ Tail Design: Determine the size of the tail wing and its distance from the main wing

These general procedures will be used to estimate the size of the prototype. After fabrication and flight tests, the actual dimensions will be adjusted accordingly.

At first, we searched the materials characteristics, shapes and dimensions used in multi-rotors (eVTOL) and we have reached many designs that can be implemented and in this chapter we will clarify the design and manufacturing processes of the project structure taking into account the simplicity and ease of manufacturing at the lowest possible cost

## 4.2 Main Frame:

As we have chosen the aluminum as the material of the main frame, we also compared the shapes and dimensions of the cross section to choose the right shape and dimensions and then we designed more than configuration for the main frame and tested its performance and the amount of tolerance, stress, strain and deformation to ensure the best configuration selection in terms of hardness, lightness of weight, ease of manufacture and clarification of this below

### 4.2.1 Cross Section Selection:

We have to decide which cross section we will be using as there is wide range of commercial aluminum bars but We found that the most suitable section is the rectangular cross section because of its strength, hardness and ease of installing motors on it and will be analyzed as follows

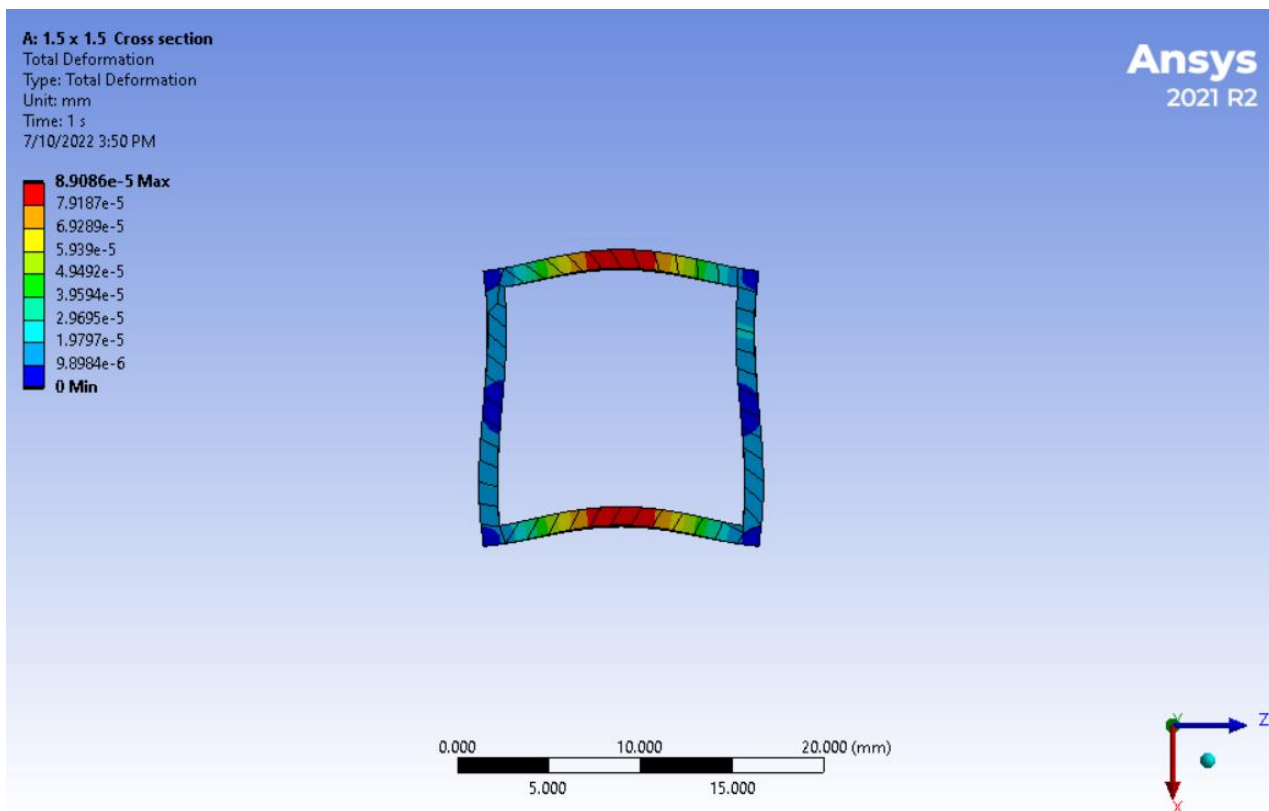


Figure 57: Structure Analysis (Square cross section (1.5×1.5 ×0.1 cm))

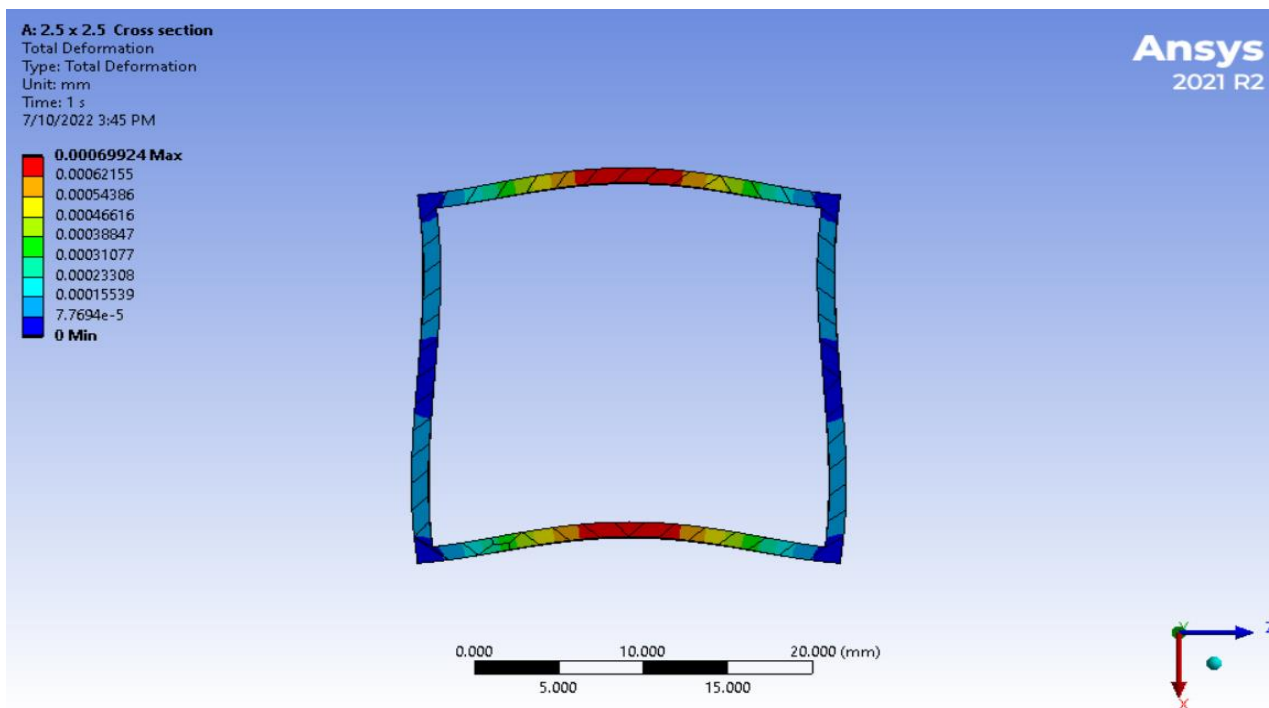


Figure 58: Structure Analysis (Square cross section (2.5×2.5 ×0.1 cm))

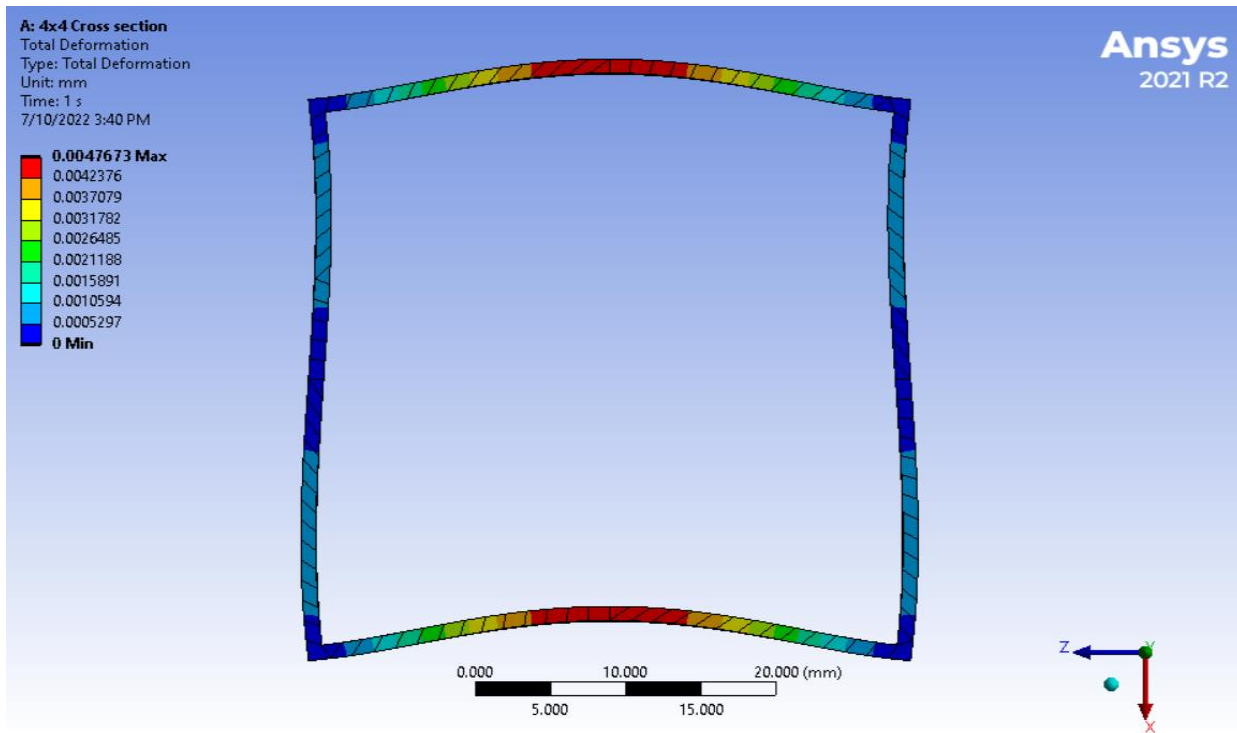


Figure 59: Structure Analysis (Square cross section 4×4×0.1 cm)

From structure analysis and test sections we found that the best choice of the cross section is  $(1.5 \times 1.5 \times 0.1)$  square tube which gives high rigidity and lighter weight and best MOS but it's not available, so we used the other two cross sections, we used two cross-sections to ensure a strong connection method as shown in the figure

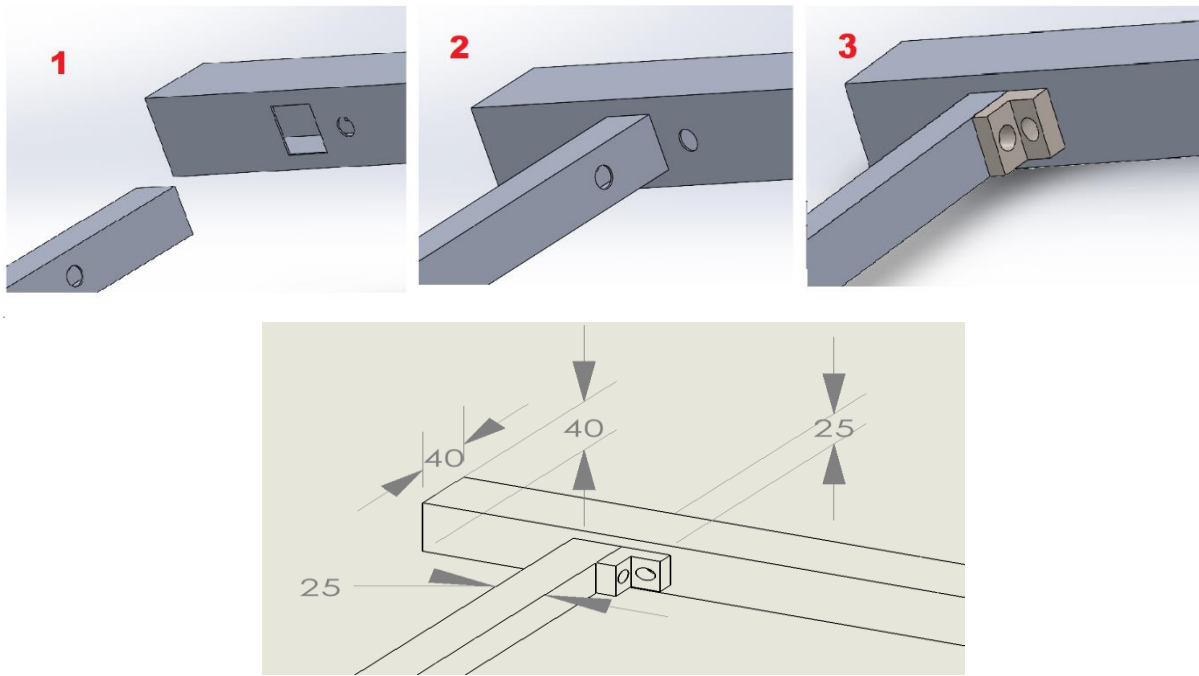


Figure 60: The first design and its dimensions

#### 4.2.2 Configuration Selection:

First design:

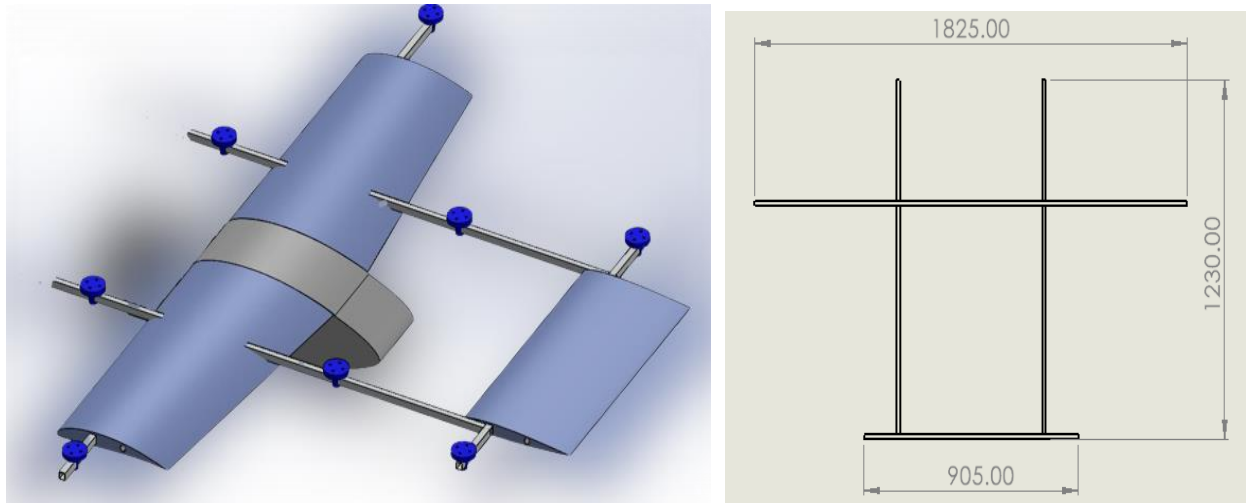


Figure 61: The first design and its dimensions

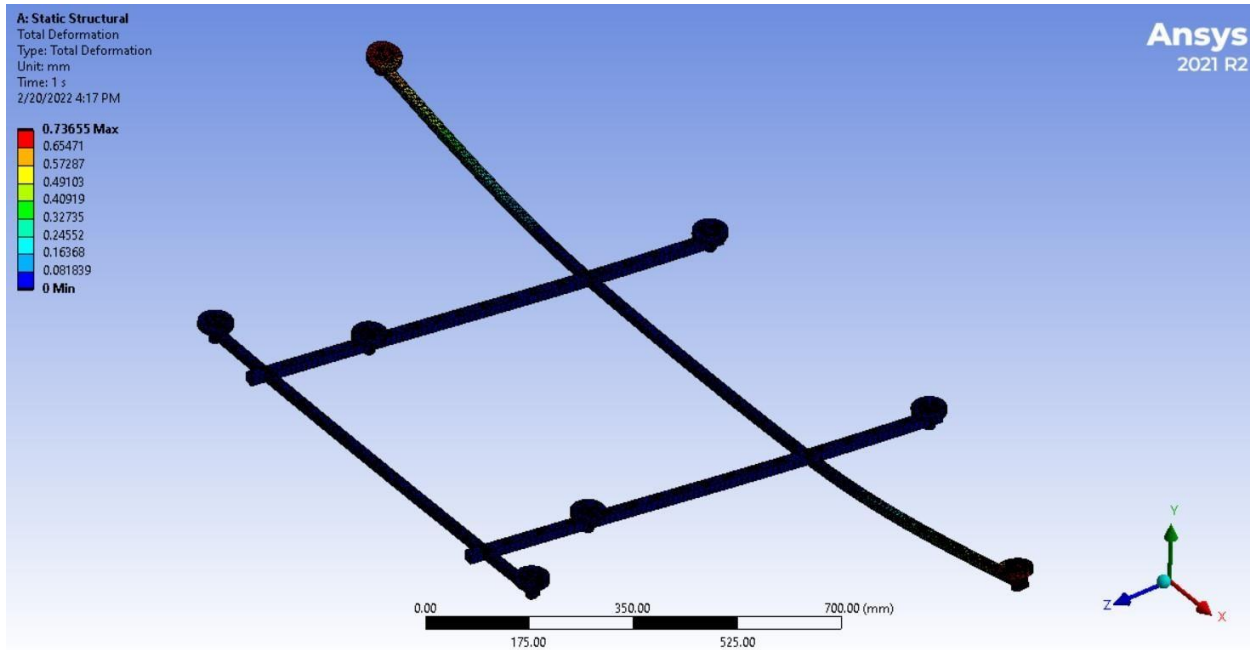


Figure 62: The first design Total deformation

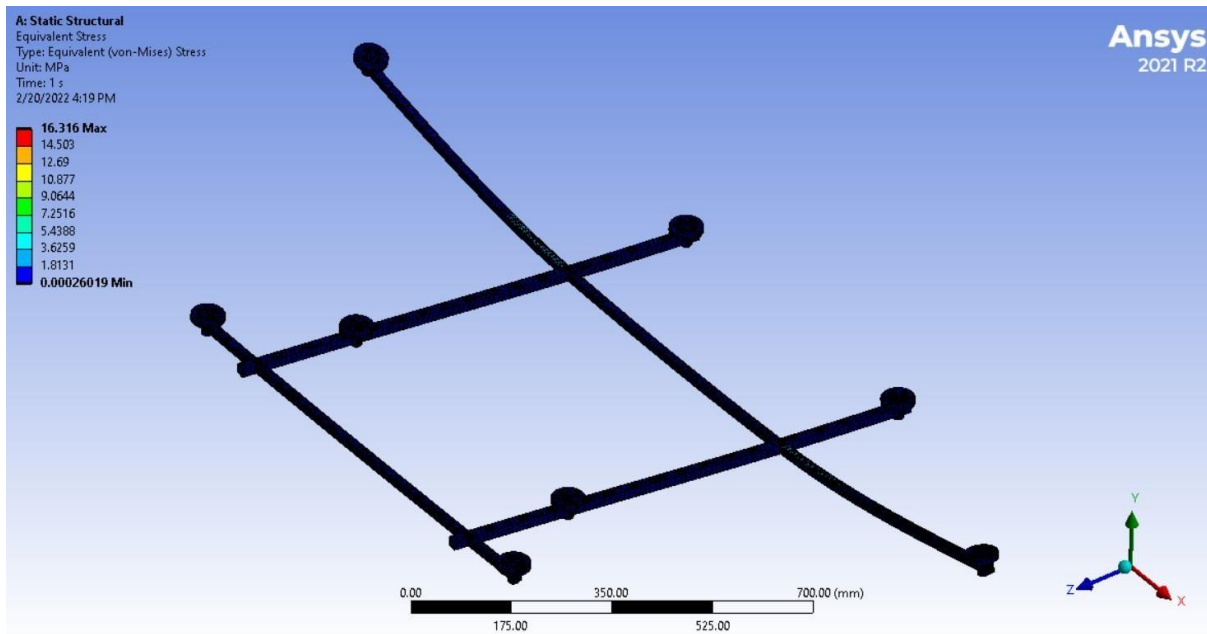


Figure 63: The first design Stress

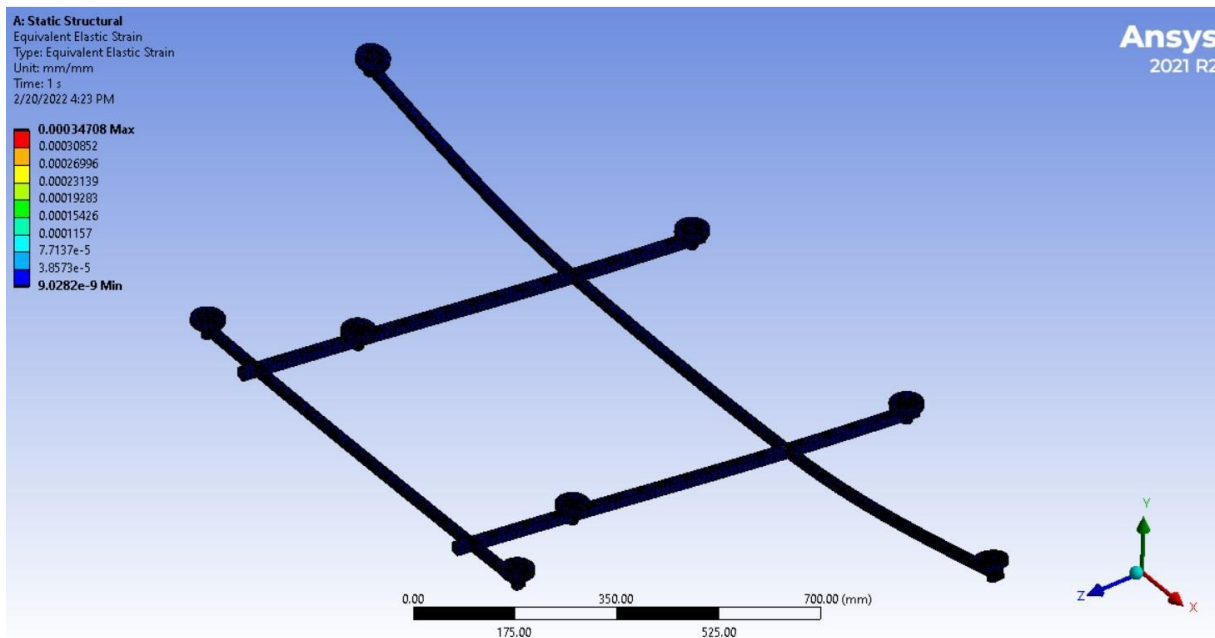


Figure 64: The first design Strain

Weight (gram)	Max Deformation (mm)	Max Stress (MPa)	Max Strain (mm)
1345	0.73655	16.316	0.000347

In this design, we made an aluminum frame with dimensions of 1825 x 1228 mm. After design and testing, it was found that the model is long and will be very long when implementing the real version, and its weight is large, as it turns out that the deformation is large due to the distance between the places of the lifting motors and the connection points

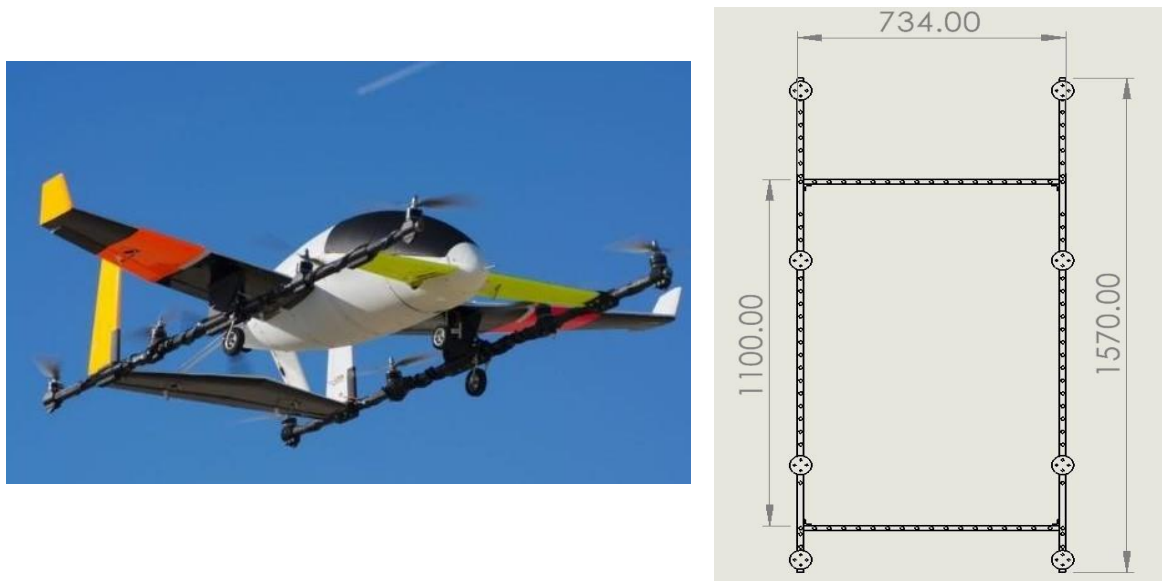
**Second design:**

Figure 65: The Second design and its dimensions

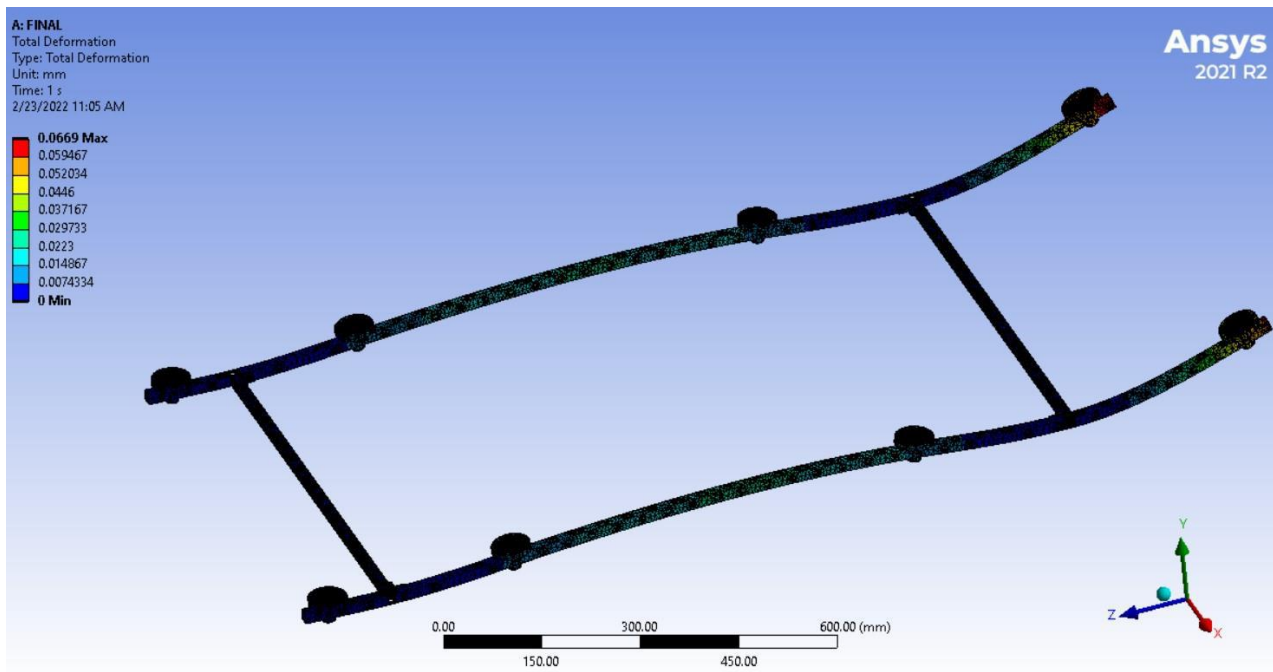


Figure 66: The second design Total deformation

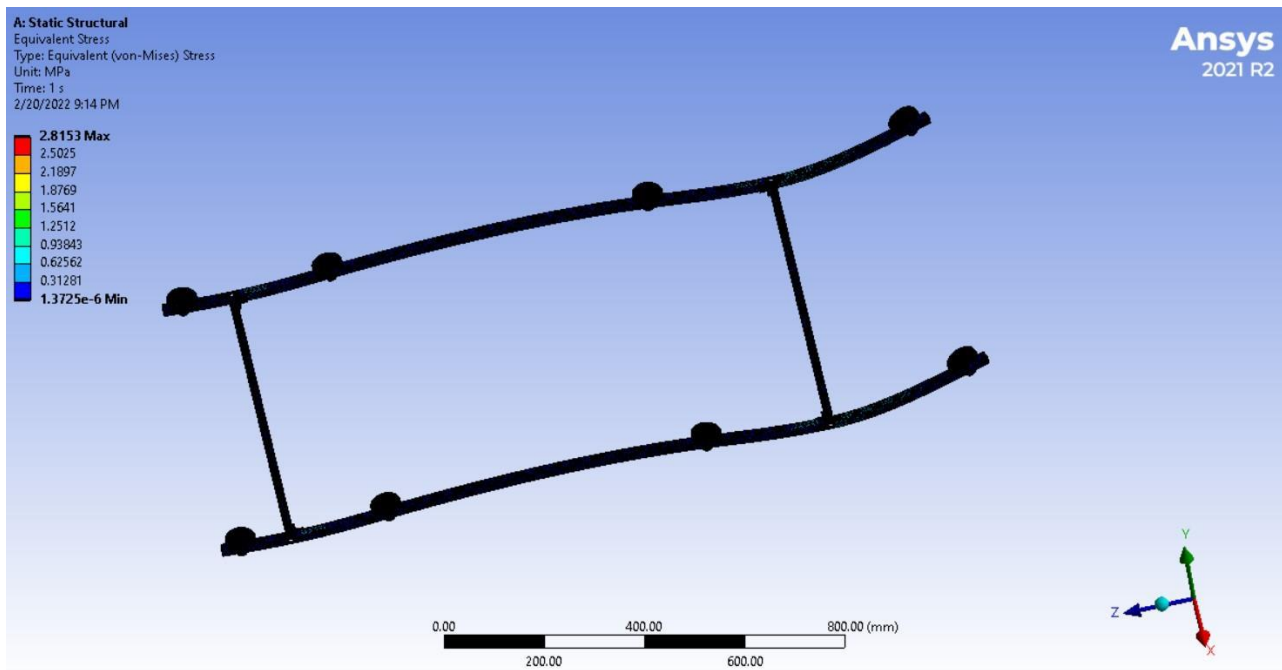


Figure 67: The second design Stress

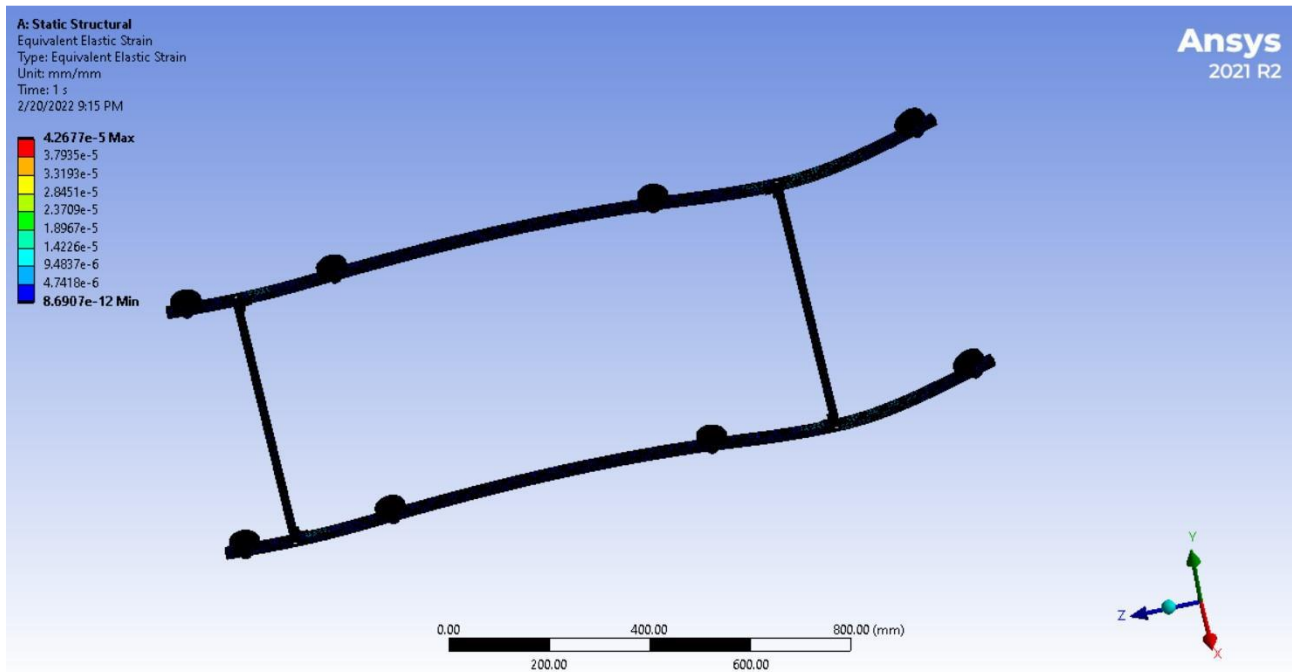


Figure 68: The second design Strain

Weight (gram)	Max Deformation (mm)	Max Stress (MPa)	Max Strain (mm)
1220	0.0669	2.8135	0.0000427

In an effort to remedy the problems in the first design we did on this construction, we made a new aluminum frame with dimensions of  $1570 \times 734$  mm. After the design and testing it turns out that the model is still long and will be very long when implementing the real version, weighing less than the first model, and less stress than the first model as it turns out to be less deformation than in the first model.

### Third design (Coaxial):

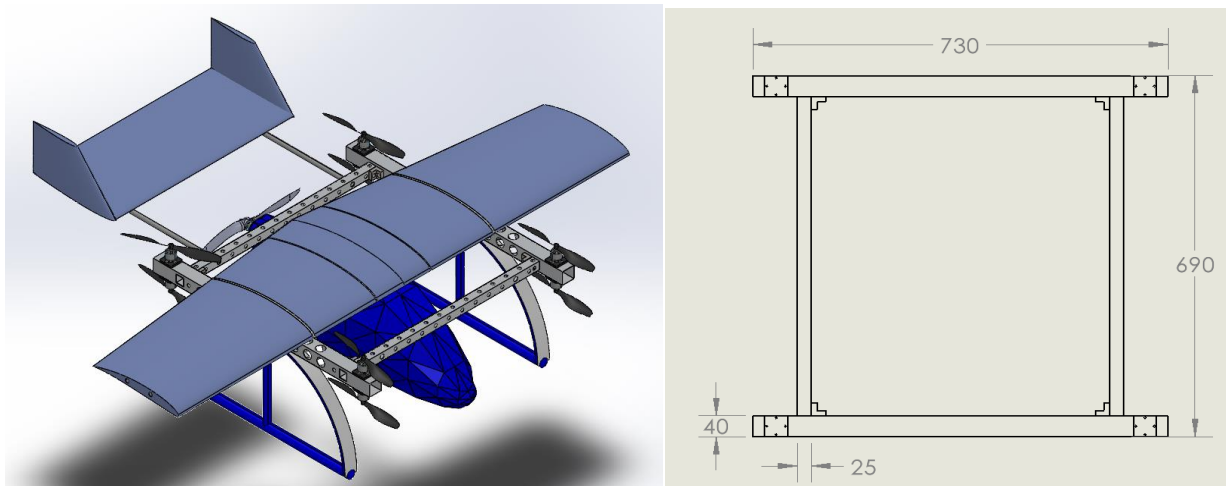


Figure 69: The Coaxial design and its dimensions

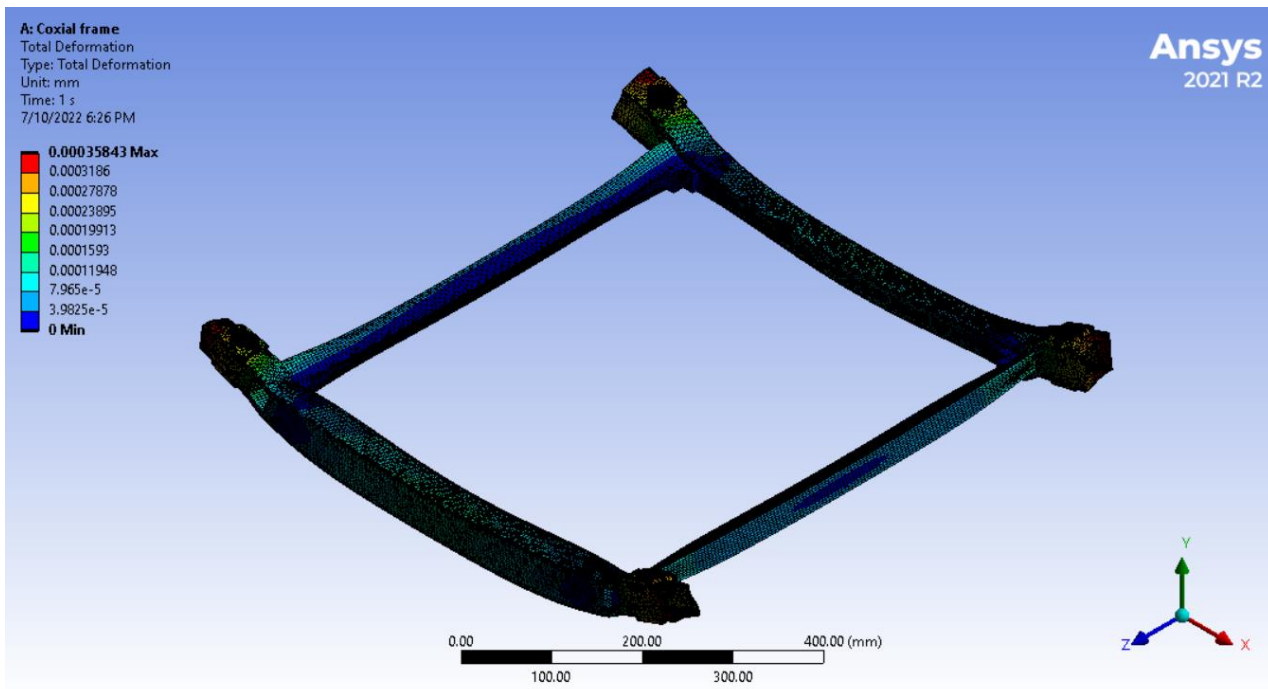


Figure 70: The Coaxial design Total deformation

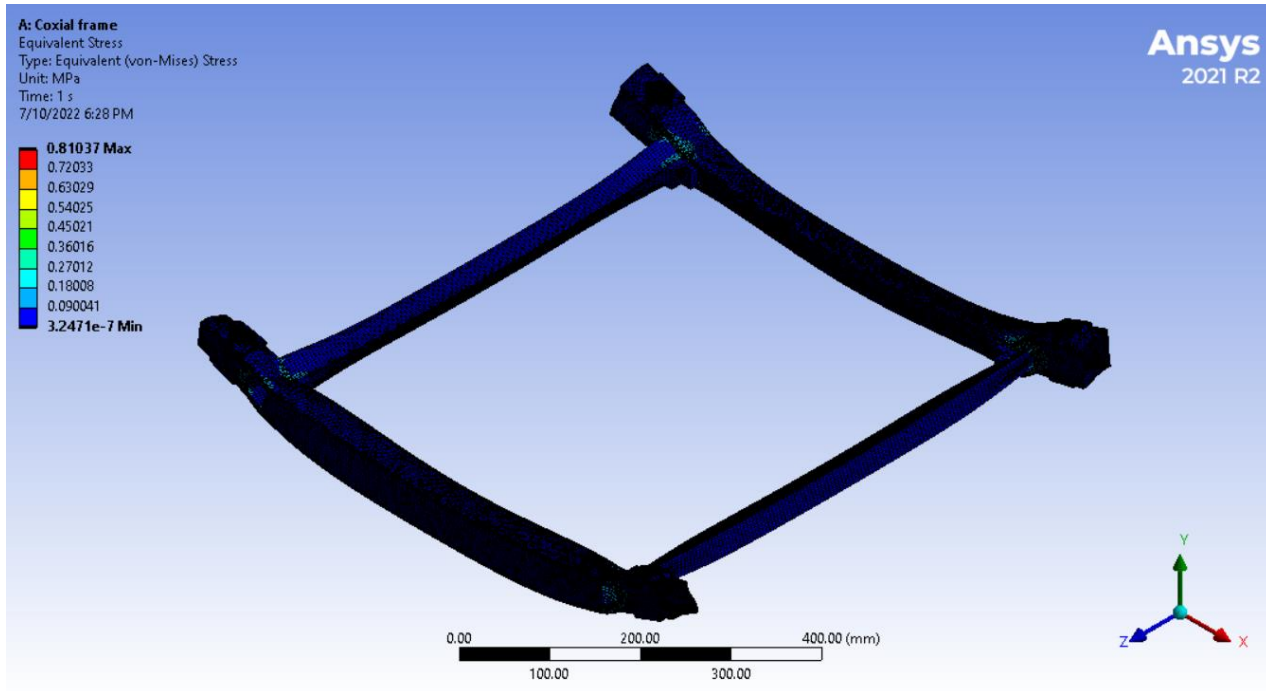


Figure 71: The Coaxial design Stress

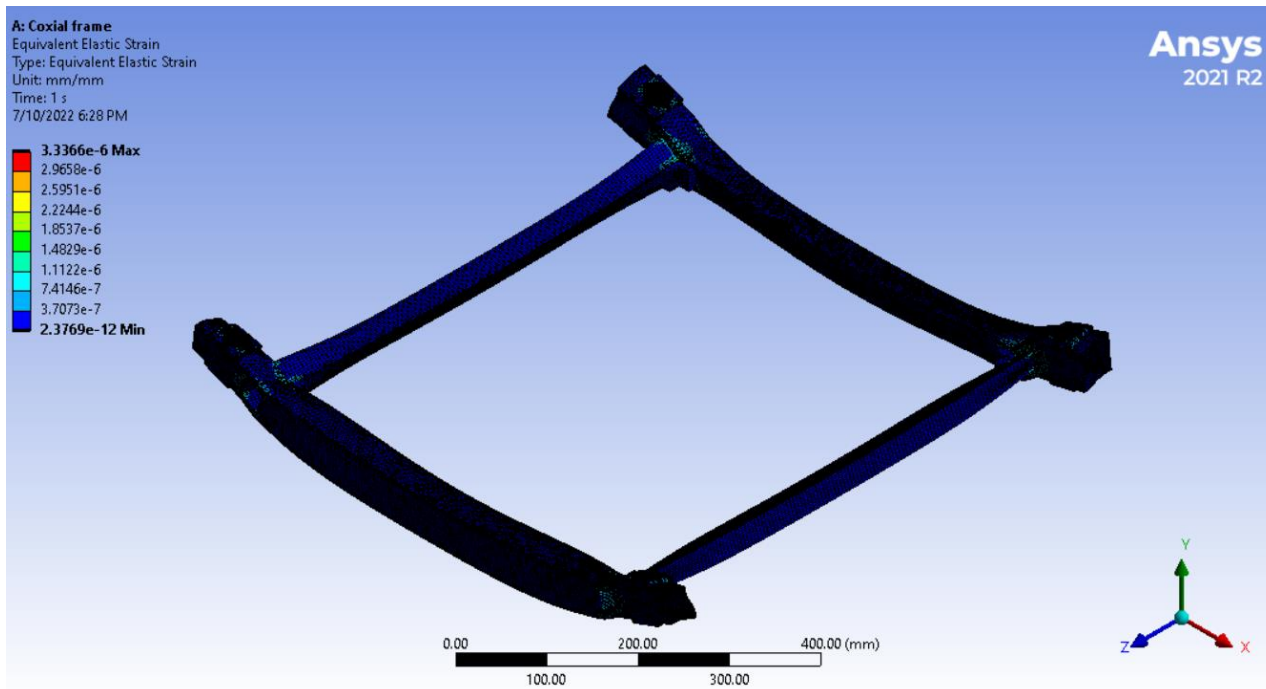


Figure 72: The Coaxial design Strain

Weight (gram)	Max Deformation (mm)	Max Stress (MPa)	Max Strain (mm)
1040	0.00035843	0.81037	0.00000334

Finally, we found that we could not reduce the weight more than that in the second design, to take into account the positions of the motors and the diameter of the propeller, so it was found that the weight loss did not decrease much from the first design, so we changed the design completely to be an OCTA-QUAD type with a coaxial motor, so we designed Frame with dimensions 690 x 734 mm. This contributed to a significant reduction in weight and deformation, due to the fact that the motors were close to the contact points.

#### 4.2.3 Weight Reduction:

From the first moment we decided to use aluminum beams for the airframe, we knew that we will have a problem with the weight, not failure. So, with a high strength material and high yield strength we decided to reduce the weight with some drilling in both sides of the beam, but the question is how it will affect the stress distribution on it.

As we know, the holes will reduce the area in some places and the stress on it will increase and there will be some stress concentration in these areas, so if we don't choose the dimensions carefully, we may increase the stress dramatically to reach the yielding point of the Aluminum

So, we used Ansys to find out where it can be drill to reduce weight, those low stress places that are not affected by the hardness and strength of the frame.

#### Coaxial drilled design:

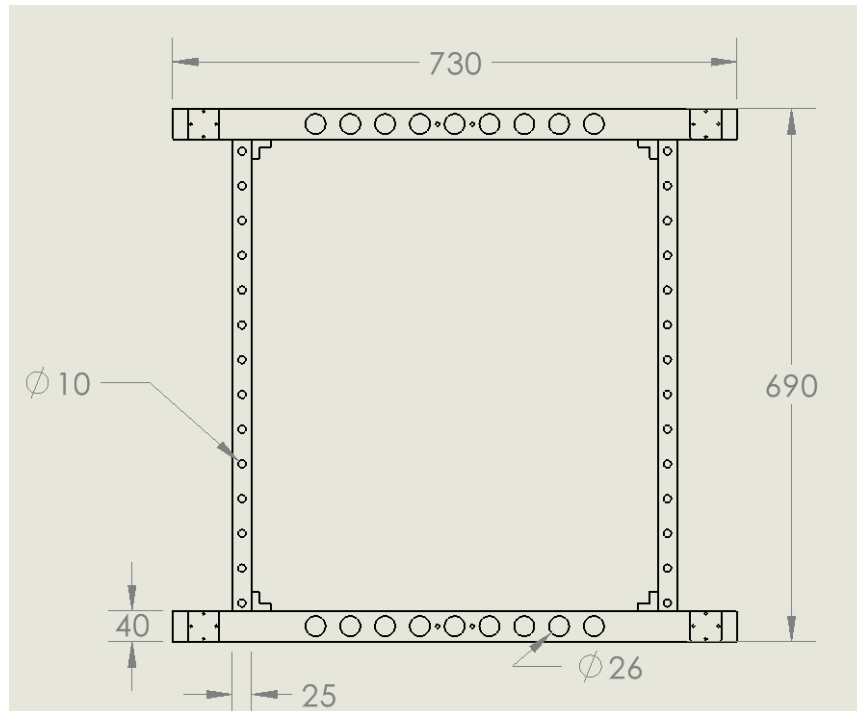


Figure 73: The Coaxial drilled design and its dimensions

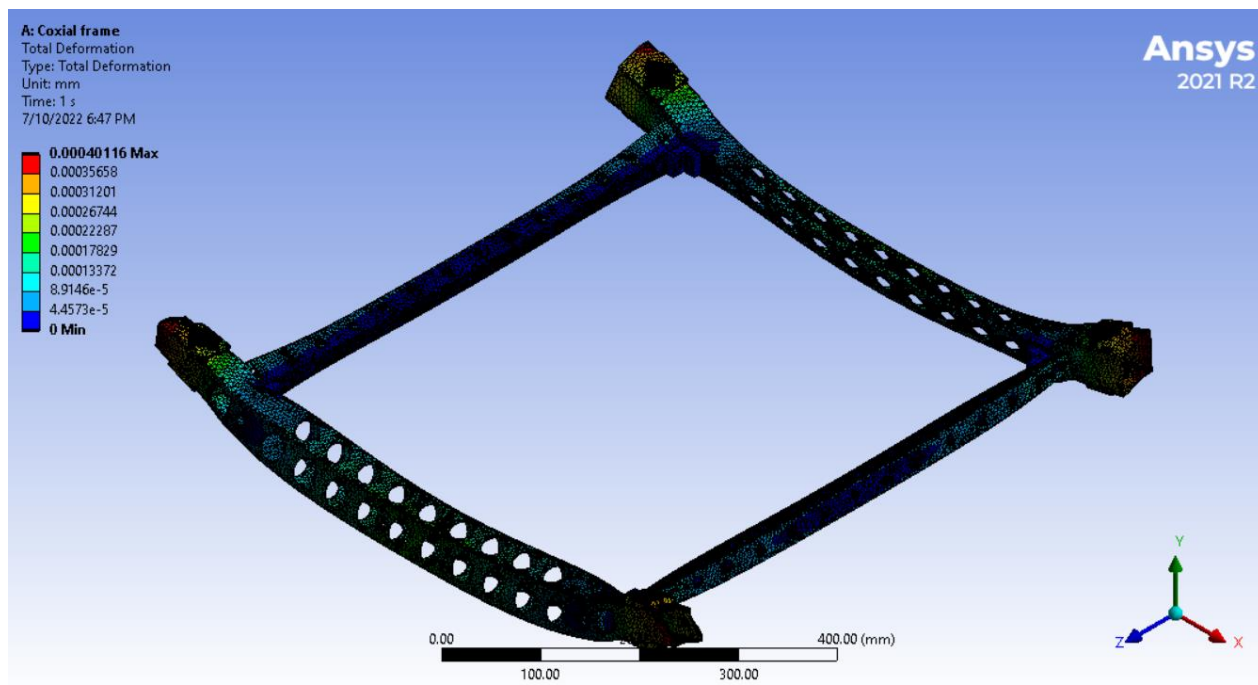


Figure 74: The Coaxial drilled design Total deformation

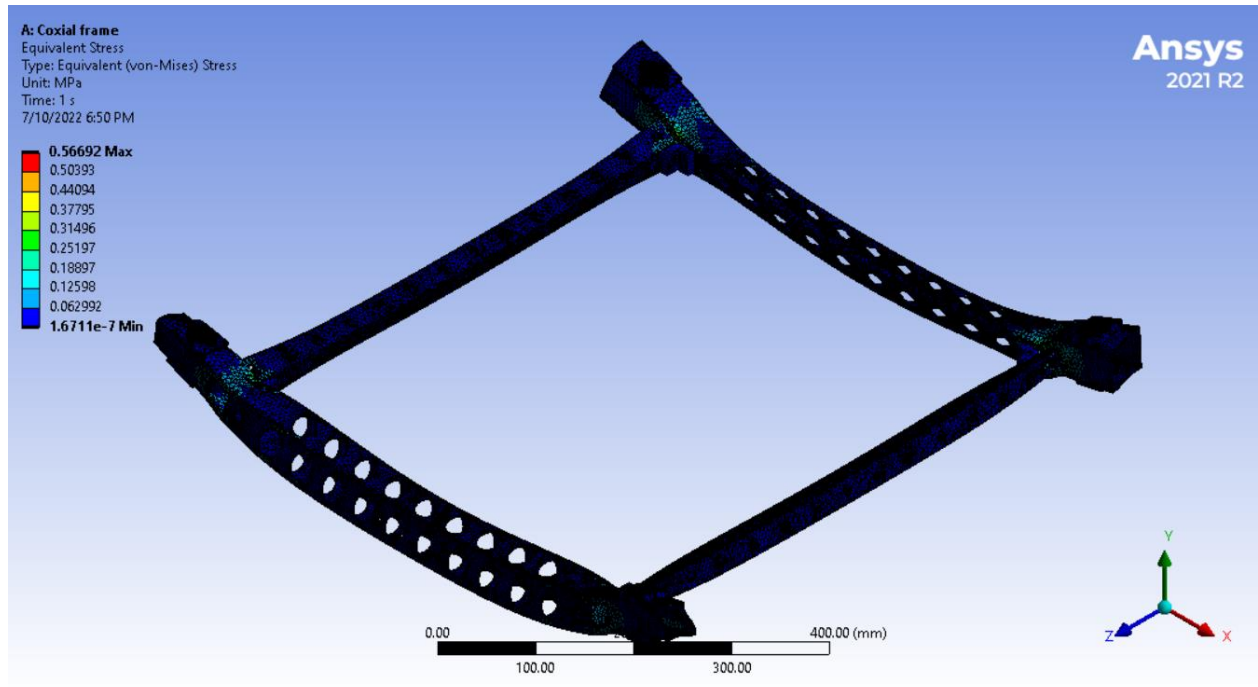


Figure 75: The Coaxial drilled design Stress

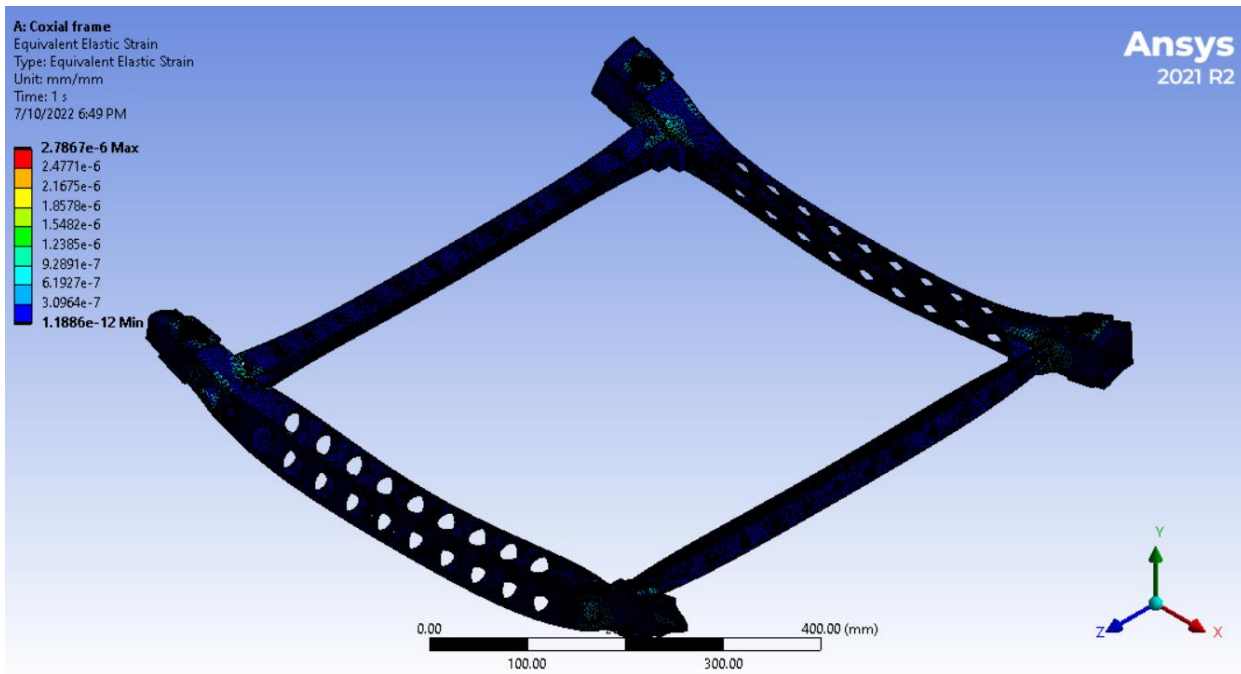


Figure 76: The Coaxial drilled design Strain

Weight (gram)	Max Deformation (mm)	Max Stress (MPa)	Max Strain (mm)
850	0.00040116	0.56692	0.000027867

Drilling contributed to significant weight loss by 19% of weight before fermentation and it does not have a significant impact on deformation, stress and strain

Model	Weight (gram)	Max Deformation (mm)	Max Stress (MPa)	Max Strain (mm)
First design	1345	0.73655	16.316	0.000347
Second design	1220	0.0669	2.8135	0.0000427
Coaxial design	1040	0.00035843	0.81037	0.00000334
Coaxial drilled design	850	0.00040116	0.56692	0.000027867

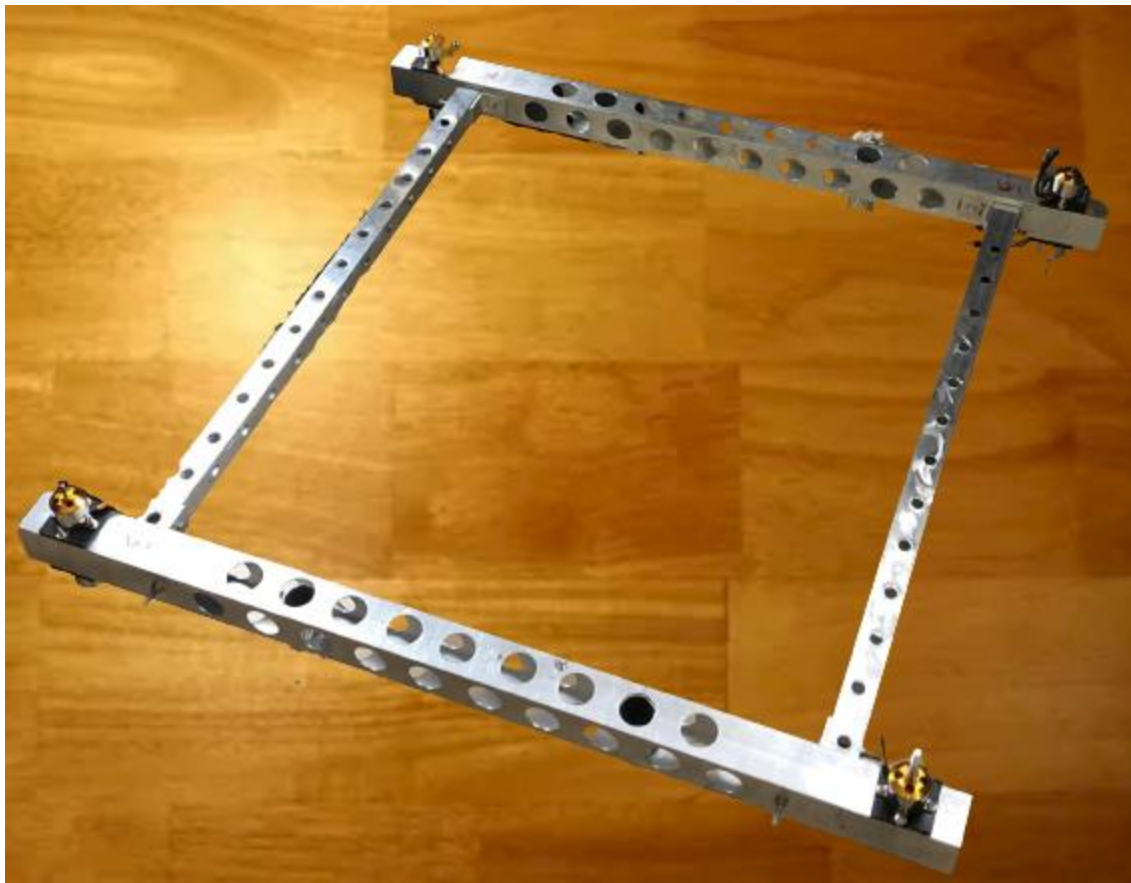


Figure 77: The Coaxial frame Implemented design

### 4.3 landing Skid:

First of all, we must ask ourselves why we use landing in most objects. What is the benefit of it? The answer is that we use them generally to latch the object onto the ground easily and safely, and also for maintain parts of control units from any shocks due to the impact with the ground because those shock may be offered these parts to damage.

For our eVTOL we need something between flexibility and rigidity, flexible in order to be the process of damping of the structure until it stabilizes and we also need to hardness in order be has the ability to with stand the stresses resulting from these shocks.

By studying similar projects implemented before, we took a relationship between the dimensions of the frame and the dimensions of landing skid and implemented them on our project.

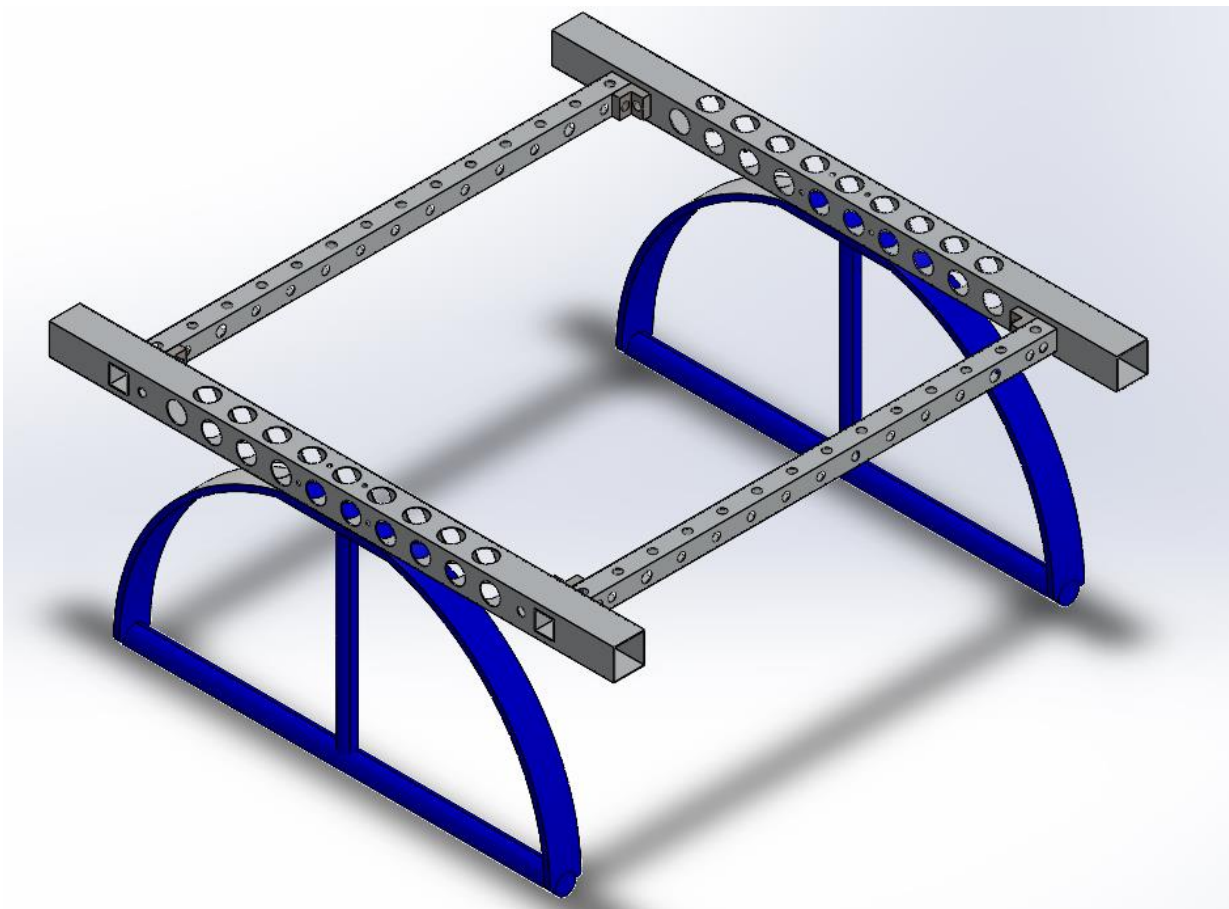


Figure 78: The Landing skid Implemented design

#### 4.3.1 Static Structure Analysis

**First design:**

Made of aluminum and wood

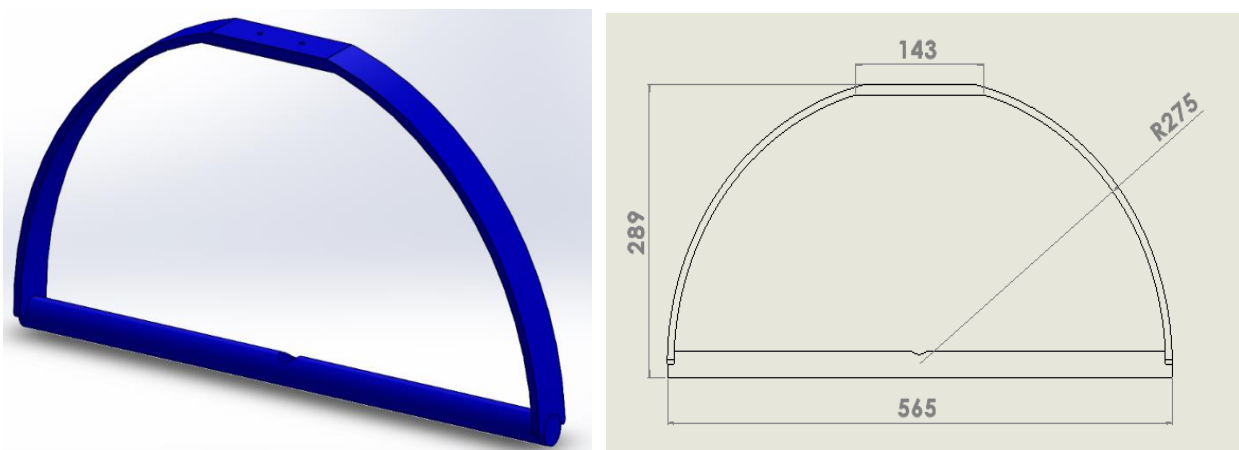


Figure 79: First Design of The Landing skid and its dimensions

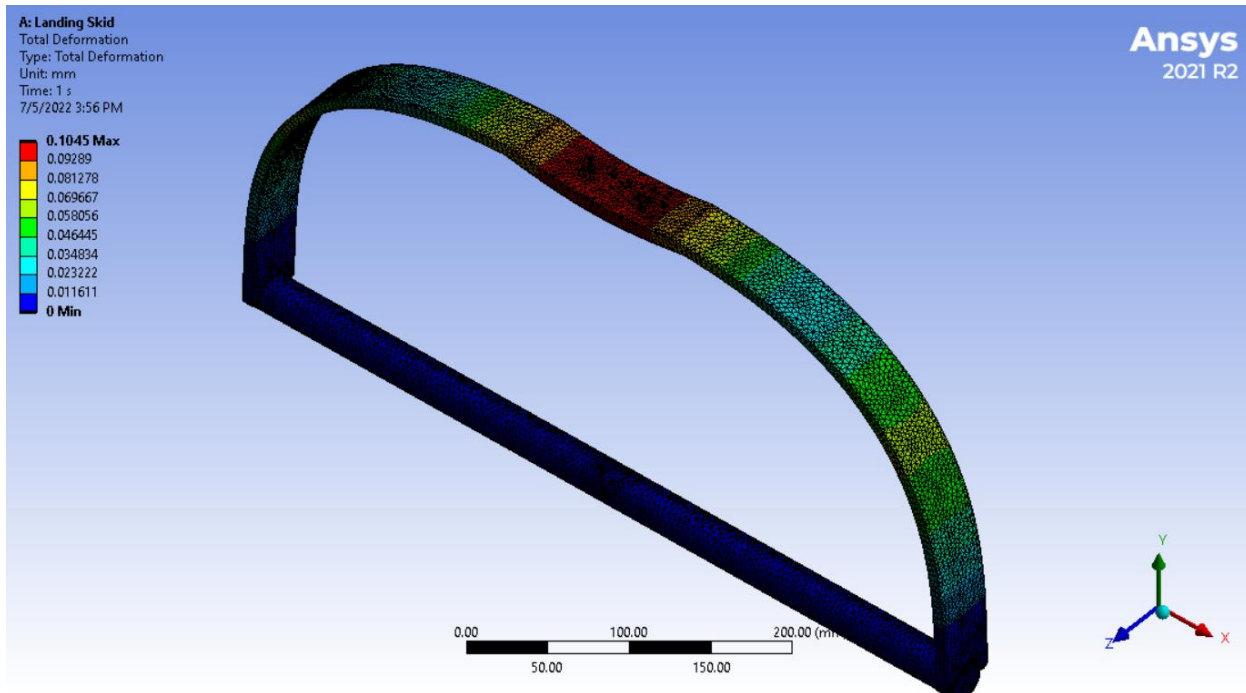


Figure 80: First Design of The Landing skid Total deformation

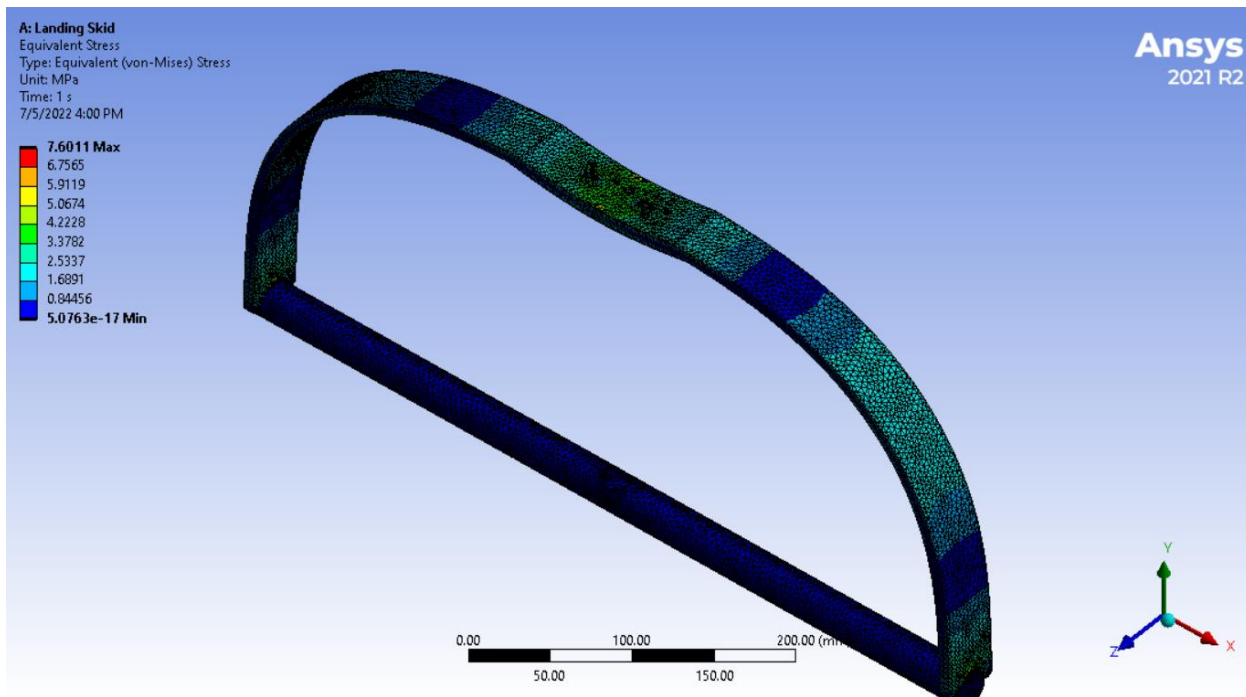


Figure 81: First Design of The Landing skid Stress

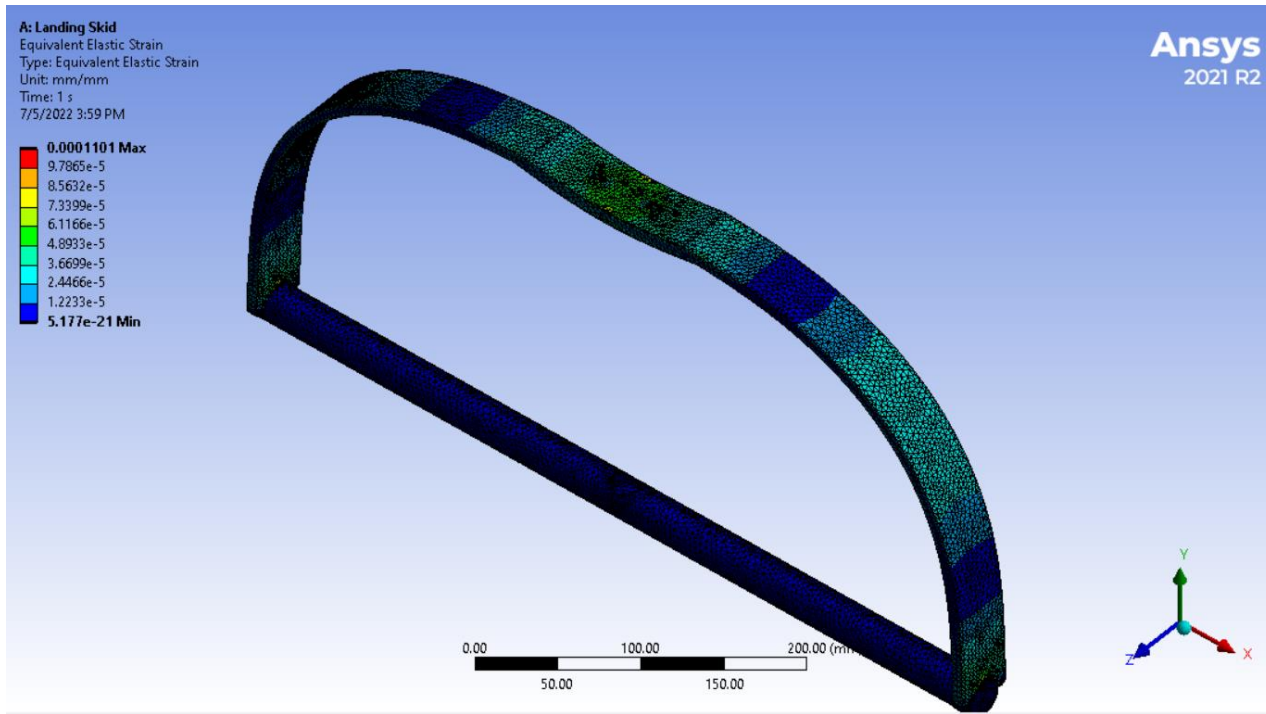


Figure 82: First Design of The Landing skid Strain

Max Deformation (mm)	Max Stress (MPa)	Max Strain (mm)
0.1045	7.6011	0.00011

We notice the increase in deformation and stress, so we're going to reduce it in the next design.

### Second design:

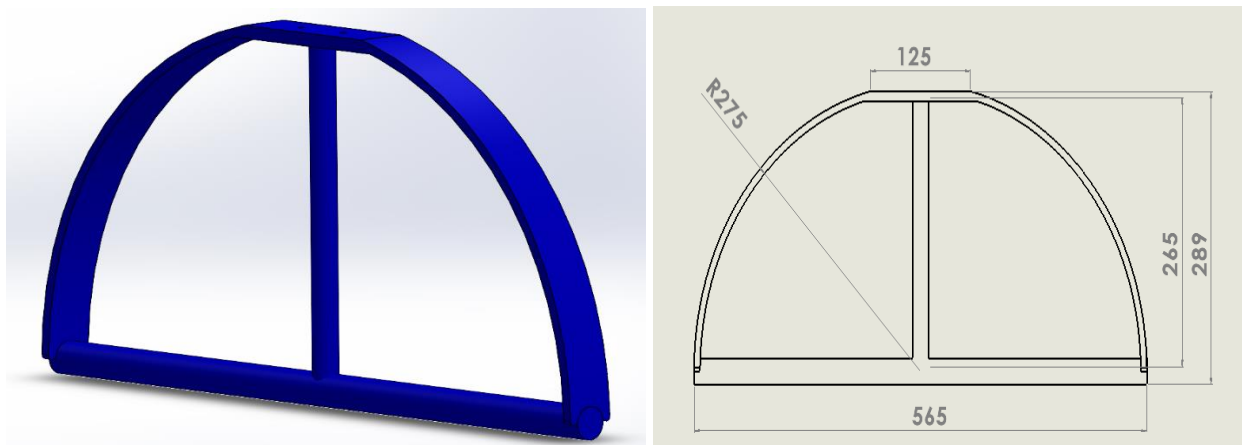


Figure 83: Second Design of The Landing skid and its dimensions

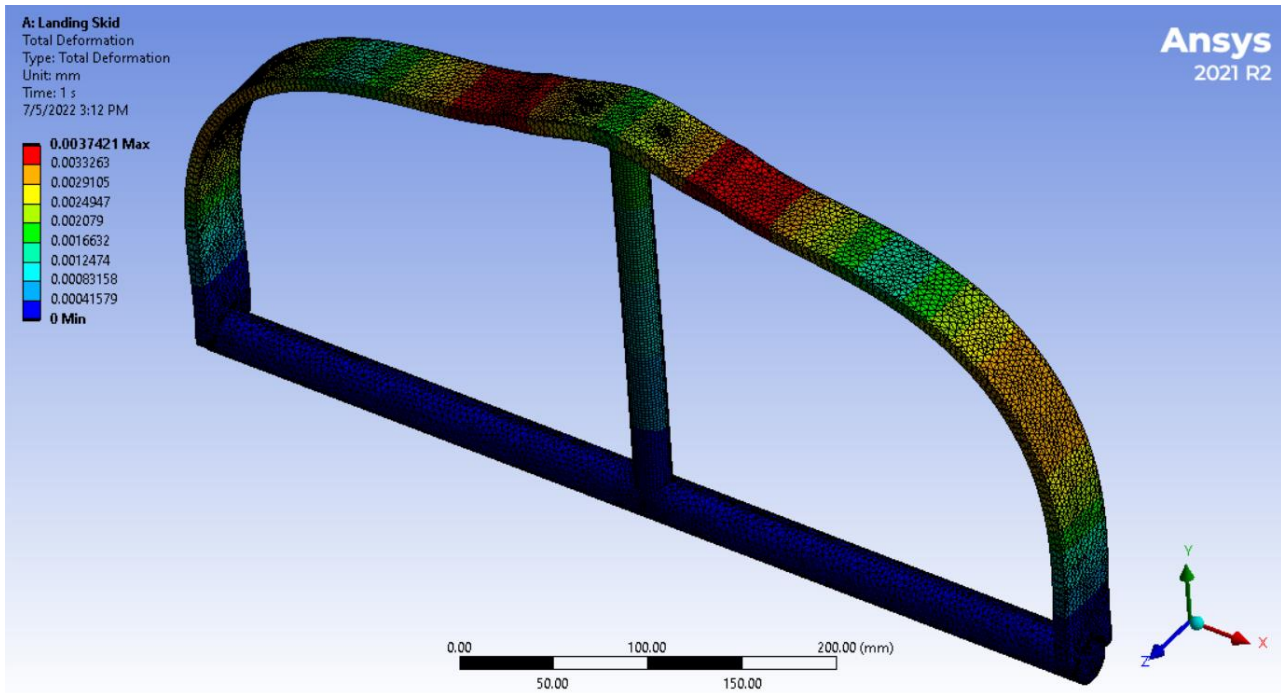


Figure 84: Second Design of The Landing skid Total deformation

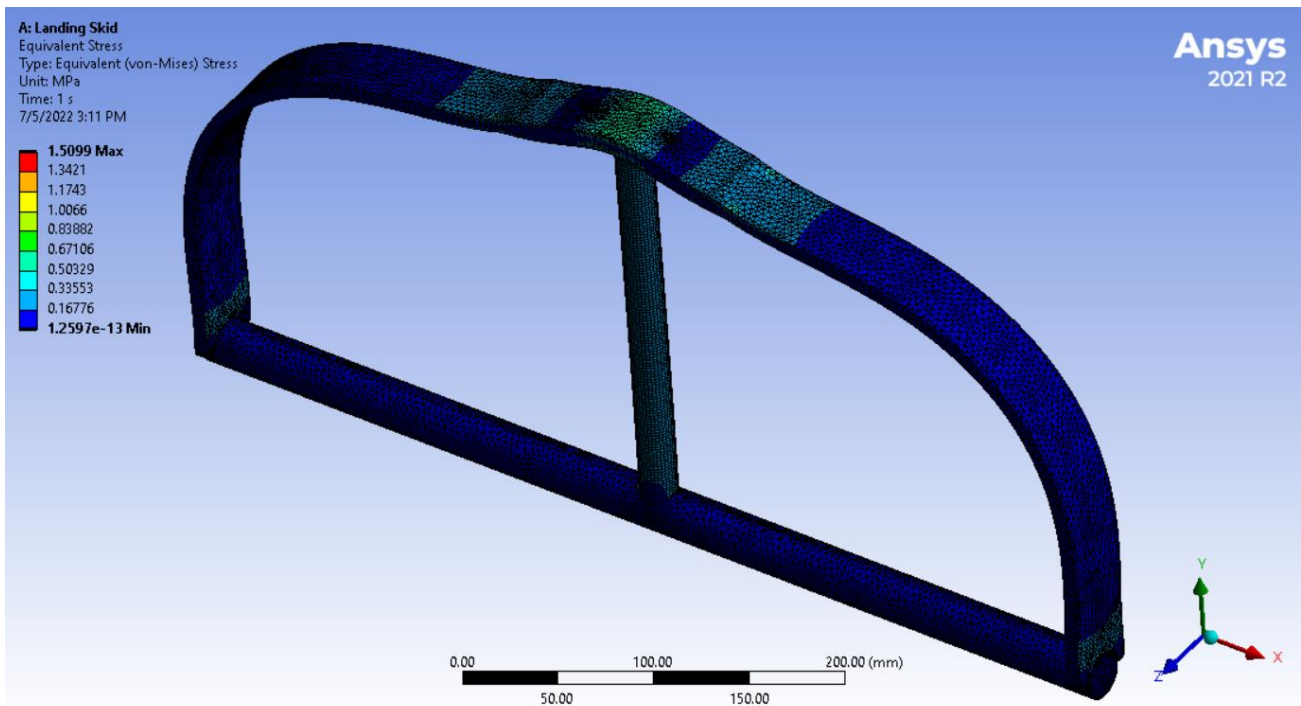


Figure 85: Second Design of The Landing skid Stress

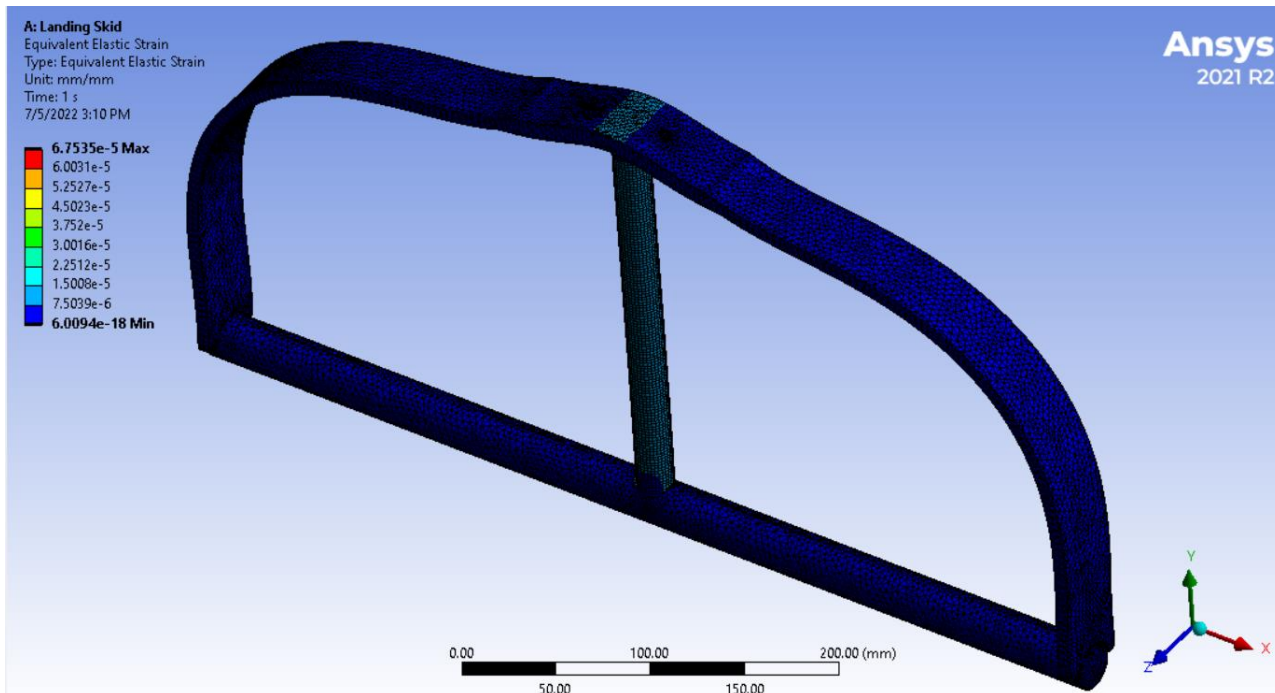


Figure 86: First Design of The Landing skid Strain

model	Max Deformation (mm)	Max Stress (MPa)	Max Strain (mm)
First Design	0.1045	7.6011	0.00011
Second Design	0.003742	1.5099	0.00006753

After we noticed the decrease in deformation and stress in the second design, the second design is better than the first one

### 4.3.2 Impact Analysis:

We had to make an amplified study of loads which could have impacted on models; we start Impact loading and the effect of the force which cause it

To analyze the landing skid, we should have the force acting on it when it falls from known height from the ground, and we get the following equations. And by combining the equations of different kinds of stresses; we can calculate the maximum stresses on it

Impact force	$F = W + ma$
Acceleration	$a = \frac{\Delta v}{\Delta t}$
Impact velocity	$v = \sqrt{2gh}$
Total force on the landing	$F = m \left( 1 + \frac{\Delta v}{\Delta t} \right)$

Compressive stress	$\sigma_{\text{comp.}} = \frac{F}{A}$
Axial stress due to bending	$\sigma_{\text{bend.}} = -\frac{Mz}{I}$
Shear stress	$\tau = \frac{F}{A}$
Max & Min axial stress	$\sigma_1, \sigma_2 = \frac{\sigma_x + \sigma_y}{2} \pm \sqrt{\left(\frac{\sigma_x - \sigma_y}{2}\right)^2 + \tau_{xy}^2}$
Max & Min shear stress	$\tau_1, \tau_2 = \pm \sqrt{\left(\frac{\sigma_x - \sigma_y}{2}\right)^2 + \tau_{xy}^2}$

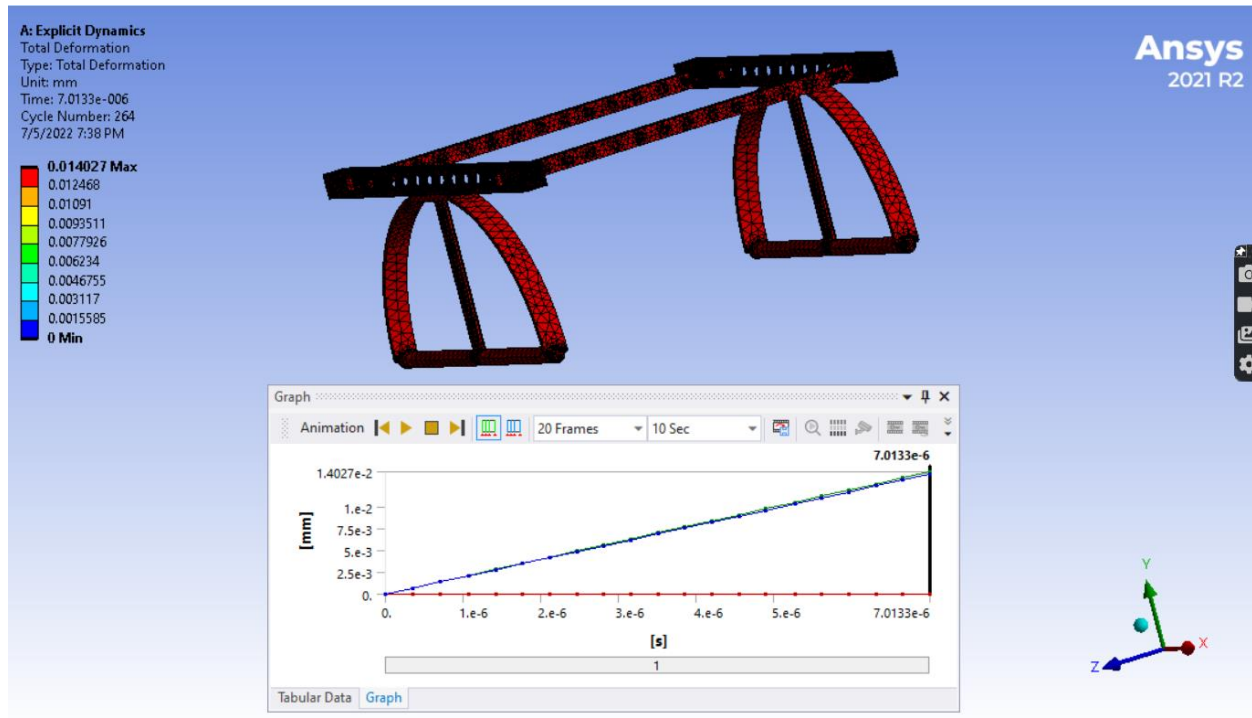


Figure 87: The Impact test of the Landing skid



Figure 88: Implemented design

#### 4.4 Fuselage:

After we defined the shape of fuselage and its dimensions and characteristics in the aerodynamics chapter now came the role of manufacturing in which we found a lot of difficulties and challenges and therefore to design a strong body and at the same time lightweight so we chose blue foam in its manufacture because of its strength and light weight, but for full scale prefers to use composite materials in manufacturing

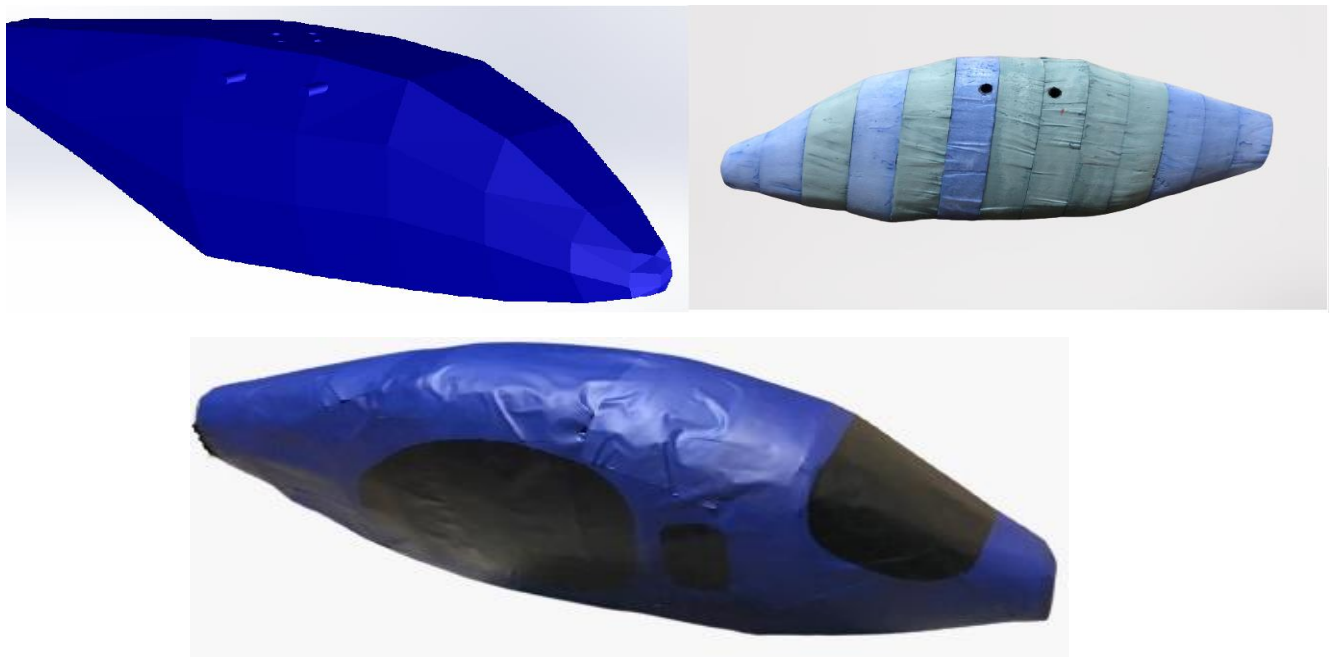


Figure 89: Fuselage CAD design and Implemented design

#### 4.4.1 Static Structure Analysis

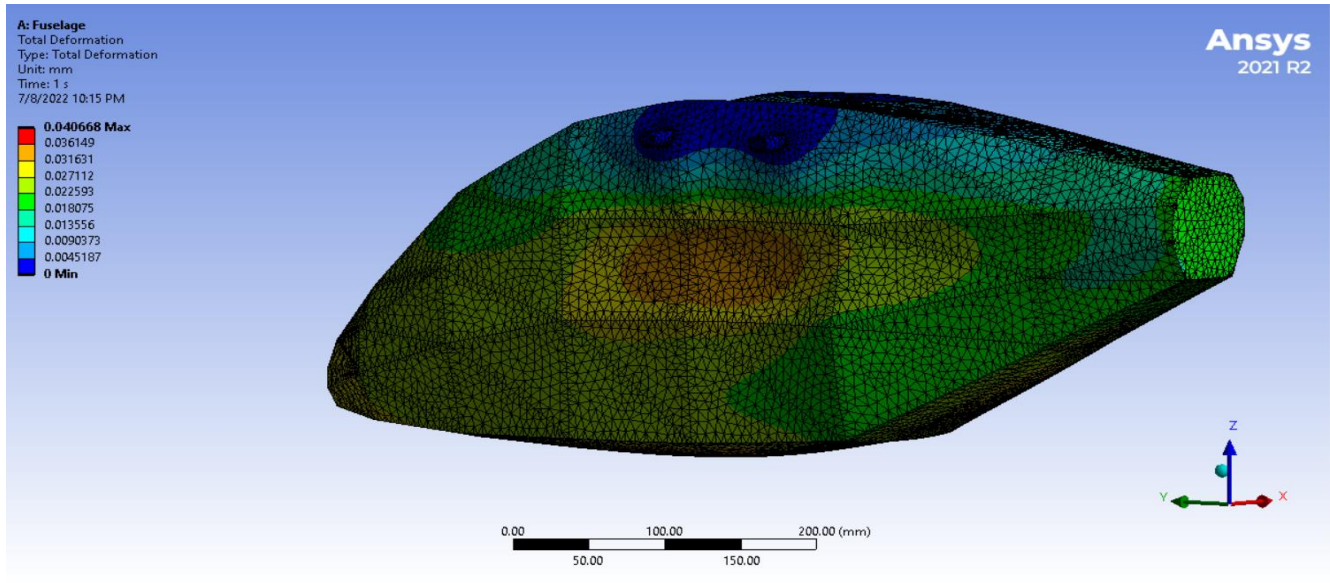


Figure 90: Fuselage CAD design Total deformation

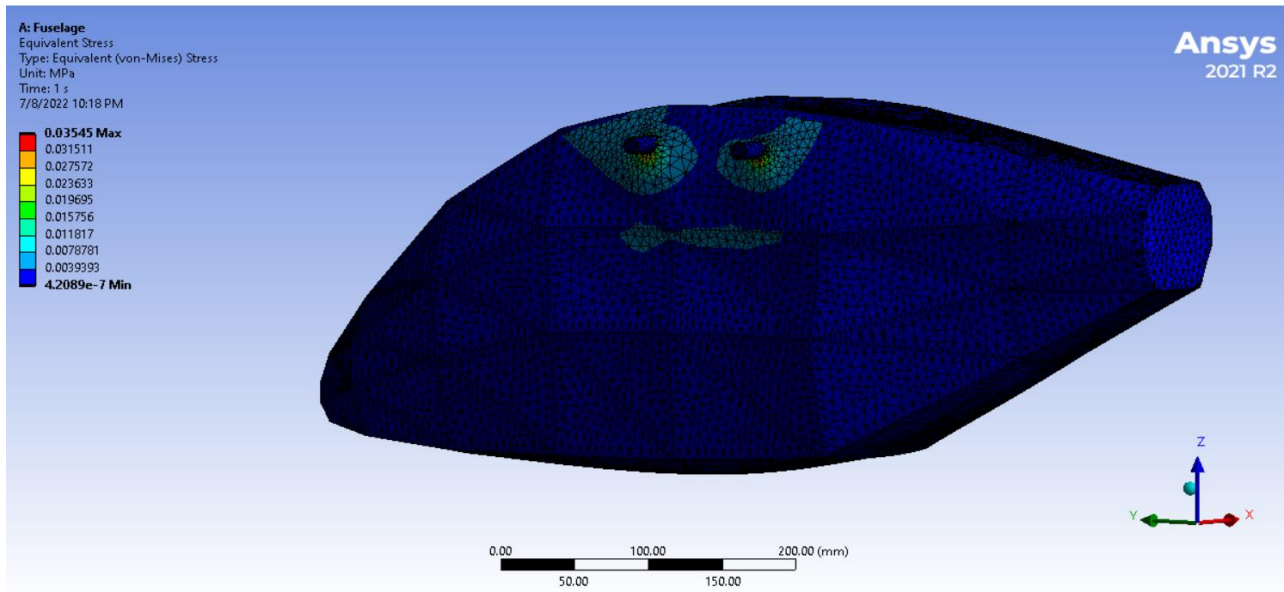


Figure 91: Fuselage CAD design Stress

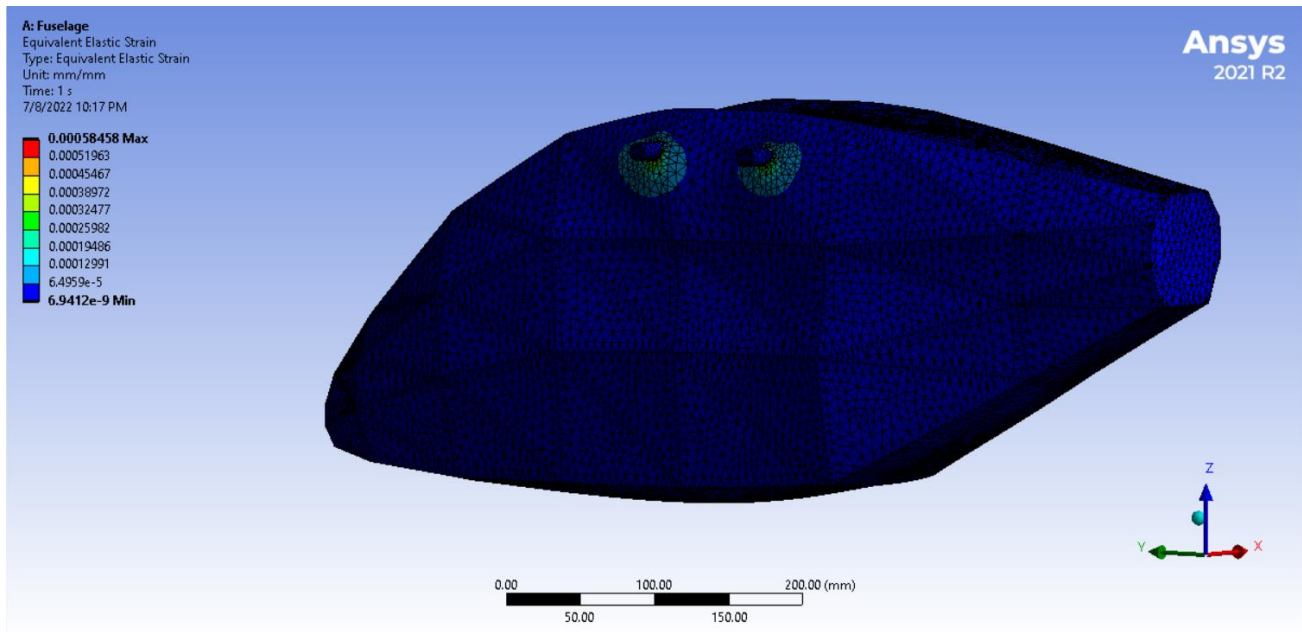


Figure 92: Fuselage CAD design Strain

#### 4.4.2 Fuselage installation:

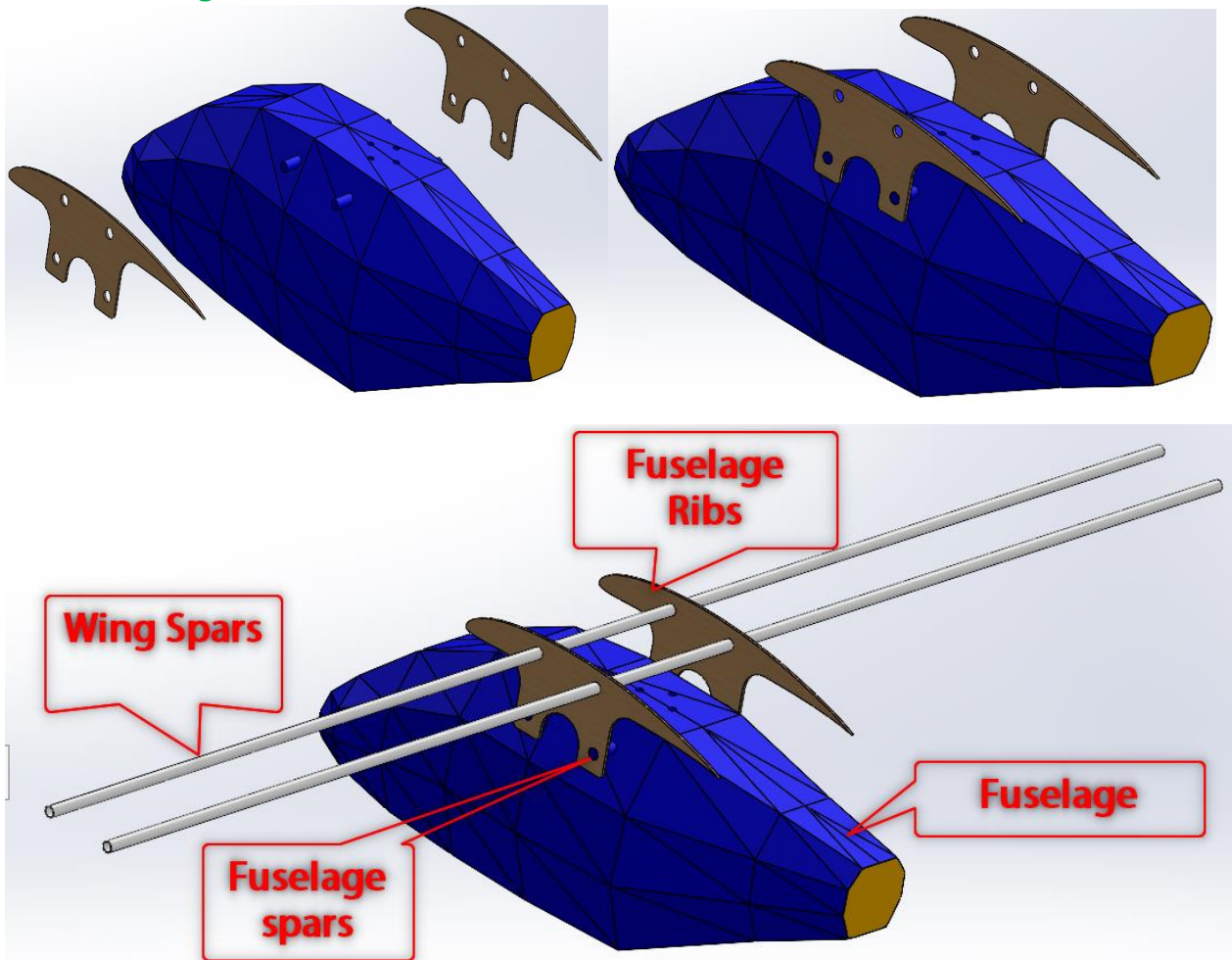


Figure 93:Fuselage installation

The fuselage is fixed to the fuselage ribs by fuselage spars and then the fuselage ribs are fixed to the wing spars

#### 4.5 Wing:

After studying the characteristics and dimensions of the wing, we entered the manufacturing stage at the beginning. We chose blue foam to manufacture and cut it in the required dimensions using hot wire. We also supported the wing with spars to strengthen it and chose aluminum for the manufacture of spar

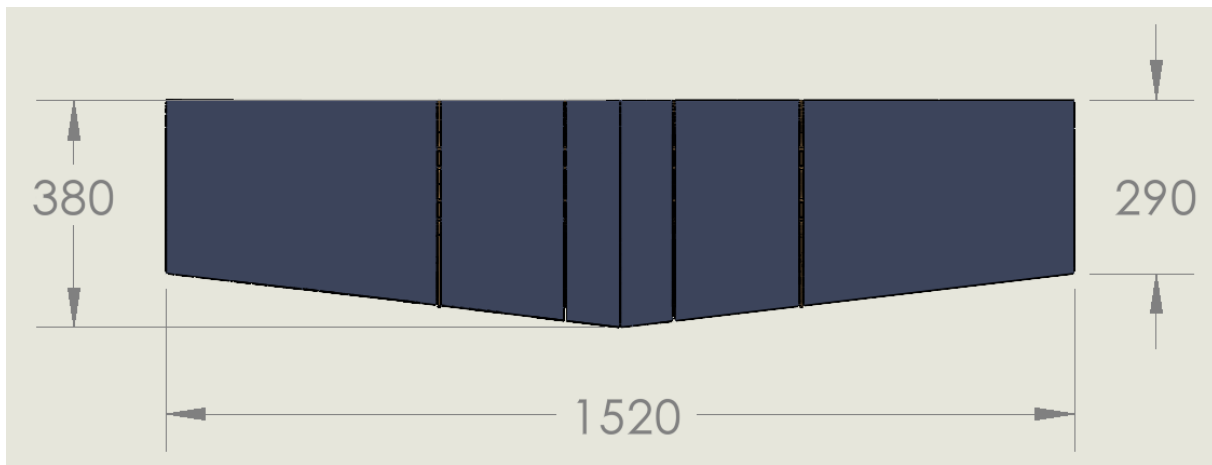


Figure 94: Wing dimension

#### 4.5.1 Static Structure Analysis

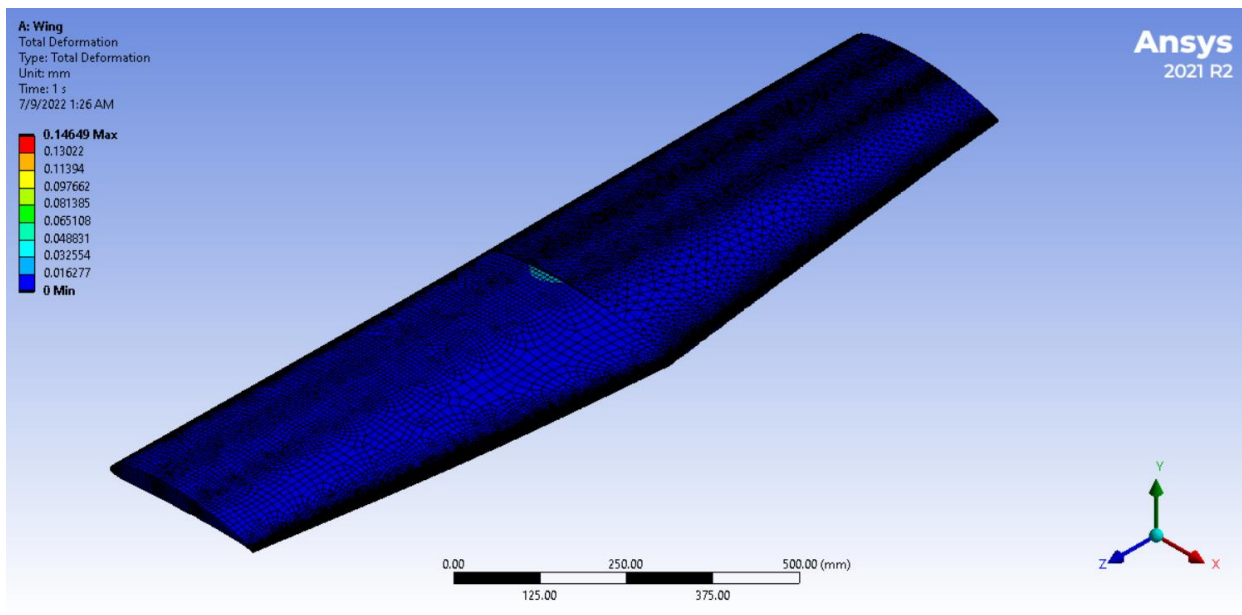


Figure 95: Wing CAD design Total deformation

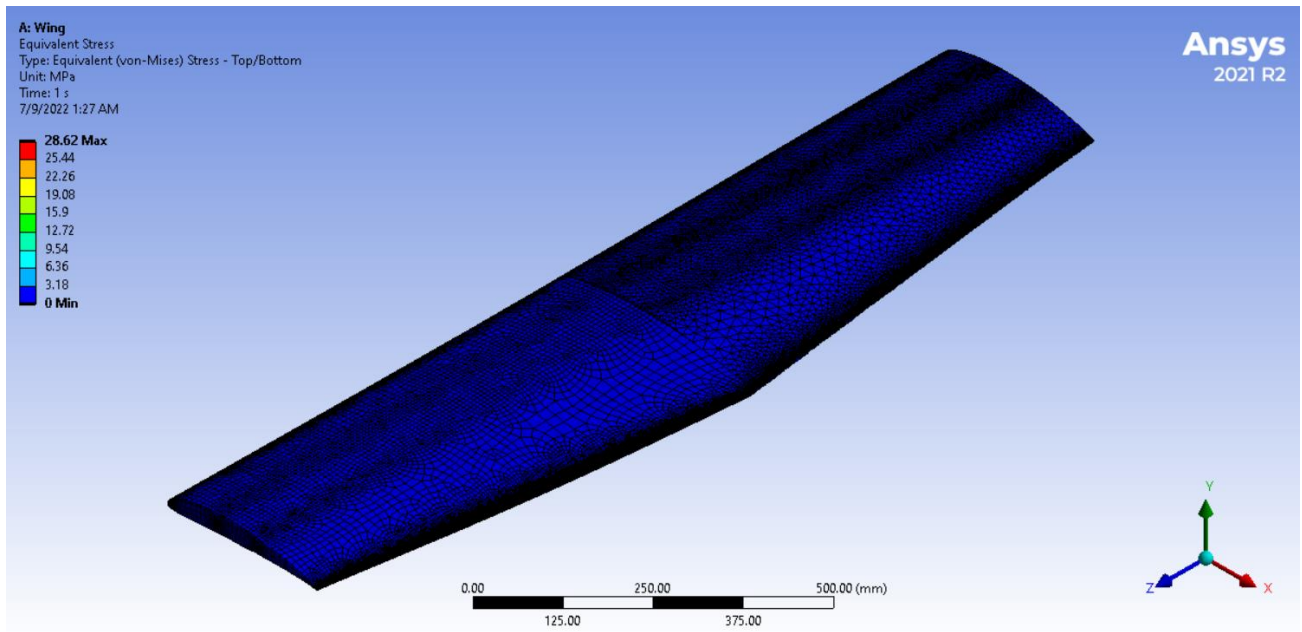


Figure 96: Wing CAD design Stress

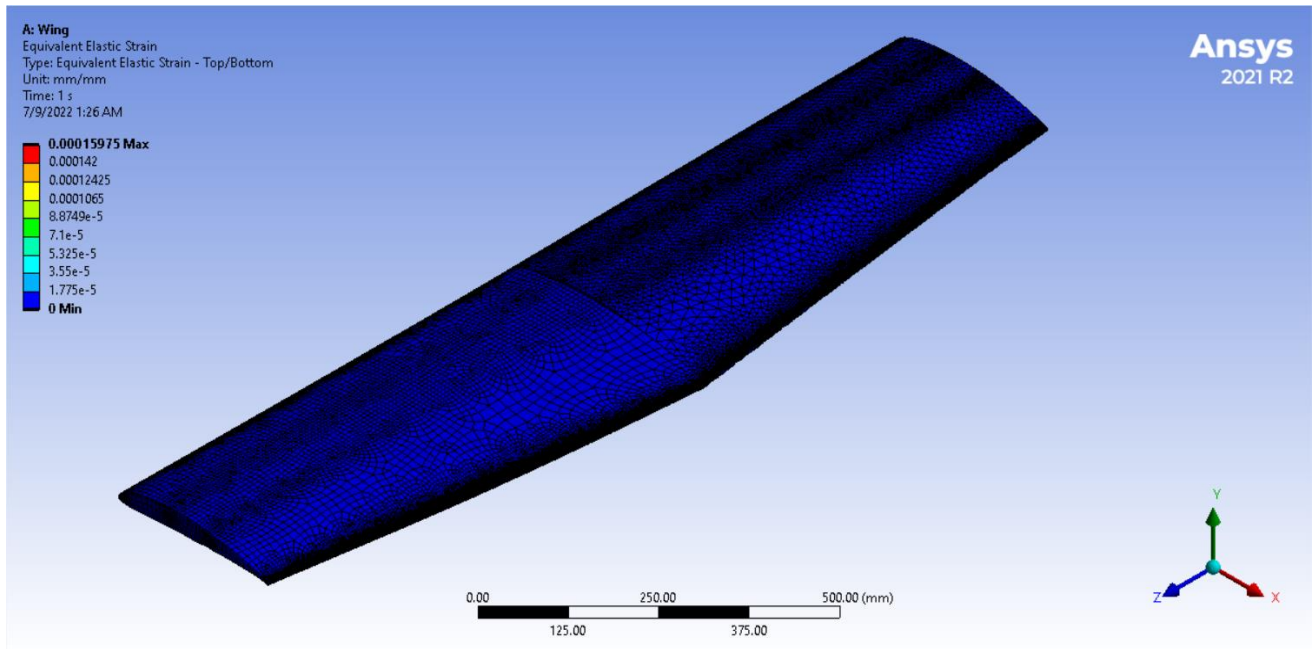


Figure 97: Wing CAD design Strain

#### 4.5.2 Wing installation:

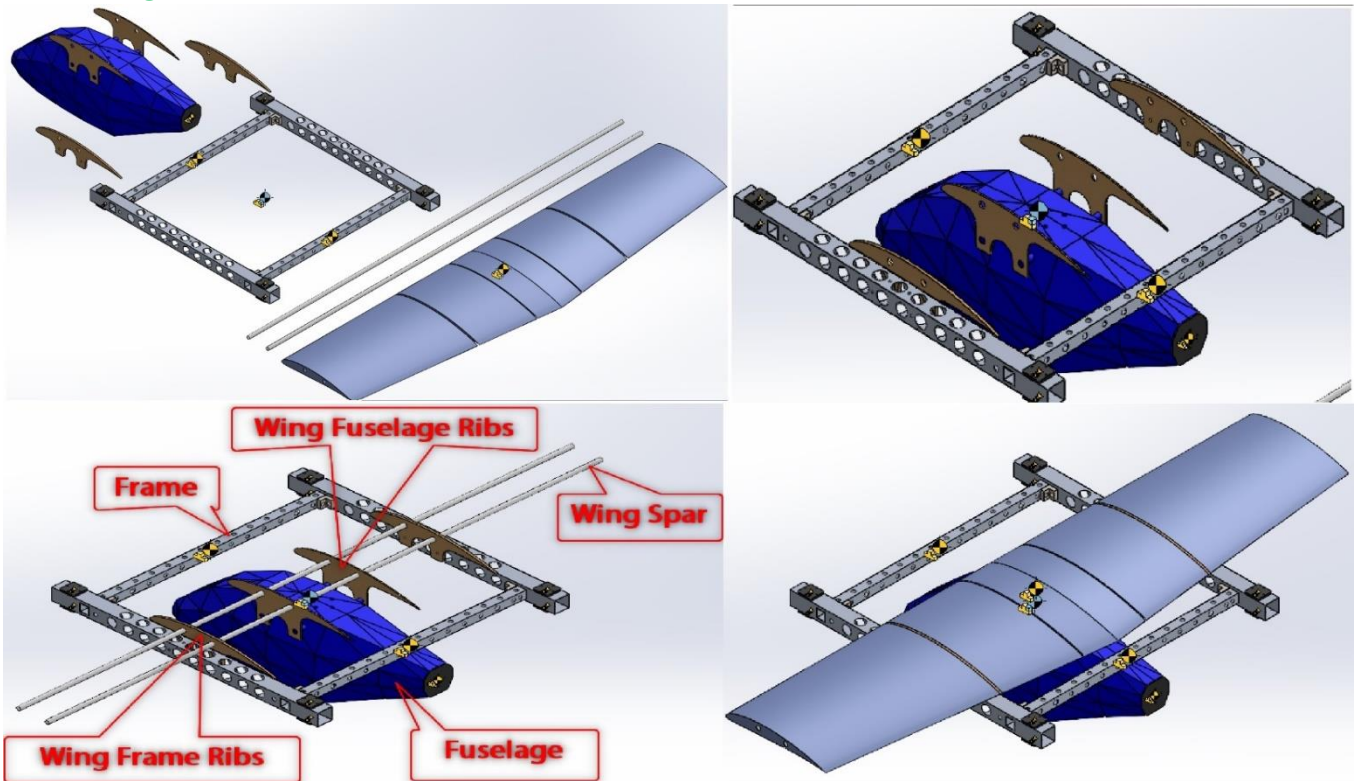


Figure 98: Wing Frame installation

The fuselage and frame are fixed to the wing spars by means of wooden ribs that are installed between the frame and the wing spar and other ribs are installed between the fuselage and the wing spar

#### 4.5.3 Wing Spar Static Structure Analysis

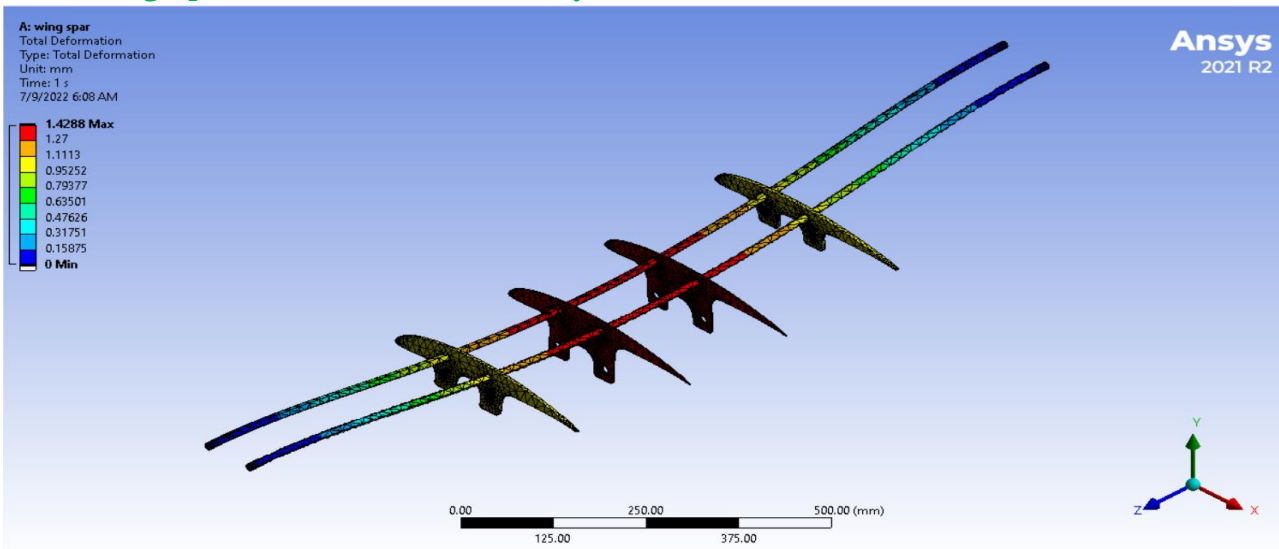


Figure 99: Wing Spar CAD design Total deformation

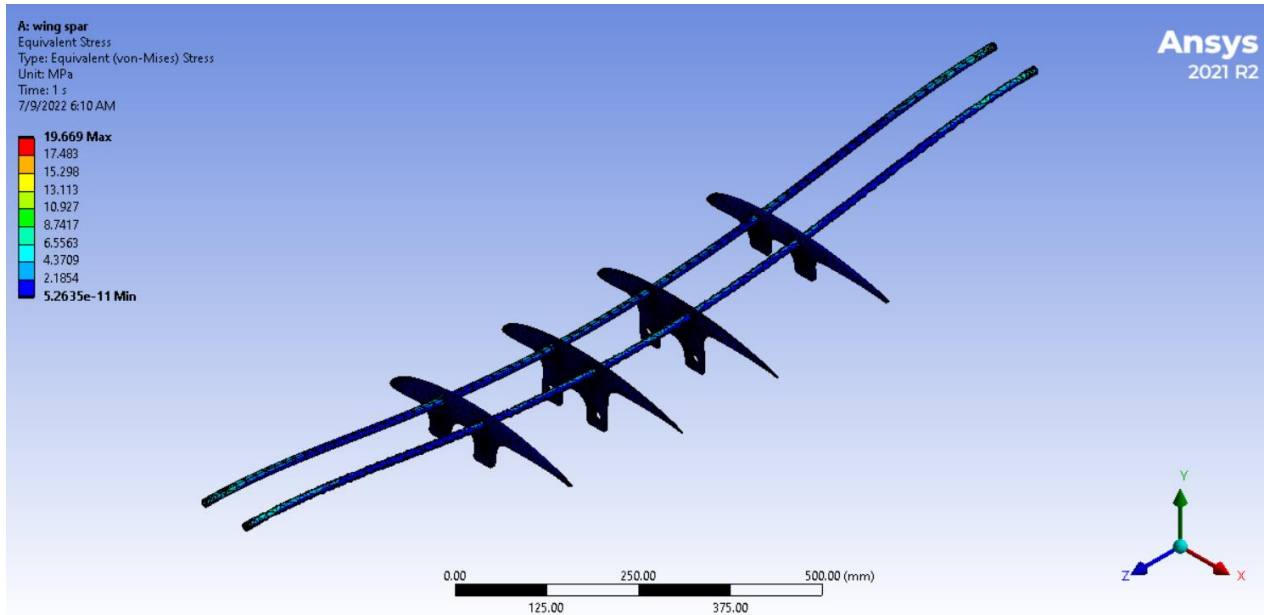


Figure 100: Wing Spar CAD design Stress

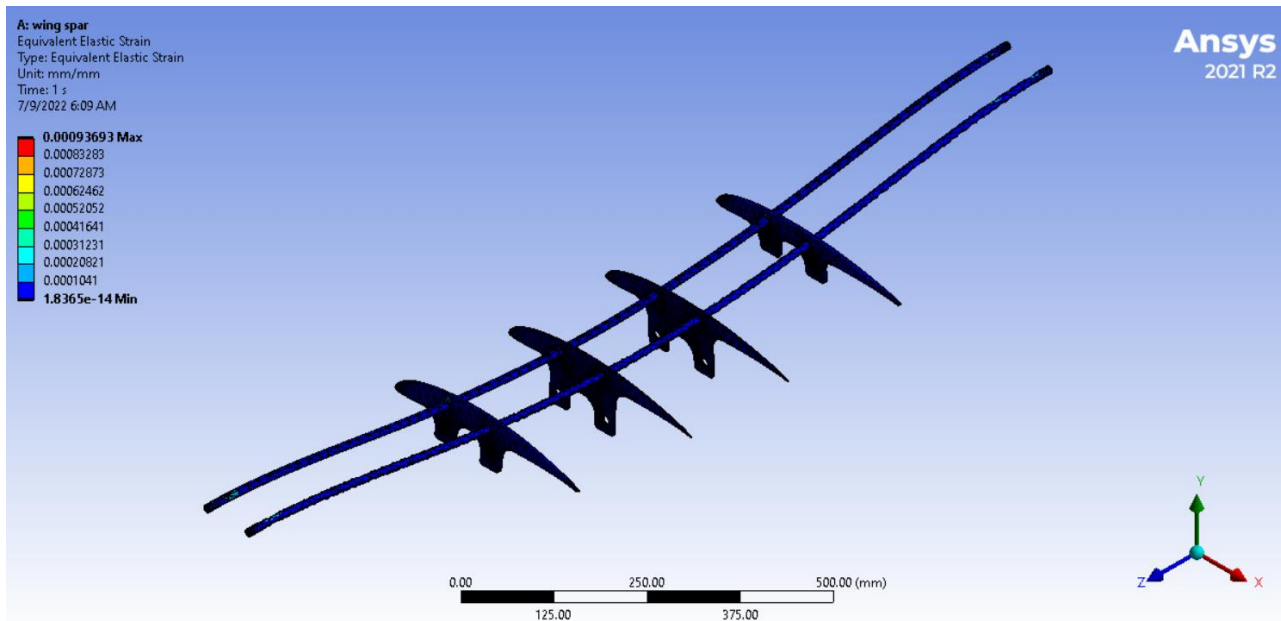


Figure 101: Wing Spar CAD design Strain

**Obviously, the wing spar is subjected to forces in more than one place and therefore is subjected to bending, so it must be very strong to withstand these loads.**

## 4.6 Tail

Finally, to manufacture the tail, we used blue foam to manufacture it due to its light weight and performance of the function required of it

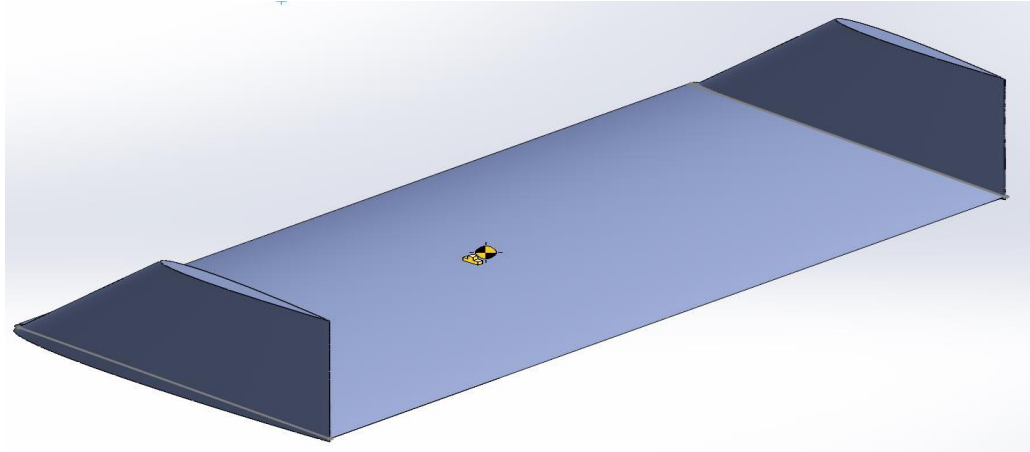


Figure 102: Tail CAD design

### 4.6.1 Tail installation:

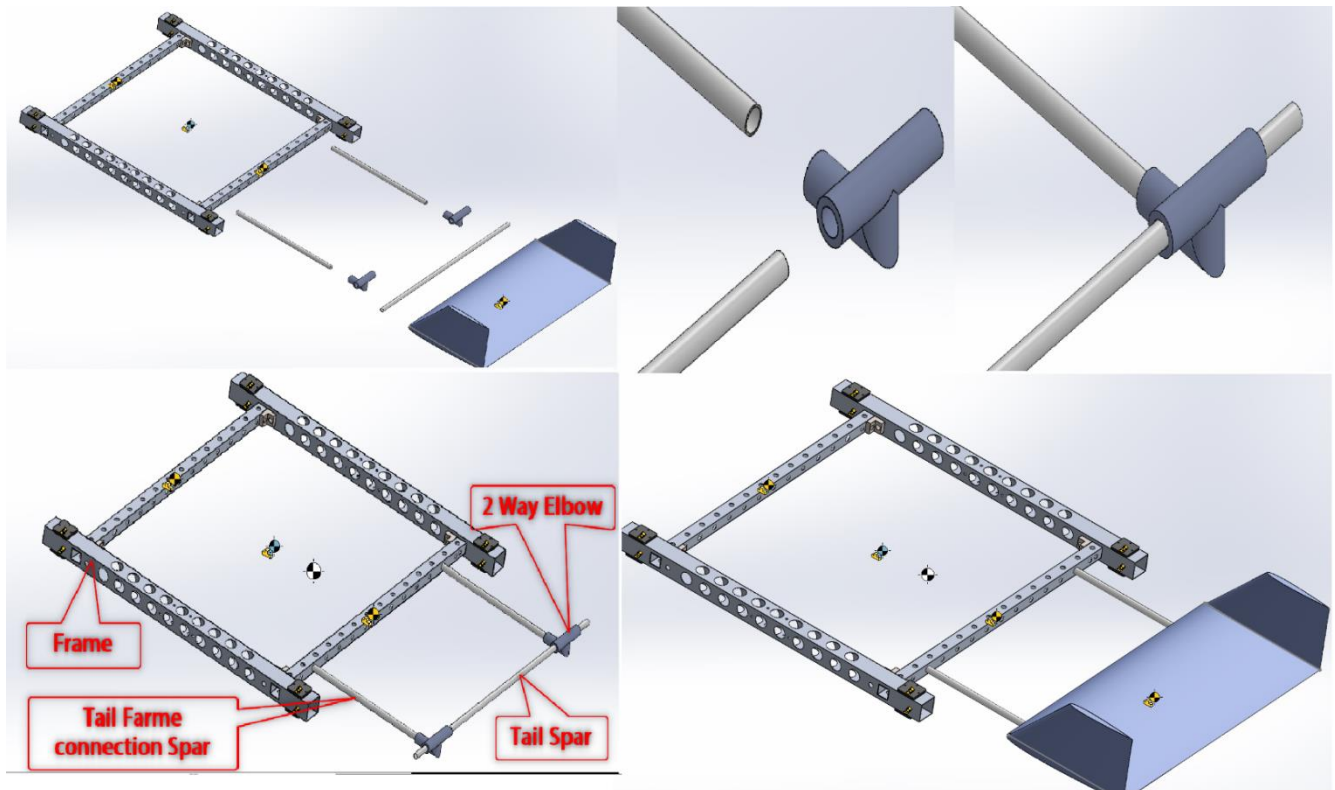


Figure 103: Tail Frame installation

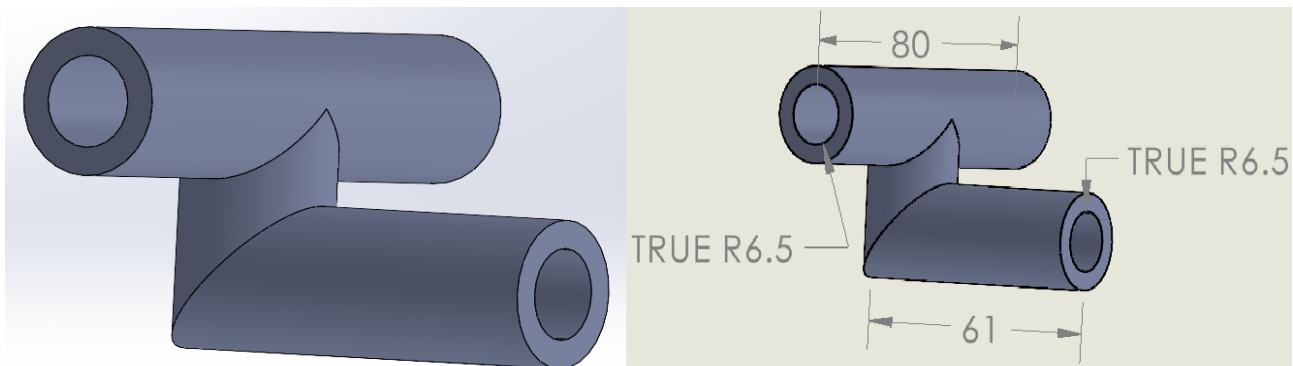


Figure 104: Two Way Elbow (3D printed)

The tail frame connection Spare is fixed in the frame from one end and the other end is held by a plastic elbow. The tail spar is held with the same elbow but in another direction, and then the tail is attached to the tail spar

#### 4.6. Tail Spar Static Structure Analysis:

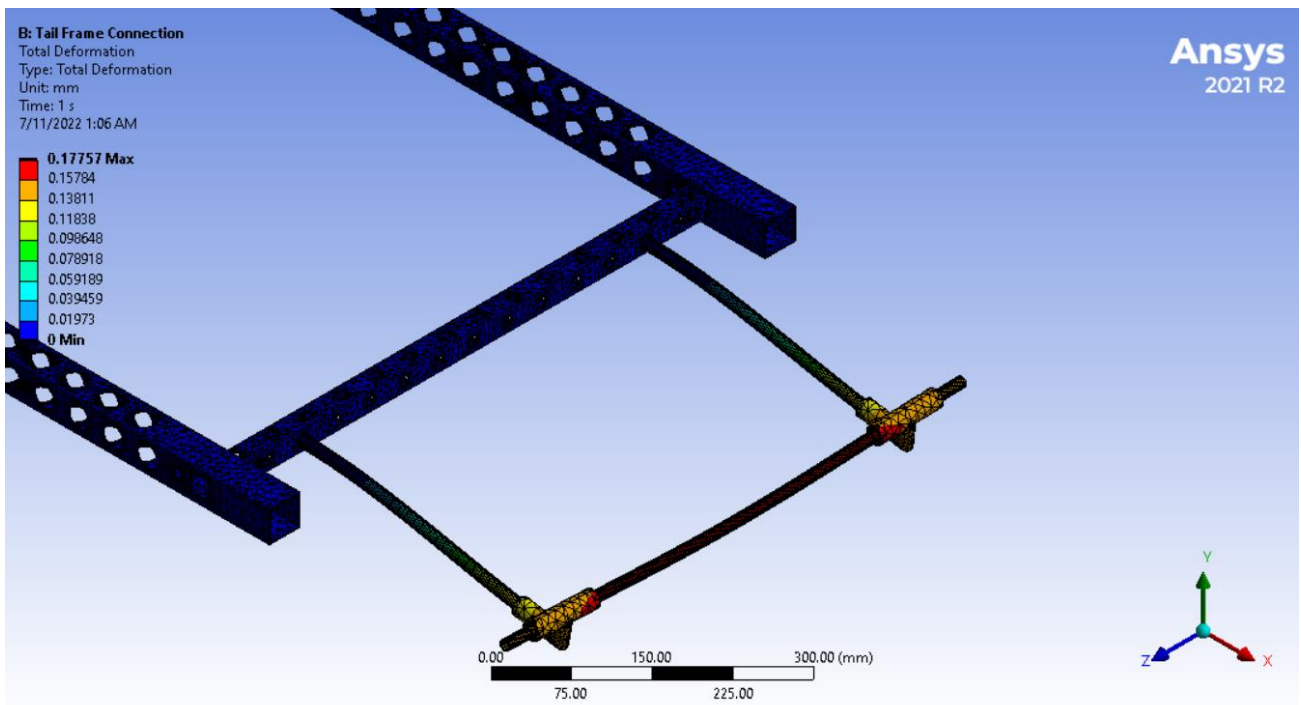


Figure 105: Tail Spar CAD design Total deformation

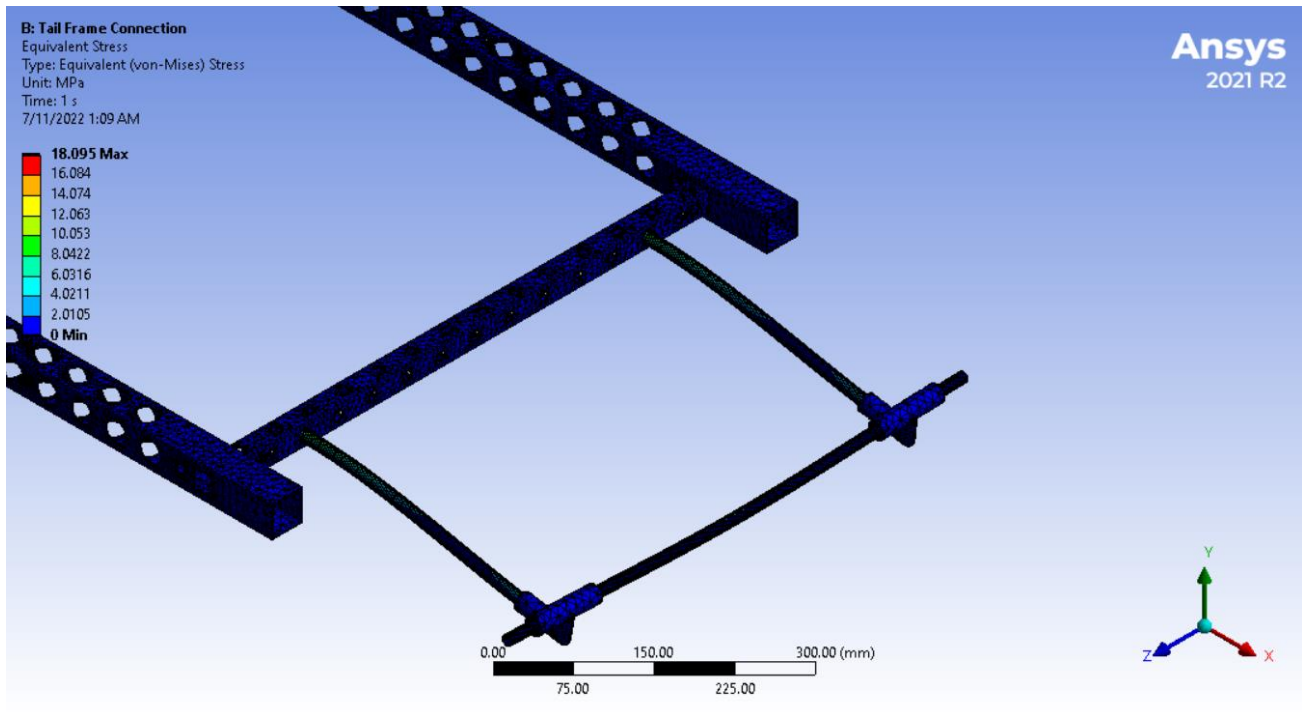


Figure 106: Tail Spar CAD design Stress

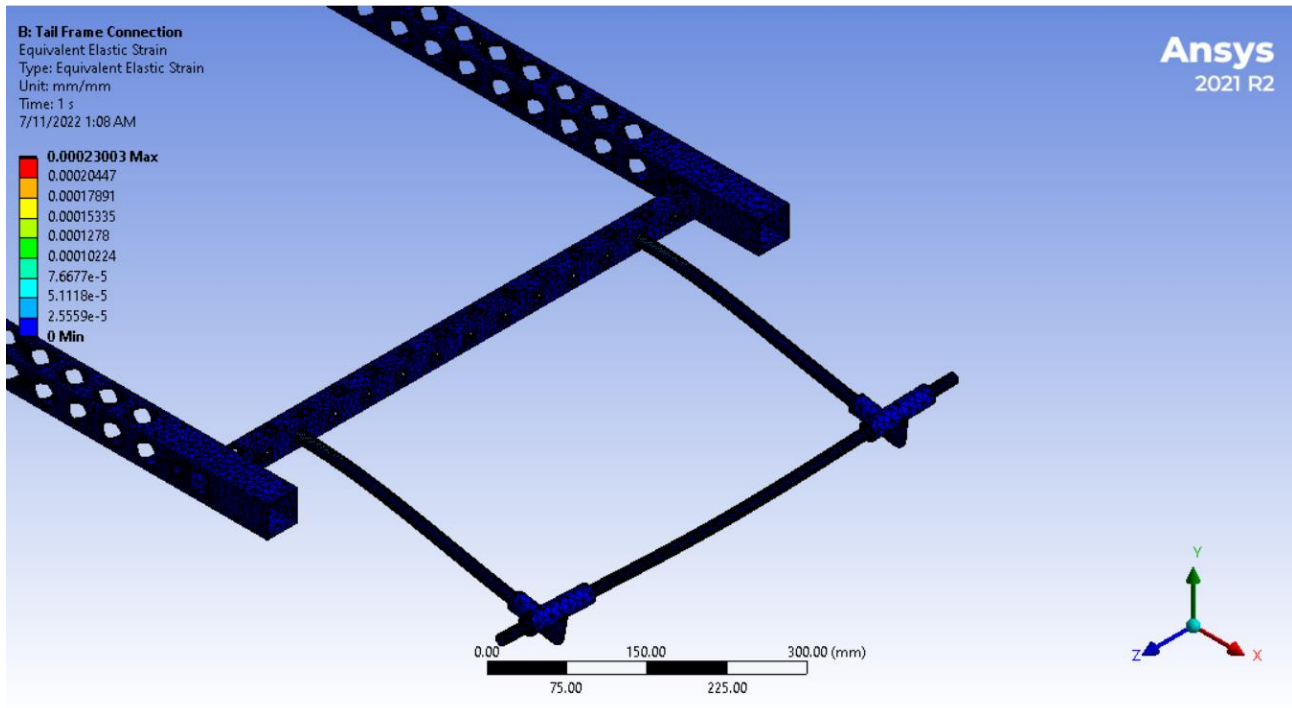


Figure 107: Tail Spar CAD design Strain

We note that the materials and dimensions used are appropriate and able to perform their task. The thickness of the spar can also be increased to reduce stress even more

#### 4.7 Assembled Structure:

After we have completed the details of all the parts of the structure of the flying vehicle, we assemble them together as shown

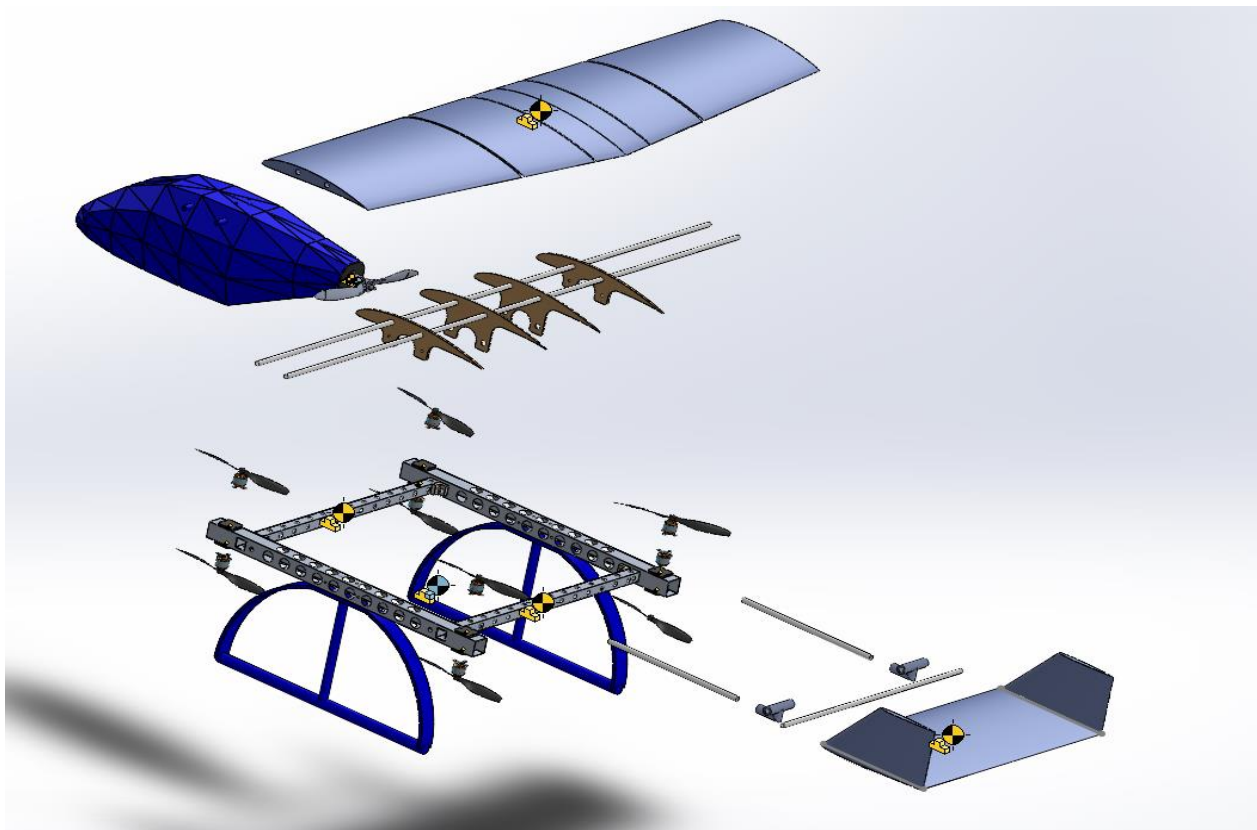


Figure 108: Assembly Exploded view

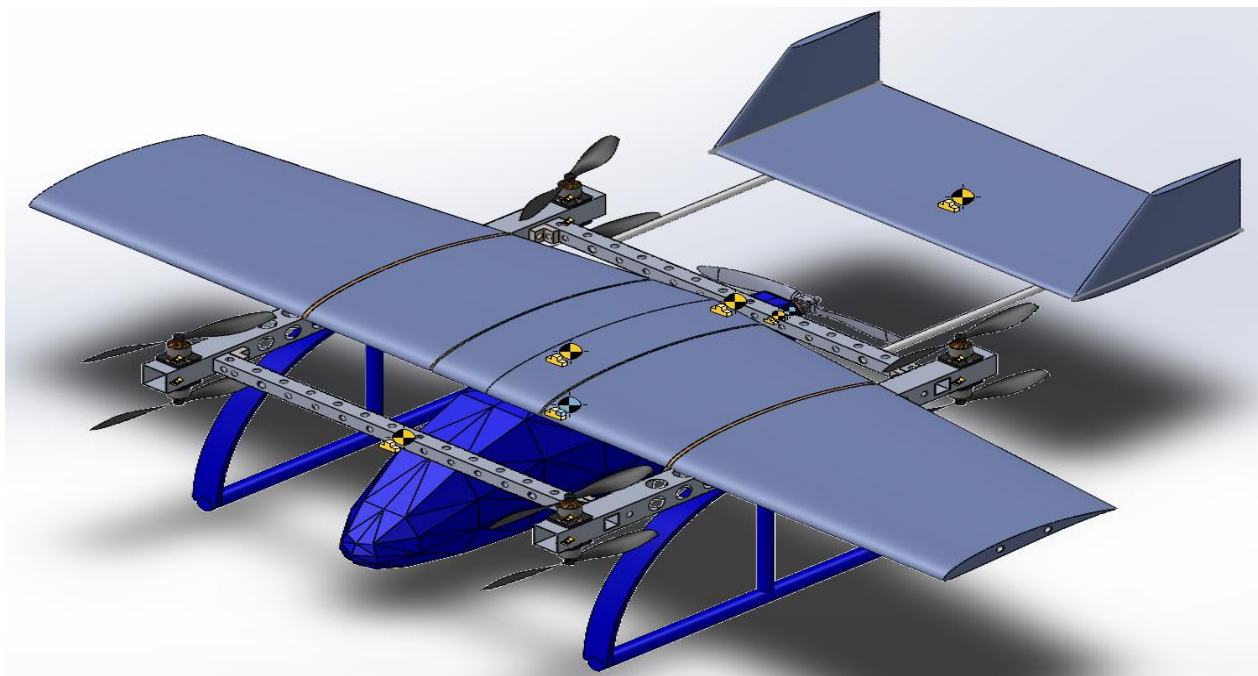


Figure 109: Final Assembly

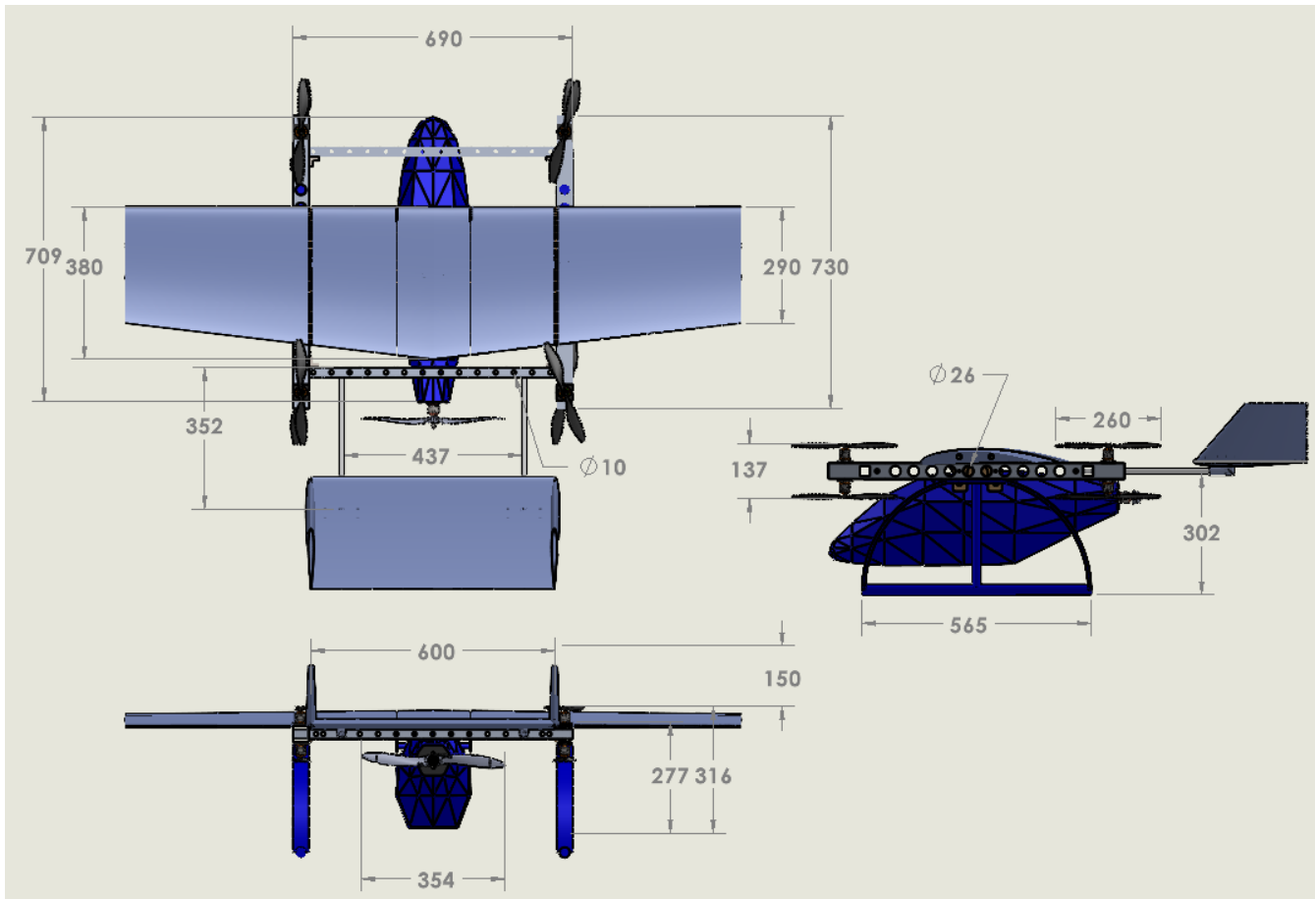


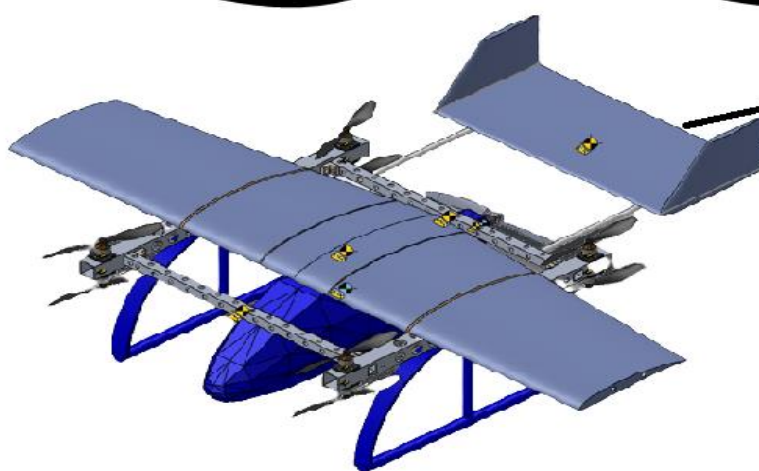
Figure 110: Final Assembly dimensions (mm)



*Figure 111: Implemented design*

# **Chapter Five:**

# **Experimental study**



## 5.1. Introduction

The main reason for going through this chapter is to study the factors that affect the performance of coaxial rotors, and to choose the most suitable setup to get the best performance. But we have limit on the current that is drawn by the ESCs.

## 5.2. Coaxial Rotors

The configuration of coaxial rotors was first used in helicopters. The idea of coaxial rotors here is to generate more lift with less space used, by using two motors rotating in opposite directions and on the same vertical axis

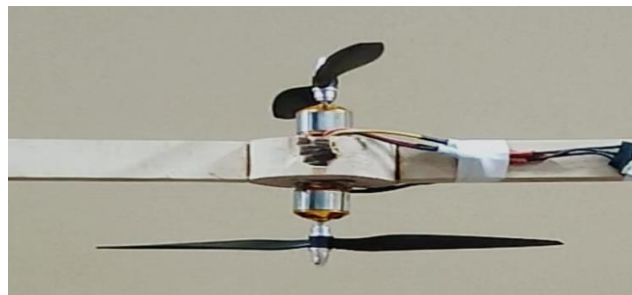


Figure 112: Coaxial test rig

### Factors that affect the performance:

- 1- Battery configuration
  - ❖ 2Cell Battery (7.4V)
  - ❖ 3Cell Battery (11.1V)
- 2- Diameter of the propellers
  - ❖ 1045 Propeller (Diameter=10 inches=25.4cm)
  - ❖ 1245 Propeller (Diameter=12 inches=30.48cm)
- 3- Coaxial rotors vertical spacing
  - ❖ 14cm
  - ❖ 16cm

The motors are connected to ESCs which are connected to an Arduino board, so the input to Arduino is the throttle taking values (0: 100), and PWM signals are sent from the Arduino to the ESC to the motor.

We can measure the force that is generated, current, voltage, and electrical power which can be calculated       $Power = V * I$

Here we make our test bench to test our motors and performance and coaxial performance.

### 5.3. Battery Comparison

#### 5.3.1. One motor with a propeller 1045

Here we are testing one motor with propeller 1045 using different batteries.

One motor using 3Cell battery with propeller 1045				
throttle	amp A	voltage V	power watt	thrust gm
0	0.1	11.95	1.1	0
15	0.5	11.71	5.855	30
20	1.1	11.71	12.881	90
25	1.8	11.7	21.06	140
30	3.1	11.65	36.115	230
35	4.9	11.5	56.35	320
40	7.5	11.52	86.4	440
45	9.9	11.42	113.058	530
50	13.1	11.31	148.161	630
55	16.1	11.18	179.998	710
60	19.4	11.06	214.564	790

One motor using 2Cell battery with propeller 1045				
throttle	amp A	voltage V	power watt	thrust gm
0	0.1	8.25	0.825	0
15	0.3	8.24	2.472	10
20	0.8	8.24	6.592	50
25	1.2	8.23	9.876	70
30	1.9	8.2	15.58	120
35	2.9	8.18	23.722	170
40	4.2	8.12	34.104	230
45	5.8	8.08	46.864	290
50	7.9	7.99	63.121	360
55	10.2	7.92	80.784	430
60	12.7	7.84	99.568	500
65	15.3	7.73	118.269	560
70	17.6	7.66	134.816	610

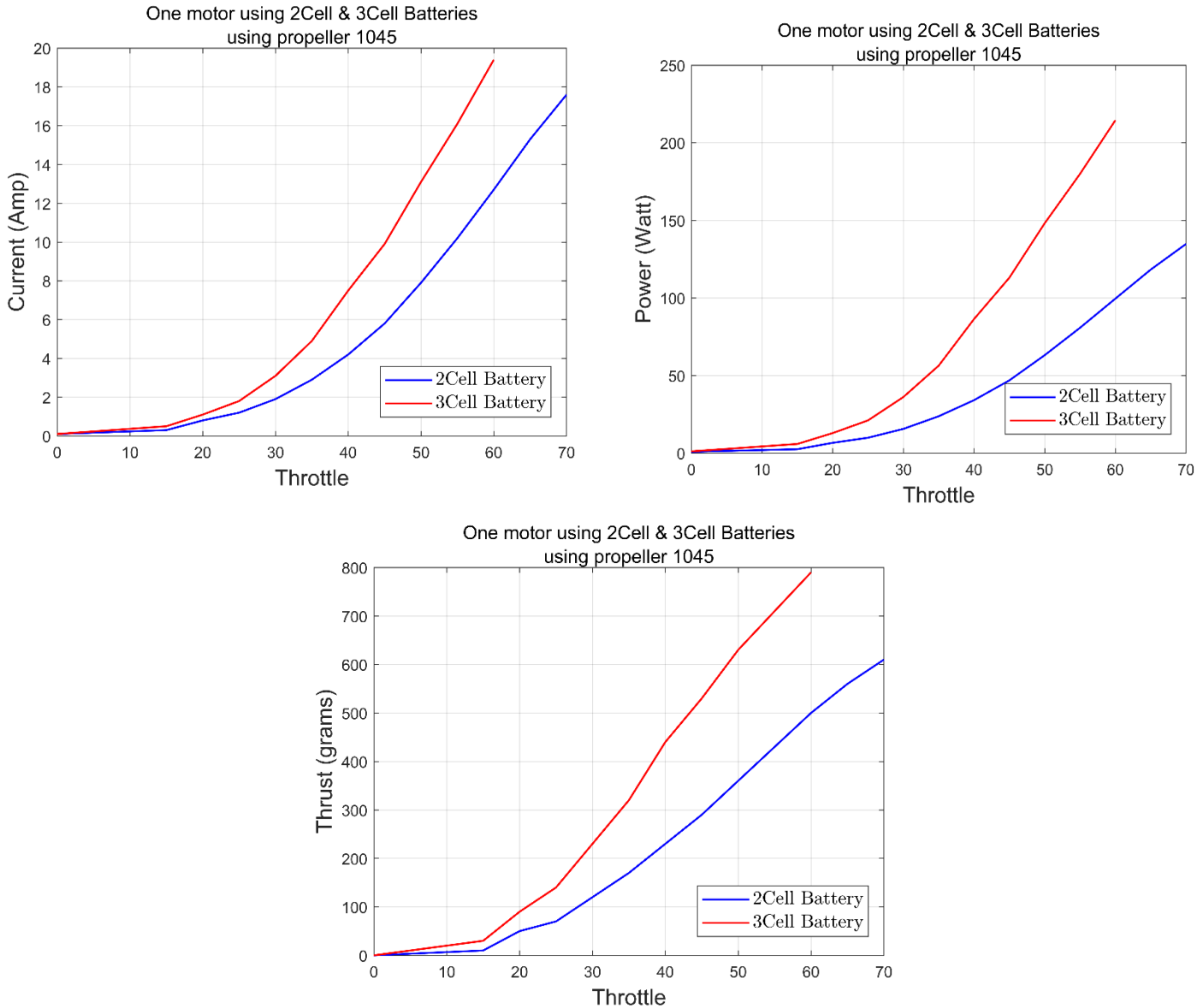


Figure 113:One motor using 2Cell battery with propeller 1045



Figure 114 :One motor using 3Cell battery with propeller 1045

After we tested and measured current, voltage, power, and thrust. We can get our graphs to compare between batteries



We can see the difference between 2Cell and 3Cell batteries. The motor takes higher current with 3Cell battery, unlike the 2Cell battery, so the result in power for 3Cell is more than the power for 2Cell, and the result in thrust we can see that 3Cell battery is more efficient than 2Cell battery and it can lift more weight.

Conclusion, 3Cell battery is better than 2Cell battery when using propeller 1045, due to the relation between power and voltage  $Power = V * I$ , so when increasing voltage then the power will increase, and the result in thrust by increasing. Due to data sheet of motor, we cannot get more cell than 3cell.

### 5.3.2. One motor with a propeller 1245

Here we are testing one motor with propeller 1245 using different batteries.

One motor using 2Cell battery with propeller 1245				
throttle %	amp A	voltage V	power watt	thrust gm
0	0.1	8.2	0.82	0
15	0.4	8.05	3.22	5
20	1	8.03	8.03	20
25	1.5	7.98	11.97	50
30	2.8	7.98	22.344	100
35	4	7.92	31.68	140
40	6	7.85	47.1	190
45	8	7.78	62.24	250
50	10.2	7.72	78.744	310
55	12.8	7.62	97.536	350
60	15.5	7.53	116.715	400
65	18.1	7.43	134.483	440



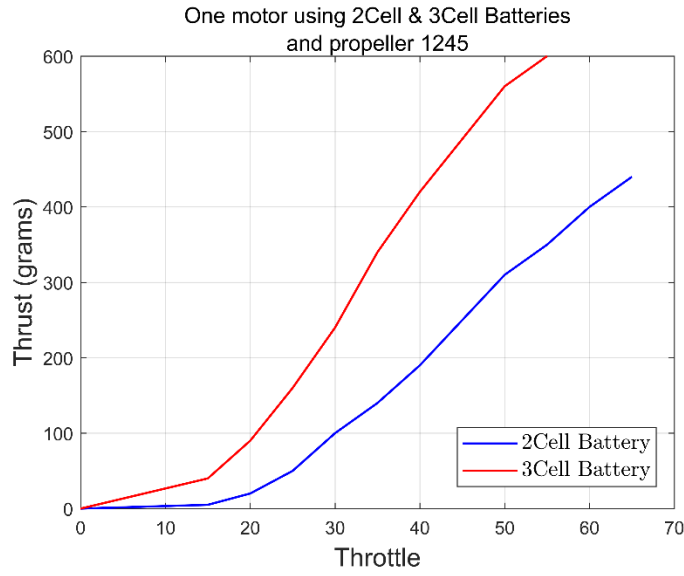
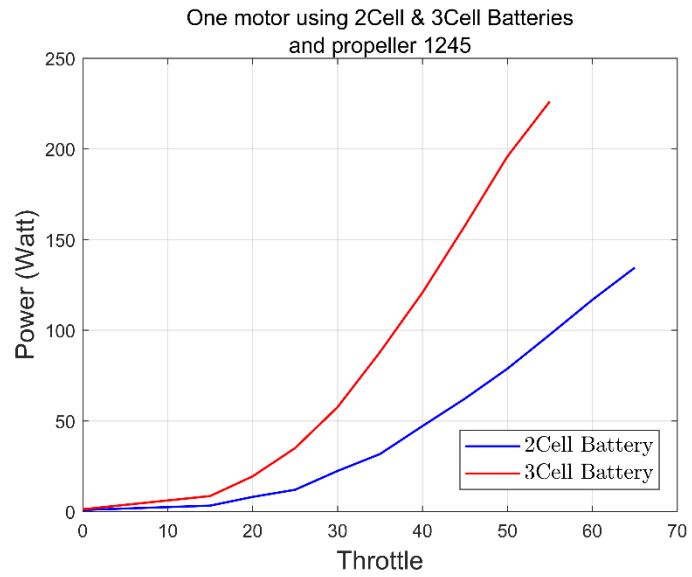
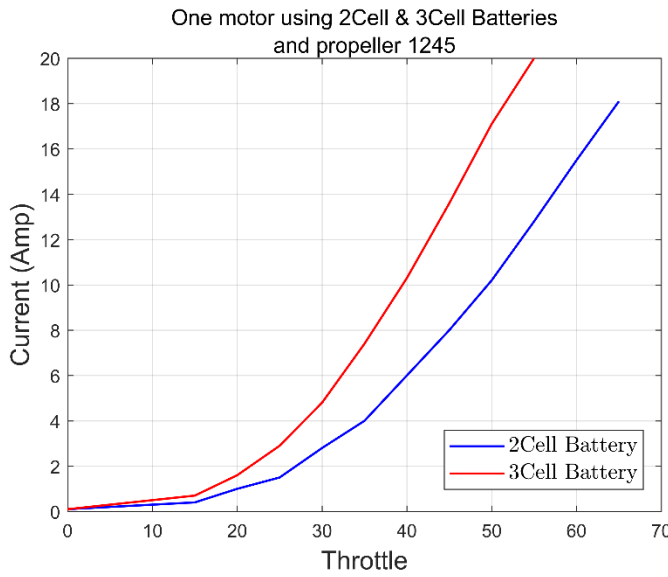
Figure 116 : One motor using 2Cell battery with propeller 1245

One motor using 3Cell battery with propeller 1245				
throttle %	amp A	voltage V	power watt	thrust gm
0	0.1	12.17	1.217	0
15	0.7	12.16	8.512	40
20	1.6	12.1	19.36	90
25	2.9	12.05	34.945	160
30	4.8	11.98	57.504	240
35	7.4	11.88	87.912	340
40	10.3	11.72	120.716	420
45	13.6	11.59	157.624	490
50	17.1	11.45	195.795	560
55	20	11.31	226.2	600



Figure 115 .One motor using 3Cell battery with propeller 1245

After we tested and measured current, voltage, power, and thrust. We can get our graphs to compare between batteries



We can see the difference between 2Cell and 3Cell batteries. The motor takes higher current with 3Cell battery, unlike the 2Cell battery, so the result in power for 3Cell is more than the power for 2Cell, and the result in thrust we can see that 3Cell battery is more efficient than 2Cell battery and it can lift more weight.

Conclusion, 3Cell battery is better than 2Cell battery when using propeller 1245, due to the relation between power and voltage  $Power = V * I$ , so when increasing voltage then the power will be increasing, and the result in thrust by increasing. Due to data sheet of motor, we cannot get more cell than 3cell.

### 5.3.3. Two motors with two propellers 1045

Here we are testing two motors (coaxial rotors) with propellers 1045 using different batteries.

Two motors using 2Cell battery with propellers 1045				
throttle	amp A	voltage V	power watt	thrust gm
0	0.1	8.25	0.825	0
15	0.8	8.18	6.544	30
20	1.7	8.18	13.906	80
25	2.6	8.11	21.086	120
30	4.2	8.09	33.978	190
35	6.1	8.02	48.922	260
40	8.9	7.92	70.488	360
45	11.9	7.82	93.058	450
50	15.9	7.69	122.271	540
55	20.2	7.54	152.308	640
60	24.6	7.39	181.794	730
65	29.4	7.26	213.444	810
70	33.6	7.12	239.232	870

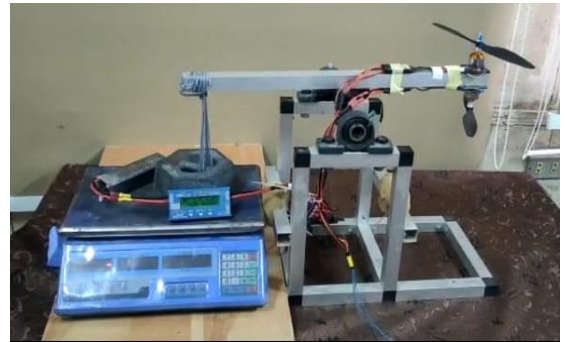


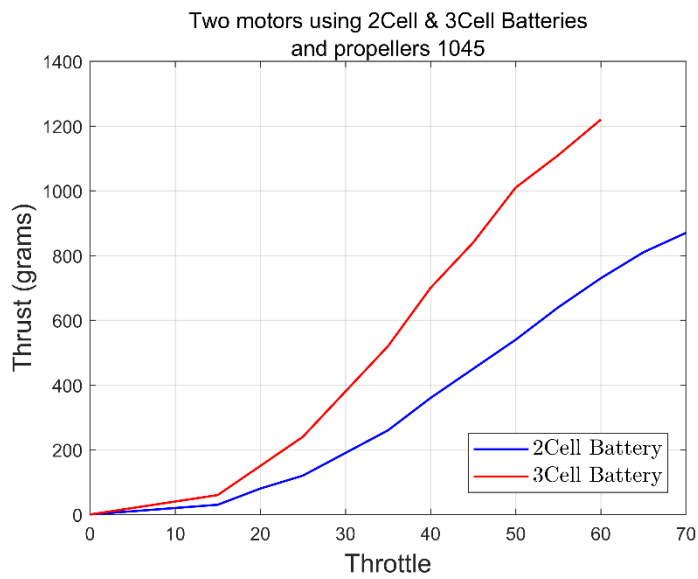
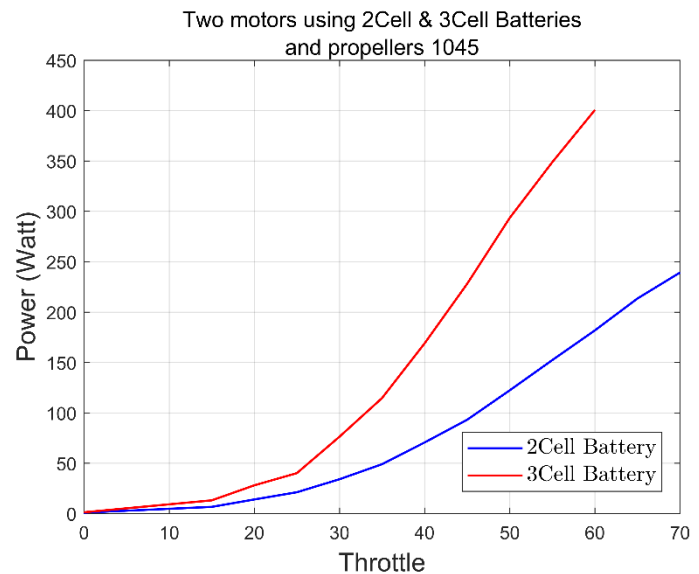
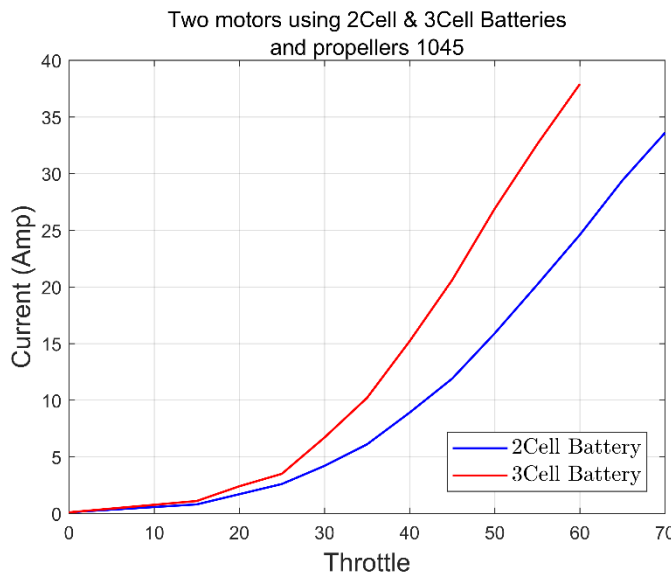
Figure 117 .Two motors using 2Cell battery with propellers 1045

Two motors using 3Cell battery with propellers 1045				
throttle	amp A	voltage V	power watt	thrust gm
0	0.1	11.95	1.195	0
15	1.1	11.84	13.024	60
20	2.4	11.64	27.936	150
25	3.5	11.44	40.04	240
30	6.7	11.37	76.179	380
35	10.2	11.23	114.546	520
40	15.2	11.11	168.872	700
45	20.6	11.07	228.042	840
50	26.9	10.91	293.479	1010
55	32.6	10.7	348.82	1110
60	37.9	10.57	400.603	1220



Figure 118 .Two motors using 3Cell battery with propellers 1045

After we tested and measured current, voltage, power, and thrust. We can get our graphs to compare between batteries



We can see the difference between 2Cell and 3Cell batteries. The two motors take higher current with 3Cell battery, unlike the 2Cell battery, so the result in power for 3Cell is more than the power for 2Cell, and the result in thrust we can see that 3Cell battery is more efficient than 2Cell battery and it can lift more weight.

Conclusion, 3Cell battery is better than 2Cell battery for coaxial rotors using propellers 1045, due to the relation between power and voltage  $\text{Power} = V * I$ , so when increasing voltage then the power will be increasing, and the result in thrust by increasing. Due to data sheet of motor, we cannot get more cell than 3cell.

### 5.3.4 Two motors with two propellers 1245

Here we are testing two motors (coaxial rotors) with propellers 1245 using different batteries.

Two motors using 3Cell battery with propellers 1245				
throttle %	amp A	voltage V	power watt	thrust gm
0	0.1	12.1	1.21	0
15	1.2	12.05	14.46	50
20	2.8	11.98	33.544	120
25	5.4	11.88	64.152	240
30	9.2	11.76	108.192	360
35	14	11.57	161.98	490
40	19.7	11.32	223.004	600
45	25.5	11.03	281.265	690
50	31.8	10.81	343.758	800
55	38.5	10.56	406.56	880

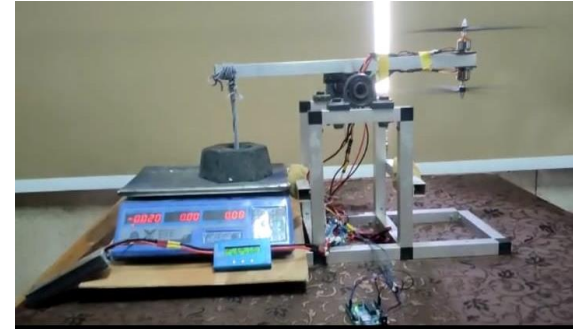


Figure 119 .Two motors using 2Cell battery with propellers 1245

Two motors using 2Cell battery with propellers 1245				
throttle %	amp A	voltage V	power watt	thrust gm
0	0.1	8.25	0.825	0
15	0.8	7.92	6.336	20
20	1.7	7.92	13.464	60
25	2.9	7.86	22.794	100
30	5	7.79	38.95	170
35	7.9	7.71	60.909	230
40	11.4	7.6	86.64	320
45	15.4	7.49	115.346	390
50	19.5	7.36	143.52	460
55	24.3	7.2	174.96	530
60	29.2	7.06	206.152	600
65	34.1	6.87	234.267	650

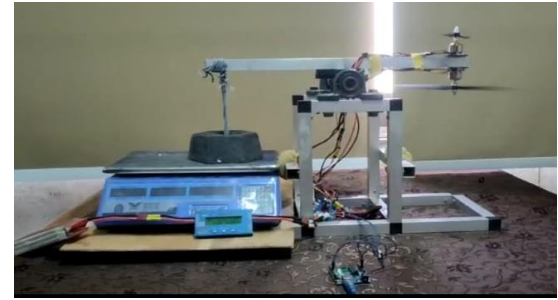
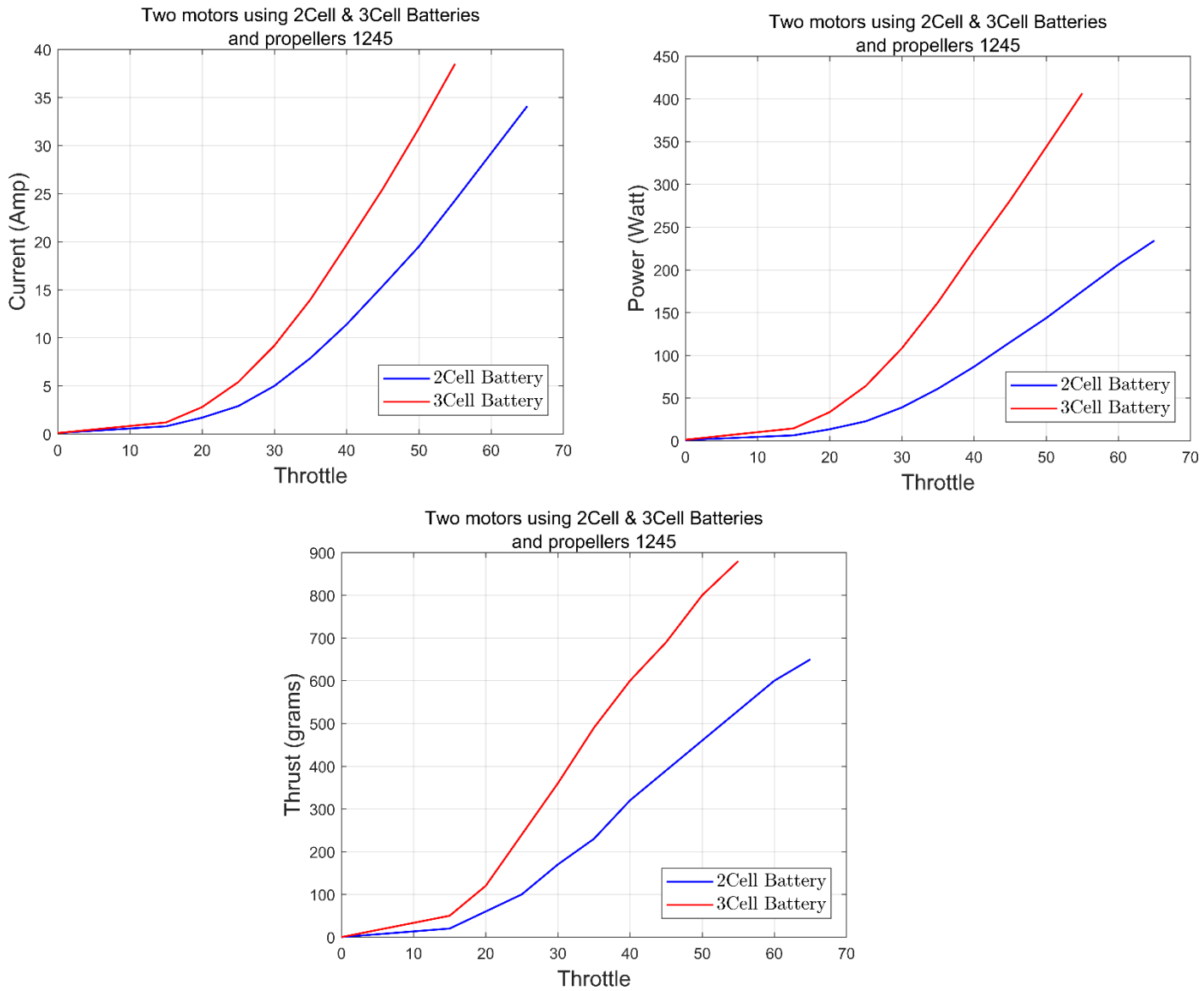


Figure 120 .Two motors using 3Cell battery with propellers 1245

After we tested and measured current, voltage, power, and thrust. We can get our graphs to compare between batteries



We can see the difference between 2Cell and 3Cell batteries. The two motors take higher current with 3Cell battery, unlike the 2Cell battery, so the result in power for 3Cell is more than the power for 2Cell, and the result in thrust we can see that 3Cell battery is more efficient than 2Cell battery and it can lift more weight.

Conclusion, 3Cell battery is better than 2Cell battery for coaxial rotors using propellers 1245, due to the relation between power and voltage  $\text{Power} = V * I$ , so when increasing voltage then the power will be increasing, and the result in thrust by increasing. Due to data sheet of motor we cannot get more cell than 3cell.

## 5.4. Propeller Comparison

### 5.4.1. One motor with a 2Cell battery

Here we are testing one motor using 2Cell battery with different propellers.

One motor using 2Cell battery with propeller 1045				
throttle	amp A	voltage V	power watt	thrust gm
0	0.1	8.25	0.825	0
15	0.3	8.24	2.472	10
20	0.8	8.24	6.592	50
25	1.2	8.23	9.876	70
30	1.9	8.2	15.58	120
35	2.9	8.18	23.722	170
40	4.2	8.12	34.104	230
45	5.8	8.08	46.864	290
50	7.9	7.99	63.121	360
55	10.2	7.92	80.784	430
60	12.7	7.84	99.568	500
65	15.3	7.73	118.269	560
70	17.6	7.66	134.816	610



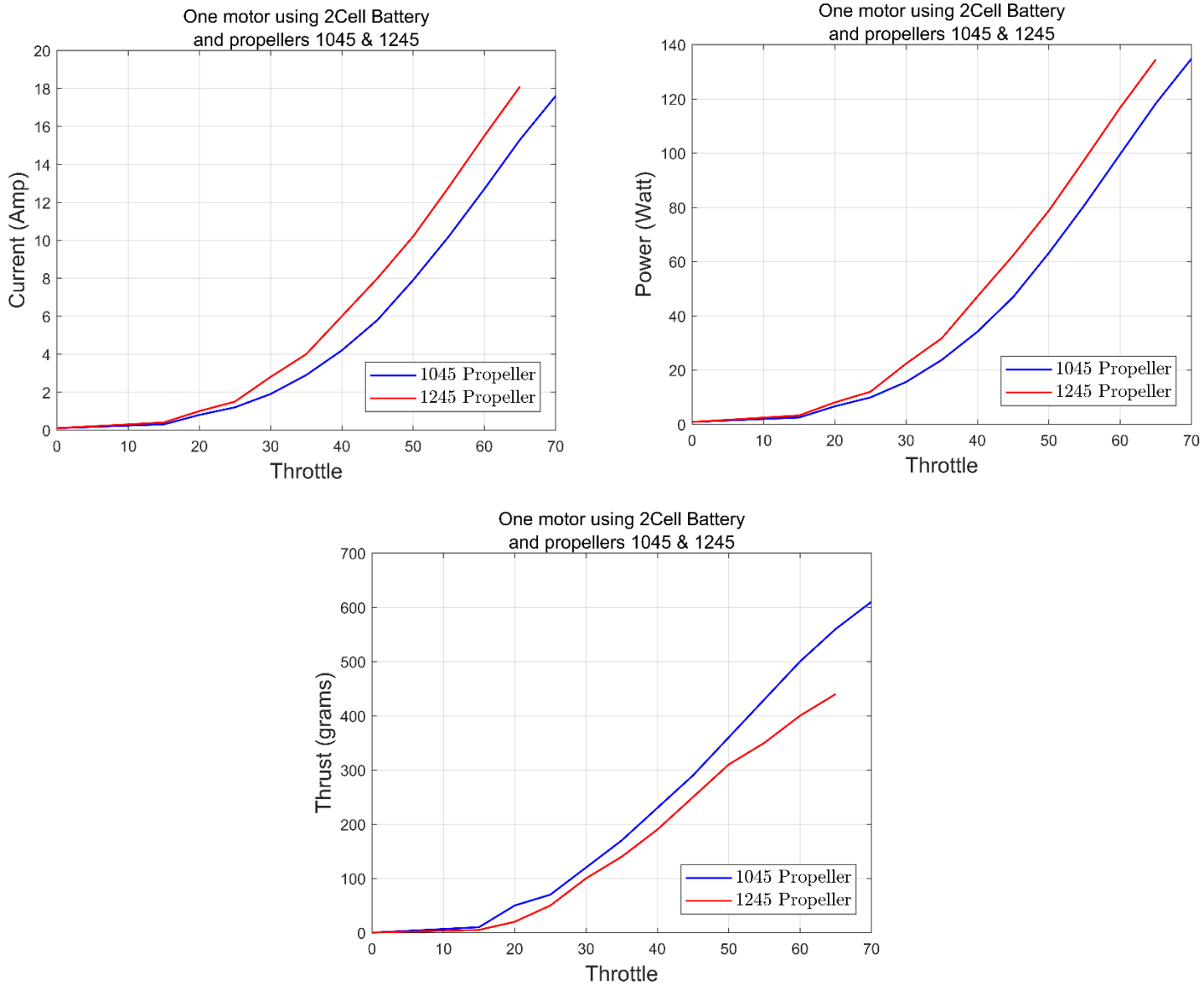
Figure 121 .One motor using 2Cell battery with propeller 1045

One motor using 2Cell battery with propeller 1245				
throttle %	amp A	voltage V	power watt	thrust gm
0	0.1	8.2	0.82	0
15	0.4	8.05	3.22	5
20	1	8.03	8.03	20
25	1.5	7.98	11.97	50
30	2.8	7.98	22.344	100
35	4	7.92	31.68	140
40	6	7.85	47.1	190
45	8	7.78	62.24	250
50	10.2	7.72	78.744	310
55	12.8	7.62	97.536	350
60	15.5	7.53	116.715	400
65	18.1	7.43	134.483	440



Figure 122 .One motor using 2Cell battery with propeller 1245

After we tested and measured current, voltage, power, and thrust. We can get our graphs to compare between batteries



We can see the difference between the two propellers for one motor using 2Cell battery. The motor takes higher current with the propeller 1245, unlike the propeller 1045, so the result in power with propeller 1245 is more than the power with propeller 1045, and the result in thrust we can see that with propeller 1045 is more efficient than with propeller 1245 and can lift more weight.

Conclusion, when using 2Cell battery the motor efficiency decreases when using a bigger propeller than 10 inches, due to data sheet of motor we cannot get more diameter of propeller than 10 inches, so if we used 12 inches or more that will influence on efficient by decreasing.

### 5.4.2. One motor with a 3Cell battery

Here we are testing one motor using 3Cell battery with different propellers.

One motor using 3Cell battery with propeller 1045				
throttle	amp A	voltage V	power watt	thrust gm
0	0.1	11.95	1.1	0
15	0.5	11.71	5.855	30
20	1.1	11.71	12.881	90
25	1.8	11.7	21.06	140
30	3.1	11.65	36.115	230
35	4.9	11.5	56.35	320
40	7.5	11.52	86.4	440
45	9.9	11.42	113.058	530
50	13.1	11.31	148.161	630
55	16.1	11.18	179.998	710
60	19.4	11.06	214.564	790

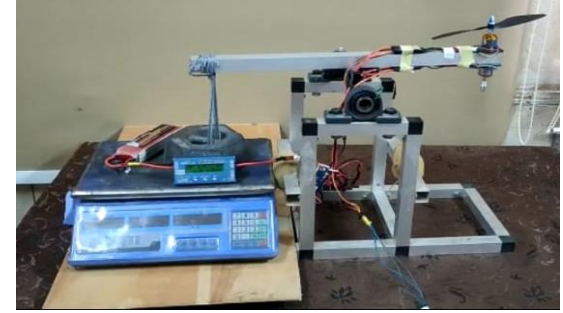


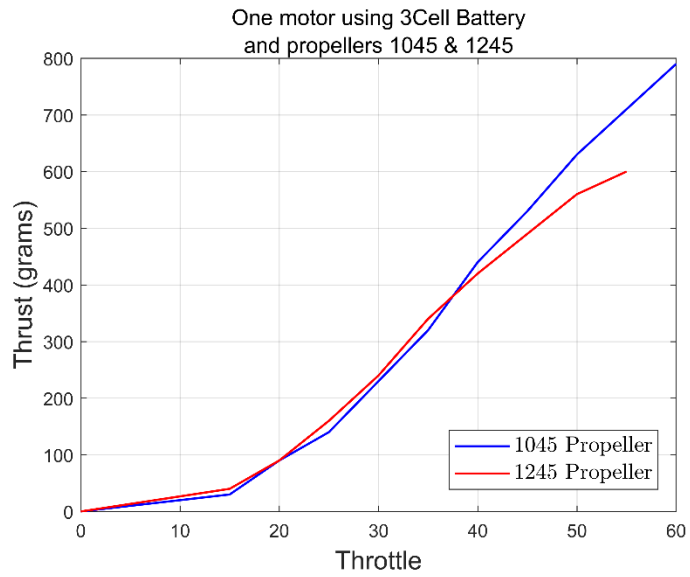
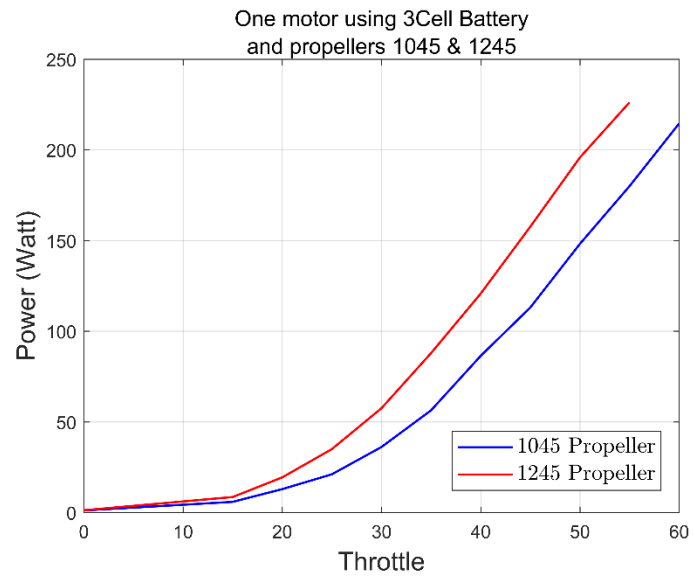
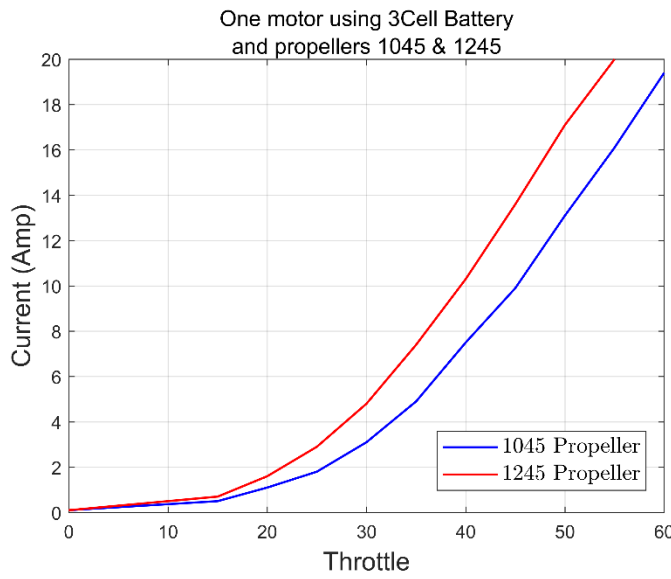
Figure 124 :One motor using 3Cell battery with propeller 1045

One motor using 3Cell battery with propeller 1245				
throttle %	amp A	voltage V	power watt	thrust gm
0	0.1	12.17	1.217	0
15	0.7	12.16	8.512	40
20	1.6	12.1	19.36	90
25	2.9	12.05	34.945	160
30	4.8	11.98	57.504	240
35	7.4	11.88	87.912	340
40	10.3	11.72	120.716	420
45	13.6	11.59	157.624	490
50	17.1	11.45	195.795	560
55	20	11.31	226.2	600



Figure 123 :One motor using 3Cell battery with propeller 1245

After we tested and measured current, voltage, power, and thrust. We can get our graphs to compare between batteries



We can see the difference between the two propellers for one motor using 3Cell battery. The motor takes higher current with the propeller 1245, unlike the propeller 1045, so the result in power with propeller 1245 is more than the power with propeller 1045, and the result in thrust we can see that with propeller 1045 is more efficient than with propeller 1245 and can lift more weight.

Conclusion, when using 3Cell battery the motor efficiency decreases when using a bigger propeller than 10 inches, due to data sheet of motor we cannot get more diameter of propeller than 10 inches, so if we used 12 inches or more that will influence on efficient by decreasing.

### 5.4.3. Two motors with two propellers of the same size using a 2Cell Battery

Here we are testing two motors (coaxial rotors) using 2Cell battery with different propellers.

Two motors using 2Cell battery with propellers 1045				
throttle	amp A	voltage V	power watt	thrust gm
0	0.1	8.25	0.825	0
15	0.8	8.18	6.544	30
20	1.7	8.18	13.906	80
25	2.6	8.11	21.086	120
30	4.2	8.09	33.978	190
35	6.1	8.02	48.922	260
40	8.9	7.92	70.488	360
45	11.9	7.82	93.058	450
50	15.9	7.69	122.271	540
55	20.2	7.54	152.308	640
60	24.6	7.39	181.794	730
65	29.4	7.26	213.444	810
70	33.6	7.12	239.232	870



Figure 126 .Two motors using 2Cell battery with propellers 1045

Two motors using 2Cell battery with propellers 1245				
throttle %	amp A	voltage V	power watt	thrust gm
0	0.1	8.25	0.825	0
15	0.8	7.92	6.336	20
20	1.7	7.92	13.464	60
25	2.9	7.86	22.794	100
30	5	7.79	38.95	170
35	7.9	7.71	60.909	230
40	11.4	7.6	86.64	320
45	15.4	7.49	115.346	390
50	19.5	7.36	143.52	460
55	24.3	7.2	174.96	530
60	29.2	7.06	206.152	600
65	34.1	6.87	234.267	650

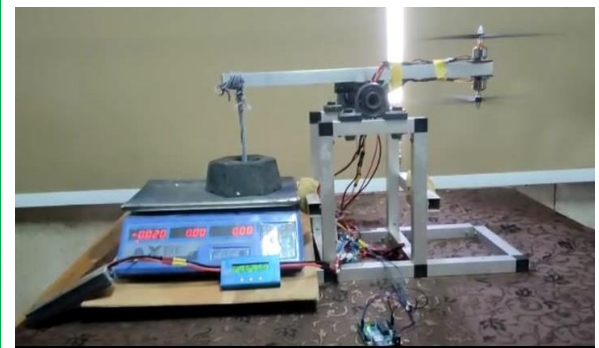
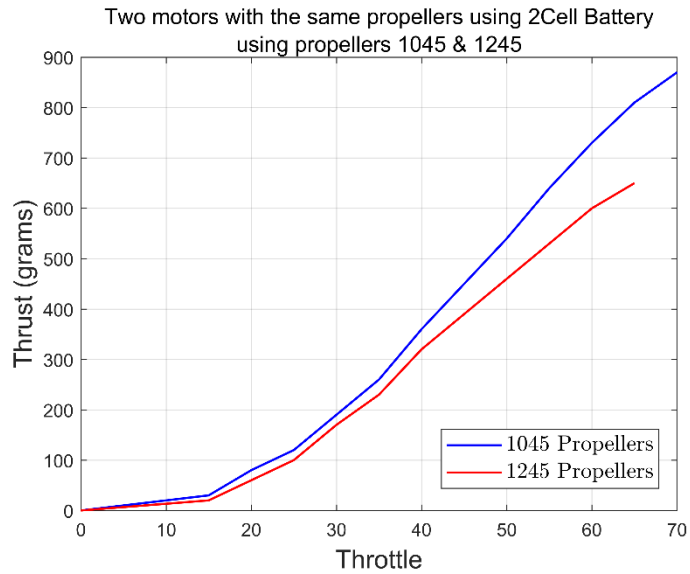
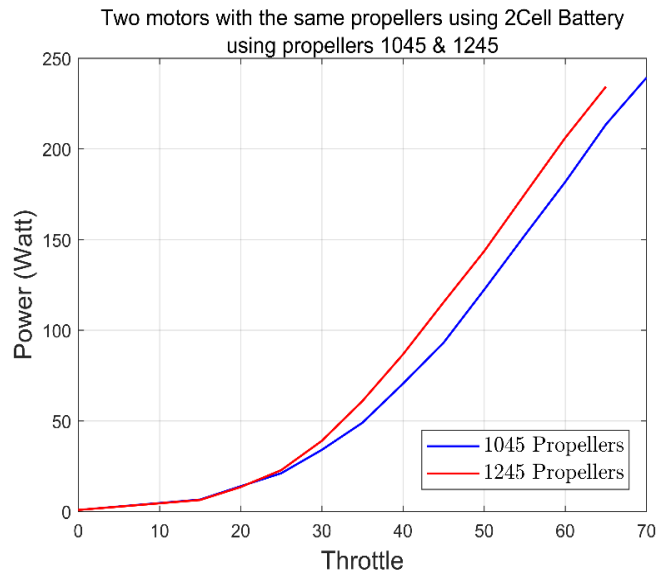
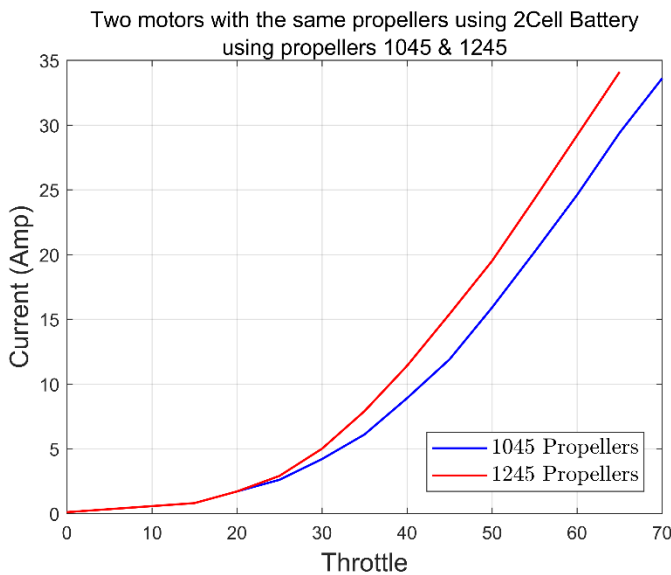


Figure 125 .Two motors using 2Cell battery with propellers 1245

After we tested and measured current, voltage, power, and thrust. We can get our graphs to compare between batteries



We can see the difference between the two propellers for two motors using 2Cell battery. The two motors take higher current with the propeller 1245, unlike the propeller 1045, so the result in power with propeller 1245 is more than the power with propeller 1045, and the result in thrust we can see that with propeller 1045 is more efficient than with propeller 1245 and can lift more weight.

Conclusion, when using 2Cell battery the efficiency decreases when using a bigger propeller than 10 inches, due to data sheet of motor we cannot get more diameter of propeller than 10 inches, so if we used 12 inches or more that will influence on efficient by decreasing.

#### 5.4.4. Two motors with two propellers of the same size using a 3Cell Battery

Here we are testing two motors (coaxial rotors) using 3Cell battery with different propellers.

Two motors using 3Cell battery with propellers 1045				
throttle	amp A	voltage V	power watt	thrust gm
0	0.1	11.95	1.195	0
15	1.1	11.84	13.024	60
20	2.4	11.64	27.936	150
25	3.5	11.44	40.04	240
30	6.7	11.37	76.179	380
35	10.2	11.23	114.546	520
40	15.2	11.11	168.872	700
45	20.6	11.07	228.042	840
50	26.9	10.91	293.479	1010
55	32.6	10.7	348.82	1110
60	37.9	10.57	400.603	1220



Figure 128 .Two motors using 3Cell battery with propellers 1045

Two motors using 3Cell battery with propellers 1245				
throttle %	amp A	voltage V	power watt	thrust gm
0	0.1	12.1	1.21	0
15	1.2	12.05	14.46	50
20	2.8	11.98	33.544	120
25	5.4	11.88	64.152	240
30	9.2	11.76	108.192	360
35	14	11.57	161.98	490
40	19.7	11.32	223.004	600
45	25.5	11.03	281.265	690
50	31.8	10.81	343.758	800
55	38.5	10.56	406.56	880

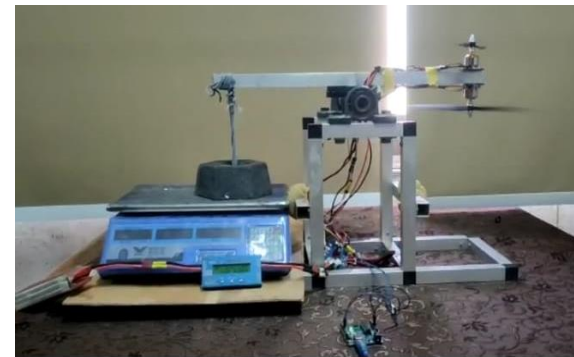
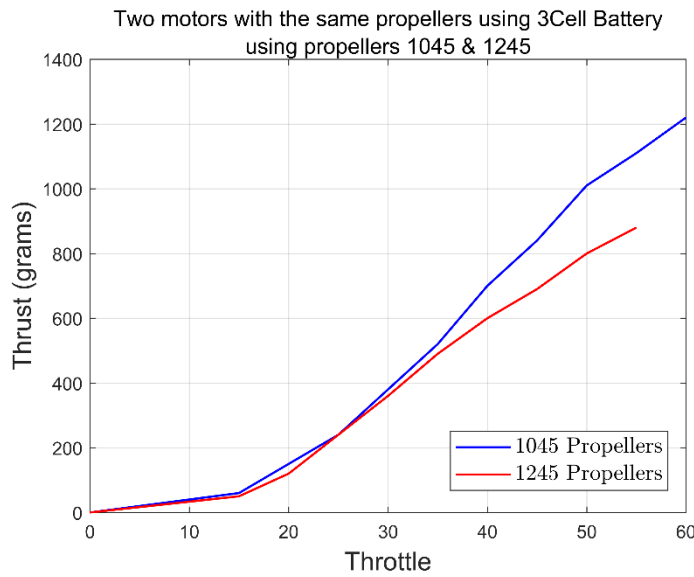
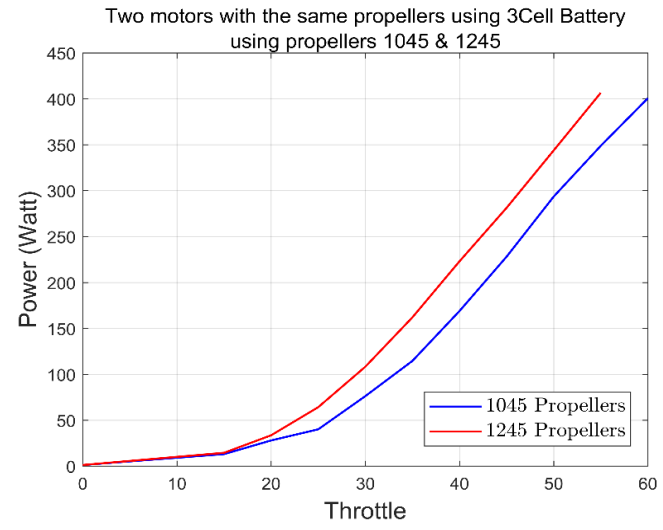
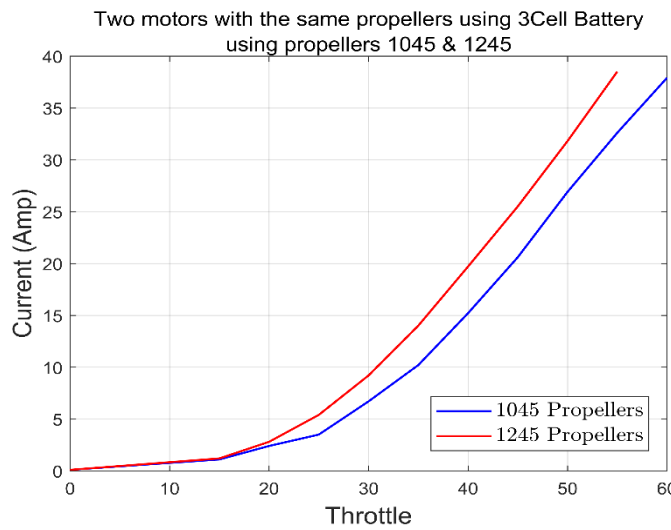


Figure 127 .Two motors using 3Cell battery with propellers 1245

After we tested and measured current, voltage, power, and thrust. We can get our graphs to compare between batteries.



We can see the difference between the two propellers for two motors using 3Cell battery. The two motors take higher current with the propeller 1245, unlike the propeller 1045, so the result in power with propeller 1245 is more than the power with propeller 1045, and the result in thrust we can see that with propeller 1045 is more efficient than with propeller 1245 and can lift more weight.

Conclusion, when using 3Cell battery the efficiency decreases when using a bigger propeller than 10 inches, due to data sheet of motor we cannot get more diameter of propeller than 10 inches, so if we used 12 inches or more that will influence on efficient by decreasing.

#### 5.4.5. Two motors with two different propellers using a 3Cell Battery

Here we are testing two motors (coaxial rotors) using 3Cell battery with different propellers.

Upper 1245 & Lower 1045				
throttle %	amp A	voltage V	power watt	thrust gm
0	0.1	12.43	1.243	0
15	1.2	12.37	14.844	60
20	2.9	12.29	35.641	140
25	5.3	12.2	64.66	250
30	9	12.04	108.36	400
35	14	11.84	165.76	540
40	20	11.64	232.8	690
45	26.5	11.4	302.1	820
50	32.9	11.16	367.164	930
55	39.1	10.92	426.972	1020

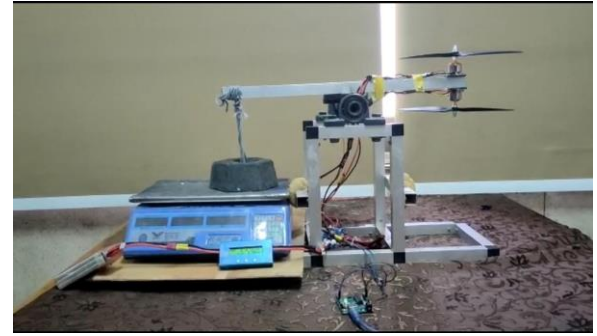


Figure 130 :Upper 1245 & Lower 1045

Upper 1045 & Lower 1245				
throttle %	amp A	voltage V	power watt	thrust gm
0	0.1	12.24	1.224	0
15	1.2	12.19	14.628	60
20	2.9	12.15	35.235	150
25	5.1	12.06	61.506	260
30	9.2	11.92	109.664	410
35	13.6	11.76	159.936	540
40	19.4	11.54	223.876	690
45	25.5	11.32	288.66	830
50	32.3	11.07	357.561	930
55	38.2	10.8	412.56	1020

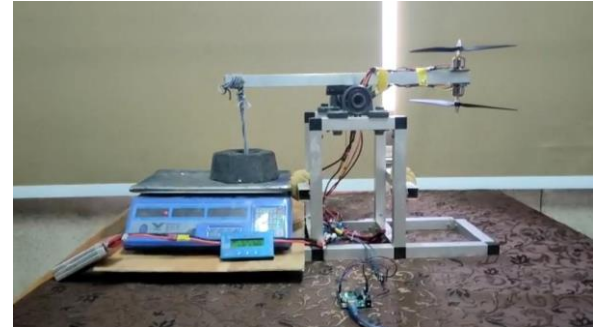
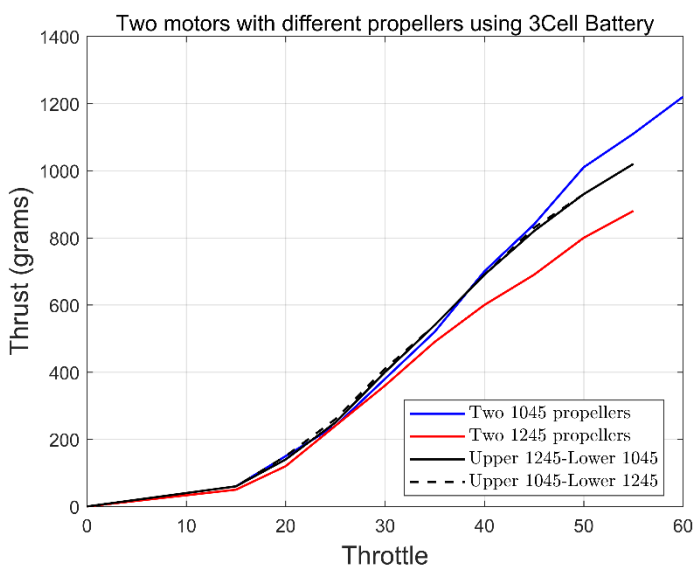
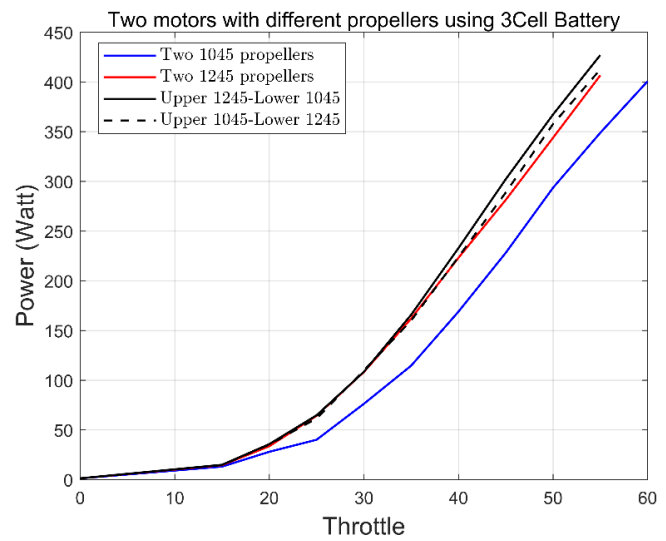
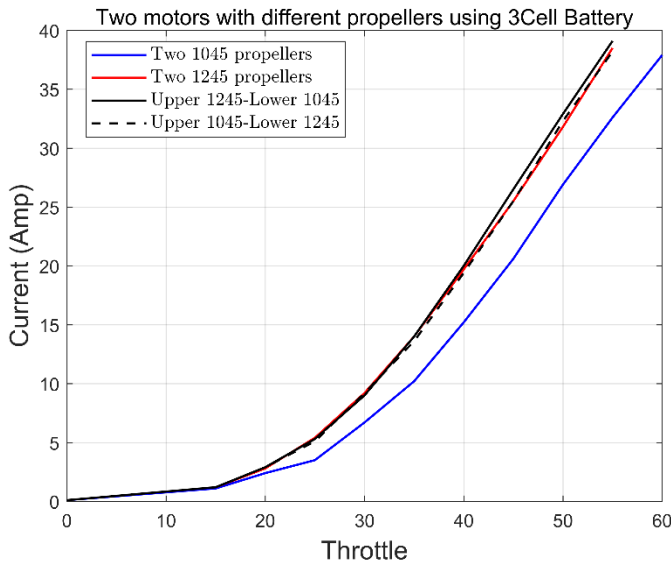


Figure 129 :Upper 1045 & Lower 1245

After we tested and measured current, voltage, power, and thrust. We can get our graphs to compare between batteries



We can see the difference between the two propellers for two motors using 3Cell battery. The two motors take the same current with the upper propeller 1245 and the lower propeller 1045, and vice versa and with two propellers 1245, which is higher than current with two propellers 1045. The result in thrust we can see that with propeller 1045 is more efficient than with propellers 1245 and can lift more weight.

Conclusion, when using 3Cell battery the efficiency decreases when using a bigger propeller than 10 inches, due to data sheet of motor we cannot get more diameter of propeller than 10 inches, so if we used 12 inches or more that will influence on efficient by decreasing.

## 5.5. And vice versa Vertical Spacing Comparison

### 5.5.1. Two motors with two propellers 1045 using a 2Cell Battery:

Here we are testing two motors (coaxial rotors) using 2Cell battery with propellers 1045, with different vertical spacing between rotors.

Vertical spacing 14cm				
throttle	amp A	voltage V	power watt	thrust gm
0	0.1	8.25	0.825	0
15	0.8	8.18	6.544	30
20	1.7	8.18	13.906	80
25	2.6	8.11	21.086	120
30	4.2	8.09	33.978	190
35	6.1	8.02	48.922	260
40	8.9	7.92	70.488	360
45	11.9	7.82	93.058	450
50	15.9	7.69	122.271	540
55	20.2	7.54	152.308	640
60	24.6	7.39	181.794	730
65	29.4	7.26	213.444	810
70	33.6	7.12	239.232	870



Figure 132 .Vertical spacing 14cm

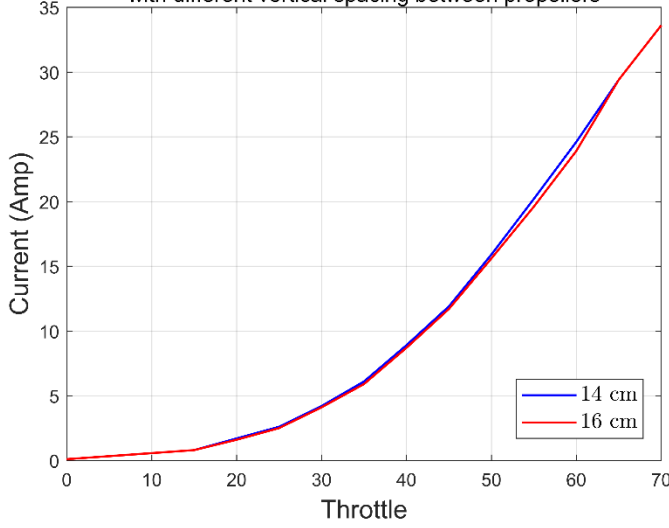
Vertical spacing 16cm				
throttle	amp A	voltage V	power watt	thrust gm
0	0.1	8.11	0.811	0
15	0.8	8.07	6.456	30
20	1.6	8.05	12.88	80
25	2.5	8.04	20.1	120
30	4.1	7.96	32.636	200
35	5.9	7.92	46.728	280
40	8.7	7.8	67.86	380
45	11.7	7.71	90.207	470
50	15.6	7.6	118.56	570
55	19.6	7.46	146.216	660
60	23.9	7.34	175.426	750
65	29.4	7.26	213.444	810
70	33.6	7.12	239.232	870



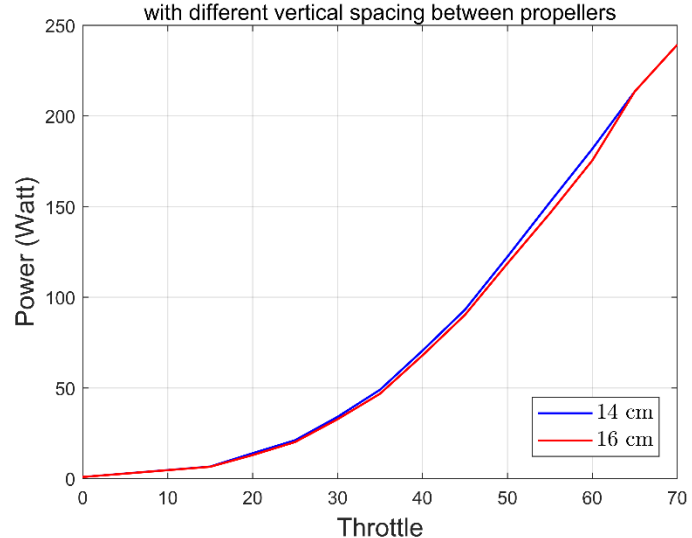
Figure 131 .Vertical spacing 16cm

After we tested and measured current, voltage, power, and thrust. We can get our graphs to compare between batteries

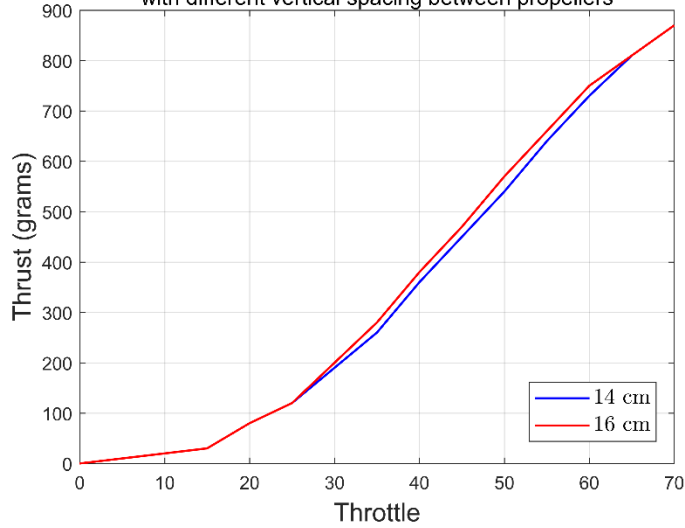
Two motors using 2Cell Battery and propellers 1045  
with different vertical spacing between propellers



Two motors using 2Cell Battery and propellers 1045  
with different vertical spacing between propellers



Two motors using 2Cell Battery and propellers 1045  
with different vertical spacing between propellers



We can see the difference between vertical spacing for 14cm and 16cm. There is almost no change in current and power. We notice that thrust increased by very small change, due to the airflow will be more comfortable around propeller.

## 5.6. Efficiency

After the experimental tests we can say that propeller 1045 is preferred than any other propeller in all conditions for coaxial rotors and for single motor, and 3Cell battery is better than 2Cell, keeping in mind the limit on the current.

For efficiency we can get the difference between single motor and coaxial rotors for 3Cell battery with propeller 1045:

throttle	thrust (gm) for coaxial rotors	thrust (gm) for single motor	efficiency
0	0	0	100
15	60	30	100
20	150	90	83
25	240	140	85
30	380	230	82
35	520	320	81
40	700	440	79
45	840	530	79
50	1010	630	80
55	1110	710	78
60	1220	790	77

$$\text{Efficiency} = \frac{\text{thrust by coaxial rotors}}{2 * \text{thrust by single motor}} * 100$$

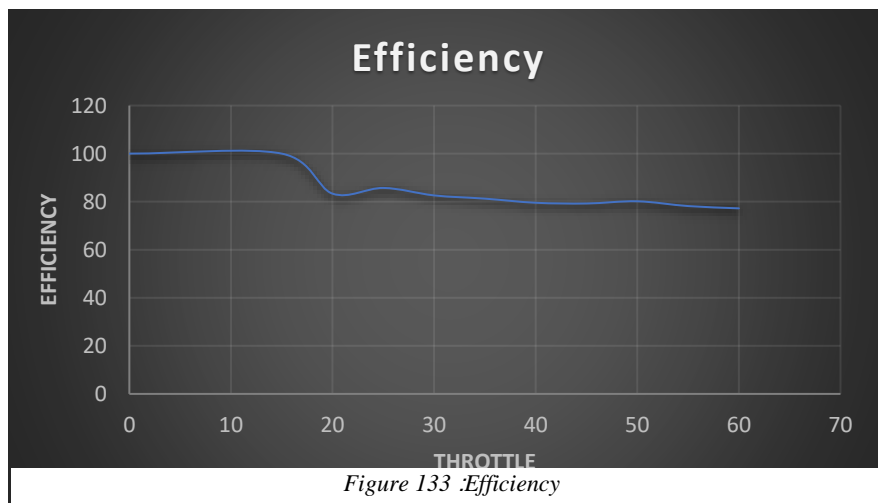
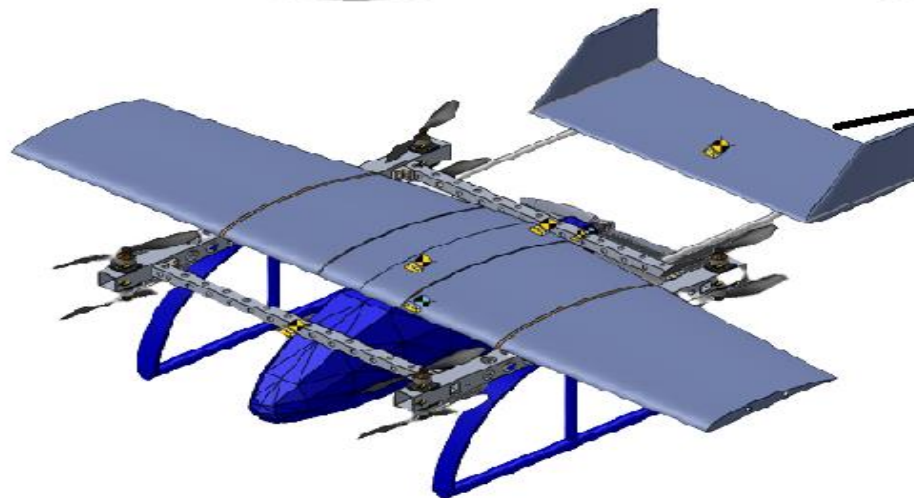


Figure 133 :Efficiency

Efficiency is good for our mission and can design on coaxial rotors to reduce the size of our eVTOL vehicle

# **Chapter Six:**

# **Hardware and Electronics**



## 6.1. Introduction

The hardware implementation is the final step in any project; it is linking all the parts of the project so the final project is ready to be tested. The components are chosen based on the requirements to develop the full project

- ❖ Brushless DC Motors
- ❖ Electronic Speed Controllers (ESCs)
- ❖ Arduino Board
- ❖ Power Distribution Board
- ❖ Inertial Measurement Unit (IMU)
- ❖ Altitude Sensor
- ❖ Global Positioning System (GPS)
- ❖ Transmitter and Receiver
- ❖ Airspeed Sensor

## 6.2. Brushless DC Electric Motor (BLDC Motor)

A DC motor converts direct current into mechanical energy by producing magnetic fields generating torque. Typical brushless DC motors use one or more permanent magnets in the rotor and electromagnets on the motor housing for the stator (brushed DC motor has rotating electromagnets and stationary magnets). A BLDC motor requires an electronic speed controller (esc) to adjust the phase and amplitude of the DC current pulses to control the speed and torque of the motor. This control system is an alternative to the brushes used in brushed DC motors. BLDC motors have three wires that are to be connected to the esc; swapping any two of these will reverse the direction of rotation of the motor

## 6.3. Electronic Speed Controller (ESC)

An electronic speed controller controls and regulates the speed of the brushless DC motor. It is powered by a battery and has separate voltage regulator for the microcontroller for providing good anti-jamming capability. It requires PWM (Pulse Width Modulation) signals from any remote control as throttle input or from the microcontroller. Throttle speed is proportional to the width of the pulse. Maximum throttle position is user programmable. In general throttle is set at zero for 1ms pulse width and full at the 2ms pulse width. The esc has three wires to connect with the BLDC motor, two wires to connect with the voltage source (battery), and three wires (red-black-orange) which are 5V, Ground, and input signal respectively to connect with the microcontroller.

Electronic speed controllers are different depending on the load current that they can drive motors with, and in our case, we have been using 30A esc, but when we used 40A esc the thrust generated by the motor was much higher, which leads us to note that the more current esc can provide, the more thrust the motor generates. We also have to keep in mind the output power is reduced when the esc get heated above a temperature depending on the quality of the esc.

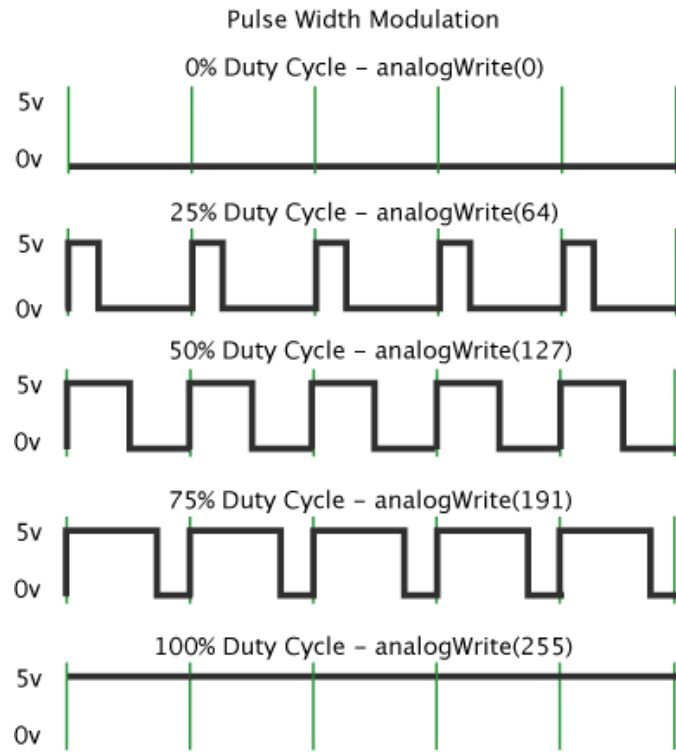


Figure 134: Pulse Width Modulation

**ESC connection with microcontroller (Arduino):**

Pulse Width Modulation (PWM) is a technique for getting analog results with digital means. Digital control is used to create a square wave, a signal switched between on and off. This on-off pattern can simulate voltages in between the full Vcc of the board (5 V) and off (0 V) by changing the portion of the time the signal spends on versus the time that the signal spends off. The duration of "on time" is called the pulse width. To get varying analog values, you change, or modulate, that pulse width. The Arduino sends PWM signals using the Servo library; this library deals with the esc the same way dealing with servo motors it takes input value in range (0:180 degrees) and the output is the width of a PWM signal in range (1:2ms)

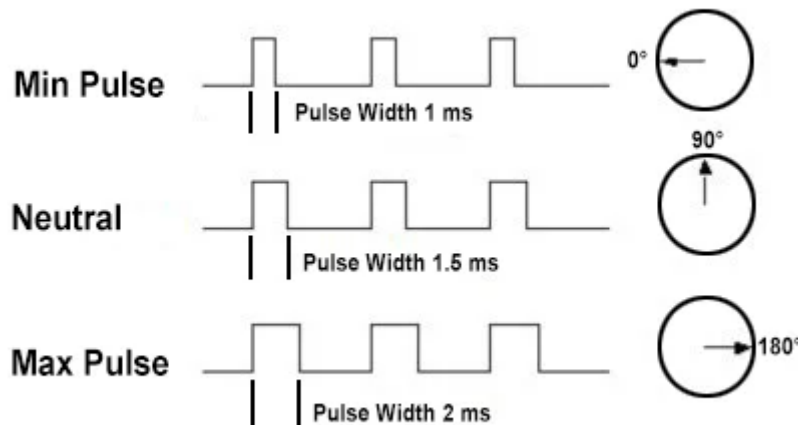


Figure 135: Servo PWM

**ESC Calibration:**

When beginning to use a new esc or when using different transmitter or microcontroller, the throttle range is reset because different transmitter has different throttle range they can be in the range of 1ms to 2ms or 0.5ms to 2.5ms at 50 to 60Hz. Calibrating esc is teaching the esc about the control signal range corresponding to the zero and full throttle.

Calibration is done by sending the maximum throttle signal to the esc (which is connected to the motor) before it is connected to the battery, then connect the battery, after a long beep is emitted that means the top point of throttle range has been confirmed, send the minimum throttle signal to the esc and another long beep is emitted that means the lowest point of throttle range has been confirmed

- 1) Connect the esc to the motor
- 2) Connect the esc to the transmitter (Microcontroller/RC Remote Control) and switch it on
- 3) Send signal of maximum throttle (100% of throttle)
- 4) Connect the esc to battery
- 5) Long beep is emitted which means the maximum point of throttle is recognized
- 6) Send signal of minimum throttle (0% of throttle)
- 7) Another beep is emitted which means the minimum point of throttle is recognized, and the esc is ready

The beeps or the tones should be mentioned in the datasheet of any electronic speed controller, as they are different for different esc

Calibration of esc should be done with no propellers

**Using Arduino to send PWM signals:**

The simple sketch for using Servo library must contain four main functions (lines) in order to rotate the servo motor by sending PWM signals, or in our case to rotate the BLDC motor by sending PWM signals to the esc, the main functions are:

- `#include <Servo.h>`
- `Servo Motor1;`
- `Motor1.attach(Pin,1000,2000);`
- `Motor1.write(Value);`

Pin is the pin number, for Arduino Uno, the signal wire is attached to any pin from (8:13) for sending PWM signals.

Value is the desired angle to rotate the servo motor in range (0:180 degrees), and this is the same range for esc as well where 0 degree means 0% of throttle, 90 degree means 50% of throttle, and 180 degree means 100% of throttle. So we should mention that when using a potentiometer to rotate a servo motor or a BLDC motor, Value should be mapped from (0:1023) to (0:180), because Value is the analogRead input from the potentiometer (0:5 Volts) and the Arduino board must be powered via the USB connection or with an external power supply.

The easier method is to just type in the Arduino IDE Serial Monitor, this is the method we have been using and our input values are in range (0:100% of throttle) and mapping from (0:100) to (0:180). This method requires powering the Arduino board via the USB cable.

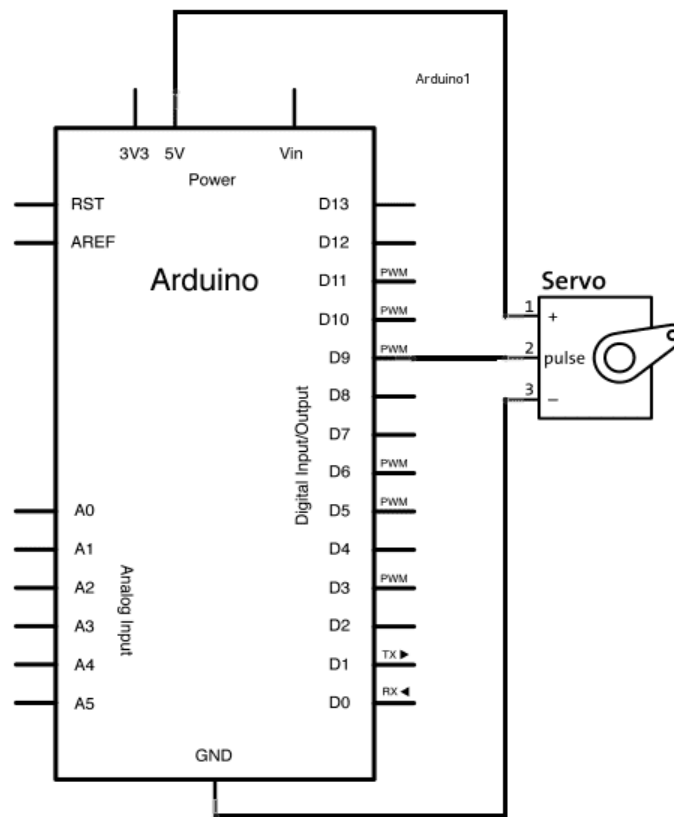


Figure 136: Servo motor connections Arduino board

**\*Important note to not burn out your Arduino board:**

If the Arduino board is powered via the USB cable or with an external power supply, connect signal and ground wires only of the esc and the Arduino board; do not connect the 5V wire in the Arduino board, when the esc is connected to the BLDC motor and battery. If the Arduino board is not powered, then you can power it with the 5V wire from the esc which is regulated from the battery, and in case of more than one motor or more than one esc, only one 5V wire from any esc is enough to power your Arduino board.

## 6.4. Power Distribution Board

A power distribution board is an important part of an electricity supply system. Its job is to split an incoming electrical power feed to the eight motors. It is important because it splits the power equally so the motors receive the same power.



Figure 137: Power Distribution Board

## 6.5. Arduino Board

Arduino is an open-source electronics platform based on easy-to-use hardware and software.

### Arduino IDE:

An open-source Arduino software can be used with any Arduino board. The Arduino Integrated Development Environment - or Arduino Software (IDE) - contains a text editor for writing code, a message area, a text console, a toolbar with buttons for common functions and a series of menus. It connects to the Arduino hardware to upload programs and communicate with them.

Programs written using Arduino Software (IDE) are called sketches. These sketches are written in the text editor and are saved with the file extension. ino. The editor has features for cutting/pasting and for searching/replacing text. The message area gives feedback while saving and exporting and also displays errors. The console displays text output by the Arduino Software (IDE), including complete error messages and other information. The bottom righthand corner of the window displays the configured board and serial port. The toolbar buttons allow you to verify and upload programs, create, open, and save sketches, and open the serial monitor.

**Arduino Board:**

One of Arduino hardware products (besides shields), it is a microcontroller that executes a set of instructions in a sketch uploaded by the user.

	Arduino Mega 2560	Arduino Uno
MICROCONTROLLER	ATmega2560	ATmega328P
OPERATING VOLTAGE	5V	5V
INPUT VOLTAGE (RECOMMENDED)	7-12V	7-12V
INPUT VOLTAGE (LIMIT)	6-20V	6-20V
DIGITAL I/O PINS	54 (of which 15 provide PWM output)	14 (of which 6 provide PWM output)
ANALOG INPUT PINS	16	6
DC CURRENT PER I/O PIN	20 mA	20 mA
DC CURRENT FOR 3.3V PIN	50 mA	50 mA
FLASH MEMORY	256 KB of which 8 KB used by bootloader	32 KB of which 0.5 KB used by bootloader
SRAM	8 KB	2 KB
EEPROM	4 KB	1 KB
CLOCK SPEED	16 MHz	16 MHz
LED_BUILTIN	13	13
LENGTH	101.52 mm	68.6 mm
WIDTH	53.3 mm	53.4 mm
WEIGHT	37 g	25 g

It is also important to take a look at the board pinout, just to make sure when connecting something that the connections are as expected

**For Arduino Uno:**

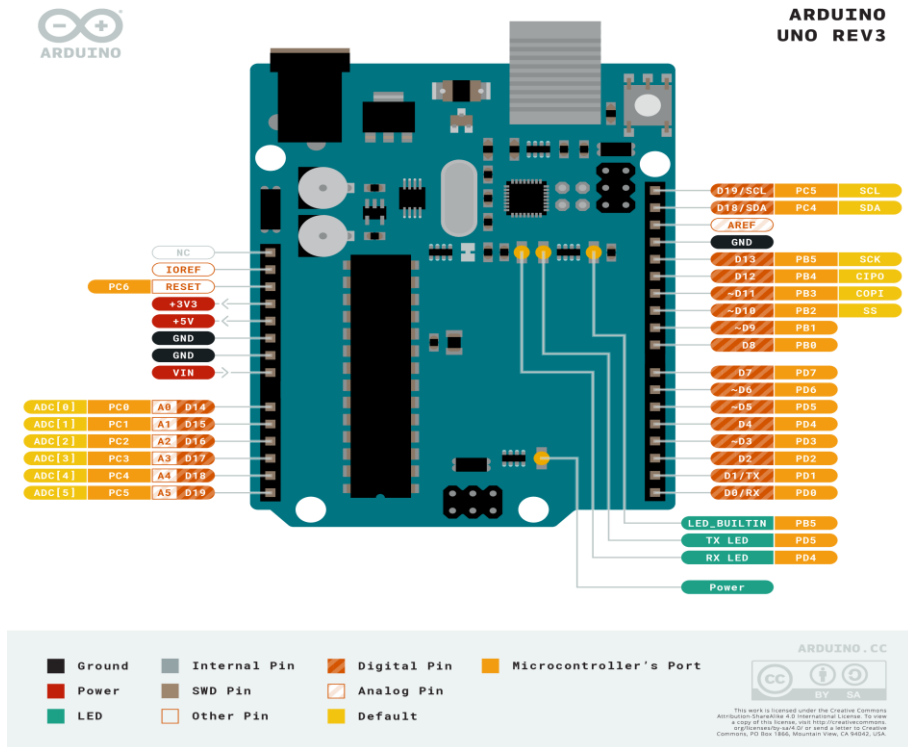


Figure 138: Arduino Uno Pinout

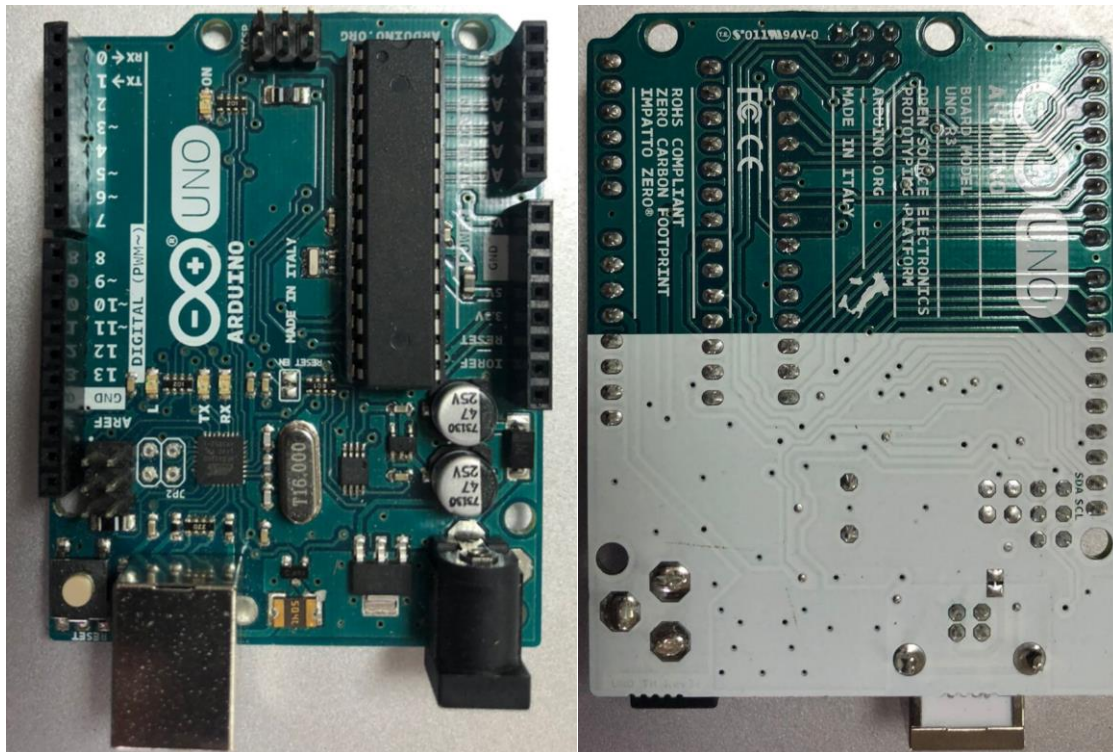


Figure 139: Arduino Uno

## For Arduino Mega:

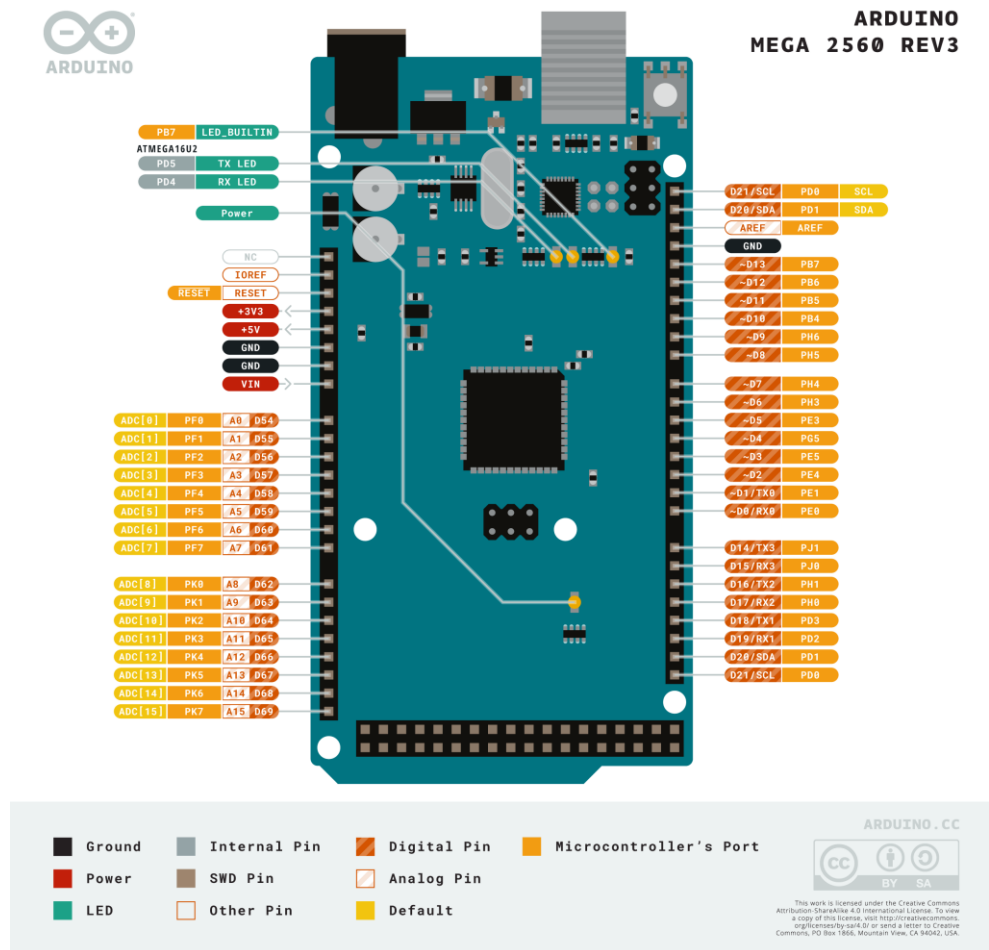


Figure 140: Arduino Mega Pinout



Figure 141: Arduino Mega

## 6.6. Sensors

Sensors are used to determine vehicle state (needed for stabilization and to enable autonomous control). The vehicle states include: position, altitude, heading, speed, airspeed, orientation (attitude), and rates of rotation in different directions.

Every sensor has a datasheet made by the manufacturer to provide details and technical specifications about the product to help the customer. These datasheets are very helpful, and it is very important to take a look at the datasheet before using any sensor.

### 6.6.1 Inertial Measurement Unit (IMU)

IMU sensor is the most important feedback unit on an aircraft. It is an electronic device that measures angular rates and accelerations using gyroscope and accelerometer. Some IMUs have 3 sensors in one device; gyroscope, accelerometer, and magnetometer, if they don't have magnetometer, then a compass is needed, as the magnetometer –or compass- is required to measure the heading of the aircraft.

**Gyroscope** is a device that measures angular rates; it is small and inexpensive. To stabilize an aircraft, gyros are used to detect the change in the attitude or the change in angular velocities.

**Accelerometer** is a device that measures linear accelerations.

**Magnetometer** is a device that measures the earth's magnetic field; to simplify the purpose of a magnetometer we can say that it works as a compass.

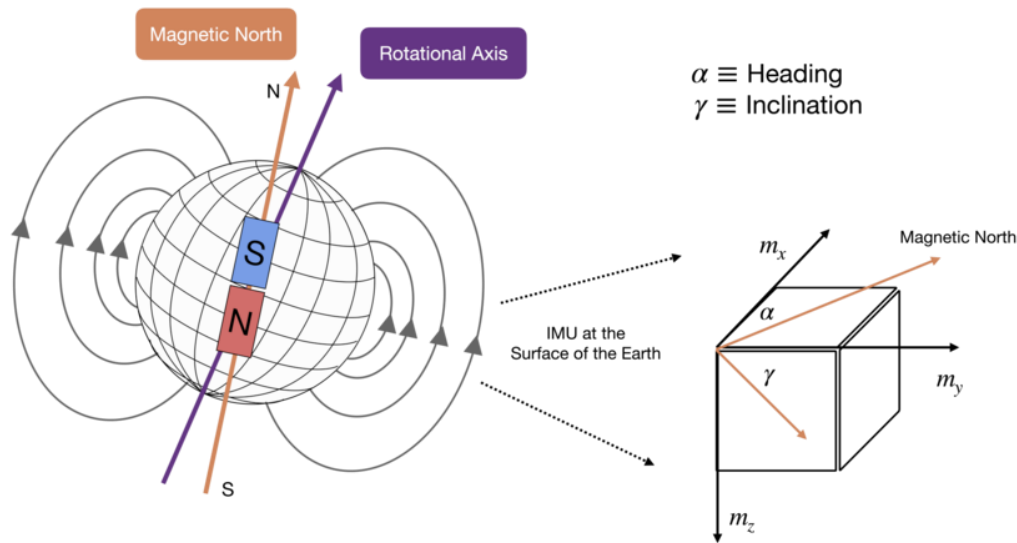


Figure 142: Magnetometer device

We could say that measuring the heading of an aircraft is the most difficult, because the sensor must be calibrated every time it is reset. The sensor is not accurate, for example when the aircraft reaches higher altitudes the accuracy becomes worse and worse, in addition to the magnetic fields around the sensor can affect the measurements and reduce the accuracy, this becomes more obvious when a magnet is brought near a compass.

To stabilize the aircraft (e.g. at hover), we need to get the orientation angles caused by any disturbance or gust. The microcontroller is connected to the IMU sensor, the sensor sends the measurement data (angular rates) to the microcontroller, and the microcontroller is programmed to calculate the orientation angles (roll-pitch-yaw) and control the aircraft to return to its stable point. The hardest part here is sending the right data to the microcontroller.

We have been using BMX055 9-axis IMU sensor (unfortunately, after a lot of trials, we couldn't get the right data for the orientation angles, because of error in the measurement data that goes into integrations which at the end results in junk data)

The BMX055 is a very small, 9-axis sensor, consisting of a triaxial 12-bit acceleration sensor, a triaxial 16 bit,  $\pm 2000^\circ/\text{sec}$  gyroscope and a triaxial geomagnetic sensor.

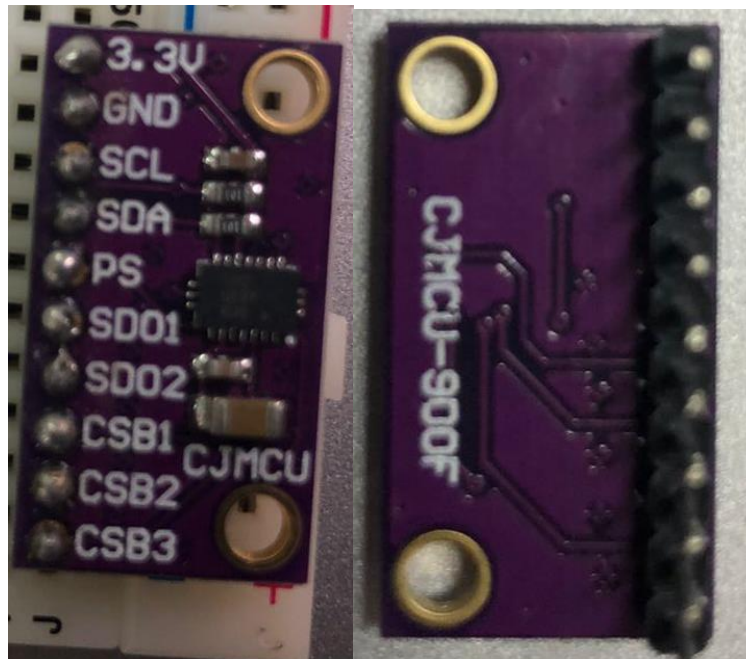
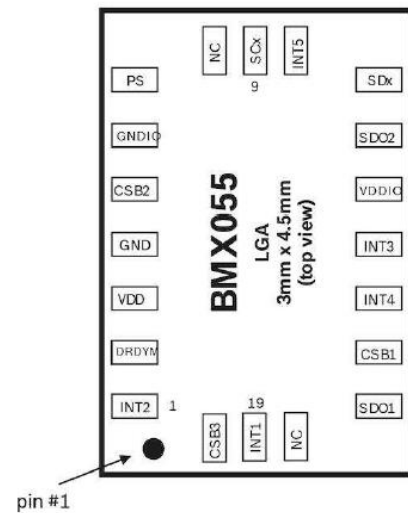


Figure 143: BMX055



Pin configuration (top view)

Figure 144: Digital interface of the device

The BMX055 supports two serial digital interface protocols for communication as a slave with a host device:

- 1- Serial Peripheral Interface or SPI (4-wire and 3-wire)
- 2- I<sup>2</sup>C

The user chooses the interface and activates it by connecting the Protocol Select (PS) pin to either Ground or VDDIO. If the PS pin is connected to Ground, then the selected interface is SPI. If the PS pin is connected to VDDIO, then the selected interface is I<sup>2</sup>C.

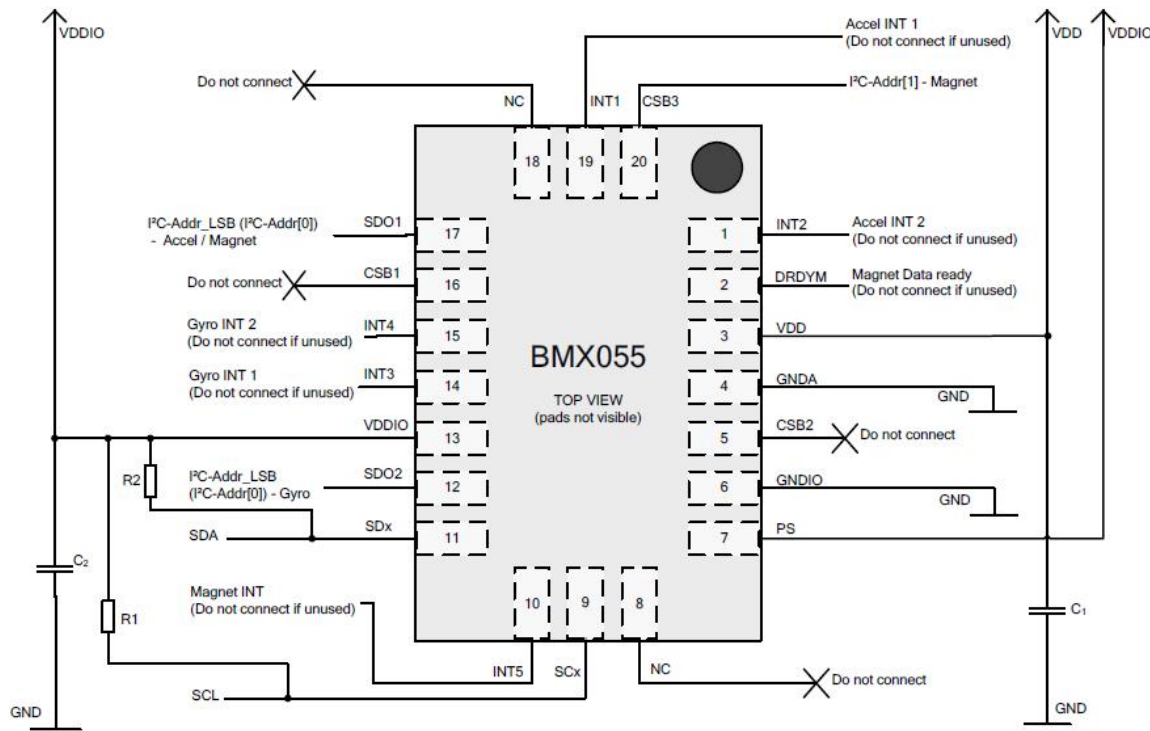
BMX055 Technical data (preliminary)		Pin		
		Pin	Name	Description
Resolution	(A): 0.98 mg, (G): 0.004 °/s (M): 0.3 µT	1	INT2	Interrupt output (A)
Measurement ranges (programmable)	(A): ±2 g, ±4 g, ±8 g, ±16 g (G): ±125 °/s, ±250 °/s, ±500 °/s, ±1000 °/s, ±2000 °/s (M): ±1300 µT (x,y), ±2500 µT (z)	2	DRDYM	Data ready (M)
Sensitivity w (calibrated)	(A): ±2 g: 1024 LSB/g ±4 g: 512 LSB/g ±8 g: 256 LSB/g ±16 g: 128 LSB/g (G): ±125 °/s: 262.4 LSB/°/s LSB/°/s ±250 °/s: 131.2 LSB/°/s ±500 °/s: 65.6 LSB/°/s ±1000 °/s: 32.8 LSB/°/s ±2000 °/s: 16.4 LSB/°/s (M): 1 µT/µT	3	V <sub>DD</sub>	Supply voltage
Zero-point offset	(A): ±70 mg (G): ±1 °/s (M): ±40 µT	4	GND	Ground
Noise density (typ.)	(A): 150 µg/√Hz (G): 0.014 °/s/√Hz (M): 0.6 µT	5	CSB2	Chip select (G)
Supply voltage (V <sub>DD</sub> )	2.4 ... 3.6 V	6	GND <sub>I/O</sub>	I/O ground
I/O supply voltage (V <sub>DDIO</sub> )	1.2 ... 3.6 V	7	PS	Protocol select
Temperature range	-40 ... +85 °C	8	NC	Not connected
Current consumption		9	SCx	SCK: SPI clock SCL: I <sup>2</sup> C clock
– Gyro @full operation	5 mA	10	INT5	Interrupt output (M)
– Acc. @full operation	130 µA	11	SDx	Serial data input/output
– Acc. @wake-up mode	<10 µA	12	SDO2	SPI: Data out (G)
– Magnet sensor @10Hz ODR	0.54 mA	13	V <sub>DDIO</sub>	I/O voltage
Package dimensions	3 x 4.5 x 0.95 mm <sup>3</sup> (LGA)	14	INT3	Interrupt input/output (G)
Shock resistance	10,000 g x 200 µs	15	INT4	Interrupt input/output (G)
		16	CSB1	Chip select (A)
		17	SDO1	SPI: Data out (A), (M)
		18	NC	Not connected
		19	INT1	Interrupt output (A)
		20	CSB3	Chip select (M)

(A) = Accelerometer  
(G) = Gyroscope  
(M) = Geomagnetic Sensor

Figure 145: BMX055 Basic Description

As we are going to connect Arduino to the BMX055 besides the other sensors, we select I<sup>2</sup>C interface

connection diagram I<sup>2</sup>C

Figure 146:  $I^2C$  connection

Note: the recommended Value for  $C_1$ ,  $C_2$ , is 100 nF

The table shows the connections and the corresponding addresses for accelerometer, gyro, and magnetometer

SDO1	SDO2	CSB3		$I^2C$ - Addr_Accel	$I^2C$ - Addr_Gyro	$I^2C$ - Addr_magnet
GND	GND	GND		0x18	0x68	0x10
GND	GND	Vddio		0x18	0x68	0x12
GND	Vddio	GND		0x18	0x69	0x10
GND	Vddio	Vddio		0x18	0x69	0x12
Vddio	GND	GND		0x19	0x68	0x11
Vddio	GND	Vddio		0x19	0x68	0x13
Vddio	Vddio	GND		0x19	0x69	0x11
Vddio	Vddio	Vddio		0x19	0x69	0x13

Figure 147: connections and the corresponding addresses

The first row is the easiest way to connect the sensor, so the connections to Arduino will be:

3.3V → Arduino output pin 3.3V

GND → Arduino Ground pin

**SCL → Pin 21 for Arduino Mega/A5 for Arduino Uno**

**SDA → Pin 20 for Arduino Mega/A4 for Arduino Uno**

**PS → VDDIO**

**SDO1 → Ground**

**SDO2 → Ground**

**CSB1 → Not connected**

**CSB2 → Not connected**

**CSB3 → Ground**

To check the connections are right and the addresses are as expected, using a simple sketch (Who am I) to get the address at which I<sup>2</sup>C device is connected. And it looks like the connections are right

```

COM5

I2C Scanner
Scanning...
I2C device found at address 0x10 !
I2C device found at address 0x18 !
I2C device found at address 0x68 !
done

Scanning...
I2C device found at address 0x10 !
I2C device found at address 0x18 !
I2C device found at address 0x68 !
done

```

Autoscroll  Show timestamp    No line ending

Figure 148: I<sup>2</sup>C scan

After connecting the sensor to the Arduino board, we need to request the data from the sensor. Requesting data from the sensor requires definition of the addresses, so we can use register maps in the sensor's datasheet. And we have to include the Wire library in the sketch so we can access (read/write) to the addresses. The Wire library allows communicating with I<sup>2</sup>C devices.

There are seven functions to use with the Wire library

- `#include <Wire.h>`
- `Wire.begin();`
- `Wire.beginTransmission(Address);`
- `Wire.write(0x00);`
- `Wire.requestFrom(Address, nBits);`
- `X = Wire.read();`
- `Wire.endTransmission();`

(0x00) is the register hexadecimal from the address of (accelerometer, gyro, or magnetometer), we can write (if possible) to the register or read (request data) from the register. nBits is the number of bits that are being requested.

The register maps show the accessibility for the byte (8 bits) carried in each register address. And for each register address that has the access for writing, the datasheet shows all the options that can be given to the sensor.

If we are interested in raw values only from the accelerometer, gyro, and magnetometer:

### Accelerometer

The width of acceleration data is 12 bits given in two's complement representation. The 12 bits for each axis are split into an MSB upper part (one byte containing bit 11 to 4) and an LSB lower part (one byte containing bits 3 to 0). Reading the acceleration data registers shall always start with the LSB part.

The entire communication with the device is performed by reading from or writing to registers. Registers have a width of 8 bits; they are mapped to a common space of 64 addresses from (ACC 0x00) to (ACC 0x3F). Within the used range there are several registers which are either completely or partially marked as 'reserved'. Any reserved bit is ignored when it is written and no specific value is guaranteed when read. It is recommended not to use registers at all which are marked as reserved. Furthermore, it is recommended to mask out (logical and with zero) reserved bits of registers which are partially marked as reserved.

Registers with addresses from (ACC 0x00) to (ACC 0x0E) are read-only. Any attempt to write to these registers will be ignored.

DATA	HAL_EN	OTHR_EN	S_tap_en	O_tap_en		Slope_en_Z	Slope_en_Y	Slope_en_X	W/R	VALU
0x15									w/r	0xF
0x14					softreset				w/o	0x0
0x13	data_high_bw	shadow_dis							w/r	0x0
0x12		lowpower_mode	sleeptimer_mode						w/r	0x0
0x11	suspend	lowpower_en	deep_suspend		sleep_dur<3:0>				w/r	0x0
0x10				bw<4:0>					w/r	0xF
0x0F					range<3:0>				w/r	0x3
0x0E	fifo_overrun				fifo_frame_counter<6:0>				ro	0x0
0x0D									w/r	0xFF
0x0C	flat		orient<2:0>		high_sign	high_first_z	high_first_y	high_first_x	ro	0x0
0x0B	tap_sign	tap_first_z	tap_first_y	tap_first_x	slope_sign	slope_first_z	slope_first_y	slope_first_x	ro	0x0
0x0A	data_int	fifo_wm_int	fifo_full_int						ro	0x0
0x09	flat_int	orient_int	s_tap_int	d_tap_int	slo_no_mot_int	slope_int	high_int	low_int	ro	0x0
0x08				temp<7:0>					ro	0x0
0x07				acc_z_lsb<3:0>					ro	0x0
0x06					acc_z_msb<11:4>				ro	0x0
0x05				acc_y_lsb<3:0>		new_data_z			ro	0x0
0x04					acc_y_msb<11:4>				ro	0x0
0x03				acc_x_lsb<3:0>		new_data_y			ro	0x0
0x02					acc_x_msb<11:4>		new_data_x		ro	0x0
0x01									ro	--
0x00					chip_id<7:0>				ro	0xFA

Figure 149: Accelerometer Register Map

The register (ACC 0x02) contains (acc\_x\_lsb<3:0>) that is 4 bits (bit4, bit5, bit6, and bit7). (acc\_x\_lsb) is the least-significant 4 bits of X-channel acceleration readout value.

The register (ACC 0x03) contains (acc\_x\_msb<11:4>) that is 8 bits (bit0:bit7). (acc\_x\_msb) is the most-significant 8 bits of the X-channel acceleration readout value.

The register (ACC 0x04) contains (acc\_y\_lsb<3:0>) that is 4 bits (bit4, bit5, bit6, and bit7). (acc\_y\_lsb) is the least-significant 4 bits of Y-channel acceleration readout value.

The register (ACC 0x05) contains (acc\_y\_msb<11:4>) that is 8 bits (bit0:bit7). (acc\_y\_msb) is the most-significant 8 bits of the Y-channel acceleration readout value.

The register (ACC 0x06) contains (acc\_z\_lsb<3:0>) that is 4 bits (bit4, bit5, bit6, and bit7). (acc\_z\_lsb) is the least-significant 4 bits of Z-channel acceleration readout value.

The register (ACC 0x07) contains (acc\_z\_msb<11:4>) that is 8 bits (bit0:bit7). (acc\_z\_msb) is the most-significant 8 bits of the Z-channel acceleration readout value.

## Gyroscope

The angular rate data can be read-out through addresses from (GYR 0x02) to (GYR 0x07). The angular rate data is 16 width bits in two's-complement formula as

Decimal value	Angular rate (in 2000°/s range mode)
+32767	+ 2000°/s
...	...
0	0°/s
...	...
-32767	- 2000°/s

Figure 150: Gyroscope Range

In order to not corrupt the angular rate data, the LSB part should always be read out first. Once the LSB part of x, y, or z read-out registers have been read, the MSB parts are locked until the MSB parts are read out.

The entire communication with the device is performed by reading from or writing to registers. Registers have a width of 8 bits; they are mapped to a common space of 64 addresses from (GYR 0x00) to (GYR 0x3F). Within the used range there are several registers which are either completely or partially marked as ‘reserved’. Any reserved bit is ignored when it is written and no specific value is guaranteed when read. It is recommended not to use registers at all which are marked as reserved. Furthermore, it is recommended to mask out (logical and with zero) reserved bits of registers which are partially marked as reserved.

Registers with addresses from (GYR 0x00) to (GYR 0x0E) are read-only. Any attempt to write to these registers will be ignored.

0x33	num_remain[3]	num_remain[2]	num_remain[1]	num_remain[0]	num_load	num_rdy	num_prog_lng	num_prog_mode	wr	0x00
0x32	auto_offset_wordlength[1]	auto_offset_wordlength[0]	fast_offset_wordlength[1]	fast_offset_wordlength[0]	fast_offset_en	fast_offset_en_z	fast_offset_en_y	fast_offset_en_x	wr	0xC0
0x31	slow_offset_th[1]	slow_offset_th[0]	slow_offset_dur[2]	slow_offset_dur[1]	slow_offset_clr[0]	slow_offset_en_z	slow_offset_en_y	slow_offset_en_x	wr	0x60
0x30									wr	0xE8
0x2F									wr	0xE0
0x2E									wr	0x01
0x2D									wr	0x40
0x2C									wr	0x42
0x2B									wr	0x22
0x2A									wr	0x08
0x29									wr	0x19
0x28									wr	0x24
0x27	high_dur_z[0]	high_dur_z[5]	high_dur_x[5]	high_dur_x[4]	high_th_z[3]	high_dur_z[2]	high_th_z[1]	high_dur_x[20]	wr	0x01
0x26	high_th_x[0]	high_th_x[5]	high_th_x[4]	high_th_x[3]	high_th_z[2]	high_th_x[2]	high_th_y[0]	high_th_x[20]	wr	0x02
0x25	high_dur_y[7]	high_dur_y[6]	high_dur_y[5]	high_dur_y[4]	high_dur_x[3]	high_dur_y[3]	high_dur_y[1]	high_dur_y[20]	wr	0x19
0x24	high_th_y[1]	high_th_y[0]	high_th_y[4]	high_th_y[3]	high_th_x[2]	high_th_y[2]	high_th_y[1]	high_th_y[20]	wr	0x02
0x23	high_dur_x[7]	high_dur_x[6]	high_dur_x[5]	high_dur_x[4]	high_th_x[3]	high_dur_x[2]	high_th_x[1]	high_dur_x[20]	wr	0x19
0x22	high_th_x[1]	high_th_x[0]	high_th_x[4]	high_th_x[3]	high_th_x[2]	high_th_x[1]	high_th_x[0]	high_th_x[20]	wr	0x02
0x21	reset_int	offset_reset		latch_status_bits	latch_int[3]	latch_int[2]	latch_int[1]	latch_int[0]	wr	0x00
0x20									wr	0x00
0x1F									wr	0x28
0x1E	fifo_wm_en								wr	0x00
0x1D									wr	0xC9
0x1C	awake_dur[1]	awake_dur[0]	any_dursample[1]	any_dursample[0]	any_en_z	any_en_y	any_en_x	any_en_y	wr	0xA0
0x1B	fast_offset_unfit	any_th[6]	any_th[5]	any_th[4]	any_th[3]	any_th[2]	any_th[1]	any_th[0]	wr	0x04
0x1A			slow_offset_unfit		high_urit_data	any_urit_data	any_urit_data	any_urit_data	wr	0x00
0x19					int2_high	int2_any	int1_high	int1_any	wo	0x00
0x18	int2_data	int2_fast_offset	int2_fifo	int2_auto_offset	int1_auto_offset	int1_fifo	int1_fast_offset	int1_data	wr	0x00
0x17					int1_high	int1_any	int1_low	int1_low	wr	0x00
0x16					int2_low	int2_M	int1_low	int1_M	wr	0x0F
0x15	data_en	tifo_en			auto_offset_en	auto_offset_en	auto_offset_en	auto_offset_en	wr	0x00
0x14	softreset[7]	softreset[6]	softreset[5]	softreset[4]	softreset[3]	softreset[2]	softreset[1]	softreset[0]	wo	0x00
0x13	data_high_bw	shadow_dis							wo	0x00
0x12	fast_powerup	power_save_mode	ext_trig_sel[1]	ext_trig_sel[0]	autosleep_dur[2]	autosleep_dur[1]	autosleep_dur[0]	autosleep_dur[0]	wr	0x00
0x11	suspend	deep_suspend			sleep_dur[2]	sleep_dur[1]	sleep_dur[0]	sleep_dur[0]	wr	0x00
0x10					bW[3]	bW[2]	bW[1]	bW[0]	wr	0x00
0x0F					range[2]	range[1]	range[1]	range[0]	wr	0x00
0x0E	Overrun	frame_counter[6]	frame_counter[5]	frame_counter[4]	frame_counter[3]	frame_counter[2]	frame_counter[1]	frame_counter[0]	ro	0x00
0x0D									ro	0x00
0x0C					high_sign	high_first_z	high_first_y	high_first_x	ro	0x00
0x0B					any_sign	any_first_z	any_first_y	any_first_x	ro	0x00
0x0A	data_int	auto_offset_int	fast_offset_int	tifo_int					ro	0x00
0x09						any_int	high_int		ro	0x00
0x08									ro	0x00
0x07	rate_z[15]	rate_z[14]	rate_z[13]	rate_z[12]	rate_z[11]	rate_z[10]	rate_z[9]	rate_z[8]	ro	0x00
0x06	rate_z[7]	rate_z[6]	rate_z[5]	rate_z[4]	rate_z[3]	rate_z[2]	rate_z[1]	rate_z[0]	ro	0x00
0x05	rate_y[15]	rate_y[14]	rate_y[13]	rate_y[12]	rate_y[11]	rate_y[10]	rate_y[9]	rate_y[8]	ro	0x00
0x04	rate_y[7]	rate_y[6]	rate_y[5]	rate_y[4]	rate_y[3]	rate_y[2]	rate_y[1]	rate_y[0]	ro	0x00
0x03	rate_x[15]	rate_x[14]	rate_x[13]	rate_x[12]	rate_x[11]	rate_x[10]	rate_x[9]	rate_x[8]	ro	0x00
0x02	rate_x[7]	rate_x[6]	rate_x[5]	rate_x[4]	rate_x[3]	rate_x[2]	rate_x[1]	rate_x[0]	ro	0x00
0x01									ro	0x00
0x00	chip_id[7]	chip_id[6]	chip_id[5]	chip_id[4]	chip_id[3]	chip_id[2]	chip_id[1]	chip_id[0]	ro	0x0F

wr	
write only	
read only	
res. future use	

Figure 151: Gyroscope Register Map

The register (GYR 0x02) contains (rate\_x\_lsb<7:0>) that is 8 bits (bit0:bit7). (rate\_x\_lsb) is the least-significant 8 bits of X-channel angular rate readout value.

The register (GYR 0x03) contains (rate\_x\_msb<15:8>) that is 8 bits (bit0:bit7). (rate\_x\_msb) is the most-significant 8 bits of X-channel angular rate readout value.

The register (GYR 0x04) contains (rate\_y\_lsb<7:0>) that is 8 bits (bit0:bit7). (rate\_y\_lsb) is the least-significant 8 bits of Y-channel angular rate readout value.

The register (GYR 0x05) contains (rate\_y\_msb<15:8>) that is 8 bits (bit0:bit7). (rate\_y\_msb) is the most-significant 8 bits of Y-channel angular rate readout value.

The register (GYR 0x06) contains (rate\_z\_lsb<7:0>) that is 8 bits (bit0:bit7). (rate\_z\_lsb) is the least-significant 8 bits of Z-channel angular rate readout value.

The register (GYR 0x07) contains (rate\_z\_msb<15:8>) that is 8 bits (bit0:bit7). (rate\_z\_msb) is the most-significant 8 bits of Z-channel angular rate readout value.

## Magnetometer

The representation of magnetic field data is different between X/Y-axis and Z-axis. The width of X-axis and Y-axis magnetic field data is 13 bits each axis and stored in two's- complement formula. The width of the Z-axis magnetic field data is 15 bit word stored in two's- complement formula. The entire communication with the device's magnetometer part is performed by reading from and writing to registers. Registers have a width of 8 bits; they are mapped to a common space of 50 addresses from (MAG 0x40) to (MAG 0x71). Within the used range there are several registers which are marked as 'reserved'. Any reserved bit is ignored when it is written and no specific value is guaranteed when read. Especially, in SPI mode the SDO pin may stay in high-Z state when reading some of these registers.

Registers with addresses from (MAG 0x40) up to (MAG 0x4A) are read-only. Any attempt to write to these registers will be ignored.

0x40	0x32	reserved							
0x41	N/A								
0x42	N/A								
0x43	N/A								
0x44	N/A								
0x45	N/A								
0x46	N/A								
0x47	N/A								
0x48	N/A								
0x49	N/A								
0x4A	0x00	REPZ Number Of Repetitions (valid for Z) [7:0]							
0x4B	0x01	REPYX Number Of Repetitions (valid for XY) [7:0]							
0x4C	0x06	High Threshold [7:0]							
0x4D	0x3F	Low Threshold [7:0]							
0x4E	0x07	Data Ready Pin En	Interrupt Pin En	Channel Z	Channel Y	Channel X	DR Polarity	Interrupt Latch	Interrupt Polarity
0x4F	0x00	Data Overrun En	Overflow Int En	High Int Z en	High Int Y en	High Int X en	Low Int Z en	Low Int Y en	Low Int X en
0x50	0x00	Adv. ST [1:0]							
0x51	0x00	Data Rate [2:0]							
0x52	0x00	Opmode [1:0]							
0x53	N/A	Self Test							
0x54	N/A	Power Control Bit							
0x55	N/A	SP1en							
0x56	N/A	Soft Reset '1'							
0x57	N/A	Power Control Bit							
0x58	N/A	RHALL [13:6] MSB							
0x59	N/A	fixed '0'							
0x5A	N/A	fixed '0'							
0x5B	N/A	fixed '0'							
0x5C	N/A	fixed '0'							
0x5D	N/A	fixed '0'							
0x5E	N/A	fixed '0'							
0x5F	N/A	fixed '0'							
0x60	N/A	fixed '0'							
0x61	N/A	fixed '0'							
0x62	N/A	fixed '0'							
0x63	N/A	fixed '0'							

Figure 152: Magnetometer Register Map

The register (MAG 0x42) contains (DATA<sub>X</sub>\_LSB [4:0]) (bit3:bit7) that is 5 bits of the 13 bits output data of the X-channel, DATA<sub>X</sub>\_LSB is the least-significant 5 bits of x-axis magnetic field data.

The register (MAG 0x43) contains (DATA<sub>X</sub>\_MSB [12:5]) (bit0:bit7) that is 8 bits of the 13 bits output data of the X-channel, DATA<sub>X</sub>\_MSB is the most-significant 8 bits of x-axis magnetic field data.

The register (MAG 0x44) contains (DATA<sub>Y</sub>\_LSB [4:0]) (bit3:bit7) that is 5 bits of the 13 bits output data of the Y-channel, DATA<sub>Y</sub>\_LSB is the least-significant 5 bits of y-axis magnetic field data.

The register (MAG 0x45) contains (DATA<sub>Y</sub>\_MSB [12:5]) (bit0:bit7) that is 8 bits of the 13 bits output data of the Y-channel, DATA<sub>Y</sub>\_MSB is the most-significant 8 bits of y-axis magnetic field data.

The register (MAG 0x46) contains (DATA<sub>Z</sub>\_LSB [6:0]) (bit3:bit7) that is 7 bits of the 15 bits output data of the Z-channel, DATA<sub>Z</sub>\_LSB is the least-significant 7 bits of z-axis magnetic field data.

The register (MAG 0x47) contains (DATA<sub>Z</sub>\_MSB [14:7]) (bit0:bit7) that is 8 bits of the 15 bits output data of the Z-channel, DATA<sub>Z</sub>\_MSB is the most-significant 8 bits of z-axis magnetic field data.

**Temperature Sensor:**

The temperature compensation is based on a resistance measurement of the hall sensor plate. The resistance value is represented by a 14 bit unsigned output word.

The register (MAG 0x48) contains (RHALL\_LSB [5:0]) (bit2:bit7) that is 6 bits of the 14 bits output data of the RHALLchannel, RHALL\_LSB is the least-significant 6 bits of hall resistance.

The register (MAG 0x49) contains (RHALL\_MSB [13:6]) (bit0:bit7) that is 8 bits of the 14 bits output data of the RHALLchannel, RHALL\_MSB is the most-significant 8 bits of hall resistance.

Out best trial using the sensor (the orientations are not accurate to the real) was getting angular rates using library (Justa AHRS Filter on github) that contains AHRS filter to get quaternion after converting the angular rates data measured by the sensor to decimal values.

The filter is a predictor-corrector for attitude and heading reference systems (AHRS) that uses the combination of accelerometer, gyro, and magnetometer.

The library's function is to get a unit quaternion which is a complex number to represent the orientations.

From the quaternions we can get the orientations, where:

$$R_1 = q_1^2 + q_2^2 - q_3^2 - q_4^2$$

$$R_2 = 2(q_2q_3 + q_1q_4)$$

$$R_3 = 2(q_1q_3 - q_2q_4)$$

$$R_4 = 2(q_1q_2 + q_3q_4)$$

$$R_5 = q_1^2 - q_2^2 - q_3^2 + q_4^2$$

And

$$\phi = \text{atan2}(R_2, R_1)$$

$$\theta = \sin^{-1}(R_3)$$

$$\psi = \text{atan2}(R_4, R_5)$$

Results from the output angular rates, using Runge-Kutta to get the orientation angles by integration

Using the equations of angular velocities to Euler angles rate:

$$\dot{\phi} = p + \sin\phi \tan\theta q + \cos\phi \tan\theta r$$

$$\dot{\theta} = \cos\phi q - \sin\phi r$$

$$\dot{\psi} = \sin\phi \sec\theta q + \cos\phi \sec\theta r$$

### 6.6.2. Altitude Sensor

Barometer (altitude sensor) is a sensor that measures atmospheric pressure and temperature. From the relation between the atmospheric pressure and altitude, it can measure altitude.

We have been using BMP180, a digital pressure sensor that consists of a piezo-resistive sensor. It is designed to be connected directly to a microcontroller via I<sup>2</sup>C interface.

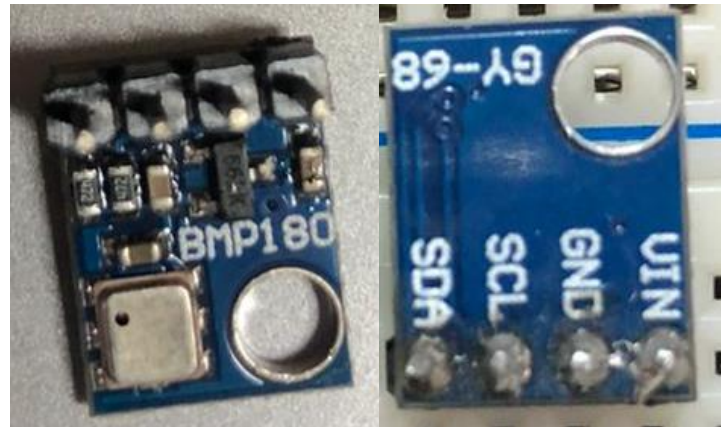


Figure 153: BMP180

The sensor has pressure range of (300:1100hPa) (+9000: -500m relating to sea-level). The sensor sensitivity is 0.06hPa (0.5m) in ultra-low power mode, 0.02hPa (0.17m) in advanced resolution mode, and the standard mode is 0.05hPa (0.4m).

The sensor has its algorithm to measure pressure and temperature

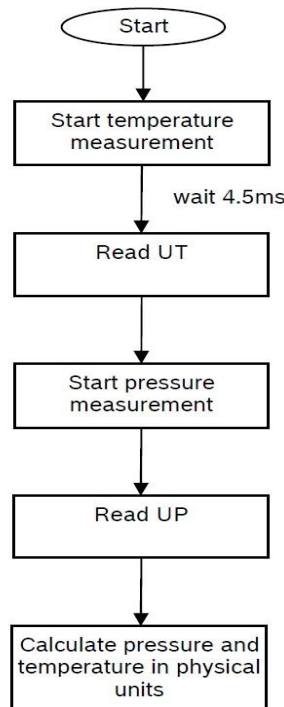


Figure 154: pressure and temperature sensor algorithm

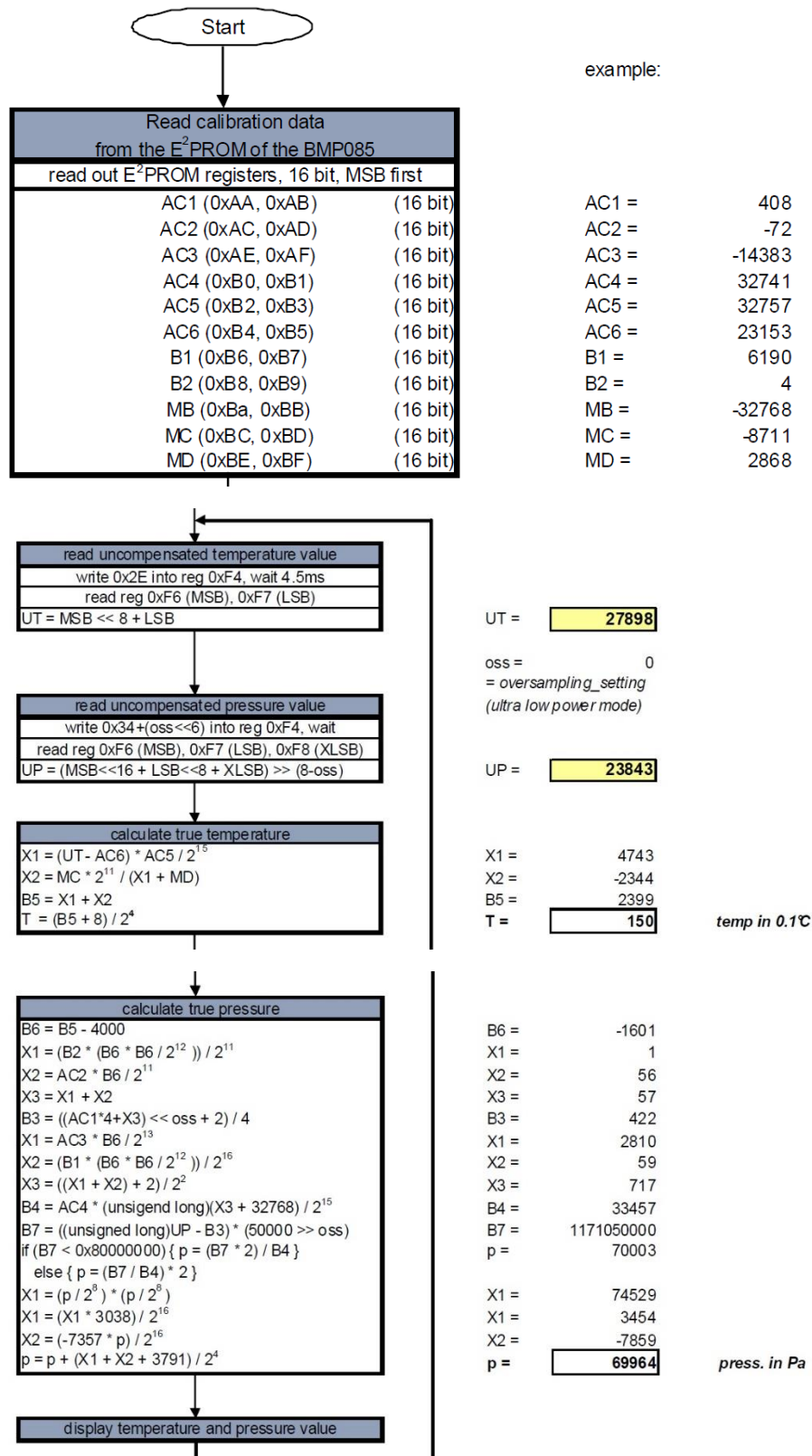


Figure 155: pressure and temperature sensor algorithm with example

And to calculate altitude from the formula

$$\text{Altitude} = 44330 \left( 1 - \left( \frac{P}{P_0} \right)^{\frac{1}{5.255}} \right)$$

Taking  $P_0 = 101325 \text{ Pa} = 1013.25 \text{ hPa}$  at sea-level

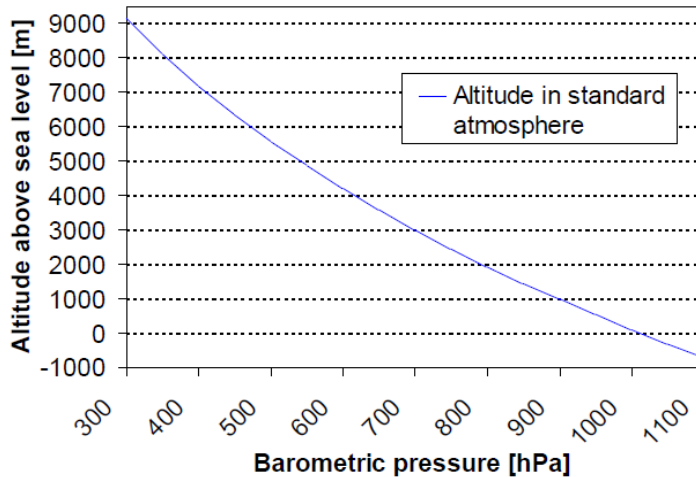


Figure 156: Altitude in Standard atmosphere

For a pressure change of 1hPa=100Pa

We used Adafruit library for BMP085, following the same algorithm for pressure and temperature measurement. BMP085 is a digital pressure sensor by the same manufacturer of BMP180, so the two sensors are the same except that BMP180 has more options for power saving.

```

COM5
Pressure at sealevel (calculated) = 99031 Pa
Real altitude = 206.75 meters

Temperature = 24.90 °C
Pressure = 99030 Pa
Altitude = 192.34 meters
Pressure at sealevel (calculated) = 99033 Pa
Real altitude = 207.09 meters

Temperature = 25.00 °C
Pressure = 99026 Pa
Altitude = 192.77 meters
Pressure at sealevel (calculated) = 99033 Pa
Real altitude = 207.43 meters

```

Autoscroll  Show timestamp      No line ending      9600 baud      Clear output

Figure 157: BMP180 measurement

### 6.6.3 Global Positioning System (GPS)

GPS module is a global positioning system device that receives signals from GPS satellites to locate a specific point on the Earth in a process named trilateration. Meanwhile, a GPS receiver measures the distances to satellites using radio signals to trilateration. And trilateration is similar to triangulation, which measures angles.

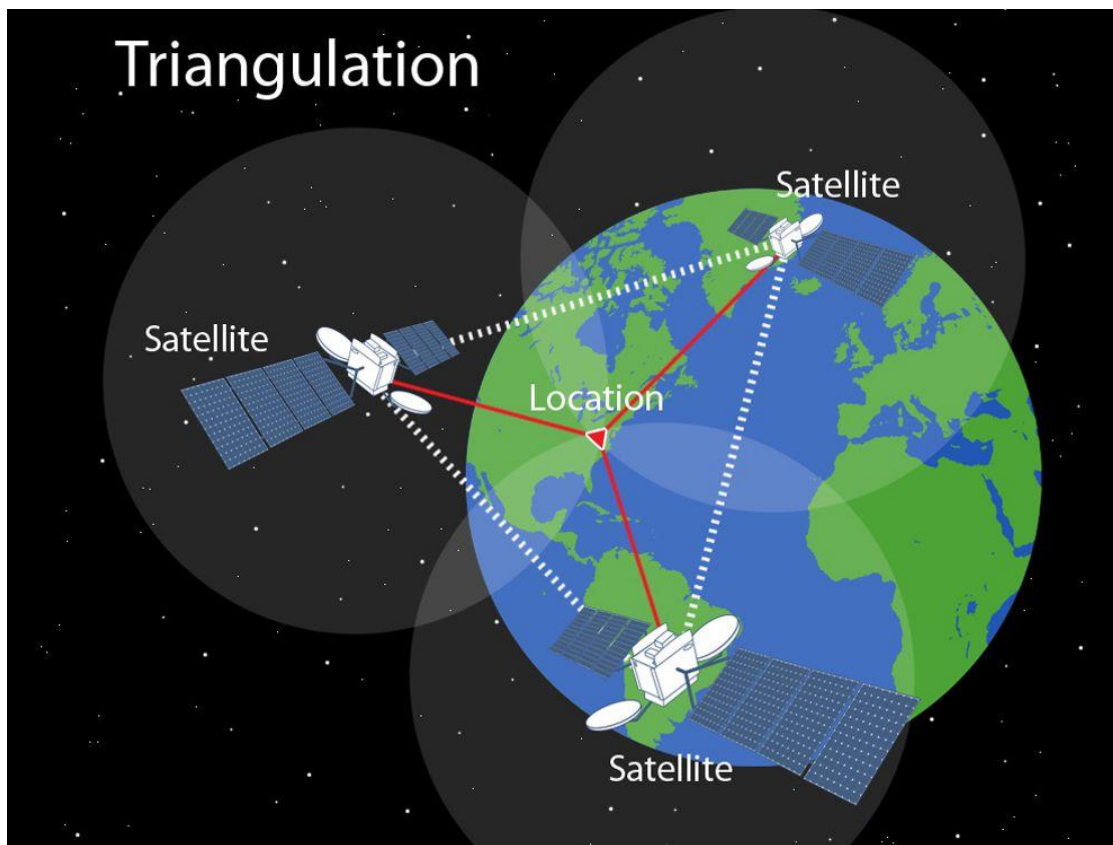


Figure 158: Triangulation

GPS module is a processor with antenna that receives signals from GPS satellites within radio frequency range. The module receives the signal with a timestamp from each satellite. If the module's antenna can spot 4 or more satellites, it is able to accurately calculate its position and time.

We have been using uBlox Neo 6M GPS module, and by entering the latitude and longitude GPS coordinates on Google Maps

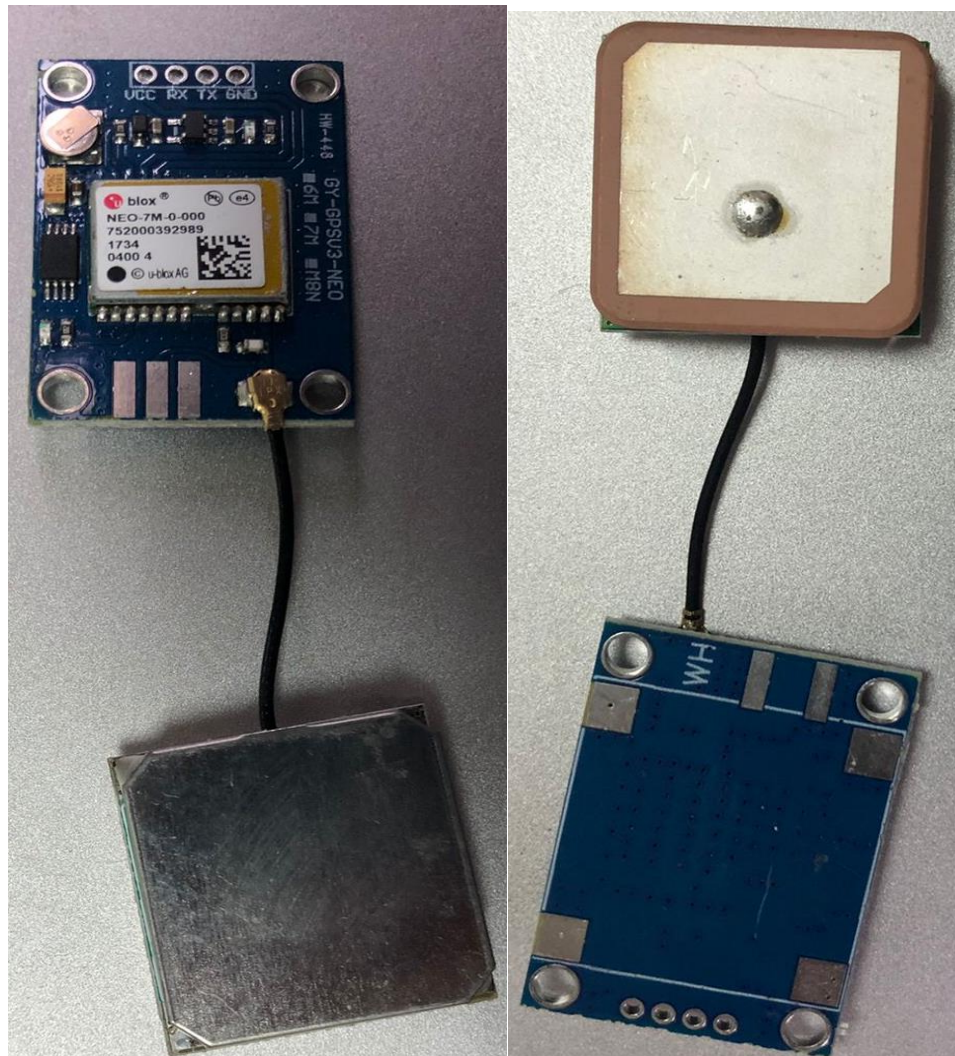


Figure 159: GPS module with Antenna

```
COM3 (Arduino/Genuino Uno) Send  
  
Position: Latitude: 30.02449 Position: Latitude: 30.024492, Longitude: 31.211536  
Position: Latitude: 30.024492, Longitude: 31.211536  
Position: Latitude: 30.024494, Longitude: 31.211532  
Position: Latitude: 30.024494, Longitude: 31.211532  
Position: Latitude: 30.024492, Longitude: 31.211530  
Position: Latitude: 30.024492, Longitude: 31.211530  
Position: Latitude: 30.024492, Longitude: 31.211532  
Position: Latitude: 30.024492, Longitude: 31.211532  
Position: Latitude: 30.024490, Longitude: 31.211528  
Position: Latitude: 30.024490, Longitude: 31.211528  
Position: Latitude: 30.024488, Longitude: 31.211528  
Position: Latitude: 30.024488, Longitude: 31.211528  
Position: Latitude: 30.024488, Longitude: 31.211526  
  
 Autoscroll  Show timestamp Newline  9600 baud  Clear output
```

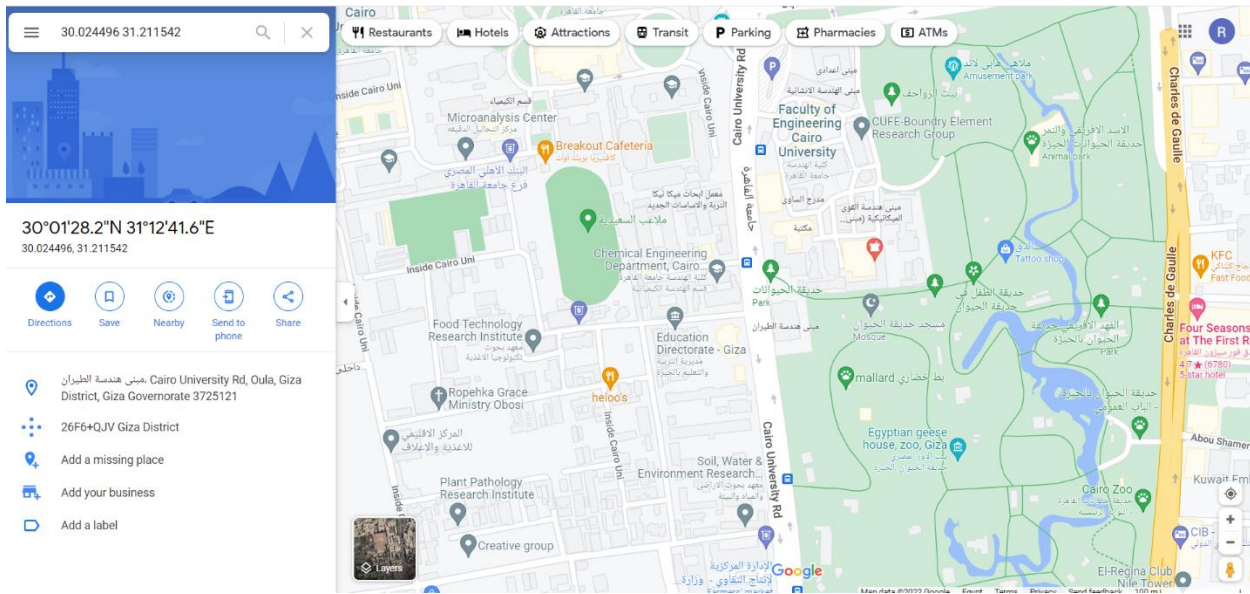


Figure 160 : Coordinates of Aerospace Engineering department building

#### 6.6.4 Transmitter and Receiver

Using a transmitter and receiver is essential when it comes to making an eVtol vehicle, as we don't have to communicate with the microcontroller directly; this will require a lot of long wires that is not applicable, instead we need to communicate with the microcontroller using wireless communication (e.g. Bluetooth, or Wi-Fi modules).

The most used Wi-Fi module with Arduino boards is ESP8266 via Blynk App. Blynk Cloud is open source cloud that connects device (smartphone) that access the application to the module via Wi-Fi connection, this connection is on a Blynk Server to allow receiving and sending messages. The application allows the user to create a template and add buttons or switches etc. as inputs to be sent to the microcontroller, or add a counter or a screen to preview data being sent from the microcontroller to the device.



Figure 161: Blynk IoT

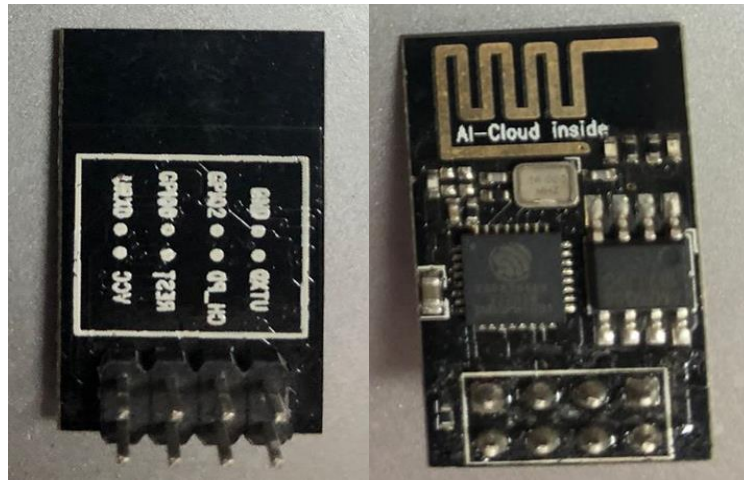


Figure 162: ESP8266

We have been using nRF24L01 as our Wi-Fi module, as we found Blynk App is a bit complicated especially the latest version is way complicated than the older one. The nRF24L01 module can be complicated because of the connections to the Arduino (microcontroller). The module operates through a Serial Peripheral Interface (SPI), as it can receive data from or send data to the microcontroller, but we will deal with a single master and a single slave.

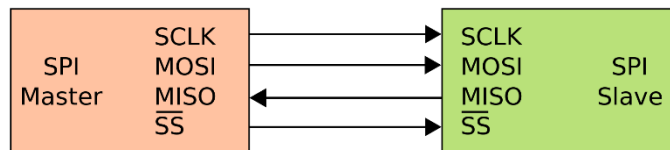


Figure 163: Serial Peripheral Interface (SPI)

We connected one Arduino board to nRF24L01 (transmitter) to send data from a laptop, and another Arduino board to nRF24L01 (receiver) to receive data and send signals to the motors. But if we want to receive data from the sensors that is on the vehicle, in addition to sending signals to the motors, the nRF24L01 Wi-Fi module works very well as a 6 data pipes MultiCeiver. The module can have an antenna to increase the range of transmission up to 1500m (based on specifications from an online store), but it will cost more than the standard. We tried the standard version to run the motors on our vehicle, but it worked within range of 10m only.

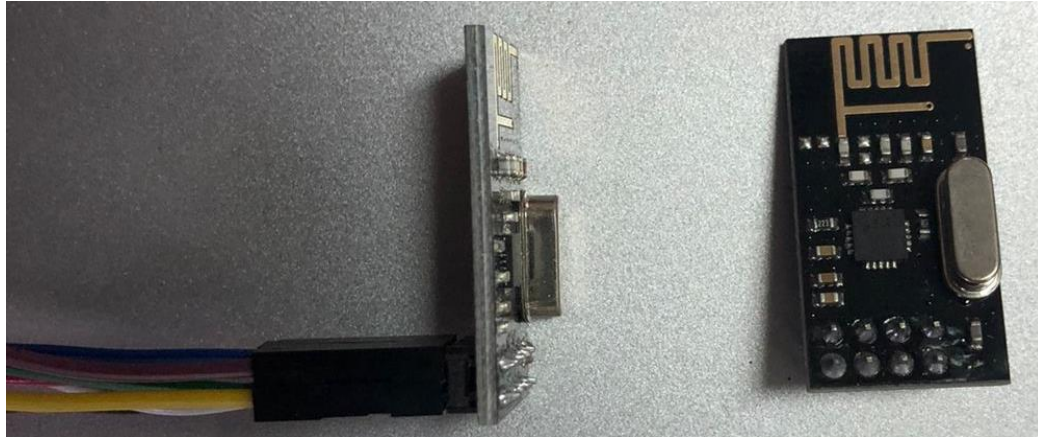


Figure 164: nRF24L01

### 6.6.5 Airspeed Sensor

Air speed sensor measures speed of aircraft relative to the air by measuring the pressure of the air (pitot pressure), and using Bernoulli's equation:

$$P = P_0 + \frac{\rho V^2}{2}$$

$$V = \sqrt{\frac{2}{\rho}(P - P_0)}$$

Where:  $P_0$  is static pressure of air inside the pitot tube, and  $\rho$  is the density

## 6.7. Arducopter

APM 2.8 is an open source fully automated system and a best-selling technology that won the prestigious 2012 Outdoor Drone Challenge competition. Allows the user to convert any stationary vehicle, rotary wing or multi-rotor vehicle (even cars and boats) into a fully autonomous vehicle; Capable of performing GPS missions programmed with waypoints. Available with top or side connectors.

This revision of the board does not have an on-board compass, which is designed for vehicles (particularly multi copters and rovers) where the compass should be placed as far away from power sources and motors as possible to avoid magnetic interference. (On a fixed wing aircraft it is often easier to mount the APM far enough from the actuators and very high sampling to avoid magnetic interference, so this is not a big deal, but APM 2.6 gives more flexibility in this location and

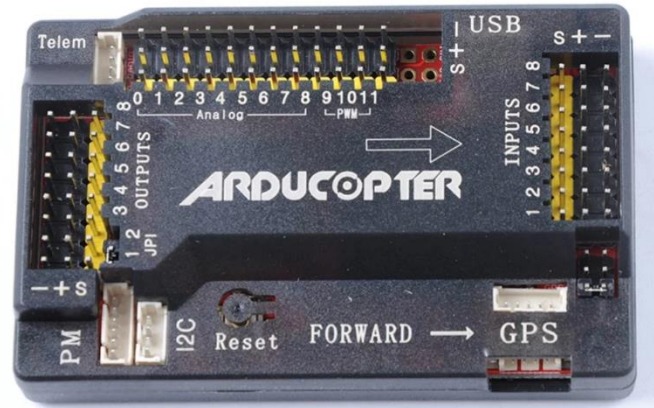


Figure 165: Arducopter

is a good choice for them too) . This is designed to be used with a 3DR GPS with a compass (see option below), so that the GPS/compass module can be mounted over noise sources from the APM itself.

### Features:

- 1) Can be ordered with top entry pins to attach connectors vertically, or as side entry pins to slide your connectors to one end horizontally
- 2) Includes 3-axis tachometer, accelerometer and magnetometer, along with a high-performance measuring scale
- 3) 4MB data flash chip on board for automatic data cleaning
- 4) Off-board positioning module, LEA-6H compass module.
- 5) One of the first open-source autopilot systems to use the MPU-6000's 4th generation 6-DoF tachometer.
- 6) Barometric pressure sensor upgraded to MS5611-01BA03, from measurement specialties.
- 7) Atmel ATMEGA2560 and ATMEGA32U-2 chips for processing usb functions respectively.

### Specifications:

- 1) Housing material: plastic Housing color: grey with housing size: 70 x 44 x 13mm, Net Weight: 31g
- 2) GPS: Built-in Compass GPS Module With fast satellite search speed, and high accuracy Compatible with APM serial port and I2C port, Includes a round plastic casing and GPS support

We are going to use autopilot Software and it is capable of controlling any vehicle like you know it can control conventional airplane quad plane multi rotors and helicopters and so many other things.

Let's talk about second system which is ground control station, so first of all what is ground control station

A ground control station is as you know a ground-based hardware and software that allows UAV operator to communicate and control a drone they can control the payload also with the help of ground control station, so if I talk about ground control station hardware it can be your computer or mobile or tablet.

There are so many open sources ground control station software available on the internet for different platforms, like there is a mission planner only for windows there is a QGS for iOS and Linux, and there is a map proxy for only for

Linux, and there is a tower and map pilot for tablets and mobiles

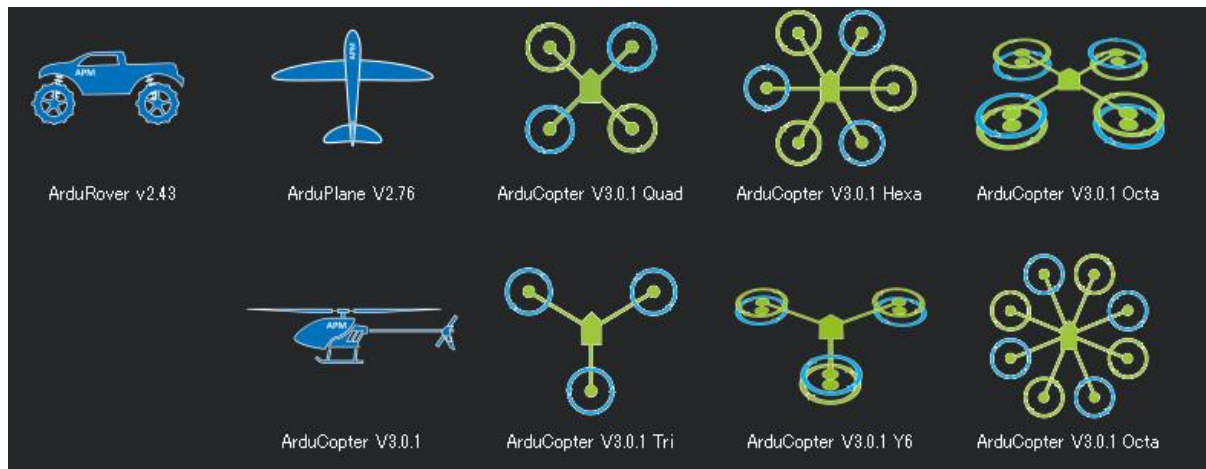


Figure 166: mission planner

From mission planner we setup firmware ArduCopter V3.0.1 Octa to our ardcopeter hardware, to use multi rotors.

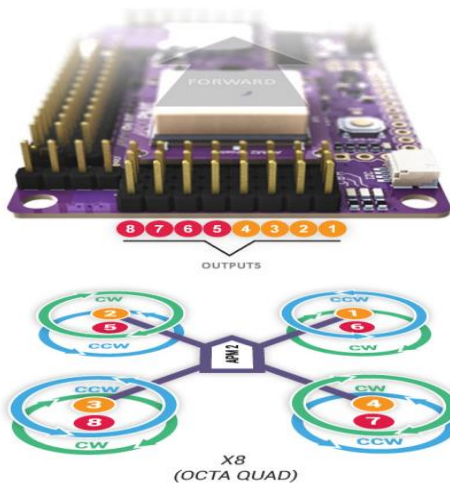


Figure 167: The configuration we have to use to our Arducopter

The last thing we need to know is communication link system, so the hardware for communication link system is basically a telemetry, and for software we will be using socket communication, as we are going to run every software in the same system and the protocol, we will be using the Mavenlink protocol for communication system

So now we are clear with the overall view of drone system, we also know the software and hardware of drones of our drone system but still something is missing like how actually we are going to program here because we can't simply make changes in the autopilot software it's a very huge

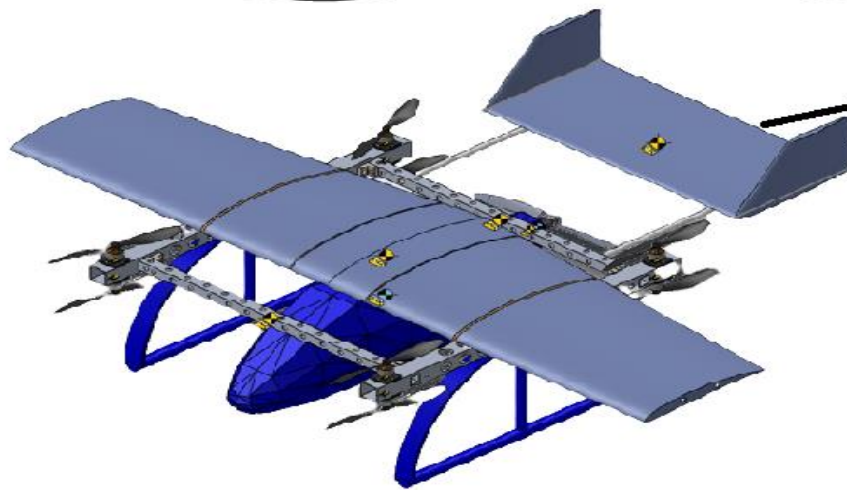
open-source software uh which consists of seven lakh code lines, so here comes the need of some sort of API which can communicate to autopilot software.

#### **Application programming interface (API):**

It is an application programming interface which allows two application or software to talk to each other and that role will be done by drone kit basically a drone kit uses a python function that creates and send messages to your drone autopilot allowing you to control your drone from a python script, for example you can write a python script to take off 10 meter and move to a particular location or follow a vehicle, and then with the help of drone kit you can directly run your python script or program in your drone.

# **Chapter Seven:**

# **Octa-Quad Modeling**



## 7.1. Introduction

We want to control the vehicle and simulate our mission. In this chapter, starting from Newton's second law, which states that the summation of external forces is equal to the time rate of change of the linear momentum, and the summation of external moments is equal to the time rate of change of the angular momentum, we study the forces and moments generated by the motors that act on the vehicle during the mission.

As we deal with two coordinate frames

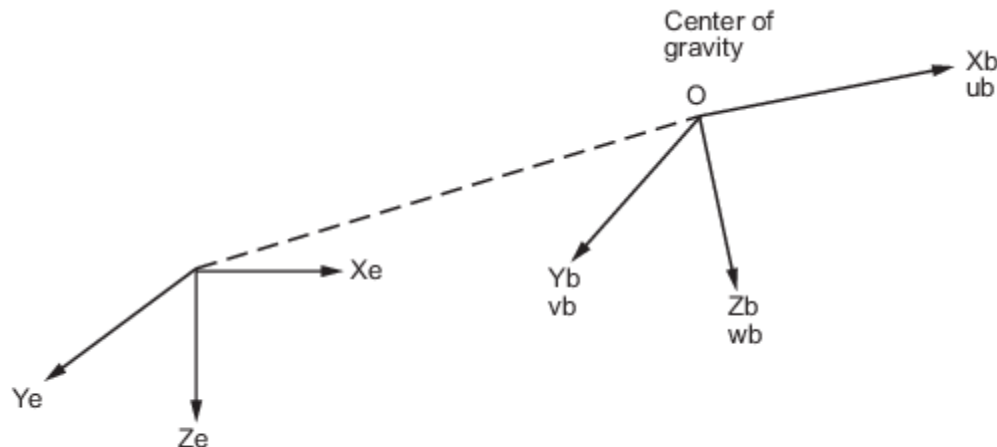
- 1- Flat earth reference frame:  $(x_E, y_E, z_E)$

This fixed frame is a reference to the vehicle's position and rotational motion.

- 2- Body fixed coordinate frame:  $(x_B, y_B, z_B)$

This frame is attached to the vehicle; its origin is the vehicle center of gravity.

The rotational motion is represented in earth axes, as the body fixed axes rotate with the vehicle



Flat Earth reference frame

Figure 168: Coordinate Frames

## 7.2. Transition from earth axes to body axes

The orientation of the vehicle is described by Euler angles. The rotation of body axes with respect to the earth axes can be represented by:

- Roll angle ( $\phi$ ) which is the rotation of the body axes about  $x_B$
- Pitch angle ( $\theta$ ) which is the rotation of the body axes about  $y_B$
- Yaw angle ( $\psi$ ) which is the rotation of the body axes about  $z_B$

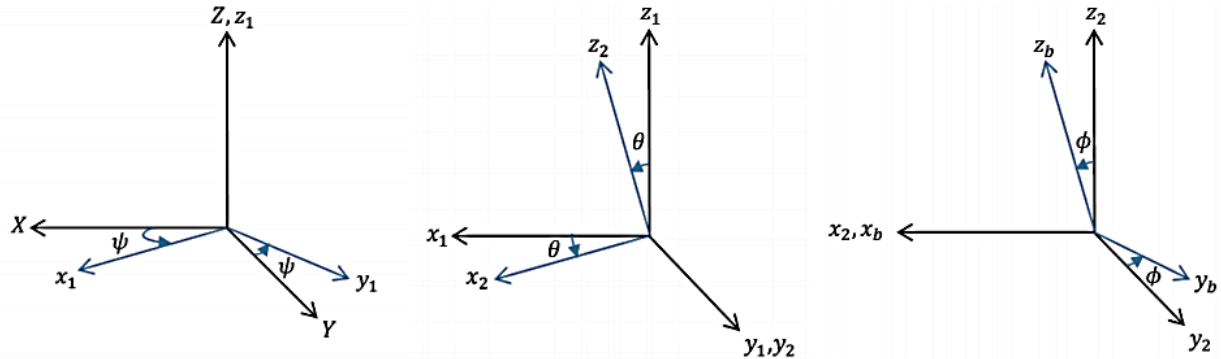


Figure 169: Transition from Body Axes to Earth Axes

### Coordinate transformation from body axes

- About  $z_B$        $R_1 = \begin{bmatrix} \cos\psi & -\sin\psi & 0 \\ \sin\psi & \cos\psi & 0 \\ 0 & 0 & 1 \end{bmatrix}$

- About  $y_B$        $R_2 = \begin{bmatrix} \cos\theta & 0 & \sin\theta \\ 0 & 1 & 0 \\ -\sin\theta & 0 & \cos\theta \end{bmatrix}$

- About  $x_B$        $R_3 = \begin{bmatrix} 1 & 0 & 0 \\ 0 & \cos\phi & -\sin\phi \\ 0 & \sin\phi & \cos\phi \end{bmatrix}$

Then the fully transformation matrix from body axes to earth axes

$$R_{BE} = R_3 R_2 R_1 = \begin{bmatrix} 1 & 0 & 0 \\ 0 & \cos\phi & -\sin\phi \\ 0 & \sin\phi & \cos\phi \end{bmatrix} \begin{bmatrix} \cos\theta & 0 & \sin\theta \\ 0 & 1 & 0 \\ -\sin\theta & 0 & \cos\theta \end{bmatrix} \begin{bmatrix} \cos\psi & -\sin\psi & 0 \\ \sin\psi & \cos\psi & 0 \\ 0 & 0 & 1 \end{bmatrix}$$

$$\begin{aligned} R_{BE} \\ = \begin{bmatrix} \cos\theta \cos\psi & \sin\phi \sin\theta \cos\psi - \cos\phi \sin\psi & \cos\phi \sin\theta \cos\psi + \sin\phi \sin\psi \\ \cos\theta \sin\psi & \sin\phi \sin\theta \sin\psi + \cos\phi \cos\psi & \cos\phi \sin\theta \sin\psi - \sin\phi \cos\psi \\ -\sin\theta & \sin\phi \cos\theta & \cos\phi \cos\theta \end{bmatrix} \end{aligned}$$

It should be mentioned that the transformation matrix from earth axes to body axes is the inverse of the matrix  $R_{BE}$  which is an orthogonal matrix

$$R_{EB} = (R_{BE})^{-1} = (R_{BE})^T$$

### 7.3. Kinetics

Newton's second law can be expressed as

#### 7.3.1 Forces

- 1- The summation of external forces is equal to the time rate of change of the linear momentum

$$\vec{F} = \frac{d}{dt}(m\vec{V})$$

If the body axes are rotating with respect to the earth axes with angular rate,  $\vec{\omega} = \begin{bmatrix} p \\ q \\ r \end{bmatrix}$

$$\vec{F} = m \left( \frac{d\vec{V}_B}{dt} + \vec{\omega} \times \vec{V}_B \right)$$

$$\begin{bmatrix} F_x \\ F_y \\ F_z \end{bmatrix} = m \left( \begin{bmatrix} \dot{u} \\ \dot{v} \\ \dot{w} \end{bmatrix} + \begin{bmatrix} p \\ q \\ r \end{bmatrix} \times \begin{bmatrix} u \\ v \\ w \end{bmatrix} \right)$$

The forces equations can be written in a scalar form

$$F_x = m (\dot{u} + qw - rv)$$

$$F_y = m (\dot{v} + ru - pw)$$

$$F_z = m (\dot{w} + pv - qu)$$

## 7.3.2 moments

- 2- The summation of external moments is equal to the time rate of change of the angular momentum

$$\vec{M} = \frac{d}{dt}(I \vec{\omega})$$

$$\begin{bmatrix} L \\ M \\ N \end{bmatrix} = \left( I \begin{bmatrix} \dot{p} \\ \dot{q} \\ \dot{r} \end{bmatrix} + \begin{bmatrix} p \\ q \\ r \end{bmatrix} \times I \begin{bmatrix} p \\ q \\ r \end{bmatrix} \right)$$

Where  $I$  is the inertia matrix

$$I = \begin{pmatrix} I_{xx} & -I_{xy} & -I_{xz} \\ -I_{yx} & I_{yy} & -I_{yz} \\ -I_{zx} & -I_{zy} & I_{zz} \end{pmatrix}$$

$$I_{xx} = \iiint (y^2 + z^2) \delta m$$

$$I_{xy} = I_{yx} = \iiint xy \delta m$$

$$I_{yy} = \iiint (x^2 + z^2) \delta m$$

$$I_{xz} = I_{zx} = \iiint xz \delta m$$

$$I_{zz} = \iiint (x^2 + y^2) \delta m$$

$$I_{yz} = I_{zy} = \iiint yz \delta m$$

(Moments of inertia are taken at the center of mass of the vehicle)

The moments equations can be written in a scalar form

$$L = I_{xx} \dot{p} - I_{xz} \dot{r} + (I_{zz} - I_{yy}) qr - I_{xz} pq$$

$$M = I_{yy} \dot{q} + I_{xz} (p^2 - r^2) + (I_{xx} - I_{zz}) pr$$

$$N = I_{zz} \dot{r} - I_{xz} \dot{p} + (I_{yy} - I_{xx}) pq + I_{xz} qr$$

## 7.4. Kinematics

- 1- The relation between the time rate of change of the Euler angles  $\begin{bmatrix} \dot{\phi} \\ \dot{\theta} \\ \dot{\psi} \end{bmatrix}$ , and body-fixed angular velocity vector  $\omega = \begin{bmatrix} p \\ q \\ r \end{bmatrix}$ , are determined by resolving the Euler rates into the body-fixed coordinate frame

$$\omega = \begin{bmatrix} \dot{\phi} \\ 0 \\ 0 \end{bmatrix} + (R_3)^{-1} \begin{bmatrix} 0 \\ \dot{\theta} \\ 0 \end{bmatrix} + (R_3)^{-1} (R_2)^{-1} \begin{bmatrix} 0 \\ 0 \\ \dot{\psi} \end{bmatrix}$$

$$\begin{bmatrix} p \\ q \\ r \end{bmatrix} = \begin{bmatrix} \dot{\phi} \\ 0 \\ 0 \end{bmatrix} + \begin{bmatrix} 1 & 0 & 0 \\ 0 & \cos\phi & \sin\phi \\ 0 & -\sin\phi & \cos\phi \end{bmatrix} \begin{bmatrix} 0 \\ \dot{\theta} \\ 0 \end{bmatrix} + \begin{bmatrix} 1 & 0 & 0 \\ 0 & \cos\phi & \sin\phi \\ 0 & -\sin\phi & \cos\phi \end{bmatrix} \begin{bmatrix} \cos\theta & 0 & -\sin\theta \\ 0 & 1 & 0 \\ \sin\theta & 0 & \cos\theta \end{bmatrix} \begin{bmatrix} 0 \\ 0 \\ \dot{\psi} \end{bmatrix}$$

$$\begin{bmatrix} p \\ q \\ r \end{bmatrix} = J^{-1} \begin{bmatrix} \dot{\phi} \\ \dot{\theta} \\ \dot{\psi} \end{bmatrix}$$

Where

$$J = \begin{bmatrix} 1 & \sin\phi \tan\theta & \cos\phi \tan\theta \\ 0 & \cos\phi & -\sin\phi \\ 0 & \sin\phi \sec\theta & \cos\phi \sec\theta \end{bmatrix}$$

The transformation from body angular velocity to Euler rate vector

$$\begin{bmatrix} \dot{\phi} \\ \dot{\theta} \\ \dot{\psi} \end{bmatrix} = J \begin{bmatrix} p \\ q \\ r \end{bmatrix}$$

The scalar form

$$\begin{aligned} \dot{\phi} &= p + \sin\phi \tan\theta q + \cos\phi \tan\theta r \\ \dot{\theta} &= \cos\phi q - \sin\phi r \\ \dot{\psi} &= \sin\phi \sec\theta q + \cos\phi \sec\theta r \end{aligned}$$

2- The relation between the velocity with respect to the earth inertial axes  $\begin{bmatrix} \dot{x}_E \\ \dot{y}_E \\ \dot{z}_E \end{bmatrix}$ , and the velocity in body axes  $\begin{bmatrix} u \\ v \\ w \end{bmatrix}$

$$\begin{bmatrix} \dot{x}_E \\ \dot{y}_E \\ \dot{z}_E \end{bmatrix} = R_{BE} \begin{bmatrix} u \\ v \\ w \end{bmatrix}$$

$$\begin{aligned} R_{BE} &= \begin{bmatrix} \cos\theta \cos\psi & \sin\phi \sin\theta \cos\psi - \cos\phi \sin\psi & \cos\phi \sin\theta \cos\psi + \sin\phi \sin\psi \\ \cos\theta \sin\psi & \sin\phi \sin\theta \sin\psi + \cos\phi \cos\psi & \cos\phi \sin\theta \sin\psi - \sin\phi \cos\psi \\ -\sin\theta & \sin\phi \cos\theta & \cos\phi \cos\theta \end{bmatrix} \end{aligned}$$

The scalar form

$$\dot{x}_E = \cos\theta \cos\psi u + (\sin\phi \sin\theta \cos\psi - \cos\phi \sin\psi) v \\ + (\cos\phi \sin\theta \cos\psi + \sin\phi \sin\psi) w$$

$$\dot{y}_E = \cos\theta \sin\psi u + (\sin\phi \sin\theta \sin\psi + \cos\phi \cos\psi) v \\ + (\cos\phi \sin\theta \sin\psi - \sin\phi \cos\psi) w$$

$$\dot{z}_E = -\sin\theta u + \sin\phi \cos\theta v + \cos\phi \cos\theta w$$

## 7.5. Modeling

Before getting into forces and moments that act on the vehicle, there are a few assumptions to apply the 6DOF rigid body equations of motion in 3D space:

- The mass and inertia are constants
- The origin of the body-fixed coordinate frame is at the center of gravity of the body, and the body is assumed to be rigid
- The earth is flat and non-rotating, then the flat earth reference frame is considered inertial
- Constant gravity
- The vehicle's body is symmetric about the x-z plane

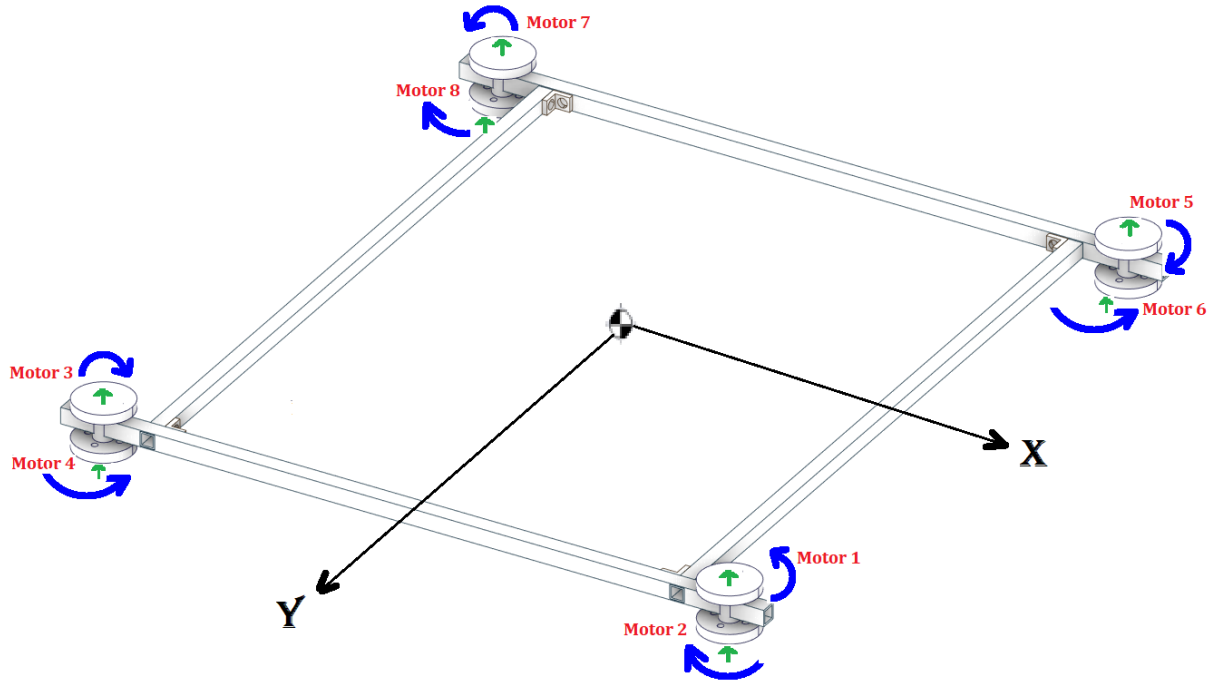


Figure 170 .The arrangement of the motors and the direction of their rotation

Forces and moments that act on the vehicle are acting along the body fixed axes, except the gravitational force which acts along the z-axis of earth axes through the vehicle's center of gravity, so it doesn't produce moments.

The transformation of the gravitational force from earth axes to body axes

$$\begin{bmatrix} F_x \\ F_y \\ F_z \end{bmatrix} = R_{EB} \begin{bmatrix} 0 \\ 0 \\ mg \end{bmatrix} = \begin{bmatrix} -mg \sin\theta \\ mg \sin\phi \cos\theta \\ mg \cos\phi \cos\theta \end{bmatrix}$$

Forces that act on the vehicle are generated by 8 brushless DC motors to generate force in negative z-axis of body fixed frame, and a brushless DC motor to generate thrust in x-axis of body fixed frame.

We can assume that force and torque generated by a motor does change linearly with the square of the motor's rotational speed as the following relations

$$F = K_t \omega^2$$

$$\text{Torque} = K_r \omega^2$$

Where  $\omega$  (rad/sec),  $F$  (N), Torque (N.m)

To verify this assumption for the two types of motors

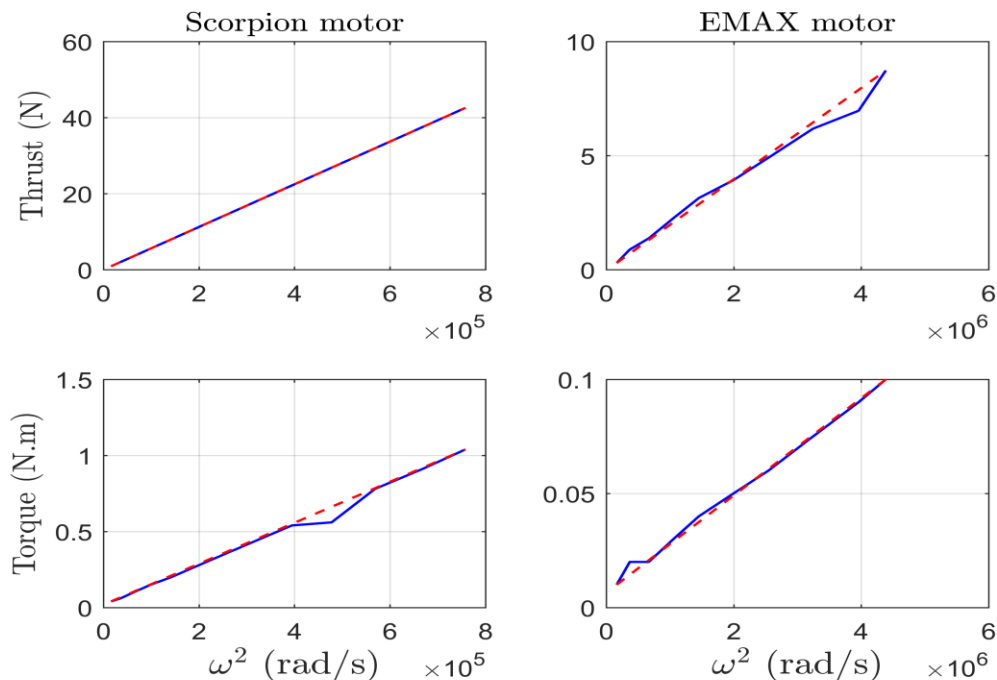


Figure 171:Comparison between two different motors

And the rotational speed is proportional to throttle input signal given to the motor

To verify this assumption for the two types of motors

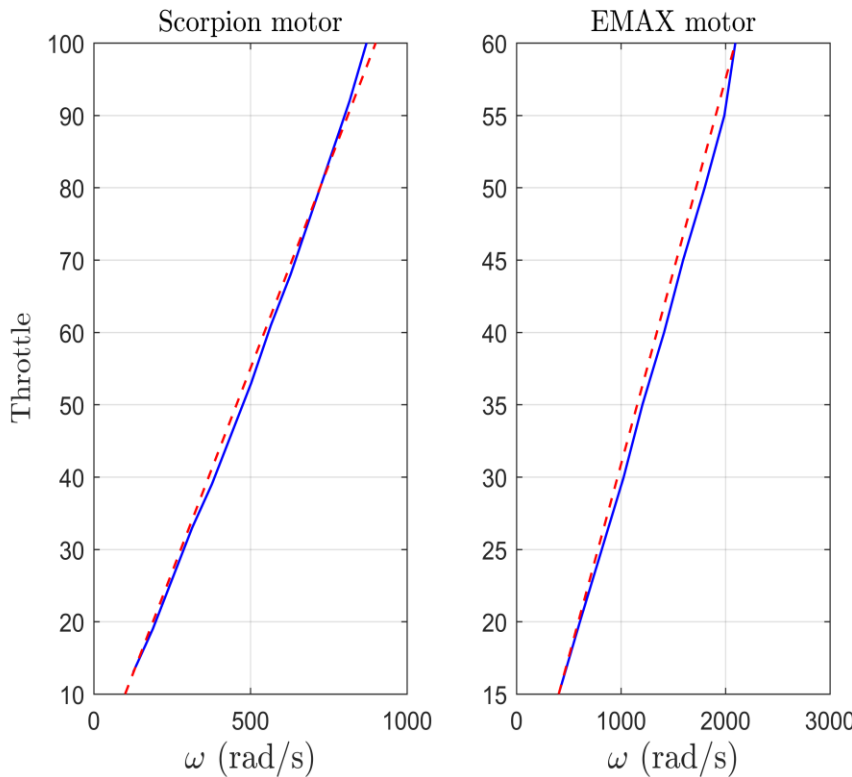


Figure 172 .Comparison between two different motors

## 7.6. Forces in body

### 7.6.1 Forces in body x-axis

- 1- Thrust force generated by Scorpion SII-4020-420 brushless DC motor **420 KV (420 rpm/volt)** with thrust coefficient  $K_t = 0.0045$
- 2- Aerodynamic drag force

$$D = \frac{1}{2} \rho V^2 S C_D$$

XFLR5 results

$$D = 0.006691V^2 + (2.768e - 08)V - (6.447e - 08)$$

The previous forces act through the vehicle's center of gravity, so they don't produce moments.

### 7.6.2 Forces in body z-axis

- 1- Aerodynamic lift force that acts through the vehicle's center of gravity, so it doesn't produce moments.

$$L = \frac{1}{2} \rho V^2 S C_L$$

XFLR5 results

$$C_L = 0.5 + 0.06375 \alpha(\text{deg})$$

- 2- Propulsive forces generated by 8 EMAX A2212 6T brushless DC motors  
2200 KV (2200 rpm/volt) with thrust coefficient  $K_t = 0.0022$

The motors (1, 4, 6, and 7) rotate counter clockwise, and (2, 3, 5, and 8) rotate clockwise to avoid yaw drift, and moments produced by the motors are due to the forces multiplied by the normal distance from the motors to the axis of the moment.

## 7.7. Moments about body axes

- 1) As the eight motors rotate with the same speed, the propulsive force generated by the motors are the same assuming the motors have the same thrust coefficient, then no moments are produced because of the symmetry about x-z and y-z planes. However, the motors may not rotate with the same speed for each motor, which produces moments about the body axes
  - ❖ Rolling moment (about the x-axis of body fixed frame) is produced by increasing the rotational speed of the motors to increase the generated forces located in the negative half of y-axis (5, 6, 7, and 8), and decreasing the rotational speed of the motors which are located in the positive half of y-axis (1, 2, 3, and 4).
  - ❖ Pitching moment (about the y-axis of body fixed frame) is produced by increasing the rotational speed of the motors which are located in the positive half of x-axis (1, 2, 5, and 6), and decreasing the rotational speed of the motors which are located in the negative half of x-axis (3, 4, 7, and 8).
  - ❖ Yawing moment (about the z-axis of body fixed frame) is produced by increasing the rotational speed of the motors rotating counter clockwise (1, 4, 6, and 7), and decreasing the rotational speed of the motors rotating clockwise (2, 3, 5, and 8). The yawing moment is a result of torque generated by the motors, as four motors rotate counter clockwise and the other four rotate clockwise, if the eight motors rotate with the same speed, from equilibrium the torque is zero, but if one set rotates faster the resultant is not zero which forces the body to rotate about its z-axis.
- 2) Aerodynamic moments, because of the control surfaces deflection.
- 3) Torque that is caused by single rotor.

## 7.8. Modeling Parameters

Parameters needed for modeling the vehicle:

Parameter	Value	Parameter	Value
Mass; $m$	5.8 kg	Gravity; $g$	9.81 m/s <sup>2</sup>
Moment of inertia (x-axis); $I_{xx}$	0.6562 kg.m <sup>2</sup>	Vehicle's arm; $L$	0.325 m
Moment of inertia (y-axis); $I_{yy}$	1.0893 kg.m <sup>2</sup>	Wing area; $S$	0.52 m <sup>2</sup>
Moment of inertia (z-axis); $I_{zz}$	0.5099 kg.m <sup>2</sup>	Air density; $\rho$	1.225 kg/m <sup>3</sup>
Thrust coefficient of each of the eight motors; $b$	0.0022 N	Torque coefficient of each of the eight motors; $d$	3.4e - 05 N.m
Thrust coefficient of the thruster motor; $K_{th}$	0.0045 N	Torque coefficient of the thruster motor; $K_q$	1.1e - 04 N.m
Stall speed; $V_s$	11 m/s	Cruise speed; $V_{cr}$	18 m/s

The minimum throttle that each of the eight motors should have to generate lift force equal to vehicle's weight is

$$Th_{min} = \sqrt{\frac{mg}{8b}} = 56.85$$

Coordinates of each motor from the origin (c.g.)

$i$	1	2	3	4	5	6	7	8
$x_i$	0.325	0.325	-0.325	-0.325	0.325	0.325	-0.325	-0.325
$y_i$	0.325	0.325	0.325	0.325	-0.325	-0.325	-0.325	-0.325

The location of each motor is to simplify the calculation of the forces, as the coaxial motors are not actually located on the same point but they are on the opposite sides of the z-axis, assuming the forces generated are along the same axis.

## 7.9 Mission Modeling:

The vehicle's mission is

- 1- Acceleration along z-axis till the vehicle reaches the desired altitude
- 2- Acceleration along x-axis till the vehicle reaches the required range
- 3- Vertical landing, negative acceleration along z-axis till the vehicle reaches the landing point

Modeling is divided into two parts:

### 7.9.1. Takeoff and landing

There are no forces generated by the motors in x-axis and y-axis, only in z-axis (upwards)

$$F_x = \mathbf{0} \quad F_y = \mathbf{0} \quad F_z = -\begin{bmatrix} b \\ b \end{bmatrix}^T \begin{bmatrix} Th_1^2 \\ Th_2^2 \\ Th_3^2 \\ Th_4^2 \\ Th_5^2 \\ Th_6^2 \\ Th_7^2 \\ Th_8^2 \end{bmatrix}$$

OR

$$F_z = -b \sum_{i=1}^8 Th_i^2$$

The moments generated by the motors about [x, y, z] axes, are [L, M, N]

$$L = -\begin{bmatrix} by_1 \\ by_2 \\ by_3 \\ by_4 \\ by_5 \\ by_6 \\ by_7 \\ by_8 \end{bmatrix}^T \begin{bmatrix} Th_1^2 \\ Th_2^2 \\ Th_3^2 \\ Th_4^2 \\ Th_5^2 \\ Th_6^2 \\ Th_7^2 \\ Th_8^2 \end{bmatrix} \quad M = \begin{bmatrix} bx_1 \\ bx_2 \\ bx_3 \\ bx_4 \\ bx_5 \\ bx_6 \\ bx_7 \\ bx_8 \end{bmatrix}^T \begin{bmatrix} Th_1^2 \\ Th_2^2 \\ Th_3^2 \\ Th_4^2 \\ Th_5^2 \\ Th_6^2 \\ Th_7^2 \\ Th_8^2 \end{bmatrix} \quad N = \begin{bmatrix} d \\ -d \\ -d \\ d \\ -d \\ d \\ d \\ -d \end{bmatrix}^T \begin{bmatrix} Th_1^2 \\ Th_2^2 \\ Th_3^2 \\ Th_4^2 \\ Th_5^2 \\ Th_6^2 \\ Th_7^2 \\ Th_8^2 \end{bmatrix}$$

OR

$$L = -b \sum_{i=1}^8 Th_i^2 y_i$$

$$M = b \sum_{i=1}^8 Th_i^2 x_i$$

$$N = d(Th_1^2 - Th_2^2 - Th_3^2 + Th_4^2 - Th_5^2 + Th_6^2 + Th_7^2 - Th_8^2)$$

The contribution on forces and moments of each motor can be put in one matrix (mixer matrix) that takes four inputs [ $Th_{late}$ ,  $Th_{long}$ ,  $Th_{norm}$ ,  $Th_z$ ], and its output is the throttle vector after adding the minimum value of throttle for each motor.

$$mixer_{mat} = \begin{bmatrix} -0.125 & 0.125 & 0.125 & 0.125 \\ -0.125 & 0.125 & -0.125 & 0.125 \\ -0.125 & -0.125 & -0.125 & 0.125 \\ -0.125 & -0.125 & 0.125 & 0.125 \\ 0.125 & 0.125 & -0.125 & 0.125 \\ 0.125 & 0.125 & 0.125 & 0.125 \\ 0.125 & -0.125 & 0.125 & 0.125 \\ 0.125 & -0.125 & -0.125 & 0.125 \end{bmatrix}$$

The contribution of each motor can be written as

$$\mathbf{Th}_1 = (-0.125)\mathbf{Th}_{late} + (0.125)\mathbf{Th}_{long} + (0.125)\mathbf{Th}_{norm} + (0.125)\mathbf{Th}_z$$

$$\mathbf{Th}_2 = (-0.125)\mathbf{Th}_{late} + (0.125)\mathbf{Th}_{long} + (-0.125)\mathbf{Th}_{norm} + (0.125)\mathbf{Th}_z$$

$$\mathbf{Th}_3 = (-0.125)\mathbf{Th}_{late} + (-0.125)\mathbf{Th}_{long} + (-0.125)\mathbf{Th}_{norm} + (0.125)\mathbf{Th}_z$$

$$\mathbf{Th}_4 = (-0.125)\mathbf{Th}_{late} + (-0.125)\mathbf{Th}_{long} + (0.125)\mathbf{Th}_{norm} + (0.125)\mathbf{Th}_z$$

$$\mathbf{Th}_5 = (0.125)\mathbf{Th}_{late} + (0.125)\mathbf{Th}_{long} + (-0.125)\mathbf{Th}_{norm} + (0.125)\mathbf{Th}_z$$

$$\mathbf{Th}_6 = (0.125)\mathbf{Th}_{late} + (0.125)\mathbf{Th}_{long} + (0.125)\mathbf{Th}_{norm} + (0.125)\mathbf{Th}_z$$

$$\mathbf{Th}_7 = (0.125)\mathbf{Th}_{late} + (-0.125)\mathbf{Th}_{long} + (0.125)\mathbf{Th}_{norm} + (0.125)\mathbf{Th}_z$$

$$\mathbf{Th}_8 = (0.125)\mathbf{Th}_{late} + (-0.125)\mathbf{Th}_{long} + (-0.125)\mathbf{Th}_{norm} + (0.125)\mathbf{Th}_z$$

Where:

$\mathbf{Th}_{late}$  is the throttle input to control roll angle  $\phi$

$\mathbf{Th}_{long}$  is the throttle input to control pitch angle  $\theta$

$\mathbf{Th}_{norm}$  is the throttle input to control yaw angle  $\psi$

$\mathbf{Th}_z$  is the throttle input to control altitude

Throttle vector contains the throttle of each motor which goes through a MATLAB function to calculate the forces and moments, and then the weight components in body fixed axes are added to the forces vector. 6DOF (Euler Angles) block in Simulink, solves the equations of motion of the body.

Our first step is to control the eight motors to stabilize the vehicle during takeoff and landing, till the vehicle reaches the desired altitude, meaning that we want roll, pitch, and yaw angles to be zero. We can use MATLAB Simulink to simulate the mission and to linearize the equations of motion. First, we create a Simulink model to get the states  $(x, y, z, \phi, \theta, \psi, u, v, w, p, q, r)$  as we have 4 inputs  $(\mathbf{Th}_{late}, \mathbf{Th}_{long}, \mathbf{Th}_{norm}, \mathbf{Th}_z)$

the model Simulink model for first model linearization

Now, after linearizing in Appendix(A) , we can get the transfer functions for each state

For input  $Th_{late}$

$$\frac{Y}{Th_{late}} = \frac{1.216}{s^4} \quad \& \quad \frac{\phi}{Th_{late}} = \frac{0.1239}{s^2}$$

For input  $Th_{long}$

$$\frac{X}{Th_{long}} = -\frac{0.7322}{s^4} \quad \& \quad \frac{\theta}{Th_{long}} = \frac{0.07464}{s^2}$$

For input  $Th_{norm}$

$$\frac{\psi}{Th_{norm}} = \frac{0.007583}{s^2}$$

For input  $Th_z$

$$\frac{Z}{Th_z} = -\frac{0.04313}{s^2}$$

We can see the difference between the responses for inputs  $Th_{late}$  &  $Th_{long}$  , as  $I_{xx} \neq I_{yy}$  despite the symmetry in forces and moments

## 7.9.2. Cruise

The forces acting on the vehicle during cruise are: Thrust force generated by a thruster motor in x-axis, and aerodynamic forces lift in negative z-axis and drag in negative x-axis

$$F_x = K_{th} x_{th}^2 - D \quad F_y = 0 \quad F_z = -L$$

Where:

$$L = \frac{1}{2} \rho u^2 S C_L$$

$$C_L = 0.5 + 0.06375 \alpha(deg) \rightarrow \alpha(deg) = 1.6^\circ + \theta(deg)$$

$$D \approx 0.006691 u^2$$

The only moment produced is a rolling moment caused by single motor.

During cruise, to control thrust

$$Thrust = Drag \quad Lift = Weight$$

The cruise velocity results from equating the weight to the lift force (in earth reference frame)

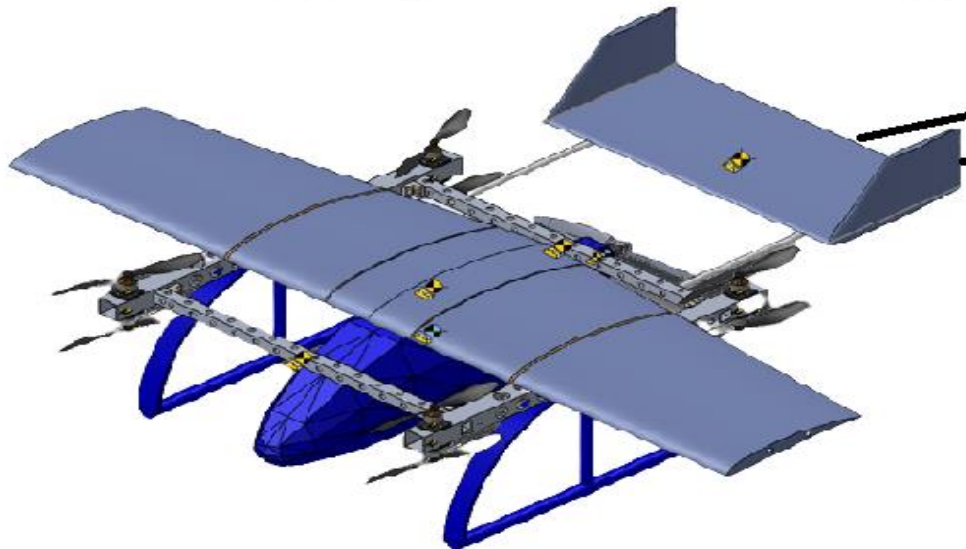
$$L = \frac{1}{2} \rho u^2 S C_L \cos \theta = mg$$

$$V_{cruise} = \sqrt{\frac{2mg}{\rho S C_L \cos \theta}}$$

$$Thrust = K_{th} Th_x^2 = (0.006691) \frac{2mg}{\rho S C_L \cos \theta}$$

# **Chapter Eight:**

## **Octa-quad Control and Simulation**



## 8.1. Takeoff and Landing:

From the linearized transfer functions, we can design controllers that achieve the desired attitude for the vehicle during takeoff and landing, we need four controllers

- 1- Altitude controller, to reach desired altitude
- 2- Roll controller, to stabilize the vehicle from any rolling moment disturbances
- 3- Pitch controller, to stabilize the vehicle from any pitching moment disturbances
- 4- Yaw controller, to stabilize the vehicle from any yawing moment disturbances

Since the transfer functions are second-order, we only need a PD controller to achieve faster response for a step input, as the steady-state error is already achieved to be zero for this system, using MATLAB SISOTOOL, we can get the gains to achieve our requirements.

### 8.1.1. Altitude Controller

The open-loop transfer function

$$\frac{z}{Th_z} = -\frac{0.04313}{s^2}$$

Using a PD controller

$$K_p = 37.7$$

$$K_d = 46.66$$

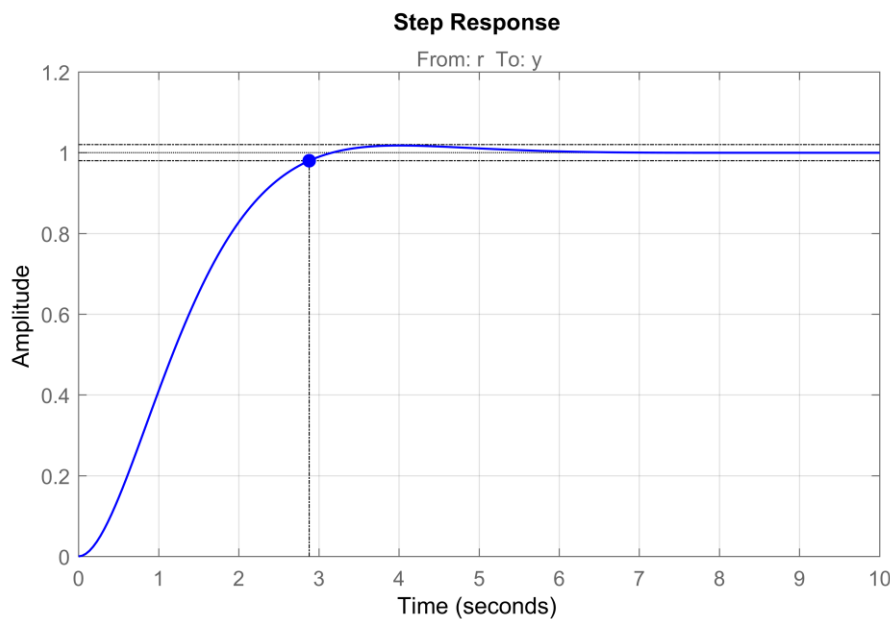


Figure 173: Altitude Controller Step Response

Settling time is 2.9 seconds

The closed-loop transfer function becomes

$$\frac{z}{z_{com}} = \frac{1.626}{s^2 + 2.012 s + 1.626}$$

Keeping in mind that the altitude is in the negative z-axis;  $h_{com} = -z_{com}$

### 8.1.2. Roll Controller

The open-loop transfer function

$$\frac{\phi}{Th_{late}} = \frac{0.1239}{s^2}$$

Using a PD controller

$$K_p = 22$$

$$K_d = 22$$

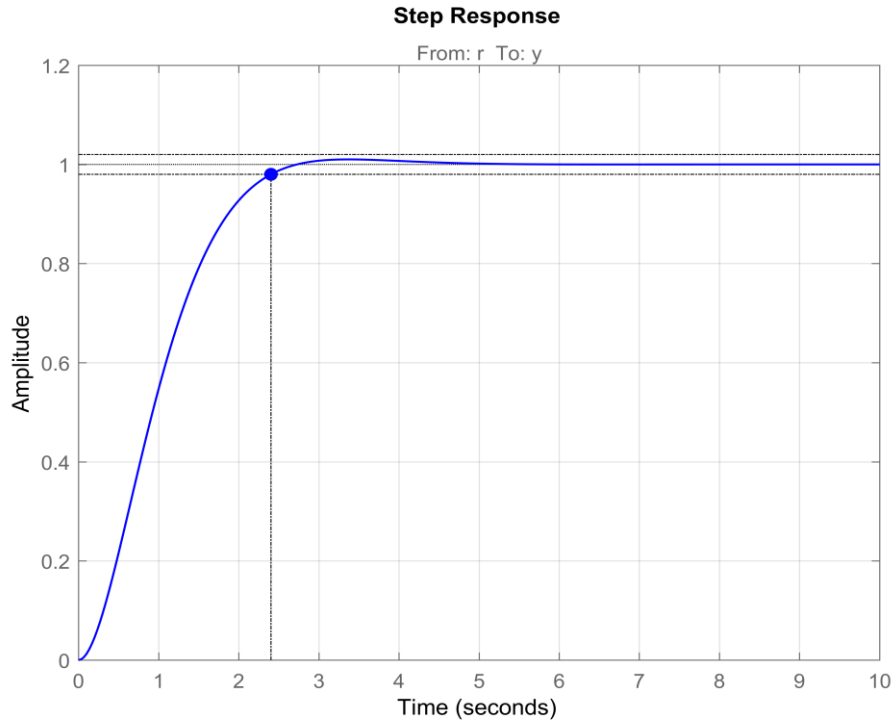


Figure 174: Roll Controller Step Response

Settling time is 2.4 seconds, and we always need the input  $\phi_{com}$  to be zero

The closed-loop transfer function becomes

$$\frac{\phi}{\phi_{com}} = \frac{2.726}{s^2 + 2.726 s + 2.726}$$

### 8.1.3. Pitch Controller

The open-loop transfer function

$$\frac{\theta}{Th_{long}} = \frac{0.07464}{s^2}$$

Using a PD controller

$$K_p = 32$$

$$K_d = 33$$

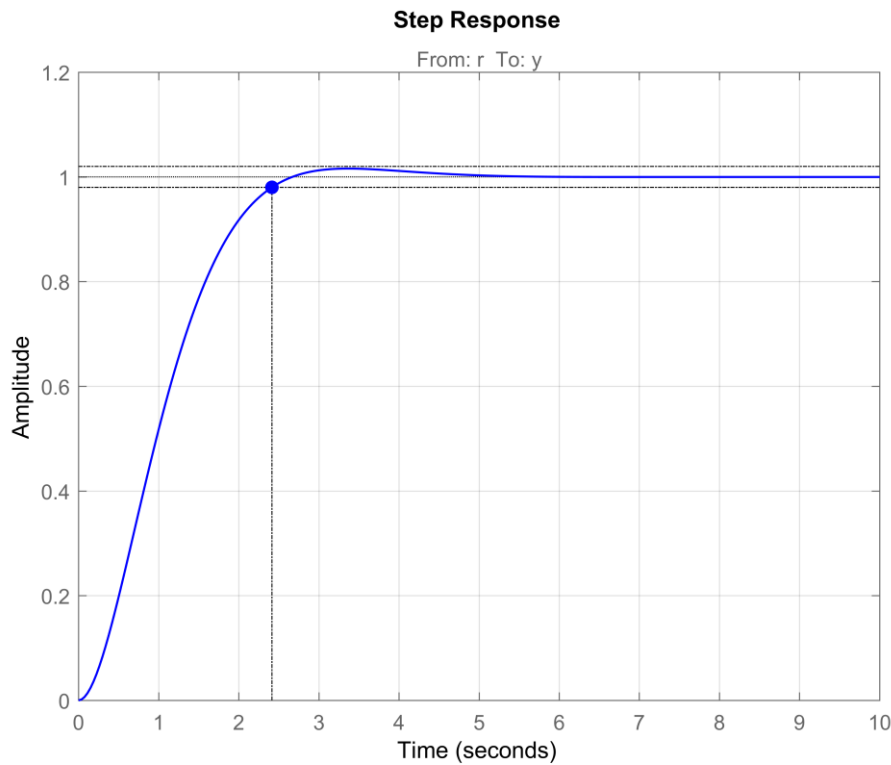


Figure 175: Pitch Controller Step Response

Settling time is 2.4 seconds, and we always need the input  $\theta_{com}$  to be zero

The closed-loop transfer function becomes

$$\frac{\theta}{\theta_{com}} = \frac{2.388}{s^2 + 2.463 s + 2.388}$$

### 8.1.4. Yaw Controller

The open-loop transfer function

$$\frac{\psi}{Th_{norm}} = \frac{0.007583}{s^2}$$

Using a PD controller

$$K_p = 170$$

$$K_d = 240$$

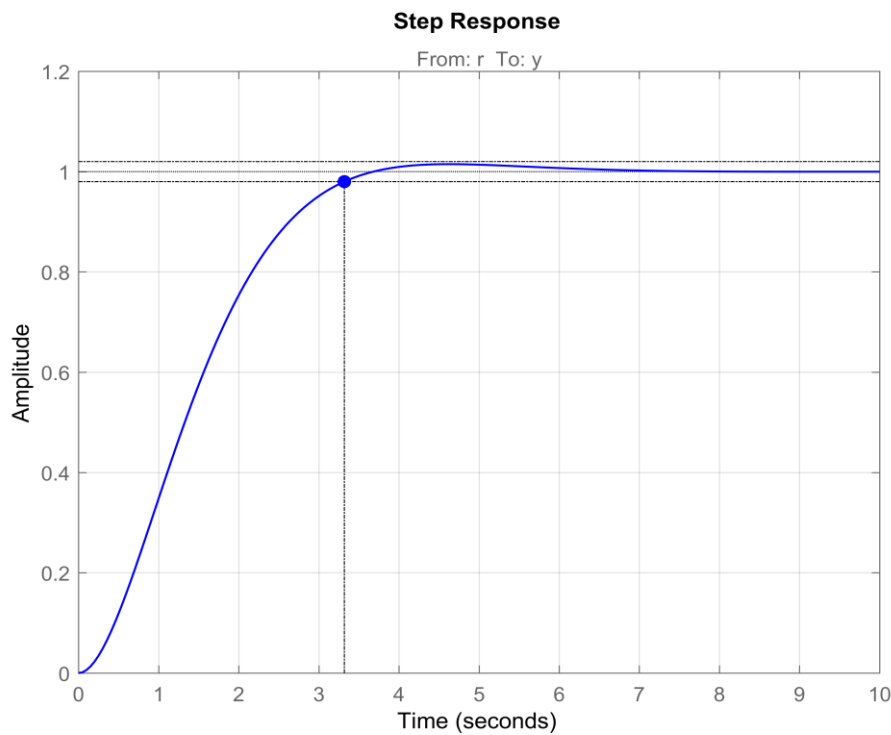


Figure 176: Yaw Controller Step Response

Settling time is 3.3 seconds, and we always need the input  $\psi_{com}$  to be zero

The closed-loop transfer function becomes

$$\frac{\psi}{\psi_{com}} = \frac{1.289}{s^2 + 1.82 s + 1.289}$$

## 8.2. Cruise:

Our next step is to design control surfaces which are necessary during cruise to

- 1- Stabilize the aircraft without using the motors, since the motors are turned off during cruising phase
- 2- Change heading angle, and turn

During cruise, when the motors are turned off, the thruster motor generates torque that forces the aircraft to roll about the x-axis, the same idea in helicopters; they require an opposite moment to compensate the torque generated by the single rotor. In helicopters, this opposite moment is produced from tail rotor. However, in fixed-wing aircrafts, the opposite moment is produced by controlling the aileron deflection. In piston single engine propeller driven aircraft, typically the propeller rotates clockwise, this tolling moment tends to rotate counter clockwise, pushing the left wing down. To counter the aircraft, roll left, the pilot applies right aileron.

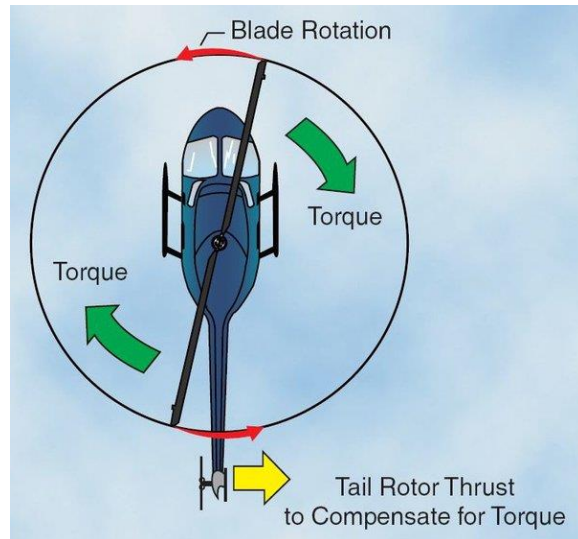


Figure 2: Helicopter Anti-Torque System

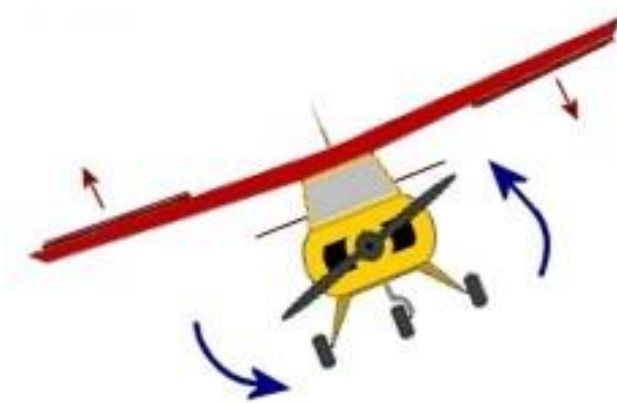


Figure 3: Ailerons

For now, we assume that ailerons compensate the torque generated by the thruster motor, so we don't need the control surfaces at the moment. We only control the thrust to sustain the forward velocity at cruise which is dependent on the pitch angle.

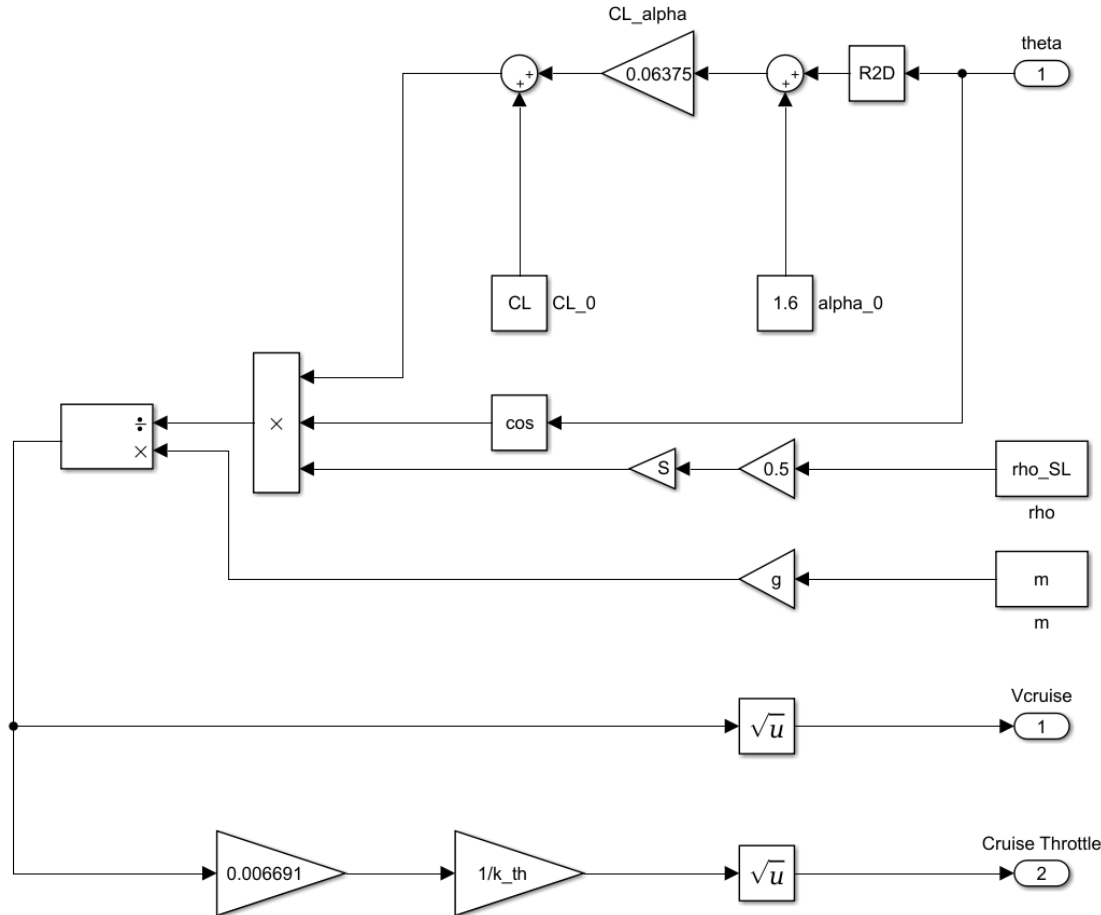


Figure 177: Controlling the cruise speed on Simulink

### 8.3. Simulation

After building the full model using MATLAB Simulink, the two inputs needed for the simulation are

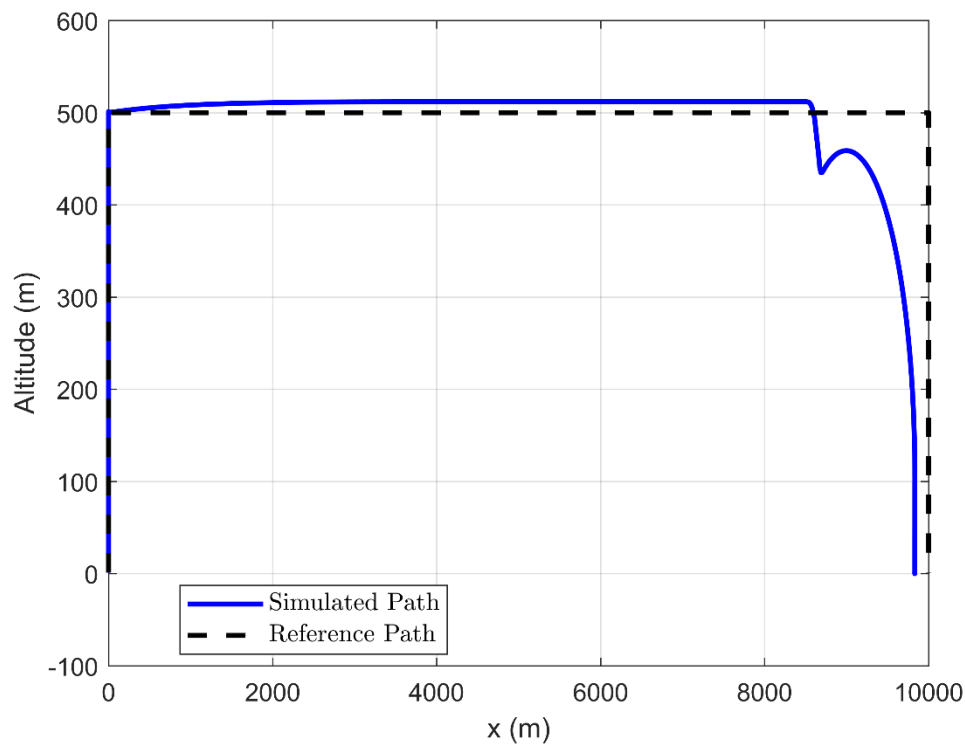
- Cruising altitude, for takeoff
- Cruising range, or descending

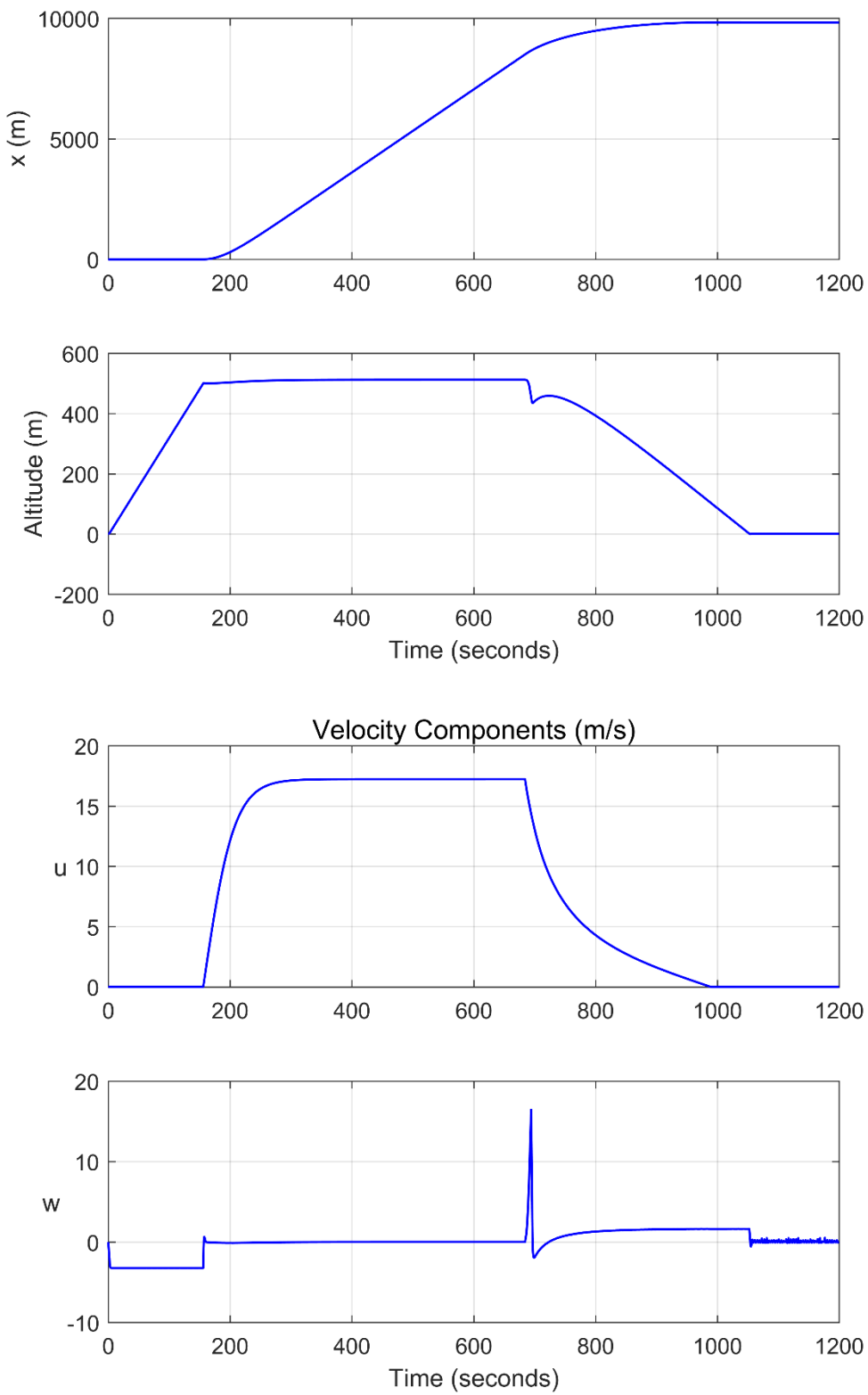
The model switches between turning off the eight motors in cruise, and turning off the thruster motor in landing. In transition between takeoff and cruise when the velocity is less than cruise velocity, then all motors (eight motors and thruster motor) are on, the eight motors are on till the velocity reaches the cruise velocity. In transition between cruise and descend, once the vehicle

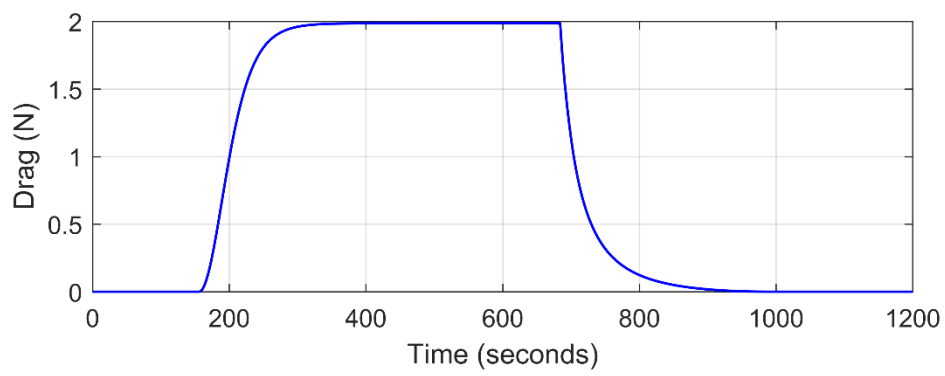
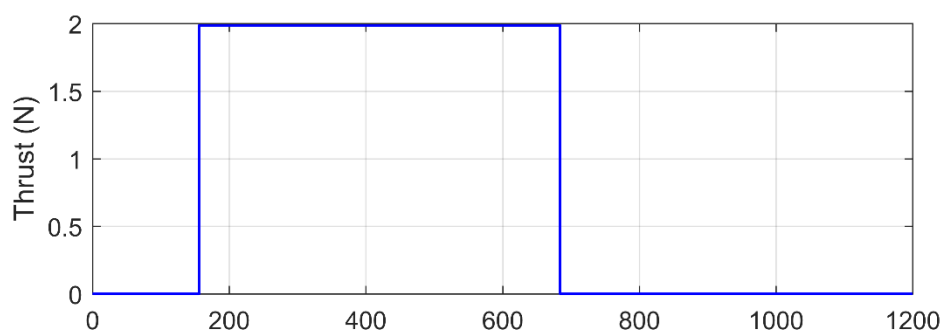
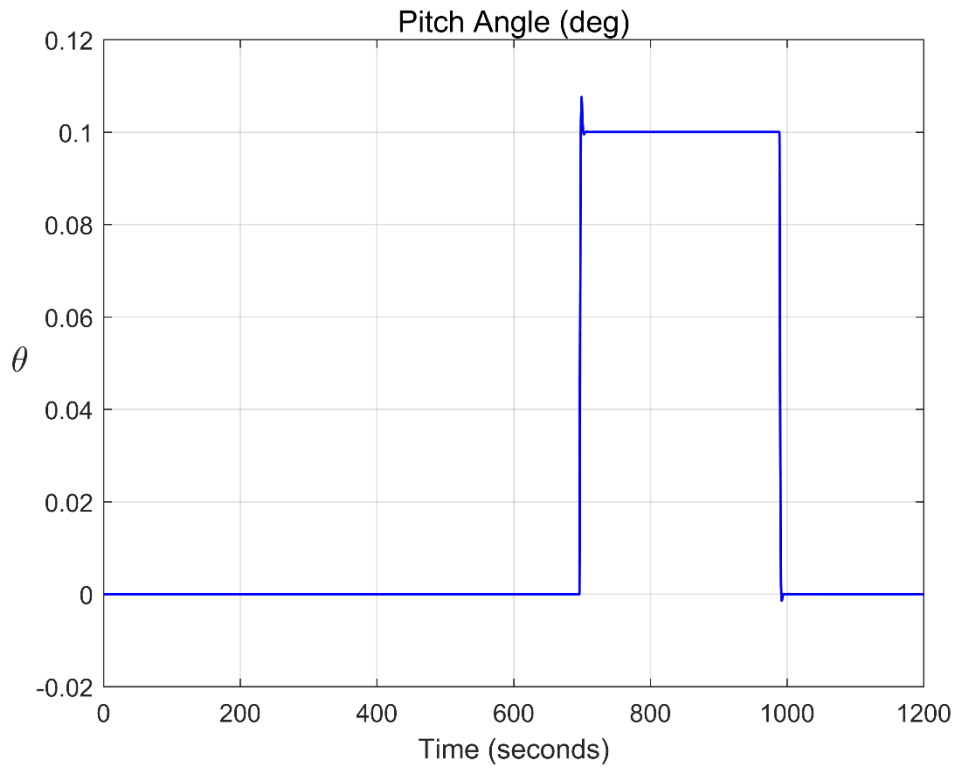
reaches the range to start descent, the thruster motor is turned off. Descending is where velocity decelerates to zero, by pitching up so the eight motors act as brakes.

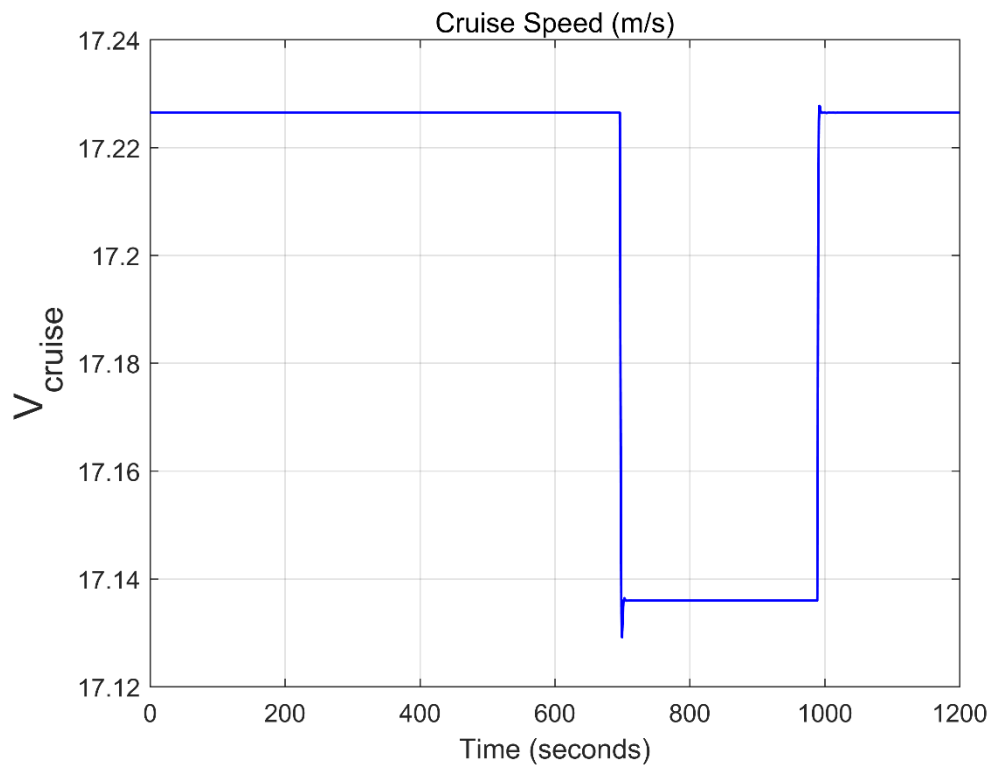
### 8.3.1. Results

Results of simulating the mission (for cruising altitude is 500m and cruising range 10000m (descending at 8500m, 85% of cruising range))

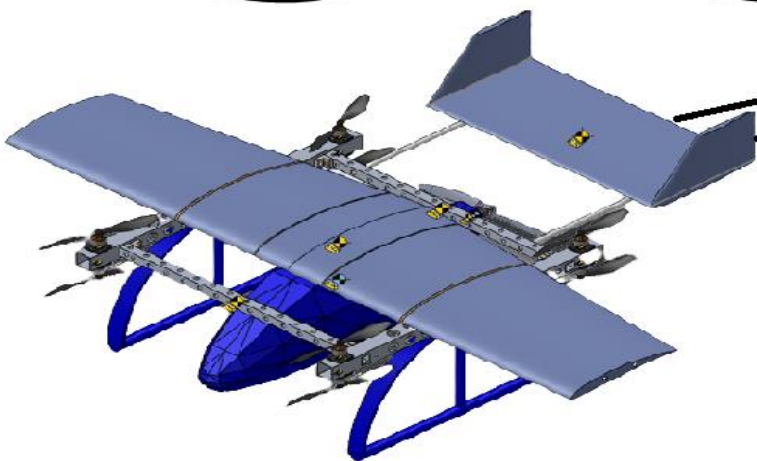








# References



## References

---

### References:

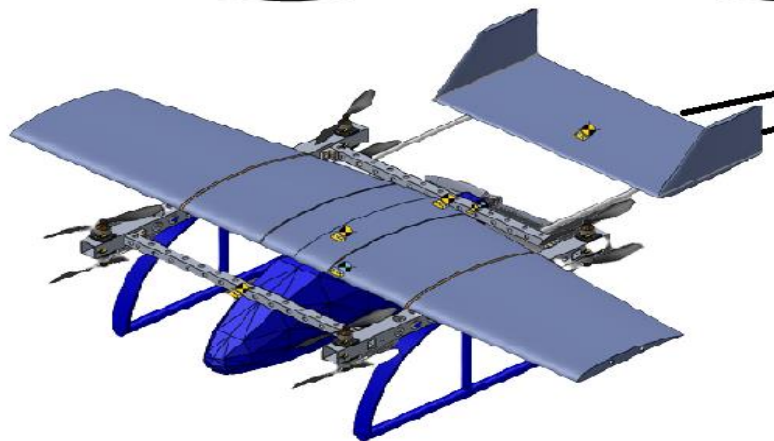
- 1) Graduation project ‘OCTOCOPTER PROJECT 2013’ supervised by “Prof. Ayman H. Kasem”.
- 2) Airplane Design Part I : Preliminary Sizing of Airplanes by Jan Roskam (Author).
- 3) Airplane Design, Part II : Preliminary Configuration Design and Integration of the Propulsion System by Jan Roskam (Author).
- 4) Airplane Design, Part III : Layout design of cockpit, fuselage, wing and empennage: cutaways and inboard profiles by Jan Roskam (Author).
- 5) Modeling Flight: The role of dynamically scaled free-flight models.
- 6) <https://docs.google.com/spreadsheets/d/17dP9XBJrdk2xVu5sA9GyqVDtclzg4MHg/edit?usp=sharing&ouid=105857420818808630627&rtpof=true&sd=true>
- 7) [https://docs.google.com/spreadsheets/d/115is7SBOu\\_rKq7qikzuBy9FIIdx1TzYML/e dit?usp=sharing&ouid=105857420818808630627&rtpof=true&sd=true](https://docs.google.com/spreadsheets/d/115is7SBOu_rKq7qikzuBy9FIIdx1TzYML/e dit?usp=sharing&ouid=105857420818808630627&rtpof=true&sd=true)
- 8) <https://aamrealityindex.com/>
- 9) <https://evtol.com/>
- 10) <https://verticalmag.com/>
- 11) [www.futureflight.aero](http://www.futureflight.aero)
- 12) <https://www.airspacemag.com/airspacemag/how-far-away-your-air-taxi-180978686/>
- 13) <https://aerotoolbox.com/>
- 14) <https://lilium.com/jet>
- 15) <https://www.theverge.com/2020/9/22/21449238/tesla-electric-car-battery-tabless-cells-day-elon-musk>
- 16) [Justa AHRS Filter], [https://github.com/Josef4Sci/AHRS\\_Filter](https://github.com/Josef4Sci/AHRS_Filter)
- 17) [Adafruit BMP085 library], <https://github.com/adafruit/Adafruit-BMP085-Library>
- 18) [Blynk IoT platform], <https://github.com/blynkkk>
- 19) [nRF24L01 Wi-Fi module interface with Arduino],  
<https://howtomechatronics.com/tutorials/arduino/arduino-wireless-communication-nrf24l01-tutorial/>
- 20) [Ardupilot Introduction], <https://ardupilot.org/copter/docs/introduction.html>

## References

---

- 21) [Ardupilot Codebase], <https://ardupilot.org/dev/docs/learning-the-ardupilot-codebase.html>
- 22) [Mission Planner Overview], <https://ardupilot.org/planner/docs/mission-planner-overview.html>
- 23) [MAVLink interface with Ardupilot], <https://ardupilot.org/dev/docs/mavlink-commands.html>
- 24) Robert C. Nelson, “Flight Stability and Automatic Control”
- 25) [MATLAB Simulink “MathWorks Help Center”],  
[https://www.mathworks.com/help/aeroblks/6dofeulerangles.html#:~:text=The%206DOF%20\(Euler%20Angles\)%20block,Ye%2C%20Ze\).](https://www.mathworks.com/help/aeroblks/6dofeulerangles.html#:~:text=The%206DOF%20(Euler%20Angles)%20block,Ye%2C%20Ze).)
- 26) [Tarek N. Deif, Ayman H. Kassem, and Gamal M. El Baioumi, “Modeling and Attitude Stabilization of Indoor Quad Rotor”],  
[https://www.researchgate.net/publication/288715443\\_Modeling\\_and\\_Attitude\\_Stabilization\\_of\\_Indoor\\_Quad\\_Rotor](https://www.researchgate.net/publication/288715443_Modeling_and_Attitude_Stabilization_of_Indoor_Quad_Rotor)

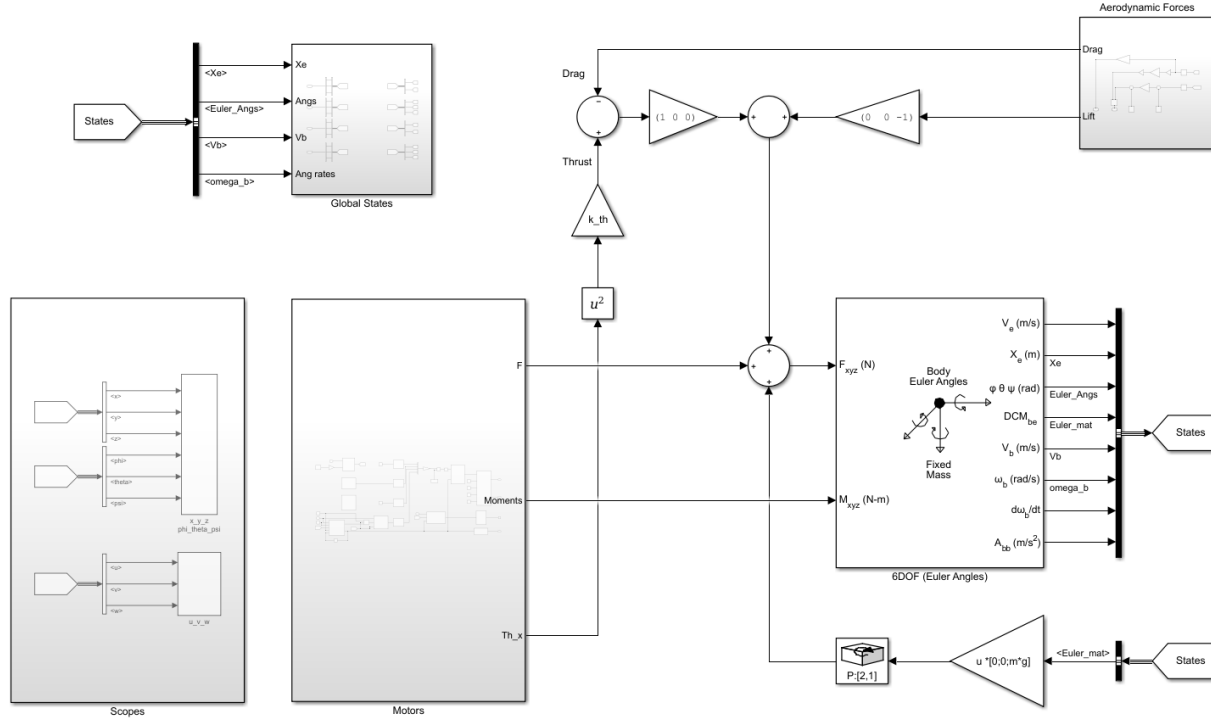
# Appendix A



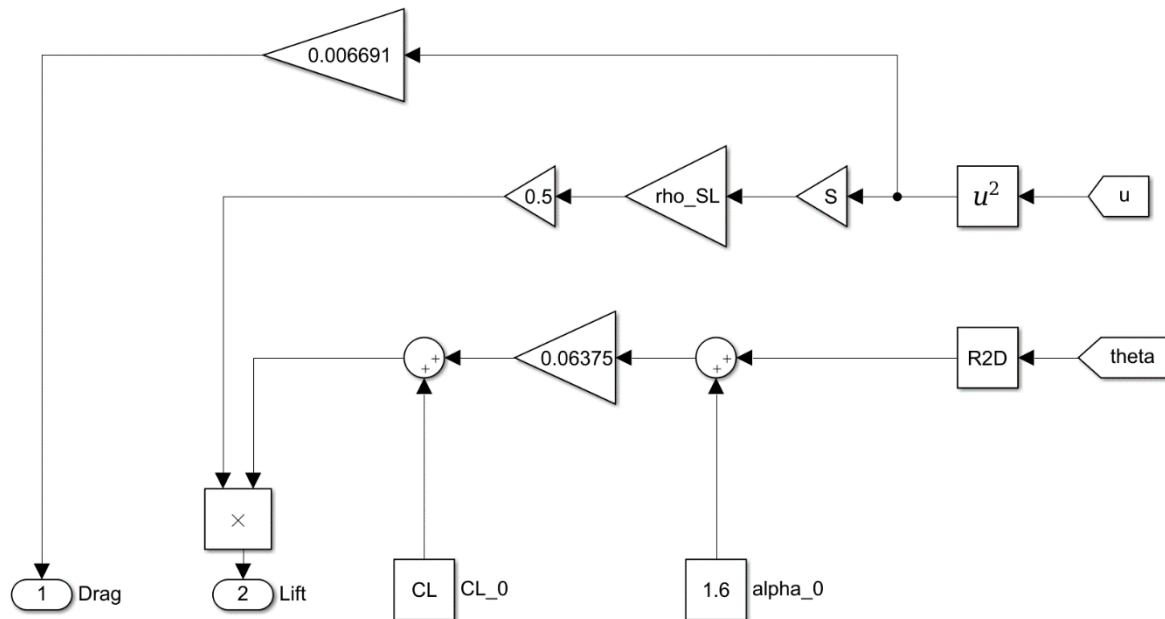
# Appendix

---

## Appendix (A): Full Model



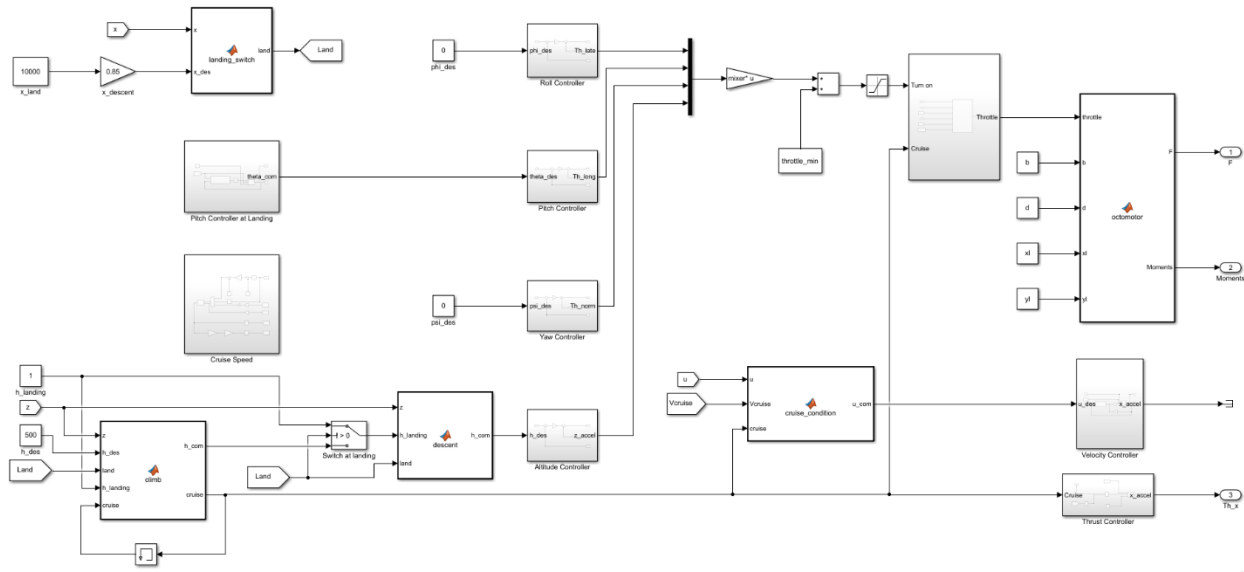
## Aerodynamic Forces



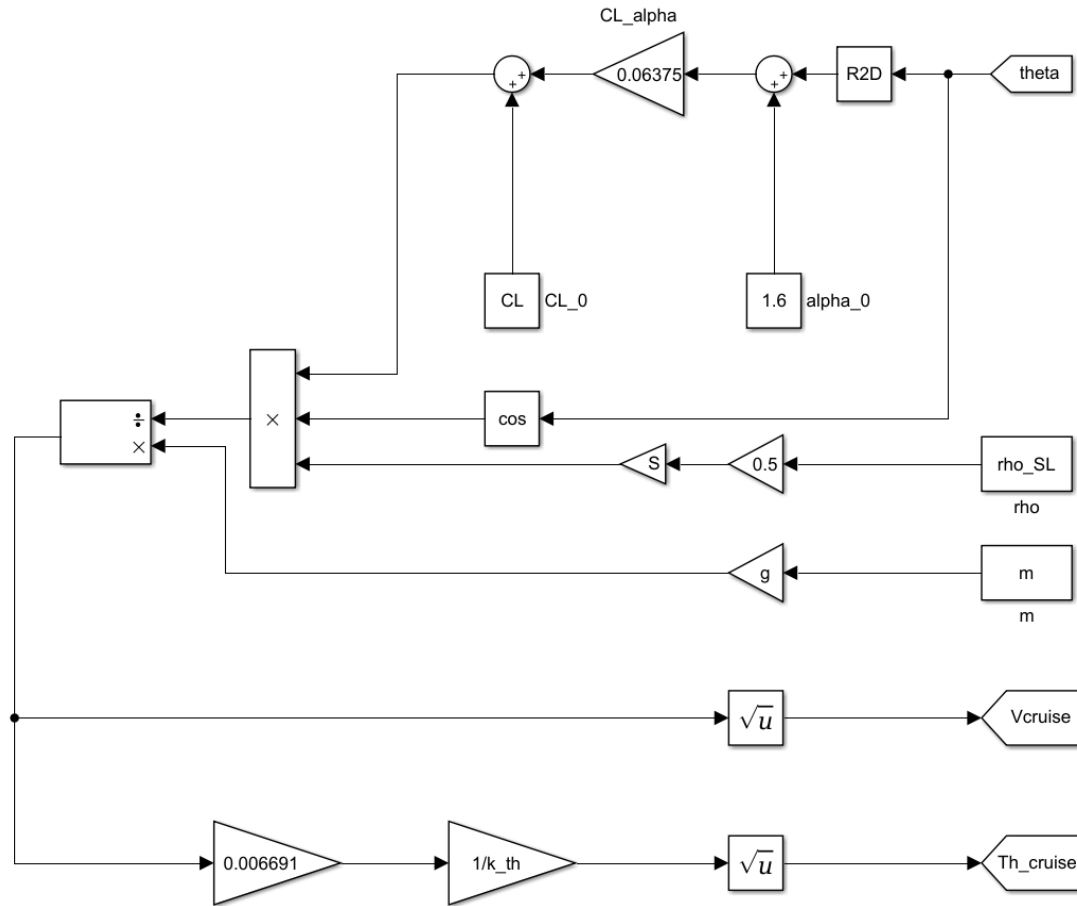
# Appendix

---

## Motors Subsystem



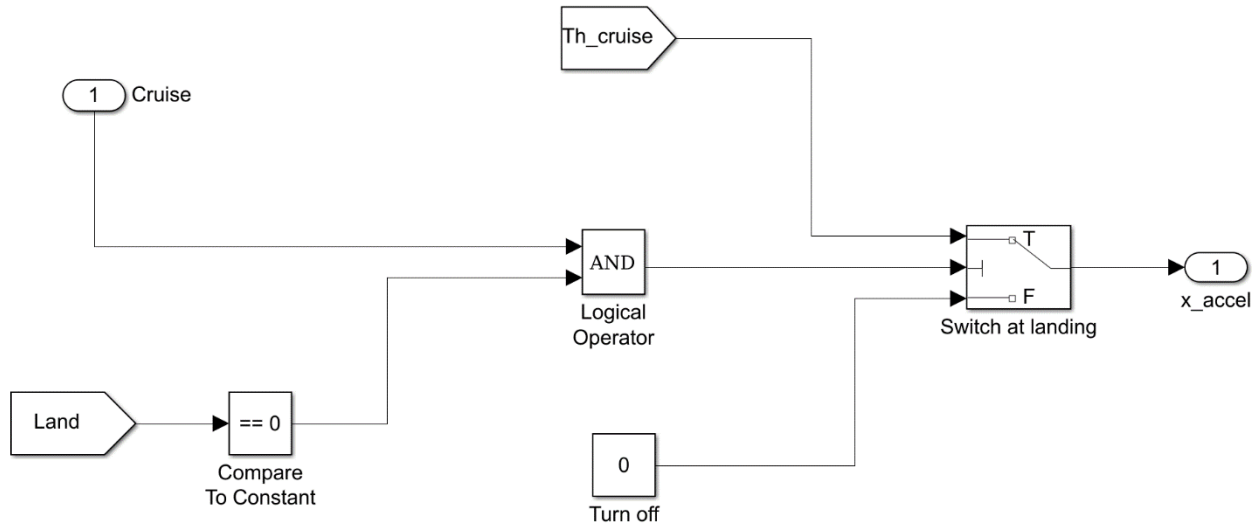
## Cruise Speed Controller



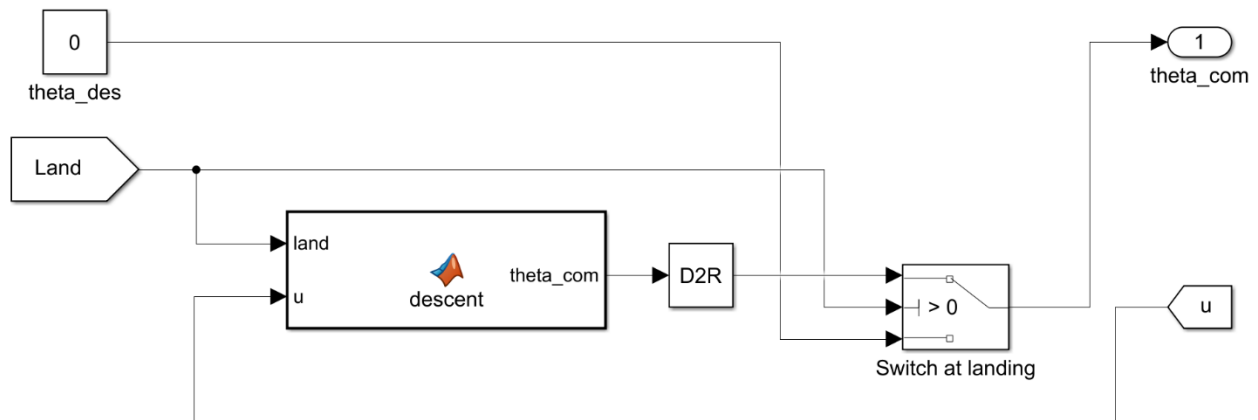
## Appendix

---

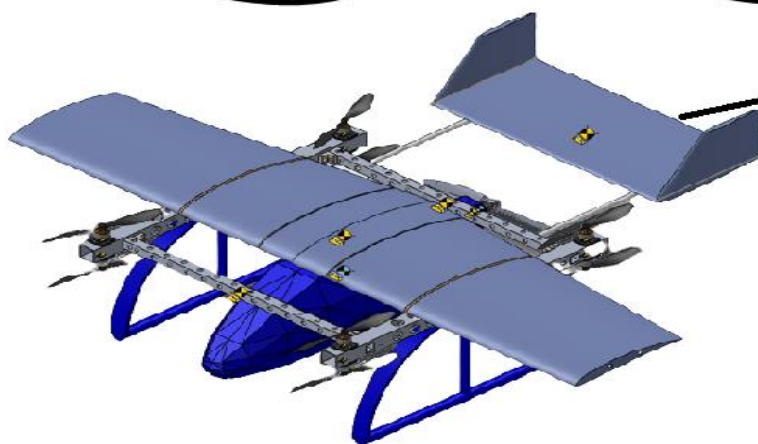
### Thrust Controller during Cruise



### Pitch Controller at Landing



## Appendix B



### Code (1) – curve fitting of full scale samples

```

clc
close all
clearvars

x = [1315    1240    2539.693      550      300   1550.037      1632.931      274.667
      700    2050.235;...
     1815    1700    3174.693      800      400   2000          2721.552      374.667
      900    2800.023;...
     500      300     635       226.796 100      449.963      453.592      100      200
749.788];
w_to = x(2,:);
w_pl = x(3,:);
w_e = x(1,:);

log_w_e = log10(w_e);
log_w_to = log10(w_to);
f=fit(log_w_e',log_w_to','poly1');
A = f(0)
B = (f(2)-f(3))/(2-3)
x = 0 : 1 : 4;
y = B*x + A;
figure(1)
plot(log_w_e,log_w_to,".")
hold on
plot(x,y)
grid minor
title("$A = "+A+" , B = "+B+"$",'interpreter','latex')
xlabel("$\log_{10} W_E$",'interpreter','latex')
ylabel("$\log_{10} W_{TO}$",'interpreter','latex')
legend off
syms w_e
eq = 10.^(A+B*log10(w_e))-(200+w_e);
s = solve(eq,w_e)
%
figure(2)
f=fit(w_pl',w_to','poly1');
A = f(0)
B = (f(2)-f(3))/(2-3)
x = 0 : 100 : 800;
y = B*x + A;
plot(w_pl,w_to,".")
hold on
plot(x,y)
grid minor
plot([200,200,0],[0,f(200),f(200)])
title("$W_{TO}(200)="+f(200)+"\nobreakspace kg$",'interpreter','latex')
xlabel("$W_{PL}$",'interpreter','latex')
ylabel("$W_{TO}$",'interpreter','latex')
legend off

```

### Code (2) - curve fitting of sub octocopter products

```
clc
close all
clearvars

x = [
2.45  0.80
2.54  0.77
8.48  2.90
6.20  2.00
15.88 11.34
9.98  0.80
19.96 3.49
11.39 9.98
16.01 4.99
18.01 5.99
13.61 7.98
13.38 12.02
8.85  12.70
4.99  6.80
4.99  2.60
6.99  1.50
7.98  1.20
11.34 9.07
24.95 9.98
4.99  2.49
4.99  2.49
12.02 6.49
2.81  0.59
7.98  2.99
5.10  2.50
2.70  0.70
3.99  1.50
4.99  3.99
3.70  0.70
9.98  8.48
24.95 16.01
3.81  1.20
19.96 7.48
11.66 9.98
11.66 9.98
8.21  4.90
8.98  2.00
12.02 5.99
11.00 8.98
9.98  7.30
19.50 13.61
19.01 6.99
12.25 2.04
16.01 5.99
7.98  2.00
];
G = 4.6086;
```

```

w_to = x(:,1);
w_pl = x(:,2);

w_e = w_to-w_pl;
f=fit(w_to,w_pl./w_to,'poly2');
figure(1)
plot(f,w_to,w_pl./w_to)
hold on
grid minor
plot([G,G,0],[0,f(G),f(G)])
title("$W_{TO} = " + G + "\nobreakspace kg \nobreakspace at \nobreakspace W_E = "
"+G*(1-f(G))+"\nobreakspace kg$",'interpreter','latex')
xlabel("$W_{TO}$",'interpreter','latex')
ylabel("$W_{PL} \% $",'interpreter','latex')
legend off
%
figure(2)
log_w_e = log10(w_e);
log_w_to = log10(w_to);
f=fit(log_w_e,log_w_to,'poly1');
A = f(0)
B = (f(2)-f(3))/(2-3)
x = 0 : 0.5 : 1.5;
y = B*x + A;
plot(log_w_e,log_w_to,".")
hold on
plot(x,y)
grid minor
title("$A = "+A+" , B = "+B+"$",'interpreter','latex')
xlabel("$\log_{10} W_E$",'interpreter','latex')
ylabel("$\log_{10} W_{TO}$",'interpreter','latex')
legend off
W_to = 10.^(A+B*log10(2.82))
W_pl = W_to-2.82

```

### Code (3) – matching plot for cruise and stall

```
clc
clear
close all
hold all
axis([0,50,0,60]);
xlabel('(W/S)_T_0','FontSize',10,...
    'FontWeight','bold')
ylabel('(W/P)_T_0','FontSize',10,...
    'FontWeight','bold')
box on
grid on

w_s=linspace(0,60,100);
w_pv=linspace(0,220,100);
```

## Givens

```
w_to= 6*2.204623;
rho_sl=0.002377;
alt_cr=0;
rho_altcr=0.002377;
g0=32; %british units
cl_max=1.5;
cl_maxto=1.7;
cl_maxL=1.7;
%all are found in the table below we take the average value
%(table 3.1)
```

Table 3.1 Typical Values For Maximum Lift Coefficient

Airplane Type	$C_{L_{max}}$	$C_{L_{max,TO}}$	$C_{L_{max,L}}$
1. Homebuilts	1.2 - 1.8	1.2 - 1.8	1.2 - 2.0*
2. Single Engine Propeller Driven	1.3 - 1.9	1.3 - 1.9	1.6 - 2.3
3. Twin Engine Propeller Driven	1.2 - 1.8	1.4 - 2.0	1.6 - 2.5
4. Agricultural	1.3 - 1.9	1.3 - 1.9	1.3 - 1.9
5. Business Jets	1.4 - 1.8	1.6 - 2.2	1.6 - 2.6
6. Regional TBP	1.5 - 1.9	1.7 - 2.1	1.9 - 3.3
7. Transport Jets	1.2 - 1.8	1.6 - 2.2	1.8 - 2.8
8. Military Trainers	1.2 - 1.8	1.4 - 2.0	1.6 - 2.2
9. Fighters	1.2 - 1.8	1.4 - 2.0	1.6 - 2.6
10. Mil. Patrol, Bomb and Transports	1.2 - 1.8	1.6 - 2.2	1.8 - 3.0
11. Flying Boats, Amphibious and Float Airplanes	1.2 - 1.8	1.6 - 2.2	1.8 - 3.4
12. Supersonic Cruise Airplanes	1.2 - 1.8	1.6 - 2.0	1.8 - 2.2

\* The Rutan Varieze reaches 2.5, based on stall speed data from Ref. 9.

```
v_crkn=18*18/5*0.5399565;
v_cr=v_crkn*1.688; % [ft/sec]
v_crmph=v_crkn*1.151; %v(knots)*1.151 [mph]
ARc=4.5;
eta_p=0.82;
```

## Stall Speed

The power-off stall speed of an airplane may be determined from:

$$V_s = \left\{ \frac{2(W/S)}{\rho C_{L_{max}}} \right\}^{1/2} \xrightarrow{\text{Clean aircraft}} \quad (3.1)$$

units are:

- $V_s \Rightarrow \text{ft/sec} = \text{knots} * 1.6878$
- $\rho \Rightarrow \text{slug/ft}^3$  [for sea-level: 0.0023769 slug/ft<sup>3</sup>]

```
% Stall curve at take off
v_s=11*18/5*0.5399565*1.688; %[ft/sec]
w_ss=0.5*rho_sl*v_s^2*c1_max
s_to=0.09290304*w_to/w_ss % to m^2 from feet
w_ssv=w_ss.*ones(1,100);
plot(w_ssv,w_pv, 'LineWidth',1.2)
```

## Cruise

[Rho Calculator](#) or you can use it in last section

$$\sigma_{CR} = \frac{\rho_{CR}}{\rho_s}$$

$$\left(\frac{W}{P}\right)_{CR} = \frac{\left(\frac{W}{S}\right)}{IP^3 * \sigma_{CR}}$$

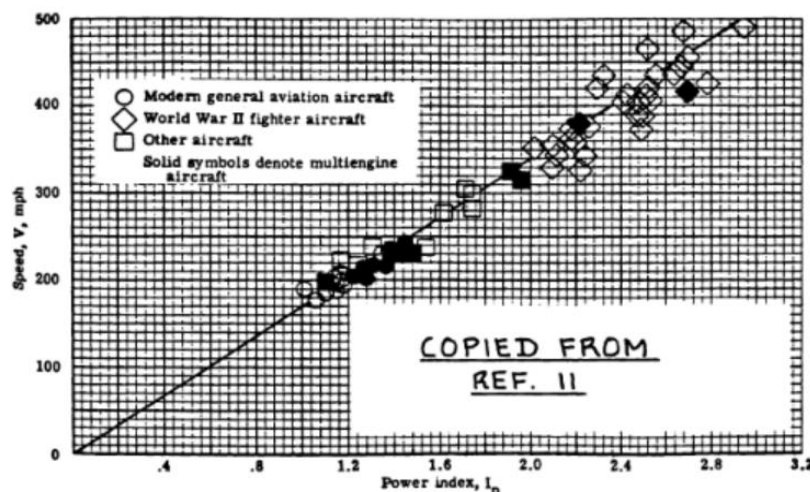


Figure 3.28 Correlation of Airplane Speed with Power Index for Retractable Gear, Cantilevered Wing Configurations

page 163 in roskam to be able to get it by a ruler  
%Inputs

```

sigma_cr=rho_altc/rho_s1
IP=0.24; % Go to figure 3.28
%Code
w_pcr=w_s/(IP^3*sigma_cr);
plot(w_s,w_pcr,'LineWidth',1.2)
legend('Stall speed ','Cruise') ;
xlim([1.5 3])
ylim([120 220])
pcr = w_to/168

```

#### Code (4) – GPS Module with Arduino

```

#include <TinyGPS.h>
float lat,lon;
TinyGPS gps;

void setup(){
Serial.println("The GPS Received Signal:");
Serial.begin(9600);

}

void loop(){
  while(Serial.available()){
    if(gps.encode(Serial.read()))
    {
      gps.f_get_position(&lat,&lon);

      Serial.print("Position: ");

      //Latitude
      Serial.print("Latitude: ");
      Serial.print(lat,6);

      Serial.print(",");
      //Longitude
      Serial.print("Longitude: ");
      Serial.println(lon,6);

    }
  }
}

```

### Code (5) – I<sup>2</sup>C Scanner (Who am I) Sketch

```
#include <Wire.h>
void setup()
{
    Wire.begin();
    Serial.begin(9600);
    while (!Serial);
    Serial.println("\nI2C Scanner");
}

void loop()
{
    byte error, address;
    int nDevices;
    Serial.println("Scanning...");
    nDevices = 0;
    for (address = 1; address < 127; address++)
    {
        Wire.beginTransmission(address);
        error = Wire.endTransmission();

        if (error == 0)
        {
            Serial.print("I2C device found at address 0x");
            if (address < 16)
                Serial.print("0");
            Serial.print(address, HEX);
            Serial.println(" !");
            nDevices++;
        }
        else if (error == 4)
        {
            Serial.print("Unknown error at address 0x");
            if (address < 16)
                Serial.print("0");
            Serial.println(address, HEX);
        }
    }
    if (nDevices == 0)
        Serial.println("No I2C devices found\n");
    else
        Serial.println("done\n");

    delay(5000);
}
```

### Code (6) – Arduino Code to Run One Motor

```
#include <Servo.h>
Servo motor1;
int inmotor1,t;
void setup() {
    Serial.begin(9600);
    t=60;
    Serial.setTimeout(t*1000);
    motor1.attach(8,1000,2000);
    motor1.write(inmotor1);
    delay(1000);
}

void loop() {
    if (Serial.available()){
        inmotor1=Serial.parseInt();
        inmotor1=map(inmotor1,0,100,0,180); //range from 0 to 100
        motor1.write(inmotor1);
        Serial.println(inmotor1);
    }
}
```

### Arduino Code to Run Two Motors:

```
#include <Servo.h>
Servo motor1, motor2;
int inmotor1, inmotor2, t;
void setup() {
    Serial.begin(9600);
    t = 60;
    Serial.setTimeout(t * 1000);
    motor1.attach(8, 1000, 2000);
    motor2.attach(9, 1000, 2000);
    motor1.write(inmotor1);
    motor2.write(inmotor2);
    delay(1000);
}

void loop() {
    if (Serial.available()) {
        inmotor1 = Serial.parseInt();
        inmotor1 = map(inmotor1, 0, 100, 0, 180); //range from 0 to 100
        delay(10);
        if (Serial.available()) {
            inmotor2 = Serial.parseInt();
            inmotor2 = map(inmotor2, 0, 100, 0, 180);
            delay(10);
            motor1.write(inmotor1);
            motor2.write(inmotor2);
            Serial.println(inmotor1);
            Serial.println(inmotor2);
        }
    }
}
```

### Code (7) – Arduino Code to Run the Eight Motors via Wi-Fi Connection and Receive Sensors' Measurement (Transmitter Code)

```
//                                         SDA   SCL
//Uno, Redboard, Pro:                      A4    A5
//Mega2560, Due:                           20    21

//Transmitter(laptop)
//Transmit -> Recieve

#include <SPI.h>
#include <nRF24L01.h>
#include <RF24.h>

RF24 radio(7, 8); // CE, CSN
int t;

struct readings {
  float phi, theta, psi;
  double a;
};

readings sensors;

struct val {
  int motor_send;
};

val input;

const byte address1[6] = "00001";
const byte address2[6] = "00002";

void setup() {
  radio.begin();
  Serial.begin(9600);
  t = 300;
  Serial.setTimeout(t * 1000);
  radio.openWritingPipe(address2); // 00002
  radio.openReadingPipe(0, address1); // 00001
  radio.setPALevel(RF24_PA_MIN);
  delay(1000);
}

void loop() {
  radio.stopListening();
  if (Serial.available()) {
    input.motor_send = Serial.parseInt();
  }

  radio.write(&input, sizeof(val));

  delay(5);

  radio.startListening();
}
```

```

if (radio.available()) {
    radio.read(&sensors, sizeof(readings));
}

Serial.print (millis()); Serial.print (" "); Serial.print (sensors.phi);
Serial.print (" "); Serial.print (sensors.theta); Serial.print (" ");
Serial.print (sensors.psi); Serial.print(" ");
Serial.println(sensors.a);
delay(10);
}

```

### Code (8) – Receiver Code

```

//                                         SDA   SCL
//Uno, Redboard, Pro:                  A4    A5
//Mega2560, Due:                      20    21

//Reciever(motors)
//Recieve -> transmit

#include <Wire.h>
#include <SFE_BMP180.h>
#include "BMX055_Minimal_Lib.h"
#include "Justa_AHRS_Filter.h"
#include <SPI.h>
#include <nRF24L01.h>
#include <RF24.h>
#include <Servo.h>

SFE_BMP180 pressure;
BMX055 bmx055;
AHRS AHRSlib;

Servo motor1;
Servo motor2;
Servo motor3;
Servo motor4;
Servo motor5;
Servo motor6;
Servo motor7;
Servo motor8;

struct readings {
    float phi, theta, psi;
    double a;
};
readings sensors;

struct val {
    int motor_send;
};


```

```

val input;

RF24 radio(7, 8); // CE, CSN
const byte address1[6] = "00001";
const byte address2[6] = "00002";

int inmotor1, inmotor2, inmotor3, inmotor4, inmotor5, inmotor6, inmotor7,
inmotor8;

float q0, q1, q2, q3, R1, R2, R3, R4, R5;
double baseline;

void setup() {
    Serial.begin(9600);

    if (pressure.begin())
        Serial.println("BMP180 init success");
    else
    {
        Serial.println("BMP180 init fail (disconnected?) \n\n");
        while (1); // Pause forever.
    }

    baseline = getPressure();
    bmx055.init();
    AHRSlib = AHRS();

    motor1.attach(30, 1000, 2000);
    motor1.write(inmotor1);

    motor2.attach(31, 1000, 2000);
    motor2.write(inmotor2);

    motor3.attach(32, 1000, 2000);
    motor3.write(inmotor3);

    motor4.attach(33, 1000, 2000);
    motor4.write(inmotor4);

    motor5.attach(34, 1000, 2000);
    motor5.write(inmotor5);

    motor6.attach(35, 1000, 2000);
    motor6.write(inmotor6);

    motor7.attach(36, 1000, 2000);
    motor7.write(inmotor7);

    motor8.attach(37, 1000, 2000);
    motor8.write(inmotor8);

    radio.begin();
    radio.openWritingPipe(address1); // 00001
    radio.openReadingPipe(0, address2); // 00002
    radio.setPALevel(RF24_PA_MIN);
}

```

```

}

void loop() {
    double P;
    byte data[18];
    float dataF[9];

    delay(5);
    radio.startListening();

    if (radio.available()) {
        radio.read(&input, sizeof(val));
    }
    inmotor1 = map(input.motor_send, 0, 100, 0, 180);
    inmotor2 = inmotor1; inmotor3 = inmotor1; inmotor4 = inmotor1; inmotor5 = inmotor1;
    inmotor6 = inmotor1; inmotor7 = inmotor1; inmotor8 = inmotor1;

    motor1.write(inmotor1);
    motor2.write(inmotor2);
    motor3.write(inmotor3);
    motor4.write(inmotor4);
    motor5.write(inmotor5);
    motor6.write(inmotor6);
    motor7.write(inmotor7);
    motor8.write(inmotor8);

    P = getPressure();
    sensors.a = pressure.altitude(P, baseline);

    bmx055.getSensorData(data);

    if (millis() < 10000) {

        AHRSlip.updateMagnetCalib(data);

    } else {

        AHRSlip.convertData(data, dataF);

        AHRSlip.updateRotationEtimation(dataF, 0.005, 0.005, 0.21 );

        q0 = AHRSlip.quaternion[0];
        q1 = AHRSlip.quaternion[1];
        q2 = AHRSlip.quaternion[2];
        q3 = AHRSlip.quaternion[3];

        R1 = (q0 * q0) + (q1 * q1) - (q2 * q2) - (q3 * q3); //1,1
        R2 = 2 * (q1 * q2 + q0 * q3); //2,1
        R3 = 2 * (q0 * q2 - q1 * q3); //3,1
        R4 = 2 * (q0 * q1 + q2 * q3); //3,2
        R5 = (q0 * q0) - (q1 * q1) - (q2 * q2) + (q3 * q3); //3,3

        sensors.phi = atan2(R2, R1) * 180.0 / M_PI;
    }
}

```

```

    sensors.theta = asin(R3) * 180.0 / M_PI;
    sensors.psi = atan2(R4, R5) * 180.0 / M_PI;
}

delay(5);
radio.stopListening();
radio.write(&sensors, sizeof(readings));

delay(10);
}

double getPressure()
{
    char status;
    double T, P, p0, a;
    status = pressure.startTemperature();
    if (status != 0)
    {
        delay(status);

        status = pressure.getTemperature(T);
        if (status != 0)
        {
            status = pressure.startPressure(3);
            if (status != 0)
            {
                delay(status);
                status = pressure.getPressure(P, T);
                if (status != 0)
                {
                    return (P);
                }
                else Serial.println("error retrieving pressure measurement\n");
            }
            else Serial.println("error starting pressure measurement\n");
        }
        else Serial.println("error retrieving temperature measurement\n");
    }
    else Serial.println("error starting temperature measurement\n");
}
}

```